Patching up the crypt

Innate immune cells orchestrate intestinal regeneration

Mónica Romera Hernández

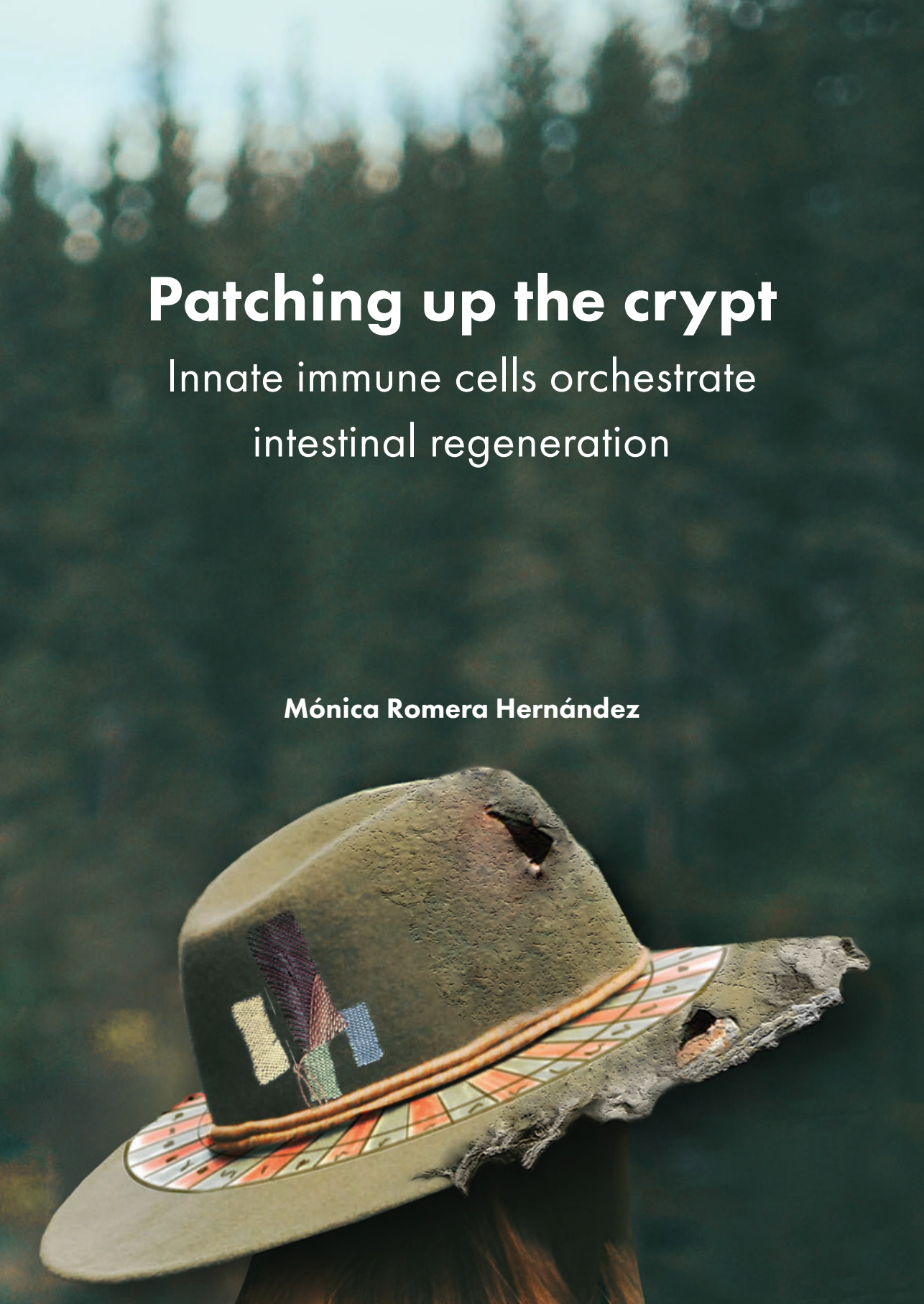

Patching up the crypt: Innate immune cells orchestrate intestinal regeneration

....

Layout: Egied Simons
Cover: Iliana Boshoven-Gkini
Printing: Ridderprint

The work described in this thesis was performed at the Department of Hematology at the Erasmus Medical Center Cancer Institute, Erasmus University Medical Center, Rotterdam, the Netherlands.

Printing of this thesis was financially supported by Erasmus University Rotterdam.

Patching up the crypt:

Innate immune cells orchestrate intestinal regeneration

Regulatie van darm herstel door cellen van het aangeboren afweer systeem

Proefschrift

ter verkrijging van de graad van doctor aan de
Erasmus Universiteit Rotterdam
op gezag van de
rector magnificus

Prof.dr. H.A.P. Pols

en volgens besluit van het College voor Promoties

De openbare verdediging zal plaatsvinden op

3 mei 2018 om 11:30 uur

door

Mónica Romera Hernández

geboren te Berga, Barcelona (Spanje)

Erasmus University Rotterdam

DOCTORAL COMMITEE

Supervisor: Prof.dr. J.J. Cornelissen

Other members: Prof.dr. I.P. Touw
Prof.dr. R.E. Mebius
Prof.dr. F. Koning

Co-supervisor: Dr. T. Cupedo

A mi iaio,
de extrema honra y dura proeza

CONTENTS

1

GENERAL INTRODUCTION

HARNESSING THE IMMUNE SYSTEM TO ENHANCE INTESTINAL BARRIER FUNCTION

Based in part on:

Damage control: Rorγt+ innate lymphoid cells in tissue regeneration. Romera-Hernández M, Aparicio-Domingo P, Cupedo T. Curr Opin Immunol. 2013 Apr;25(2):156-60.

ABSTRACT

Innate lymphoid cells (ILCs) are critical effectors of innate immunity and facilitate homeostasis as well as sustained adaptive immune responses, in particular to pathological infections. Recently, ILCs have emerged as novel orchestrators of tissue remodeling after injury, in the skin, thymus and intestine. In the intestine, group 3 innate lymphoid cells (ILC3s) and their IL-22 production are critical to maintain local crypt stem cells from T cell mediated killing in graft-versus-host (GVHD) disease[1], yet their mechanisms of action are not completely understood. Intestinal regeneration relies on the continuous replacement of the damaged epithelium by local stem cells, that are contained within a niche in the crypts of Lieberkühn. Interestingly, in mammals, hundreds of lymphoid clusters, namely cryptopatches and containing ILC3s, dendritic cells (DCs) and stromal cells, locate adjacent to the intestinal crypts. We hypothesized that cryptopatches play an important role in intestinal regeneration by conveying damage-associated signals to epithelial stem cell regulation. We set out to elucidate whether interactions between innate immune cells in cryptopatches and intestinal stem cells are significant to enhance mucosal healing, with the ultimate goal of improving epithelial barrier function in pathological conditions, such as alimentary mucositis and inflammatory bowel disease.

INTRODUCTION

The intestinal immune cell system

The intestinal barrier is a multi-layered functional system essential for uptake of nutrients and water and for the prevention of microbial translocation[2,3]. Key physical components include a monolayer of epithelial cells linked by tight junctions and a layer of mucus, which efficiently segregate the commensal gut microbiota from our body. The epithelium is in constant exposure to food antigens and commensal bacteria. Underlying the epithelial barrier is the lamina propria (LP), which is formed mostly of connective tissue, and the muscularis mucosa that consists of a layer of smooth muscle cells whose main function is to enhance the transport of lumenenal contents along the gastrointestinal (GI) tract. Smooth muscle cells contract and relax generating peristaltic movements that are controlled by the self-contained enteric nervous system.

The intestines contain the largest accumulation of lymphoid tissues in the body in the form of lymphoid aggregates, including Peyer's Patches (PPs), colonic patches and solitary intestinal lymphoid tissues (SILTs), which include cryptopatches (CPs) and isolated lymphoid follicles (ILFs). In addition, scattered lymphocyte and myeloid populations are found in LP as well as interspersed between epithelial cells, and these contain cell types belonging to both the innate and the adaptive immune systems. Like SILTs, lymph nodes (LNs) receive antigens from the gut, providing another mechanism for containing microbes. In the case of LNs these antigens are transported via lymph vessels, often after engulfment by DCs. A dynamic balance between the immune system and the epithelium is vital to ensure the establishment of host protective immune responses while maintaining intestinal homeostasis and controlled immune responses against infections[4–6].

Innate lymphoid cells: general insights

Innate lymphoid cells (ILCs) are members of a recently identified branch of the innate immune system. ILCs develop normally in the absence of microbiota, although maturation, expansion and acquisition of some of their tissue-effector functions is influenced by the environment.

ILCs combine innate and adaptive modes of function and are involved in barrier immunity, tissue homeostasis and immune regulation within multiple organs, mucosal and non-mucosal. ILCs orchestrate early immune defenses, aided by their strategic positioning within epithelial-associated (lymphoid) tissues at barrier surfaces such as the lung, skin and gastrointestinal tract[7–10].

ILCs respond to alarmins and cytokine signals by enhancing their effector functions. ILCs are a prominent source of cytokines with profiles similar to those of T Helper (T_H) cells[9], yet ILCs lack antigen-specific receptors and their sequential production of cytokines precedes adaptive immune responses.

The family of ILCs can be subdivided in three main types based on their master transcription factor usage and cytokine profile: group1 ILCs, which are dependent on the T-box transcription factor T-bet and include NK cells and ILC1s; group 2 ILCs, that depend on GATA3 and, group 3 ILCs, that can further be classified in NKp46^{+} or CCR6^{+} ILC3 subtypes and require retinoic acid-related orphan receptor γt (RORγt) for their development. A recent study has also identified regulatory innate lymphoid cells, named ILCregs, which are distinct from other ILC subsets and regulatory T cells (Tregs).

Similar to adaptive lymphocytes, ILCs originate from common lymphoid progenitors (CLPs) in the fetal liver during embryonic development or in the bone marrow (BM) after birth (Figure 1)[11,12]. These progenitor cells possess precursor potential for T, B, NK cells and ILCs, as lymphoid-restricted gene programs (including expression of CD127, Rag1 and Rag2) are activated, whereas the myeloid program is strongly repressed. Like T and B lymphocytes, ILCs depend on γ_c cytokines in their generation from hematopoietic progenitors[13,14] but in contrary, ILCs require the transcriptional repressor inhibitor of DNA binding 2 (Id2). Some of the progenitors identified using mice report expression of Id2, PLZF (encoded by Zbtb16) and CXCR6 and are the earliest α-lymphoid progenitors (αLP or CXCR6^{+} integrin $\alpha_4\beta_7^{+}$-expressing CLPs), which further differentiate into the common helper ILC precursor ($\alpha_4\beta_7^{+}$ Id2^{hi} CHILP) and into the earliest precursor to the ILC lineages, the common ILC progenitor (ILCP)[12,15–20] (Figure 1). Of note, CHILP precursors have lost the potential to generate NK cells, and ILCP progenitors are able to generate ILC1, ILC2 and NKp46^{+} ILC3s but not CCR6^{+} ILC3s[15]. Id2^{+} PLZF^{-} progenitors expressing CXCR5, $\alpha_4\beta_7$ and CCR6 generate adult CCR6^{+} ILC3s[12,20]. The development of ILCregs depends on CHILPs but not ILCP progenitors and their diversification requires Id3 transcription factor (Figure 1)[21]. NK cell-restricted progenitors (NKP) have also been identified originating from CLPs, although their ability to generate other ILC subsets is not known[22–24]. The second stage of ILC differentiation involves the diversification of different ILC groups under the influence of a multitude of transcription factors including GATA3, TOX, TCF-1 and NFIL3 [12,25–31].

Each ILC subfamily is specialized in the production of a specific array of cytokines, closely mirroring T_H cell subsets[9,32].

ILC1s express T-bet, produce IFN-γ in response to IL-12, IL-15 and IL-18 and fight intracellular pathogen infections, thus representing the innate T helper 1 (T_H1) cells[15,33,34].

GATA-3^{hi} ILC2s secrete IL-5, IL-9, IL-13 and Areg in response to tissue-derived IL-25 and IL-33, as T_H2 cells, and contribute to immune responses against multicellular pathogens as well as the pathogenesis of type 2 inflammatory diseases including asthma and atopic dermatitis[35–38].

The Th17 equivalent is denoted ILC3s. These cells can produce IL-22, IL-17A and IL-17F and depend on RORγt for their development.

Finally, the most recent subset of ILCs discovered is the regulatory ILC subset (ILCregs). ILCregs are able to inhibit ILC1- and ILC3-, but not ILC2-effector functions, during innate

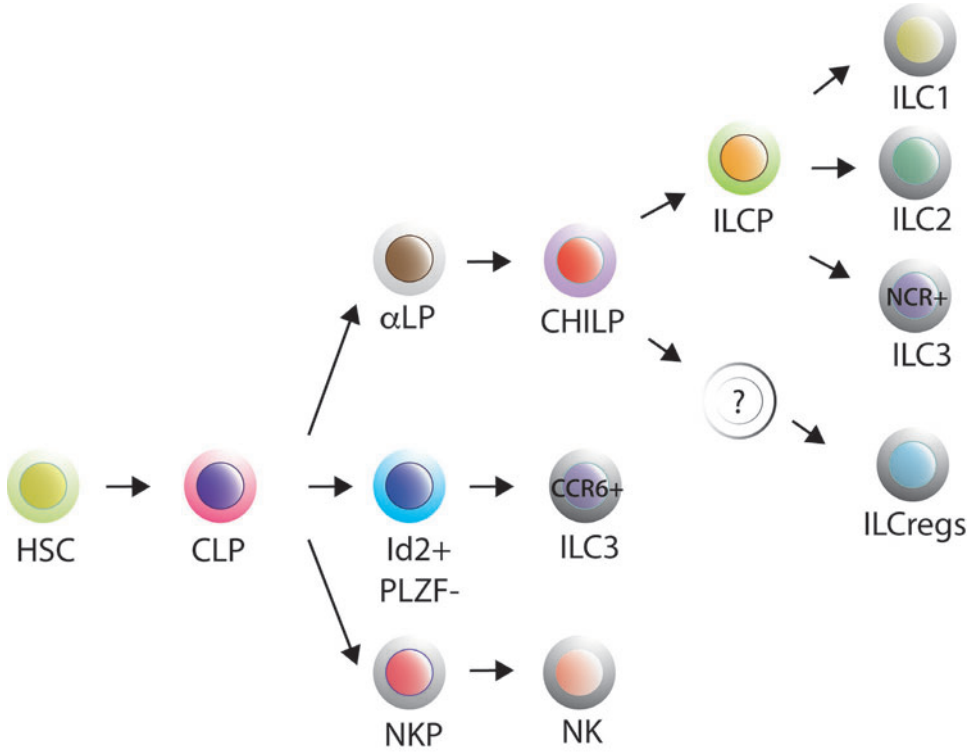

Figure 1: Development of innate lymphoid cells. Hematopoietic stem cells (HSC) give rise to common lymphoid progenitor cells (CLP). The earliest α-lymphoid progenitor (αLP) generates the common helper-like progenitor cells (CHILP), which further differentiates into a commited innate lymphoid cell progenitor (ILCP). ILC1, ILC2 and NCR+ ILC3 subtypes derive from ILCP. Alternatively, the development of regulatory ILCs (ILCregs) require CHILP progenitors but it is independent of the ILCP. In addition, the subset of ILC3s that express CCR6 derives from a lymphoid progenitor that has not expressed PLZF. Finally, cytotoxic innate lymphoid cells, NK cells are developed from NK cell progenitor cells, that are distinct from the other innate lymphoid precursors.

intestinal inflammation[19]. The ILCregs signature cytokine is IL-10 and interestingly, although ILCregs inhibit ILC3-derived IL-17/IFNγ, they do not impact IL-22 production by ILC3s[19].

Conventional NK cells are considered to represent the cytotoxic innate counterpart of $CD8^+$ T cells due to its developmentally dependence on T-bet and Eomes as well as their ability to secrete IFN-γ, granzyme and perforins[9]. In contrast to ILC1s, NK cells are localized in secondary lymphoid tissues.

Importantly, mature ILCs show substantial plasticity in peripheral tissues that is influenced by Notch ligands and cytokines[13,39–42]. It is well reported under inflammatory conditions that $NKp46^+$ ILC3s can produce IFNγ as they adopt an ILC1 phenotype by expressing T-bet and downregulating RORγt[43–49]. Also, $NKp46^+$ ILC3s can convert to $CCR6^+$ ILC3s[50–52]. Recently, plasticity has also been reported for human and mouse ILC2s towards an ILC1-like phenotype[53–56].

Deciphering transcriptional control of human ILC development remains rudimentary, although multipotent lymphoid-restricted progenitors, NK precursors, ILC3-restricted precursors and highly heterogeneous subsets of tissue-resident ILCs[61] have been characterized in humans[57–60]. Recently, a new study has identified human blood circulating and tissue-resident human ILC precursors, using humanized mice[21]. Hopefully, further analysis in humanized mice models will help in elucidating key regulatory pathways controlling human ILC development[62,63].

Single cell RNA sequencing as well as the study of chromatin landscapes has demonstrated its power in advancing our understanding of ILC developmental pathways and relationships between precursor populations[64]. These findings demonstrate why ILCs are much quicker in responding to stimulation compared to naïve T cells, as their epigenetic modifications that imprint their gene expression are established very early during development compared to T helper cells in which these are only observed after antigen-specific expansion. Another important discovery is the fact that ILC groups segregate depending on the tissue they are isolated from, which highlights the strong influence of the environment and microbial communities to control their specific gene expression profiles[56,65]. In line with this, human ILC3s from non-inflamed lymph nodes and spleen showed a more quiescent transcriptomic profile compared to their phenotypic counterparts in inflamed tonsils and blood, although these ILC3s express activating cytokine receptors and have acquired the ability to be recruited to immune responses by inflammatory cytokines (Bar-Ephraim, YE et al. Cell Reports. 2017 – in press).

One area that requires further investigation is ILC re-circulation and generation. It has been shown that ILCs are generated in the bone-marrow or fetal liver and then migrate to peripheral tissues due to the expression of homing receptors, such as $\alpha_4\beta_7$, CCR9, CCR6, CCR7 and CXCR6[66]. There is evidence, nonetheless, that intestinal CCR6$^+$ ILC3s migrate to the mesenteric lymph nodes (MLNs) using afferent lymphatics[67] and delete auto-reactive T cells[68]. It has also been demonstrated in parabiotic adult mice that ILCs are mainly tissue resident and maintained by self-renewal in various microenvironments, but hematogenous sources are required to partially replenish the ILC pool post-infection[69]. Therefore, it is still possible that committed ILC3 precursors can migrate from the bone-marrow (BM) to the periphery to fully mature locally in the tissue[13,16,70,71] . Similarly, human adult CD34$^+$ hematopoietic precursors have been described in adult tonsils expressing RORγt and an ILC3 transcriptional programe[72]. Recently, a concept of "ILC-poiesis" proposed a model in which human ILC precursors circulate throughout the organism via blood (similar to naïve T cells) and will be activated in tissues upon local inflammatory signals (such as cytokines, metabolites and other co-stimulatory molecules) that trigger their expansion and dictate their differentiation into mature tissue-resident ILC subsets[21]. However, the signals that orchestrate the recruitment of ILC progenitors to the tissues and their differentiation remain to be defined.

GROUP 3 INNATE LYMPHOID CELLS (ILC3S)

ILC3s as architects in lymphoid tissue development

The organogenesis of LNs and intestinal lymphoid aggregates, including PPs, CPs and ILFs depend on a subset of ILC3s which are RORγt-dependent and were first discovered in fetal lymph nodes and called lymphoid tissue inducer (LTi)[73–76] cells. Accordingly, mice lacking ILC3s, such as RORγt$^{-/-}$ mice, are devoid of these tissues[75,77].

Fetal LTi cells interact with endothelial and mesenchymal lymphoid tissue organizer populations to initiate and orchestrate lymph node and PP development in the small intestine during embryogenesis[73,76,78]. Post-birth, LTi cell counterparts also interact with mesenchymal stromal cells to form discrete ILC3 clusters termed cryptopatches[79,80]. PP are developmentally programmed tissues that originate around embryonic day E15.5 in mice[81] whereas SILTs form 1-2 weeks after birth[82,83]. In more detail, the primary events leading to PP formation require lymphoid tissue initiator (LTin) cells via RET-ARTN interactions. Subsequently, interactions between LTα1β2^{+} LTi cells and LTβR^{+} mesenchymal cells, termed lymphoid tissue organizer (LTo) cells lead to further growth of PP anlage[84–87]. In addition, Tumor necrosis factor-a (TNFα) and TNF receptor-I signaling pathways are engaged during PP development[88,89]. Also, PP are absent in mice with simultaneous defects in both CXCL13-CXCR5 and CCL19/21-CCR7 axes[90].

Cryptopatches predominantly contain adult LTi cells and DCs organized around stromal cell populations situated close to the bottom of intestinal crypt structures. Interestingly, cryptopatches develop independent of colonization, whereas their maturation into isolated lymphoid follicles requires bacterial presence. Cryptopatch development require IL-7-IL-7R and LT-LTBR signaling pathways[76,79,80]. Also, RANKL controls the density of CPs in the small intestine, but not in the colon. RANKL$^{-/-}$ mice have a fourfold reduction in the overall density of CPs in the small intestine and no B cells are present in CPs, thus ILF formation is completely abrogated. The recognition of peptidoglycans via NOD1 receptor expressed on epithelial cells drives the expression of CCL20 and β-defensin-3, both ligands of CCR6 expressed by LTi cells in CPs[82,91]. In turn, activation of stromal cells drives chemokine and cytokine release, including CCL20[74], which recruit B cells[92], which further grow into mature B cell follicles with the help of TNFα, produced by DCs and macrophages in response to bacterial compounds recognized by toll-like receptors (TLR)[91,93]. Mature ILFs generate IgA-producing B cells that target the microbiota, controlling the bacterial community during homeostasis[91,94,95]. RANKL is also essential for stromal cell-derived CXCL13, a B cell chemoattractant and is also linked to regulation of the expression of LT$\alpha_1\beta_2$ by LTi cells[96–98]. These organized structures provide the mammalian intestine with specialized locations at which immune activation can take place and immune responses can be efficiently mounted.

Although the function of cryptopatches in transitioning to ILFs is important for IgA-mediated protective functions of the intestinal mucosa, it is still incompletely understood

whether cryptopatches interact with intestinal epithelial cells during homeostasis or in response to damage.

ILC3s as orchestrators of epithelial barrier integrity

In general, adult ILC3s are defined by the expression of the IL-7 receptor (IL-7R), the surface protein CD90.2 or Thy1.2 and the tyrosine kinase receptor c-Kit or CD117[99]. ILC3s produce IL-17A, IL-17F and IL-22[44,100,101]. ILC3s are subdivided by the mutually exclusive expression of the chemokine receptor CCR6 and the NK-cell associated receptor NKp46. The adult $CCR6^+$ ILC3s phenotypically mirror fetal lymphoid tissue-inducer (LTi) cells and mainly cluster in SILTs[76]. $NKp46^+$ ILC3s are scattered through the lamina propria, together with ILC2s and ILC1s. Expression of MHCII by lymph node-resident $CCR6^+$ ILC3s has been identified in mice as well as HLA^+ ILC3s in humans, and these cells are able to regulate $CD4^+$ T cell responses to intestinal microflora[102].

ILC3s are amongst the first immune cells to seed the intestinal tissue before birth and are influenced by commensal microbiota-derived signals as well as diet-derived metabolites. In utero, LTi development is modulated via maternal retinoids[103]. Prior to colonization, aryl hydrocarbon receptor (AhR) ligands increase the number of $NKp46^+$ ILC3s, through transmitted maternal antibodies[104]. Later in life, AhR acts to sense aromatic hydrocarbons which are essential for the development of both populations of ILC3s as well as their effector function mediated by IL-22[16,39,47,105,106]. Vitamin A is critical for the appearance and expansion of intestinal ILC3s in adult mice[107,108]. In addition, gut ILC3s have been suggested to regulate circadian rhythms in the epithelium to control fat storage and other host metabolic homeostasis (unpublished data).

ILC3s play critical roles in controlling bacterial communities in the gut by interacting with the epithelial barrier through cytokines, as well as with adaptive immune cells. ILC3s can be activated by cytokines released by the intestinal epithelium or by antigen presenting cells, primarily IL-23 and IL-1β, which stimulate IL-22 production. IL-22 signals through IL-22R expressed on epithelial and stromal cells, activating downstream STAT3 signaling pathways involved in proliferation and activation. ILC3s are the major source of IL-22 in the intestine, and IL-22 is critical to regulate epithelial barrier responses, the balance of commensal bacterial species and to prevent translocation of bacteria to peripheral organs. On one hand, IL-22 stimulates the expression of antimicrobial peptides (including RegIII, S100a8 and S100a9) and the production of mucus-associated molecules by the intestinal epithelium[101,109]. This, in turn, serves to create a spatial segregation of commensal bacteria and enteric pathogens. ILC3-derived IL-22 also induces serum amyloid protein (SAA) production by the epithelium, which drives the recruitment of Th17 cells that play important roles in the homeostatic containment of commensal segmented filamentous bacteria (SFB)[110,111]. On the other hand, IL-22 produced by ILC3s drives fucosylation of epithelial cell-associated carbohydrate chains following colonization, which favors diversity of bacterial communities. Fucosylation

is critical against the outgrowth of the opportunistic pathogen *Enterococous faecalis* and protects from infections against *Salmonella spp* and *Citrobacter rodentium*[112–114].

ILC3s as defense against enteric pathogens

During infection, bacterial-sensing CX3CR1 macrophages upregulate their production of IL-23, which stimulates IL-22 production by ILC3s[115].

ILC3-derived IL-22 contributes to immunity in a diverse range of clinically-relevant infections in the gut, including *Clostridium difficile*[116], *Rotavirus*[117], *Candida albicans*[118], as well as intestinal worms[119]. Extensive research has demonstrated that ILC3s prevent morbidity in the early phase of *C. rodentium* infection prior to the generation of bacteria-specific T cell responses[45,47,120–122] via IL-22 production. The relative contribution of different subsets of ILC3s in the intestine is still controversial[123,124]. *Salmonella*, for example, has evolved to exploit the ILC3 responses to infection, and competes with the commensal microbiota for IL-22-dependent antimicrobial response to colonize the inflamed gut[125].

CCR6$^+$ ILC3s produce IL-17A in response to *Klebsiella pneumoniae* and *Candida albicans* infection and this IL-17A is critical for their clearance[126,127].

ILC3s as originators of pathological conditions

In contrast to their protective and homeostatic roles, ILC3s may also take on pro-inflammatory roles and contribute to tissue damage and inflammation during disease.

ILC3s drive pro-inflammatory cytokine production, such as IFNγ and GM-CSF, in an innate anti-CD40- or *Helicobacter hepaticus*- driven model of colitis, in an IL-23 dependent manner[128,129].

Pediatric Crohn's disease patients have reduced HLA-DR expression on intestinal ILC3s, which is inversely correlating with inflammatory colonic Th17 cells and the amount of circulating, commensal bacteria-specific IgG[68]. MHCII$^+$ ILC3s in lymph nodes limit intestinal inflammation via deletion of commensal bacterial-specific CD4$^+$ T cells from intestine and associated lymphoid tissues[68,102,130]. MHCII$^+$ ILC3s do not have co-stimulatory molecules CD80 and CD86, in line with an inhibitory role for ILC3-mediated antigen presentation[102,131]. However, under inflammatory conditions, co-stimulatory molecules, not only CD80 or CD86, but also OX40L and CD30L which aid T cell-dependent antibody responses, are upregulated and ILC3s can promote immune responses[132]. Targeting RORγt efficiently inhibits the pathological role in chronic intestinal inflammation of Th17 while preserves the function of ILC3s[127].

Crohn's disease patients have also confirmed the role of ILC3s in promoting chronic inflammation. These patients exhibit increased frequency of CCR6$^+$ ILC3s and have elevated levels of IL-17A[133].

Although not completely understood yet, there is evidence that patients with inflammatory bowel disease show aberrant ILC3 crosstalk with myeloid cells, defective ILC3 responses or aberrant B cell responses, even long before disease onset.

The formation of psoriatic lesions is driven by IL-23 and IL-17RA and it is dependent on RORγt. Similar to the intestinal mucosa, IL-23 and IL-1β induces IL-22 expression on ILC3s in the skin. Both γδ T cells and ILC3s are the dominant source of IL-17A, IL-17F and IL-22[134]. It is shown that inhibiting IL-23 or IL-17A ameliorates disease and that ILC3s are sufficient to induce skin pathology. In humans, psoriatic patients show an increase of ILC3s expressing NKp44 in the skin and blood[135].

ILC3s have also been linked to contribute to pathology in rheumatoid arthritis[136,137], ankylosing spondylitis[138], systemic sclerosis[139], experimental autoimmune encephalomyelitis[140], but further investigation is indispensable to completely comprehend the detrimental role of the referred ILC3 subsets. In parallel, ILC3s develop tertiary lymphoid organs, typically found in locations of chronic immune stimulation that can arise from microbial infection, chronic allograft rejection or autoimmune diseases[141]. Ultimately, ILC3s have also been implicated in the development of cancer, such as in the gut where a dysregulated antimicrobial response can ultimately lead to tumorigenesis[142].

ILC3s as integrators of environmental-derived signals

Microbiota-induced IL-1β production by intestinal macrophages activates ILC3s to secrete GM-CSF[143]. GM-CSF maintains $CD103^+$ intestinal DC subsets and further stimulates its capacity to produce retinoic acid (RA)[144]. In turn, GM-CSF modulates mononuclear phagocyte function to promote local Treg differentiation and reinforce tolerance[143]. In addition, it is suggested that blocking ILC3-derived production of GM-CSF and ILC3 mobilization from cryptopatches, may help reduce intestinal inflammation[128].

Conversely, epithelial-derived cytokines such as TSLP and IL-25 suppress IL-22 production by ILC3s[145,146], likely through myeloid cells.

ILC3s, in particular LTi cells have a well-documented role in interacting with mesenchymal stromal cells and endothelial cells to facilitate the formation of lymphoid organs. In addition, many of the cytokines expressed by different subsets of stromal cells are believed to play important roles in ILC homeostasis, although future research in this trajectory is in progress.

Similarly, a new emerging area is the study of ILC3-enteric nervous axis. It has been recently shown that glial cells in the intestine produce neurofactors that control the function of adult ILC3s.

Intestinal ILC3s are directly linked to epithelial stem cell function. ILC3-derived IL-22 is required for an effective DNA-damage response, thus decreasing cancer incidence and progression. IL-22 has also been shown to protect intestinal stem cells from alloreactive T cell-mediated killing in the context of GvHD. And in this thesis, we show that ILC3s contribute to intestinal stem cell reprogramming after chemotherapeutic-induced tissue damage, and also provide evidence that ILC3s contribute to the homeostasis of intestinal stem cell pool.

ILC3s and tissue regeneration

In addition to the well-defined roles of ILC-derived IL-22 during mucosal homeostasis and the early stages of enteric infections, recent studies highlighted novel functions of ILC3s in various tissues as enhancing epithelial cell regeneration.

The intestinal epithelial cell system

The small intestinal epithelial barrier is composed of a monolayer of epithelial cells that extends throughout the gut tube and is organized in finger-like projections towards the lumen called villi, and deep invaginations into the lamina propria known as crypts of Lieberkühn[147–150]. Epithelial barrier function is essential since the intestine is constantly exposed to bacteria, dietary antigens, mutagens and immunological cytokines and oxidative stress. Epithelial renewal requires constant proliferation of intestinal stem cells (ISCs) located within the crypts. One of the unique capabilities of ISCs is their potential to divide and repopulate the entire epithelium within 3-5 days[151], both under basal conditions and in response to injury. ISCs give rise to transit-amplifying (TA) progenitors which will differentiate into all specialized cell types of the intestinal epithelium, both absorptive and secretory cells[152–154].

Intestinal epithelial cells

Enterocytes are the most frequent intestinal epithelial cell type and their function is to absorb nutrients and water. Goblet cells secrete mucus-associated molecules that generate a mucus layer to keep microorganisms separated from the epithelium[155]; enteroendocrine cells produce hormones, which are essential to regulate digestion, appetite, gut motility and metabolism[156]; Tuft cells are chemosensory cells [157–159]; and Paneth cells the only terminally differentiated cell type that do not travel towards the villi but are found interspersed along crypt base columnar cells (CBCs) at the base of the crypt[160]. Paneth cells are also a source of Notch ligands and EGF, and support the growth of $Lgr5^+$ ISCs in in vitro cultures, thus being considered a pivotal component of the ISC niche[161]. In addition, they contain granules filled with bactericidal products that keep the crypt in a sterile environment, which is critical for host-defense.

Intestinal stem cells

The identification of intestinal stem cell populations has been subjected to substantial research. Currently, there is mounting evidence supporting the existence of a hierarchically organized stem cell compartment. Actively proliferating CBCs cells were the first genetically marked ISC population shown to give rise to all cell types in the intestinal epithelium through lineage tracing experiments. CBCs locate at the bottom of the crypts and are characterized by the expression of the Wnt pathway target gene leucine-rich repeat-containing G-protein coupled receptor 5 (Lgr5)[152]. However, specific ablation of $Lgr5^+$ ISCs

showed that they are dispensable for intestinal homeostasis, yet play an important role in response to DNA-damaging injury[162]. This suggested that additional epithelial cells are capable of compensating for CBC loss.

A second population of ISCs expresses the polycomb complex protein BMI-1. In contrast to CBCs, Bmi1$^+$ ISCs are indispensable for epithelial maintenance at steady-state[163]. They were termed "+4 cells" due to its position within the crypt[164] and label-retaining cells or quiescent due to their slow cycling properties[163,165–169]. Numerous reports have attributed similar characteristics to crypt cells expressing either Hopx[166,168,170], mTert[167,171], Krt19[172], Lrig[173] or Sox9-CreER[174]. However, these genes are broadly expressed by numerous cells in the crypt, making it difficult to address cell identity. These alternative ISC populations are resistant to DNA-damaging injury and generate progeny in response to such injury, therefore they have also been termed reserve ISCs[167–169,175]. Single-cell expression profiling confirmed overlapping identities of the majority of cells marked by Hopx-CreER and Bmi1-CreER. In addition, Bmi1-GFP$^+$ cells and Prox1$^+$ cells, as well as enteroendocrine lineage cells possess intestinal stem cell activity during homeostasis and injury-induced regeneration[176]. In parallel, another study has reported that Bmi1-GFP$^+$ cells and other secretory cells, including CD69$^+$ CD274$^+$ goblet cell precursors acquire an enhancer signature similar to Lgr5$^+$ stem cells in response to injury[177].

Clearly, the achievement of new technologies with better single-cell sensitivity has provided the resolution required to address the astonishing degree of heterogeneity in the stem cell compartment. Taken together these studies show that the normal intestine has enormous plasticity, and controversy exists regarding the mechanisms that control the regenerative process after ISC injury[178].

Signaling pathways controlling intestinal stem cell function

It is well stablished that a defined set of evolutionary conserved signaling pathways control the cycling properties and differentiation potential of intestinal stem cells, and perturbations of these pathways can substantially affect the ISC niche, leading to increased susceptibility to intestinal diseases. Therefore, a thorough understanding of these pathways, not only during homeostasis but also during regeneration after injury due to overt inflammation, nutritional deprivation or anti-cancer treatments, is essential to elucidate the molecular mechanisms of tissue dysfunction, including malignant transformation.

Wnt signaling

The Wnt/β-catenin pathway is critical for maintaining self-renewal and proliferation of ISCs. Gradients of Wnt ligands exist with high expression in crypts and lower expression towards the villi [179]. Multiple studies have demonstrated that the intestinal stem cells and intestinal crypt compartments are dependent on Wnt/β-catenin signaling pathway. By knocking-out secreted Wnt antagonists, such as *Tcf*, *Dkk1*, *Ctnmb1* and the Wnt target gene *c-Myc*[180–183]

proliferation was greatly affected, whereas dampening the function of Wnt agonists, like roof plate-specific spondin 1 (R-spondin1) or APC knock-outs drive hyperplasia in the intestine[184]. Recently, *Fzd7* has been linked to Wnt signaling through the Lgr5 receptor in ISCs in vivo[185]. Besides mitogenic activity, Wnt signaling pathways also control the differentiation of Paneth cells. At the same time, Paneth cells support stem cells by secreting canonical Wnt ligands[186]. Mesenchymal cells, that underlie the epithelium of the crypts, have also been reported to enhance Wnt signaling pathway in ISCs. Even though there is also redundancy when compared to Paneth cells, it is thought that non-epithelial Wnt signals could provide a secondary physiological source of Wnt[187].

BMP signaling

Mesenchymal cells express bone morphogenetic proteins (BMP), a member of transforming growth factor-β family, that upon binding to its specific epithelial receptors inhibits cell proliferation through Wnt/β-catenin suppression. Consequently, BMP levels are higher in the villi boundaries compared to the base of the crypt, inhibiting cell renewal and supporting epithelial differentiation towards the villi[188]. At the base of the crypt, mesenchymal-derived Noggin, a BMP inhibitor, enhances cell proliferation[189]. Noggin-1 and Noggin-2, as well as chordin-like 1 are also highly expressed in the submucosa region by the mesenchyme to suppress BMP signaling[188–190].

Notch signaling

Notch signaling targets the ISCs via cell-cell interactions. Inhibition of Notch signaling leads to a loss of the stem cell compartment, reduced proliferation and enhanced differentiation of epithelial progenitors towards the secretory cell lineage[191,192].

Hedgehog signaling

The Hedgehog (Hh) pathway functions as an indicator of the state of the epithelium. One of the main ligands in the small and large intestinal epithelium is Indian Hedgehogh (Ihh)[193] and signaling is exclusively paracrine to the mesenchyme or to intestinal myeloid cells. Inhibition of Ihh activates a regenerative response, characterized by an activation of mesenchymal immune responses and epithelial crypt proliferation[194,195].

EGF signaling

EGF signaling regulates cellular processes that include cell-cycle progression, survival and DNA repair after genotoxic stress. EGFRs are expressed in stem cells and ligands have been demonstrated in the underlying mesenchymal cells[196] and in Paneth cells[161]. EGF is currently used in organoid cultures as a stem cell growth factor and it activates proliferation and inhibits apoptosis of intestinal stem cells. Alterations in EGFR affects sensitivity to radiation and proliferation of intestinal stem cells, potentially contributing to tumor development[197].

Hippo-Yap signaling

Although Yap1 signaling is not required during normal intestinal homeostasis, its activity is essential for intestinal regeneration after injury. In the intestine, endogenous YAP1 protein expression is restricted to the stem cell niche at the bottom of the crypt, suggesting an association with ISC regulation. Several studies suggest that Yap1 regulates intestinal tissue regeneration by increasing ISC proliferation. IEC-specific conditional knockout of Yap1 leads to loss of crypts 2-5 days after DSS-induced colitis and decreased crypt proliferation after whole body irradiation[196]. Furthermore, Yap1 reprograms ISCs 2-4 days after ionizing radiation. On one hand, Yap1 induction leads to the expression of Notch ligands and receptors, which maintains proliferation of ISCs and TA cells, whereas it inhibits the generation of secretory and absorptive cell types[198]. On the other hand, Yap1 transiently suppresses Wnt signaling and activates EGFR pathway in the first few days of the regeneration phase. Later during regeneration, hyperproliferation is critical to regain the number of damaged epithelial cells and this is controlled by increasing Wnt signaling. In addition, there is evidence of non-canonical Wnt signaling directly activating Yap1[199].

Non-epithelial-intrinsic regulation of ISCs

As discussed in the previous paragraphs, there are intrinsic epithelial mechanisms that regulate proliferation and differentiation of the intestinal stem cells within the crypt unit. This notwithstanding, there is evidence that external interactions are also playing important roles in sensing and translating environmental signals to the intestinal stem cells located in the crypts and inducing epithelial responses, especially after injury. Of note, macromolecules of the extracellular matrix (ECM) form a peculiar scaffold with different physical and biochemical properties that are able to influence stem cell behavior, as it influences how cells sense the external forces and respond to the environment[200–202]. In addition, enteric neurons, intraepithelial lymphocytes, smooth muscle cells of the muscularis mucosa, lymph and vascular endothelial cells and a variety of mesenchymal cells, such as pericryptal myofibroblasts are also part of the ISC niche[203,204]. Recently, IL-22 from group 3 innate lymphoid cells (ILC3) was shown to act directly on intestinal stem cells after damage elicited by irradiation and protect from graft-versus-host- associated mortality[205,206].

ILC3s in intestinal epithelial regeneration

Allogenic hematopoietic stem cell transplantation (HSCT) is used to treat several hematological malignancies. One of the major side effects limiting successful stem cell transplantation is the occurrence of intestinal GvHD[207] mediated by alloreactive T cells that recognize recipient tissues as foreign and cause severe inflammatory disease.

Reasoning that factors important during wound healing might also be involved in limiting the extent of damage provoked by intestinal GvHD, experiments were initiated in experimental GvHD models to define a possible role for IL-22 in GvHD severity[205].

Bone marrow transfer (BMT) recipient mice that lacked IL-22 suffered from increased GvHD severity and significantly increased GvHD mortality. Instead, transplantation with IL22-deficient donor marrow did not have any impact on GvHD-associated organ pathology. These findings implied the post-transplant presence of a subset of cells essential for IL-22 production and limiting GVHD-induced intestinal damage. Using bone-marrow chimeras as secondary transplant recipients it became clear that recipient-derived hematopoietic cells were responsible for the production of protective IL-22. Detailed analysis revealed that IL-22 production was restricted to a radio-resistant population of NKp46$^-$ IL7Rα$^+$ CCR6$^+$ RORγt+ ILC3s that survives pre-transplant conditioning. IL-22 production by ILC3s was positively regulated by IL-23 derived from intestinal dendritic cells.

In order to unravel the mechanisms of GvHD induced tissue damage, expression of the IL-22R was analyzed by immunohistology and found to be present on epithelial stem and progenitor cells in the small intestinal crypts. Moreover, intestinal stem cells are a direct target cell of the GvHD and stem cell apoptosis is increased during GvHD. Interestingly, also host-derived ILCs appeared to be targeted by the GvHD as their numbers subsided during disease, concomitant with an increase in the number of apoptotic stem cells[205]. Combined these data suggest a role for ILC3-derived IL-22 in protecting epithelial stem cells from GvHD-induced cell death.

The fact that intestinal stem cells as well as their downstream progenitors express IL-22R[205,208,209] has led to the notion that IL-22 could act as an instructor of the epithelial cell function at the level of progenitor cell compartment. ILC3s, by virtue of their high radiation tolerance and IL-22 production, protect the ISC compartment from GvHD-induced cell death ensuring proper epithelial regeneration and barrier function (Figure 2).

ILC3s in thymic epithelial regeneration

ILC3s thus seem to have important functions in tissue regeneration that go well beyond their appreciated roles in organogenesis and innate immunity to infections. This notion is strengthened by the fact that a similar subset of radioresistant NKp46$^-$ IL7Rα$^+$ CCR6$^+$ RORγt$^+$ ILC3s is involved in regeneration of epithelial cells in the thymus after radiation damage[210].

After lethal total body irradiation (TBI) or targeted radiation to the thymus followed by syngeneic or allogenic hematopoietic stem cell transplantation (HSCT), IL22-deficient mice displayed reduced thymic cellularity when compared to wild-type (WT) control mice[210]. Conversely, absolute levels of IL-22 in the thymus were increased 2 to 3-fold in experimental models of sublethal-TBI without HSCT, lethal TBI and syngeneic HSCT, and T cell-depleted allogeneic HSCT, when compared to non-irradiated WT mice. Particularly, the peak of intrathymic IL-22 was inversely correlated with the thymic cellularity[210].

Importantly, IL-22 signaling through IL-22Rα enhances viability of cortical-TECs and immature mTECs in vitro. Likewise, administration of recombinant IL-22 to mice given SL-TBI led to an enhancement of thymopoiesis. Thus, the thymic ILC3s are not responsible for

IL-22 production under steady-state conditions but are an essential radio-resistant source of IL-22 required for thymic regeneration after damage[210] (Figure 2).

The mechanisms that regulated ILC-derived IL-22 also showed overlap with those found in the intestine. Intrathymic IL-23 was detected in-vivo and was associated with an increase in IL-23 producing $CD103^+$ thymic DCs, suggesting that up-regulation of IL-23 by radio-resistant thymic DCs induces IL-22 production by ILC3s. However, further studies are needed to elucidate the requirements for DC and ILC activation for thymic regeneration.

ILC3s in skin regeneration

The skin also forms a highly organized physical and immunological barrier against the external environment and the microbiota. It is well established that a correct recruitment of immune cells locally is essential for conventional skin repair.

The contribution of ILC3s in normal physiology of skin repair have only been recently assessed. In an elegant study, ILC3s were shown to favor wound healing by enhancing the recruitment of myeloid cells and promoting re-epithelization of the injured epidermis.

During wound repair, epidermal Notch1 signaling is indispensable for wound closure and innate immune cell recruitment. Notch1 downstream effectors, in particular TNFα, mediated the recruitment of ILC3s into wounded areas of the skin. ILC3 were required to control epidermal proliferation and macrophage entry by producing IL-17F and CCL3[211].

Altogether, Notch1 serve as an injury signal that activates ILC3s to orchestrate the organization of the skin epithelium to undergo skin repair.

Concluding remarks

ILC3s were initially identified as inducers of lymphoid tissues during fetal development and subsequently appreciated for their role in mucosal immunity in the early stages after enteric infections. However, recent studies unveiled a novel role for ILC3s as mediators of epithelial tissue regeneration after radiation damage in the intestines and thymus. It is tempting to speculate with these findings that we are getting closer to understanding the possible original function of ILC3s as regulators of tissue-specific precursor cells long before the emergence of adaptive immunity and secondary lymphoid tissues. There are clear parallels between regeneration and tissue organogenesis as in both cases ILCs function by activating the local microenvironment of either epithelial cells in the thymus and intestines or of mesenchymal and endothelial cells in lymph node anlagen.

Another intriguing observation is the central function of DCs as activators of ILC3s in thymus and intestines after damage, but also at basal conditions. This suggests that the well-known system of T cell activation and functional differentiation by DCs might have been modelled to a more ancient system in which DCs sensing tissue damage activate ILCs and induce the production of cytokines important for homeostasis and tissue repair.

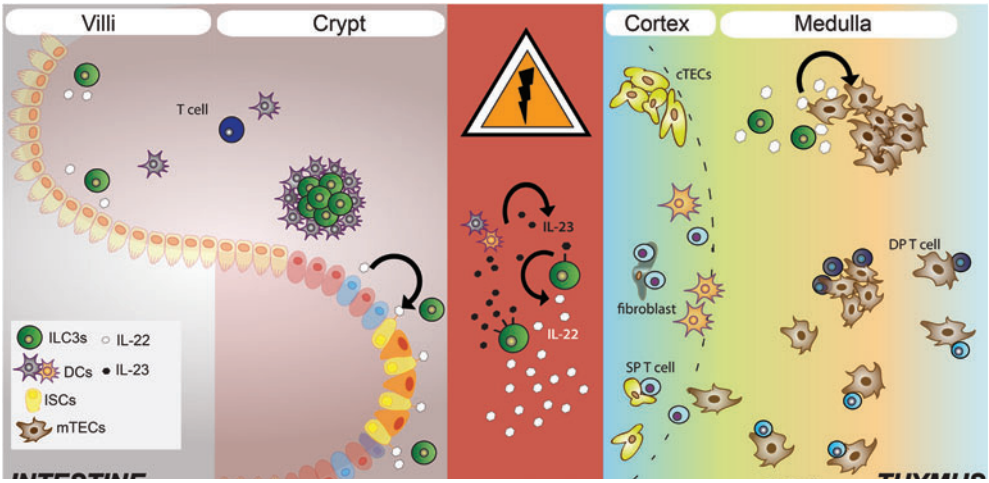

Figure 2: RORγt+ ILCs enhance tissue regeneration after radiation damage in mice. Radio resistant NCR$^-$RORγt$^+$ ILCs are activated by DC-derived IL-23 after radiation induced tissue damage in the intestines or thymus. As a result RORγt$^+$ ILCs secrete IL-22 that is essential for regeneration of thymic epithelium and for preventing crypt cell apoptosis during intestinal GvHD.

AIMS AND OUTLINE OF THE THESIS

It is firmly established that Innate lymphoid cells (ILCs) are key components of the innate immune system and play important roles at mucosal surfaces. In the intestine, a subset of ILCs, Group 3 ILCs (ILC3s) control epithelial homeostasis, protect the host against extracellular pathogens and contribute to the containment of commensals. ILC3s exert anti-infectious functions in the intestinal epithelium and contribute to bacterial clearance by producing IL-22. However, ILC3 contribution to epithelial function and regeneration after damage, in the absence of infection, has not been extensively assessed. We believe that deciphering the mechanisms by which ILC3s enhance mucosal healing will have important future therapeutic implications in intestinal disorders characterized by excessive inflammation fueled by the loss of epithelial barrier function.

The **overall aim of this thesis** is to explore the importance of ILC3s during intestinal epithelial regeneration through control of intestinal stem cell function, and the mechanisms through which this is achieved.

Chapter 1 provides an overview of current knowledge on ILC development and function and on intestinal epithelial cell homeostasis.

In **chapter 2** we used a model of Methotrexate-induced tissue damage that specifically targets intestinal stem cells of the small intestine to assess whether the immune system was required to modulate epithelial regeneration. We demonstrated that ILC3s are essential for epithelial activation, intestinal stem cell maintenance, as well as for crypt regeneration after MTX-induced intestinal damage. In addition, we identify IL-22 as an important mediator of stem cell maintenance post-damage.

In **chapter 3** we further examine the function of IL-22 in epithelial responses to tissue damage. We show that IL-22 is dispensable for crypt regeneration preventing pathology. In contrast, we show that activation of Yap1 signaling in $Lgr5^{+}$ ISCs is critically dependent on the presence of ILC3s and require activation through IL-6/IL-11-Gp130-Src axis.

While ILC3s directly regulate the function of intestinal stem cells during damage responses, their contribution to maintaining normal epithelial homeostasis is completely unknown. **Chapter 4** explores the contribution of ILC3s and IL-22 to intestinal epithelium homeostasis. In the absence of ILC3s, alterations are induced in the intestinal stem cell pool, which resembled responses occurring during epithelial damage. This chapter proposes a model that supports a direct link between ILC3s in cryptopatches and the maintenance of active versus reserve intestinal stem cells at steady-state.

In **chapter 5** we interrogated the role of myeloid cells in activating ILC3-mediated intestinal regeneration after MTX. We identified the phenotype and transcriptional profile of cryptopatch dendritic cells and established the importance of mononuclear phagocytes for epithelial regeneration after MTX-induced damage.

Finally, a general discussion of the thesis is presented in **chapter 6** where findings of this thesis are explained in the context of intestinal immunology and epithelial biology. Ultimately, we present an outlook with future experiments that expand our findings.

REFERENCES

1. Hanash, A. M. *et al.* Interleukin-22 protects intestinal stem cells from immune- mediated tissue damage and regulates sensitivity to graft vs. host disease. *Immunity* **37,** 339–350 (2012).
2. Keita, A. & Söderholm, J. D. The intestinal barrier and its regulation by neuroimmune factors. *Neurogastroenterology and Motility* **22,** 718–733 (2010).
3. Lopetuso, L. R., Scaldaferri, F., Bruno, G., Petito, V., Franceschi, F. & Gasbarrini, A. The therapeutic management of gut barrier leaking: The emerging role for mucosal barrier protectors. *European Review for Medical and Pharmacological Sciences* **19,** 1068–1076 (2015).
4. Messina, V. *et al.* Gut Mesenchymal Stromal Cells in Immunity. *Stem Cells Int.* **2017,** (2017).
5. Kayama, H. & Takeda, K. Functions of innate immune cells and commensal bacteria in gut homeostasis. *J. Biochem.* **159,** 141–149 (2015).
6. Strobel, S. & Mowat, A. M. Immune responses to dietary antigens: Oral tolerance. *Immunology Today* **19,** 173–181 (1998).
7. Klose, C. S. N. & Artis, D. Innate lymphoid cells as regulators of immunity, inflammation and tissue homeostasis. *Nat. Immunol.* **17,** 765–774 (2016).
8. Walker, J. a, Barlow, J. L. & McKenzie, A. N. J. Innate lymphoid cells--how did we miss them? *Nat. Rev. Immunol.* **13,** 75–87 (2013).
9. Spits, H. *et al.* Innate lymphoid cells--a proposal for uniform nomenclature. *Nat. Rev. Immunol.* **13,** 145–9 (2013).
10. Diefenbach, A., Colonna, M. & Koyasu, S. Development, differentiation, and diversity of innate lymphoid cells. *Immunity* **41,** 354–365 (2014).
11. Serafini, N., Vosshenrich, C. A. J. & Di Santo, J. P. Transcriptional regulation of innate lymphoid cell fate. *Nat. Rev. Immunol.* **15,** 415–428 (2015).
12. Ishizuka, I. E., Chea, S., Gudjonson, H., Constantinides, M. G., Dinner, A. R., Bendelac, A. & Golub, R. Single-cell analysis defines the divergence between the innate lymphoid cell lineage and lymphoid tissue–inducer cell lineage. *Nat. Immunol.* **17,** 269–276 (2016).
13. Cherrier, M., Sawa, S. & Eberl, G. Notch, Id2, and RORγt sequentially orchestrate the fetal development of lymphoid tissue inducer cells. *J. Exp. Med.* **209,** 729–740 (2012).
14. Satoh-Takayama, N., Lesjean-Pottier, S., Vieira, P., Sawa, S., Eberl, G., Vosshenrich, C. A. J. & Di Santo, J. P. IL-7 and IL-15 independently program the differentiation of intestinal CD3 $^{-}$ NKp46 $^{+}$ cell subsets from Id2-dependent precursors. *J. Exp. Med.* **207,** 273–280 (2010).
15. Klose, C. S. N. *et al.* Differentiation of type 1 ILCs from a common progenitor to all helper-like innate lymphoid cell lineages. *Cell* **157,** 340–356 (2014).
16. Possot, C., Schmutz, S., Chea, S., Boucontet, L., Louise, A., Cumano, A. & Golub, R. Notch signaling is necessary for adult, but not fetal, development of RORγt+ innate lymphoid cells. *Nat. Immunol.* **12,** 949–958 (2011).
17. Constantinides, M. G., McDonald, B. D., Verhoef, P. A. & Bendelac, A. A committed precursor to innate lymphoid cells. *Nature* **508,** 397–401 (2014).
18. Yu, X., Wang, Y., Deng, M., Li, Y., Ruhn, K. A., Zhang, C. C. & Hooper, L. V. The basic leucine zipper transcription factor NFIL3 directs the development of a common innate lymphoid cell precursor. *Elife* **3,** (2014).
19. Wang, S. *et al.* Regulatory Innate Lymphoid Cells Control Innate Intestinal Inflammation. *Cell* (2017).
20. Chea, S. *et al.* Single-Cell Gene Expression Analyses Reveal Heterogeneous Responsiveness of Fetal Innate Lymphoid Progenitors to Notch Signaling. *Cell Rep.* **14,** 1500–1516 (2016).

21. Lim, A. I. *et al.* Systemic Human ILC Precursors Provide a Substrate for Tissue ILC Differentiation. *Cell* **168,** 1086–1100.e10 (2017).
22. Rosmaraki, E. E., Douagi, I., Roth, C., Colucci, F., Cumano, A. & Di Santo, J. P. Identification of committed NK cell progenitors in adult murine bone marrow. *Eur. J. Immunol.* **31,** 1900–1909 (2001).
23. Carotta, S., Pang, S. H. M., Nutt, S. L. & Belz, G. T. Identification of the earliest NK-cell precursor in the mouse BM. *Blood* **117,** 5449–5452 (2011).
24. Fathman, J. W., Bhattacharya, D., Inlay, M. A., Seita, J., Karsunky, H. & Weissman, I. L. Identification of the earliest natural killer cell-committed progenitor in murine bone marrow. *Blood* **118,** 5439–5447 (2011).
25. Serafini, N., Klein Wolterink, R. G. J., Satoh-Takayama, N., Xu, W., Vosshenrich, C. A. J., Hendriks, R. W. & Di Santo, J. P. Gata3 drives development of RORgammat+ group 3 innate lymphoid cells. *J. Exp. Med.* **211,** 199–208 (2014).
26. Yagi, R. *et al.* The transcription factor GATA3 is critical for the development of all IL-7Ralpha-expressing innate lymphoid cells. *Immunity* **40,** 378–388 (2014).
27. Mielke, L. A., Groom, J. R., Rankin, L. C., Seillet, C., Masson, F., Putoczki, T. & Belz, G. T. TCF-1 Controls ILC2 and NKp46+ROR t+ Innate Lymphocyte Differentiation and Protection in Intestinal Inflammation. *J. Immunol.* **191,** 4383–4391 (2013).
28. Seillet, C., Rankin, L. C., Groom, J. R., Mielke, L. A., Tellier, J., Chopin, M., Huntington, N. D., Belz, G. T. & Carotta, S. Nfil3 is required for the development of all innate lymphoid cell subsets. *J. Exp. Med.* **211,** 1733–1740 (2014).
29. Hoyler, T., Klose, C. S. N., Souabni, A., Turqueti-Neves, A., Pfeifer, D., Rawlins, E. L., Voehringer, D., Busslinger, M. & Diefenbach, A. The Transcription Factor GATA-3 Controls Cell Fate and Maintenance of Type 2 Innate Lymphoid Cells. *Immunity* **37,** 634–648 (2012).
30. Yang, Q. *et al.* T cell factor 1 is required for group 2 innate lymphoid cell generation. *Immunity* **38,** 694–704 (2013).
31. Zook, E. C. & Kee, B. L. Development of innate lymphoid cells. *Nat. Immunol.* **17,** 775–782 (2016).
32. Artis, D. & Spits, H. The biology of innate lymphoid cells. *Nature* **517,** 293–301 (2015).
33. Constantinides, M. G., Gudjonson, H., McDonald, B. D., Ishizuka, I. E., Verhoef, P. A., Dinner, A. R. & Bendelac, A. PLZF expression maps the early stages of ILC1 lineage development. *Proc Natl Acad Sci U S A* **112,** 5123–5128 (2015).
34. Fuchs, A., Vermi, W., Lee, J. S., Lonardi, S., Gilfillan, S., Newberry, R. D., Cella, M. & Colonna, M. Intraepithelial type 1 innate lymphoid cells are a unique subset of il-12- and il-15-responsive IFNg-producing cells. *Immunity* **38,** 769–781 (2013).
35. Mjösberg, J. *et al.* The Transcription Factor GATA3 Is Essential for the Function of Human Type 2 Innate Lymphoid Cells. *Immunity* **37,** 649–659 (2012).
36. Moro, K. *et al.* Innate production of TH2 cytokines by adipose tissue-associated c-Kit+Sca-1+ lymphoid cells. *Nature* **463,** 540–544 (2010).
37. Neill, D. R. *et al.* Nuocytes represent a new innate effector leukocyte that mediates type-2 immunity. *Nature* **464,** 1367–1370 (2010).
38. Monticelli, L. A. *et al.* Innate lymphoid cells promote lung-tissue homeostasis after infection with influenza virus. *Nat. Immunol.* **12,** 1045–1054 (2011).
39. Lee, J. S. *et al.* AHR drives the development of gut ILC22 cells and postnatal lymphoid tissues via pathways dependent on and independent of Notch. *Nat. Immunol.* **13,** 144–151 (2011).
40. Yang, Q. *et al.* TCF-1 upregulation identifies early innate lymphoid progenitors in the bone marrow. *Nat. Immunol.* **16,** 1044–1050 (2015).

41. Califano, D., Cho, J. J., Uddin, M. N., Lorentsen, K. J., Yang, Q., Bhandoola, A., Li, H. & Avram, D. Transcription Factor Bcl11b Controls Identity and Function of Mature Type 2 Innate Lymphoid Cells. *Immunity* **43,** 354–368 (2015).

42. Yu, Y. *et al.* The transcription factor Bcl11b is specifically expressed in group 2 innate lymphoid cells and is essential for their development. *J. Exp. Med.* **212,** 865–874 (2015).

43. Ishizuka, I. E., Constantinides, M. G., Gudjonson, H. & Bendelac, A. The Innate Lymphoid Cell Precursor. *Annu. Rev. Immunol.* **34,** 299–316 (2016).

44. Klose, C. S. N. *et al.* A T-bet gradient controls the fate and function of CCR6−RORγt+ innate lymphoid cells. *Nature* **494,** 261–265 (2013).

45. Cella, M., Fuchs, A., Vermi, W., Facchetti, F., Otero, K., Lennerz, J. K. M., Doherty, J. M., Mills, J. C. & Colonna, M. A human natural killer cell subset provides an innate source of IL-22 for mucosal immunity. *Nature* **457,** 722–725 (2008).

46. Rankin, L., Groom, J., Mielke, L. A., Seillet, C. & Belz, G. T. Diversity, function, and transcriptional regulation of gut innate lymphocytes. *Frontiers in Immunology* **4,** (2013).

47. Satoh-Takayama, N. *et al.* Microbial Flora Drives Interleukin 22 Production in Intestinal NKp46+ Cells that Provide Innate Mucosal Immune Defense. *Immunity* **29,** 958–970 (2008).

48. Vonarbourg, C. *et al.* Regulated expression of nuclear receptor RORγt confers distinct functional fates to NK cell receptor-expressing RORγt+ innate lymphocytes. *Immunity.* **33,** 736–751 (2010).

49. Bernink, J. H. *et al.* Human type 1 innate lymphoid cells accumulate in inflamed mucosal tissues. *Nat. Immunol.* **14,** 221–229 (2013).

50. Verrier, T., Satoh-Takayama, N., Serafini, N., Marie, S., Di Santo, J. P. & Vosshenrich, C. A. J. Phenotypic and Functional Plasticity of Murine Intestinal NKp46+ Group 3 Innate Lymphoid Cells. *J. Immunol.* **196,** 4731–8 (2016).

51. Viant, C. *et al.* Transforming growth factor- and Notch ligands act as opposing environmental cues in regulating the plasticity of type 3 innate lymphoid cells. *Sci. Signal.* **9,** ra46-ra46 (2016).

52. Cortez, V. S. *et al.* Transforming Growth Factor-β Signaling Guides the Differentiation of Innate Lymphoid Cells in Salivary Glands. *Immunity* **44,** 1127–1139 (2016).

53. Bal, S. M. *et al.* IL-1β, IL-4 and IL-12 control the fate of group 2 innate lymphoid cells in human airway inflammation in the lungs. *Nat. Immunol.* **17,** 636–645 (2016).

54. Silver, J. S. *et al.* Inflammatory triggers associated with exacerbations of COPD orchestrate plasticity of group 2 innate lymphoid cells in the lungs. *Nat. Immunol.* **17,** 626–635 (2016).

55. Ohne, Y., Silver, J. S., Thompson-Snipes, L., Collet, M. A., Blanck, J. P., Cantarel, B. L., Copenhaver, A. M., Humbles, A. A. & Liu, Y.-J. IL-1 is a critical regulator of group 2 innate lymphoid cell function and plasticity. *Nat. Immunol.* **17,** 646–655 (2016).

56. Shih, H. Y. *et al.* Developmental Acquisition of Regulomes Underlies Innate Lymphoid Cell Functionality. *Cell* **165,** 1120–1133 (2016).

57. Kohn, L. A., Hao, Q.-L., Sasidharan, R., Parekh, C., Ge, S., Zhu, Y., Mikkola, H. K. A. & Crooks, G. M. Lymphoid priming in human bone marrow begins before expression of CD10 with upregulation of L-selectin. *Nat. Immunol.* **13,** 963–971 (2012).

58. Renoux, V. M., Zriwil, A., Peitzsch, C., Michaëlsson, J., Friberg, D., Soneji, S. & Sitnicka, E. Identification of a Human Natural Killer Cell Lineage-Restricted Progenitor in Fetal and Adult Tissues. *Immunity* **43,** 394–407 (2015).

59. Montaldo, E. & Romagnani, C. Human rorgt+CD34+ cells are lineage-specified progenitors of group 3 rorgt+ innate lymphoid cells. *Immunity* **41,** 988–1000 (2014).

60. Kyoizumi, S., Kubo, Y., Kajimura, J., Yoshida, K. & Hayashi, T. Fate Decision Between Group 3 Innate Lymphoid and Conventional NK Cell Lineages by Notch Signaling in Human Circulating Hematopoietic Progenitors. (2017).

61. Björklund, Å. K., Forkel, M., Picelli, S., Konya, V., Theorell, J., Friberg, D., Sandberg, R. & Mjösberg, J. The heterogeneity of human CD127(+) innate lymphoid cells revealed by single-cell RNA sequencing. *Nat. Immunol.* **17,** 451–60 (2016).
62. ter Horst, R. *et al.* Host and Environmental Factors Influencing Individual Human Cytokine Responses. *Cell* **167,** 1111–1124.e13 (2016).
63. Duffy, D. *et al.* Functional analysis via standardized whole-blood stimulation systems defines the boundaries of a healthy immune response to complex stimuli. *Immunity* **40,** 436–450 (2014).
64. Yu, Y. *et al.* Single-cell RNA-seq identifies a PD-1hi ILC progenitor and defines its development pathway. *Nature* **539,** 102–106 (2016).
65. Gury-BenAri, M. *et al.* The Spectrum and Regulatory Landscape of Intestinal Innate Lymphoid Cells Are Shaped by the Microbiome. *Cell* **166,** 1231–1246.e13 (2016).
66. Zlotoff, D. A., Sambandam, A., Logan, T. D., Bell, J. J., Schwarz, B. A. & Bhandoola, A. CCR7 and CCR9 together recruit hematopoietic progenitors to the adult thymus. *Blood* **115,** 1897–1905 (2010).
67. Mackley, E. C. *et al.* CCR7-dependent trafficking of RORγ+ ILCs creates a unique microenvironment within mucosal draining lymph nodes. *Nat. Commun.* **6,** 5862 (2015).
68. Hepworth, M. R. *et al.* Group 3 innate lymphoid cells mediate intestinal selection of commensal bacteria-specific CD4+ T cells. *Science (80-.).* **348,** 1031–1035 (2015).
69. Gasteiger, G., Fan, X., Dikiy, S., Lee, S. Y. & Rudensky, A. Y. Tissue residency of innate lymphoid cells in lymphoid and nonlymphoid organs. *Science (80-.).* **350,** 981–985 (2015).
70. Montaldo, E. *et al.* Human RORgammat(+)CD34(+) cells are lineage-specified progenitors of group 3 RORgammat(+) innate lymphoid cells. *Immunity* **41,** 988–1000 (2014).
71. Sawa, S., Cherrier, M., Lochner, M., Satoh-Takayama, N., Fehling, H. J., Langa, F., Di Santo, J. P. & Eberl, G. Lineage Relationship Analysis of ROR t+ Innate Lymphoid Cells. *Science (80-.).* **330,** 665–9 (2010).
72. Scoville, S. D. *et al.* A Progenitor Cell Expressing Transcription Factor RORγt Generates All Human Innate Lymphoid Cell Subsets. *Immunity* **44,** 1140–1150 (2016).
73. Eberl, G., Marmon, S., Sunshine, M.-J., Rennert, P. D., Choi, Y. & Littman, D. R. An essential function for the nuclear receptor RORgamma(t) in the generation of fetal lymphoid tissue inducer cells. *Nat. Immunol.* **5,** 64–73 (2004).
74. Tsuji, M., Suzuki, K., Kitamura, H., Maruya, M., Kinoshita, K., Ivanov, I. I., Itoh, K., Littman, D. R. & Fagarasan, S. Requirement for Lymphoid Tissue-Inducer Cells in Isolated Follicle Formation and T Cell-Independent Immunoglobulin A Generation in the Gut. *Immunity* **29,** 261–271 (2008).
75. Sun, Z. Requirement for RORgamma in Thymocyte Survival and Lymphoid Organ Development. *Science (80-.).* **288,** 2369–2373 (2000).
76. Mebius, R. E., Rennert, P. & Weissman, I. L. Developing lymph nodes collect CD4+CD3- LTbeta+ cells that can differentiate to APC, NK cells, and follicular cells but not T or B cells. *Immunity* **7,** 493–504 (1997).
77. Yokota, Y., Mansouri, A., Mori, S., Sugawara, S., Adachi, S., Nishikawa, S.-I. & Gruss, P. Development of peripheral lymphoid organs and natural killer cells depends on the helix-loop-helix inhibitor Id2. *Nature* **397,** 702–706 (1999).
78. Onder, L., Danuser, R., Scandella, E., Firner, S., Chai, Q., Hehlgans, T., Stein, J. V. & Ludewig, B. Endothelial cell–specific lymphotoxin-β receptor signaling is critical for lymph node and high endothelial venule formation. *J. Exp. Med.* **210,** 465–473 (2013).
79. van de Pavert, S. A. & Mebius, R. E. New insights into the development of lymphoid tissues. *Nat. Rev. Immunol.* **10,** 664–674 (2010).
80. Eberl, G. Inducible lymphoid tissues in the adult gut: recapitulation of a fetal developmental pathway? *Nat. Rev. Immunol.* **5,** 413–20 (2005).

81. Adachi, S., Yoshida, H., Kataoka, H. & Nishikawa, S. I. Three distinctive steps in Peyer's patch formation of murine embryo. *Int. Immunol.* **9,** 507–514 (1997).

82. Hamada, H. *et al.* Identification of Multiple Isolated Lymphoid Follicles on the Antimesenteric Wall of the Mouse Small Intestine. *J. Immunol.* **168,** 57–64 (2002).

83. Kanamori, Y., Ishimaru, K., Nanno, M., Maki, K., Ikuta, K., Nariuchi, H. & Ishikawa, H. Identification of novel lymphoid tissues in murine intestinal mucosa where clusters of c-kit+ IL-7R+ Thy1+ lympho-hemopoietic progenitors develop. *J. Exp. Med.* **184,** 1449–1459 (1996).

84. Cao, X. *et al.* Defective lymphoid development in mice lacking expression of the common cytokine receptor γ chain. *Immunity* **2,** 223–238 (1995).

85. Park, S. Y. *et al.* Developmental defects of lymphoid cells in Jak3 kinase-deficient mice. *Immunity* **3,** 771–782 (1995).

86. Miyawaki, S., Nakamura, Y., Suzuka, H., Koba, M., Shibata, Y., Yasumizu, R. & Ikehara, S. A new mutation, aly, that induces a generalized lack of lymph nodes accompanied by immunodeficiency in mice. *Eur. J. Immunol.* **24,** 429–434 (1994).

87. Rennert, P. D., James, D., Mackay, F., Browning, J. L. & Hochman, P. S. Lymph node genesis is induced by signaling through the lymphotoxin beta receptor. *Immunity* **9,** 71–79 (1998).

88. Neumann, B., Luz, A., Pfeffer, K. & Holzmann, B. Defective Peyer's patch organogenesis in mice lacking the 55-kD receptor for tumor necrosis factor. *J. Exp. Med.* **184,** 259–64 (1996).

89. Körner, H., Cook, M., Riminton, D. S., Lemckert, F. a, Hoek, R. M., Ledermann, B., Köntgen, F., Fazekas de St Groth, B. & Sedgwick, J. D. Distinct roles for lymphotoxin-alpha and tumor necrosis factor in organogenesis and spatial organization of lymphoid tissue. *Eur. J. Immunol.* **27,** 2600–2609 (1997).

90. Patel, A. *et al.* Differential RET Signaling Pathways Drive Development of the Enteric Lymphoid and Nervous Systems. *Sci. Signal.* **5,** ra55-ra55 (2012).

91. Bouskra, D., Brézillon, C., Bérard, M., Werts, C., Varona, R., Boneca, I. G. & Eberl, G. Lymphoid tissue genesis induced by commensals through NOD1 regulates intestinal homeostasis. *Nature* **456,** 507–510 (2008).

92. McDonald, K. G., McDonough, J. S., Wang, C., Kucharzik, T., Williams, I. R. & Newberry, R. D. CC chemokine receptor 6 expression by B lymphocytes is essential for the development of isolated lymphoid follicles. *Am. J. Pathol.* **170,** 1229–1240 (2007).

93. Lorenz, R. G., Chaplin, D. D., McDonald, K. G., McDonough, J. S. & Newberry, R. D. Isolated lymphoid follicle formation is inducible and dependent upon lymphotoxin-sufficient B lymphocytes, lymphotoxin beta receptor, and TNF receptor I function. *J. Immunol. (Baltimore, Md 1950)* **170,** 5475–5482 (2003).

94. Fagarasan, S., Muramatsu, M., Suzuki, K., Nagaoka, H., Hiai, H. & Honjo, T. Critical roles of activation-induced cytidine deaminase in the homeostasis of gut flora. *Science* **298,** 1424–1427 (2002).

95. Macpherson, A. J. Induction of Protective IgA by Intestinal Dendritic Cells Carrying Commensal Bacteria. *Science (80-.).* **303,** 1662–1665 (2004).

96. Knoop, K. A., Butler, B. R., Kumar, N., Newberry, R. D. & Williams, I. R. Distinct developmental requirements for isolated lymphoid follicle formation in the small and large intestine: RANKL is essential only in the small intestine. *Am. J. Pathol.* **179,** 1861–1871 (2011).

97. Buettner, M. & Lochner, M. Development and function of secondary and tertiary lymphoid organs in the small intestine and the colon. *Frontiers in Immunology* **7,** (2016).

98. Yoshida, H., Naito, A., Inoue, J. I., Satoh, M., Santee-Cooper, S. M., Ware, C. F., Togawa, A., Nishikawa, S. & Nishikawa, S. I. Different cytokines induce surface lymphotoxin-αβ on IL-7 receptor-α cells that differentially engender lymph nodes and Peyer's patches. *Immunity* **17,** 823–833 (2002).

99. Montaldo, E., Juelke, K. & Romagnani, C. Group 3 innate lymphoid cells (ILC3s): Origin, differentiation, and plasticity in humans and mice. *Eur. J. Immunol.* **45,** 2171–2182 (2015).

100. Buonocore, S., Ahern, P. P., Uhlig, H. H., Ivanov, I. I., Littman, D. R., Maloy, K. J. & Powrie, F. Innate lymphoid cells drive IL-23 dependent innate intestinal pathology. *Nature* **464,** 1371–1375 (2010).

101. Sonnenberg, G. F., Fouser, L. A. & Artis, D. Border patrol: regulation of immunity, inflammation and tissue homeostasis at barrier surfaces by IL-22. *Nat. Immunol.* **12,** 383–390 (2011).

102. Hepworth, M. R. *et al.* Innate lymphoid cells regulate CD4+ T-cell responses to intestinal commensal bacteria. *Nature* **498,** 113–117 (2013).

103. van de Pavert, S. A. *et al.* Maternal retinoids control type 3 innate lymphoid cells and set the offspring immunity. *Nature* **508,** 123–7 (2014).

104. Gomez de Aguero, M. *et al.* The maternal microbiota drives early postnatal innate immune development. *Science (80-.).* **351,** 1296–1302 (2016).

105. Kiss, E. A. & Diefenbach, A. Role of the aryl hydrocarbon receptor in controlling maintenance and functional programs of RORgt+ innate lymphoid cells and intraepithelial lymphocytes. *Frontiers in Immunology* **3,** (2012).

106. Qiu, Ju; Heller, Jennifer J; Guo, Xiaohuan; Zong-ming E Chen, K. F., Yang-Xin Fu, and L. Z., Qiu, J., Heller, J. J., Guo, X., Chen, Z. E. M. E., Fish, K., Fu, Y.-X. X. & Zhou, L. The Aryl Hydrocarbon Receptor Regulates Gut Immunity through Modulation of Innate Lymphoid Cells. *Immunity* **36,** 92–104 (2012).

107. Goverse, G., Labao-Almeida, C., Ferreira, M., Molenaar, R., Wahlen, S., Konijn, T., Koning, J., Veiga-Fernandes, H. & Mebius, R. E. Vitamin A Controls the Presence of RORγ+ Innate Lymphoid Cells and Lymphoid Tissue in the Small Intestine. *J. Immunol.* **196,** 5148–55 (2016).

108. Spencer, S. P. *et al.* Adaptation of Innate Lymphoid Cells to a Micronutrient Deficiency Promotes Type 2 Barrier Immunity. *Science (80-.).* **343,** 432–437 (2014).

109. Mukherjee, S. & Hooper, L. V. Antimicrobial Defense of the Intestine. *Immunity* **42,** 28–39 (2015).

110. Qui, J., Zhou, L., Qiu, J. & Zhou, L. Aryl Hydrocarbon Receptor Promotes RORγt+ ILCs and Controls Intestinal Immunity and Inflammation. *Semin Immunopathol* **35,** 657–670 (2013).

111. Sano, T. *et al.* An IL-23R/IL-22 Circuit Regulates Epithelial Serum Amyloid A to Promote Local Effector Th17 Responses. *Cell* **163,** 381–393 (2015).

112. Pham, T. A. N. *et al.* Epithelial IL-22RA1-mediated fucosylation promotes intestinal colonization resistance to an opportunistic pathogen. *Cell Host Microbe* **16,** 504–516 (2014).

113. Pickard, J. M. *et al.* Rapid fucosylation of intestinal epithelium sustains host–commensal symbiosis in sickness. *Nature* **514,** 638–641 (2014).

114. Goto, Y., Obata, T., Kunisawa, J., Sato, S. & Ivanov, I. I. Innate lymphoid cells regulate intestinal epithelial cell glycosylation. *Science (80-.).* **345,** 1–11 (2014).

115. Longman, R. S. *et al.* CX_3CR1^+ mononuclear phagocytes support colitis-associated innate lymphoid cell production of IL-22. *J. Exp. Med.* **211,** 1571–83 (2014).

116. Abt, M. C., Lewis, B. B., Caballero, S., Xiong, H., Carter, R. A., Susac, B., Ling, L., Leiner, I. & Pamer, E. G. Innate immune defenses mediated by two ilc subsets are critical for protection against acute clostridium difficile infection. *Cell Host Microbe* **18,** 27–37 (2015).

117. Hernández, P. P. *et al.* Interferon-λ and interleukin 22 act synergistically for the induction of interferon-stimulated genes and control of rotavirus infection. *Nat. Immunol.* **16,** 698–707 (2015).

118. Zelante, T. *et al.* Tryptophan catabolites from microbiota engage aryl hydrocarbon receptor and balance mucosal reactivity via interleukin-22. *Immunity* **39,** 372–385 (2013).

119. Turner, J. E., Stockinger, B. & Helmby, H. IL-22 Mediates Goblet Cell Hyperplasia and Worm Expulsion in Intestinal Helminth Infection. *PLoS Pathog.* **9,** 1–7 (2013).

120. Zheng, Y. *et al.* Interleukin-22 mediates early host defense against attaching and effacing bacterial pathogens. *Nat. Med.* **14,** 282–9 (2008).

121. Guo, X., Qiu, J., Tu, T., Yang, X., Deng, L., Anders, R. A., Zhou, L. & Fu, Y. X. Induction of innate lymphoid cell-derived interleukin-22 by the transcription factor STAT3 mediates protection against intestinal infection. *Immunity* **40,** 25–39 (2014).

122. Basu, R., O'Quinn, D. B., Silberger, D. J., Schoeb, T. R., Fouser, L., Ouyang, W., Hatton, R. D. & Weaver, C. T. Th22 Cells Are an Important Source of IL-22 for Host Protection against Enteropathogenic Bacteria. *Immunity* **37,** 1061–1075 (2012).

123. Rankin, L. C. *et al.* Complementarity and redundancy of IL-22-producing innate lymphoid cells. *Nat. Immunol.* **17,** 179–186 (2016).

124. Song, C., Lee, J. S., Gilfillan, S., Robinette, M. L., Newberry, R. D., Stappenbeck, T. S., Mack, M., Cella, M. & Colonna, M. Unique and redundant functions of NKp46 $^{+}$ ILC3s in models of intestinal inflammation. *J. Exp. Med.* **212,** 1869–1882 (2015).

125. Behnsen, J., Jellbauer, S., Wong, C. P., Edwards, R. A., George, M. D., Ouyang, W. & Raffatellu, M. The Cytokine IL-22 Promotes Pathogen Colonization by Suppressing Related Commensal Bacteria. *Immunity* **40,** 262–273 (2014).

126. Xiong, H., Keith, J. W., Samilo, D. W., Carter, R. A., Leiner, I. M. & Pamer, E. G. Innate Lymphocyte/Ly6Chi Monocyte Crosstalk Promotes Klebsiella Pneumoniae Clearance. *Cell* **165,** 679–689 (2016).

127. Withers, D. R. *et al.* Transient inhibition of ROR-γt therapeutically limits intestinal inflammation by reducing TH17 cells and preserving group 3 innate lymphoid cells. *Nat. Med.* **22,** 319–323 (2016).

128. Pearson, C. *et al.* ILC3 GM-CSF production and mobilisation orchestrate acute intestinal inflammation. *Elife* **5,** 1–21 (2016).

129. Vonarbourg, C. *et al.* Regulated expression of nuclear receptor RORgammat confers distinct functional fates to NK cell receptor-expressing RORgammat(+) innate lymphocytes. *Immunity.* **33,** 736–751 (2010).

130. Goto, Y., Panea, C., Nakato, G., Cebula, A., Lee, C., Diez, M. G., Laufer, T. M., Ignatowicz, L. & Ivanov, I. I. Segmented filamentous bacteria antigens presented by intestinal dendritic cells drive mucosal Th17 cell differentiation. *Immunity* **40,** 594–607 (2014).

131. Hepworth, M. R. *et al.* Immune tolerance. Group 3 innate lymphoid cells mediate intestinal selection of commensal bacteria-specific CD4^{+} T cells. TL - 348. *Science* **348 VN-,** 1031–1035 (2015).

132. von Burg, N. *et al.* Activated group 3 innate lymphoid cells promote T-cell-mediated immune responses. *Proc Natl Acad Sci U S A* **111,** 12835–12840 (2014).

133. Geremia, A., Arancibia-Cárcamo, C. V, Fleming, M. P. P., Rust, N., Singh, B., Mortensen, N. J., Travis, S. P. L. & Powrie, F. IL-23–responsive innate lymphoid cells are increased in inflammatory bowel disease. *J. Exp. Med.* **208,** 1127–1133 (2011).

134. Pantelyushin, S., Haak, S., Ingold, B., Kulig, P., Heppner, F. L., Navarini, A. A. & Becher, B. Rorgammat+ innate lymphocytes and gammadelta T cells initiate psoriasiform plaque formation in mice. *J Clin Invest* **122,** 2252–2256 (2012).

135. Teunissen, M. B. M. *et al.* Composition of Innate Lymphoid Cell Subsets in the Human Skin: Enrichment of NCR+ ILC3 in Lesional Skin and Blood of Psoriasis Patients. *J. Invest. Dermatol.* **134,** 2351–2360 (2014).

136. Ren, J., Feng, Z., Lv, Z., Chen, X. & Li, J. Natural killer-22 cells in the synovial fluid of patients with rheumatoid arthritis are an innate source of interleukin 22 and tumor necrosis factor-α. *J. Rheumatol.* **38,** 2112–2118 (2011).

137. Koo, J., Kim, S., Jung, W. J., Lee, Y. E., Song, G. G., Kim, K.-S. & Kim, M.-Y. Increased Lymphocyte Infiltration in Rheumatoid Arthritis Is Correlated with an Increase in LTi-like Cells in Synovial Fluid. *Immune Netw.* **13,** 240–8 (2013).

138. Ciccia, F. *et al.* Type 3 innate lymphoid cells producing IL-17 and IL-22 are expanded in the gut, in the peripheral blood, synovial fluid and bone marrow of patients with ankylosing spondylitis. *Ann. Rheum. Dis.* **74,** 1739–1747 (2015).

139. Roan, F., Stoklasek, T. A., Whalen, E., Molitor, J. A., Bluestone, J. A., Buckner, J. H. & Ziegler, S. F. CD4+ Group 1 Innate Lymphoid Cells (ILC) Form a Functionally Distinct ILC Subset That Is Increased in Systemic Sclerosis. *J. Immunol.* **196,** 2051–2062 (2016).

140. Hatfield, J. K. & Brown, M. A. Group 3 innate lymphoid cells accumulate and exhibit disease-induced activation in the meninges in EAE. *Cell. Immunol.* **297,** 69–79 (2015).

141. Shikhagaie, M. M., Germar, K., Bal, S. M., Ros, X. R. & Spits, H. Innate lymphoid cells in autoimmunity: emerging regulators in rheumatic diseases. *Nat. Rev. Rheumatol.* **13,** 164–173 (2017).

142. Chan, I. H. *et al.* Interleukin-23 is sufficient to induce rapid de novo gut tumorigenesis, independent of carcinogens, through activation of innate lymphoid cells. *Mucosal Immunol.* **7,** 842–856 (2014).

143. Mortha, A., Chudnovskiy, A., Hashimoto, D., Bogunovic, M., Spencer, S. P., Belkaid, Y. & Merad, M. Microbiota-dependent crosstalk between macrophages and ILC3 promotes intestinal homeostasis. *Science (80-.).* **343,** 1249288–1249288 (2014).

144. Ohoka, Y., Yokota-Nakatsuma, A., Maeda, N., Takeuchi, H. & Iwata, M. Retinoic acid and GM-CSF coordinately induce retinal dehydrogenase 2 (RALDH2) expression through cooperation between the RAR/RXR complex and Sp1 in dendritic cells. *PLoS One* **9,** (2014).

145. Giacomin, P. R. *et al.* Epithelial-intrinsic IKKα expression regulates group 3 innate lymphoid cell responses and antibacterial immunity. *J. Exp. Med.* **212,** 1513–28 (2015).

146. Sawa, S., Lochner, M., Satoh-Takayama, N., Dulauroy, S., Bérard, M., Kleinschek, M., Cua, D., Di Santo, J. P. & Eberl, G. RORγt+ innate lymphoid cells regulate intestinal homeostasis by integrating negative signals from the symbiotic microbiota. *Nat. Immunol.* **12,** 320–326 (2011).

147. Marshman, E., Booth, C. & Potten, C. S. The intestinal epithelial stem cell. *BioEssays* **24,** 91–98 (2002).

148. Bjerknes, M., Cheng, H. & Irina Klimanskaya and Robert, L. in *Methods in Enzymology* (2006).

149. Barker, N., Van Es, J. H., Jaks, V., Kasper, M., Snippert, H., Toftgård, R. & Clevers, H. Very long-term self-renewal of small intestine, colon, and hair follicles from cycling Lgr5+ve stem cells. in *Cold Spring Harbor Symposia on Quantitative Biology* **73,** 351–356 (2008).

150. Bjerknes, M. & Cheng, H. Clonal analysis of mouse intestinal epithelial progenitors. *Gastroenterology* **116,** 7–14 (1999).

151. Potten, C. S. Stem cells in gastrointestinal epithelium: numbers, characteristics and death. *Philos. Trans. R. Soc. Lond. B. Biol. Sci.* **353,** 821–830 (1998).

152. Barker, N. *et al.* Identification of stem cells in small intestine and colon by marker gene Lgr5. *Nature* **449,** 1003–1007 (2007).

153. van der Flier, L. G. & Clevers, H. Stem Cells, Self-Renewal, and Differentiation in the Intestinal Epithelium. *Annu. Rev. Physiol.* **71,** 241–260 (2009).

154. Barker, N., Van Oudenaarden, A. & Clevers, H. Identifying the stem cell of the intestinal crypt: Strategies and pitfalls. *Cell Stem Cell* **11,** 452–460 (2012).

155. Birchenough, G. M. H., Johansson, M. E., Gustafsson, J. K., Bergström, J. H. & Hansson, G. C. New developments in goblet cell mucus secretion and function. *Mucosal Immunol.* **8,** 1–8 (2015).

156. Rehfeld, J. F. A centenary of gastrointestinal endocrinology. *Hormone and Metabolic Research* **36,** 735–741 (2004).

157. Gerbe, F. *et al.* Intestinal epithelial tuft cells initiate type 2 mucosal immunity to helminth parasites. *Nature* **529,** (2016).

158. Middelhoff, M., Westphalen, C. B., Hayakawa, Y., Yan, K. S., Gershon, M. D., Wang, T. C. & Quante, M. Dclk1-expressing tuft cells: Critical modulators of the intestinal niche? *Am. J. Physiol. - Gastrointest. Liver Physiol.* ajpgi.00073.2017 (2017). doi:10.1152/ajpgi.00073.2017

159. Gerbe, F., Legraverend, C. & Jay, P. The intestinal epithelium tuft cells: Specification and function. *Cellular and Molecular Life Sciences* **69,** 2907–2917 (2012).

160. Clevers, H. The intestinal crypt, a prototype stem cell compartment. *Cell* **154,** (2013).

161. Sato, T. *et al.* Paneth cells constitute the niche for Lgr5 stem cells in intestinal crypts. *Nature* **469,** 415–418 (2011).

162. Metcalfe, C., Kljavin, N. M., Ybarra, R. & De Sauvage, F. J. Lgr5+ stem cells are indispensable for radiation-induced intestinal regeneration. *Cell Stem Cell* **14,** 149–159 (2014).

163. Sangiorgi, E. & Capecchi, M. R. Bmi1 is expressed in vivo in intestinal stem cells. *Nat. Genet.* **40,** 915–20 (2008).

164. Gordon, J. I., Schmidt, G. H. & Roth, K. A. Studies of intestinal stem cells using normal, chimeric, and transgenic mice. *Faseb J* **6,** 3039–3050 (1992).

165. Zhu, Y., Huang, Y. F., Kek, C. & Bulavin, D. V. Apoptosis differently affects lineage tracing of lgr5 and bmi1 intestinal stem cell populations. *Cell Stem Cell* **12,** 298–303 (2013).

166. Li, N., Yousefi, M., Nakauka-Ddamba, A., Jain, R., Tobias, J., Epstein, J. A., Jensen, S. T. & Lengner, C. J. Single-cell analysis of proxy reporter allele-marked epithelial cells establishes intestinal stem cell hierarchy. *Stem Cell Reports* **3,** 876–891 (2014).

167. Montgomery, R. K. *et al.* Mouse telomerase reverse transcriptase (mTert) expression marks slowly cycling intestinal stem cells. *Proc. Natl. Acad. Sci.* **108,** 179–184 (2011).

168. Li, N., Nakauka-Ddamba, A., Tobias, J., Jensen, S. T. & Lengner, C. J. Mouse Label-Retaining Cells Are Molecularly and Functionally Distinct From Reserve Intestinal Stem Cells. *Gastroenterology* **151,** 298–310. e7 (2016).

169. Yousefi, M. *et al.* Msi RNA-binding proteins control reserve intestinal stem cell quiescence. *Journal of Cell Biology* **215,** 401–413 (2016).

170. Takeda, N., Jain, R., LeBoeuf, M. R., Wang, Q., Lu, M. M. & Epstein, J. A. Interconversion between intestinal stem cell populations in distinct niches. *Science* **334,** 1420–1424 (2011).

171. Breault, D. T. *et al.* Generation of mTert-GFP mice as a model to identify and study tissue progenitor cells. *Proc. Natl. Acad. Sci. U. S. A.* **105,** 10420–5 (2008).

172. Asfaha, S. *et al.* Krt19+/Lgr5- Cells Are Radioresistant Cancer-Initiating Stem Cells in the Colon and Intestine. *Cell Stem Cell* **16,** 627–638 (2015).

173. Powell, A. E. *et al.* The pan-ErbB negative regulator lrig1 is an intestinal stem cell marker that functions as a tumor suppressor. *Cell* **149,** 146–158 (2012).

174. Roche, K. C., Gracz, A. D., Liu, X. F., Newton, V., Akiyama, H. & Magness, S. T. SOX9 Maintains Reserve Stem Cells and Preserves Radioresistance in Mouse Small Intestine. *Gastroenterology* **149,** 1553–1563.e3 (2015).

175. Yan, K., Chia, L. & Li, X. The intestinal stem cell markers Bmi1 and Lgr5 identify two functionally distinct populations. *Pnas* **109,** 466–471 (2012).

176. Yan, K. S. *et al.* Intestinal Enteroendocrine Lineage Cells Possess Homeostatic and Injury-Inducible Stem Cell Activity. *Cell Stem Cell* **21,** 78–90.e6 (2017).

177. Jadhav, U., Saxena, M., O'Neill, N. K., Saadatpour, A., Yuan, G. C., Herbert, Z., Murata, K. & Shivdasani, R. A. Dynamic Reorganization of Chromatin Accessibility Signatures during Dedifferentiation of Secretory Precursors into Lgr5+ Intestinal Stem Cells. *Cell Stem Cell* **21,** 65–77.e5 (2017).

178. Buczacki, S. J. A., Zecchini, H. I., Nicholson, A. M., Russell, R., Vermeulen, L., Kemp, R. & Winton, D. J. Intestinal label-retaining cells are secretory precursors expressing Lgr5. *Nature* **495,** 65–9 (2013).

179. Vries, R. G. J., Huch, M. & Clevers, H. Stem cells and cancer of the stomach and intestine. *Mol. Oncol.* **4,** 373–84 (2010).

180. Kuhnert, F., Davis, C. R., Wang, H.-T., Chu, P., Lee, M., Yuan, J., Nusse, R. & Kuo, C. J. Essential requirement for Wnt signaling in proliferation of adult small intestine and colon revealed by adenoviral expression of Dickkopf-1. *Proc. Natl. Acad. Sci.* **101,** 266–271 (2004).

181. Muncan, V. *et al.* Rapid Loss of Intestinal Crypts upon Conditional Deletion of the Wnt/Tcf-4 Target Gene c-Myc. *Mol. Cell. Biol.* **26,** 8418–8426 (2006).

182. Fevr, T., Robine, S., Louvard, D. & Huelsken, J. Wnt/beta-catenin is essential for intestinal homeostasis and maintenance of intestinal stem cells. *Mol. Cell. Biol.* **27,** 7551–9 (2007).

183. van Es, J. H. *et al.* Dll1+ secretory progenitor cells revert to stem cells upon crypt damage. *Nat. Cell Biol.* **14,** 1099–104 (2012).

184. Kim, K.-A. Mitogenic Influence of Human R-Spondin1 on the Intestinal Epithelium. *Science (80-.).* **309,** 1256–1259 (2005).

185. Flanagan, D. J. *et al.* Frizzled7 functions as a Wnt receptor in intestinal epithelial Lgr5^{+} stem cells. *Stem Cell Reports* **4,** 759–767 (2015).

186. Tan, S. & Barker, N. Epithelial stem cells and intestinal cancer. *Semin. Cancer Biol.* (2014). doi:10.1016/j.semcancer.2014.02.005

187. Gregorieff, A., Pinto, D., Begthel, H., Destrée, O., Kielman, M. & Clevers, H. Expression pattern of Wnt signaling components in the adult intestine. *Gastroenterology* **129,** 626–638 (2005).

188. Kosinski, C. *et al.* Gene expression patterns of human colon tops and basal crypts and BMP antagonists as intestinal stem cell niche factors. *Proc. Natl. Acad. Sci. U. S. A.* **104,** 15418–23 (2007).

189. He, X. C. *et al.* BMP signaling inhibits intestinal stem cell self-renewal through suppression of Wnt-beta-catenin signaling. *Nat. Genet.* **36,** 1117–21 (2004).

190. Pinchuk, I. V., Mifflin, R. C., Saada, J. I. & Powell, D. W. Intestinal mesenchymal cells. *Current Gastroenterology Reports* **12,** 310–318 (2010).

191. Pellegrinet, L. *et al.* Dll1- and Dll4-mediated notch signaling are required for homeostasis of intestinal stem cells. *Gastroenterology* **140,** 1230–1240 (2011).

192. VanDussen, K. L. *et al.* Notch signaling modulates proliferation and differentiation of intestinal crypt base columnar stem cells. *Development* **139,** 488–497 (2012).

193. Batts, L. E., Polk, D. B., Dubois, R. N. & Kulessa, H. Bmp signaling is required for intestinal growth and morphogenesis. *Dev. Dyn.* **235,** 1563–1570 (2006).

194. Zacharias, W. J., Li, X., Madison, B. B., Kretovich, K., Kao, J. Y., Merchant, J. L. & Gumucio, D. L. Hedgehog Is an Anti-Inflammatory Epithelial Signal for the Intestinal Lamina Propria. *Gastroenterology* **138,** (2010).

195. Van Dop, W. A. *et al.* Loss of Indian hedgehog activates multiple aspects of a wound healing response in the mouse intestine. *Gastroenterology* **139,** (2010).

196. Taniguchi, K. *et al.* A gp130-Src-YAP Module Links Inflammation to Epithelial Regeneration. *Nature* **519,** 57–62 (2015).

197. Iyer, R., Thames, H. D., Tealer, J. R., Mason, K. A. & Evans, S. C. Effect of reduced EGFR function on the radiosensitivity and proliferative capacity of mouse jejunal crypt clonogens. in *Radiotherapy and Oncology* **72,** 283–289 (2004).

198. Gregorieff, A., Liu, Y., Inanlou, M. R., Khomchuk, Y. & Wrana, J. L. Yap-dependent reprogramming of Lgr5+ stem cells drives intestinal regeneration and cancer. *Nature* **526,** 715–8 (2015).

199. Park, H. W. *et al.* Alternative Wnt Signaling Activates YAP/TAZ. *Cell* **162,** 780–794 (2015).

200. Gjorevski, N., Sachs, N., Manfrin, A., Giger, S., Bragina, M. E., Ordóñez-Morán, P., Clevers, H. & Lutolf, M. P. Designer matrices for intestinal stem cell and organoid culture. *Nature* **539,** 560–564 (2016).

201. Hynes, R. O. The extracellular matrix: not just pretty fibrils. *Science* **326,** 1216–9 (2009).

202. DuFort, C. C., Paszek, M. J. & Weaver, V. M. Balancing forces: architectural control of mechanotransduction. *Nat. Rev. Mol. Cell Biol.* **12,** 308–319 (2011).

203. Yeung, T. M., Chia, L. A., Kosinski, C. M. & Kuo, C. J. Regulation of self-renewal and differentiation by the intestinal stem cell niche. *Cellular and Molecular Life Sciences* **68,** 2513–2523 (2011).

204. Powell, D. W., Pinchuk, I. V, Saada, J. I., Chen, X. & Mifflin, R. C. Mesenchymal cells of the intestinal lamina propria. *Annu. Rev. Physiol.* **73,** 213–237 (2011).

205. Hanash, A. M. *et al.* Interleukin-22 Protects Intestinal Stem Cells from Immune-Mediated Tissue Damage and Regulates Sensitivity to Graft versus Host Disease. *Immunity* **37,** 339–350 (2012).

206. Lindemans, C. A. *et al.* Interleukin-22 promotes intestinal-stem-cell-mediated epithelial regeneration. *Nature* **528,** 560–564 (2015).

207. Blazar, B. R., Murphy, W. J. & Abedi, M. Advances in graft-versus-host disease biology and therapy. *Nat. Rev. Immunol.* **12,** 443–458 (2012).

208. Pickert, G. *et al.* STAT3 links IL-22 signaling in intestinal epithelial cells to mucosal wound healing. *J. Exp. Med.* **206,** 1465–72 (2009).

209. Witte, E., Witte, K., Warszawska, K., Sabat, R. & Wolk, K. Interleukin-22: A cytokine produced by T, NK and NKT cell subsets, with importance in the innate immune defense and tissue protection. *Cytokine Growth Factor Rev.* **21,** 365–379 (2010).

210. Dudakov, J. A. *et al.* Interleukin-22 Drives Endogenous Thymic Regeneration in Mice. *Science (80-.).* **336,** 91–95 (2012).

211. Li, Z. *et al.* Epidermal Notch1 recruits RORγ+ group 3 innate lymphoid cells to orchestrate normal skin repair. *Nat. Commun.* **7,** 11394 (2016).

2

TYPE 3 INNATE LYMPHOID CELLS MAINTAIN INTESTINAL EPITHELIAL STEM CELLS AFTER TISSUE DAMAGE

Patricia Aparicio-Domingo[1,5], Mónica Romera-Hernández[1,5], Julien J. Karrich[1], Ferry Cornelissen[1], Natalie Papazian[1], Dicky Lindenbergh-Kortleve[2], James A. Butler[3], Louis Boon[4], Mark C. Coles[3], Janneke N. Samsom[2] and Tom Cupedo[1]

[1]Department of Hematology, Erasmus University Medical Center, Rotterdam, The Netherlands; [2]Department of Pediatrics, Division of Gastroenterology and Nutrition, Erasmus University Medical Center, Rotterdam, The Netherlands; [3]Centre for Immunology and Infection, Department of Biology and Hull York Medical School, York, UK; [4]Bioceros, Utrecht, The Netherlands
[5]These authors contributed equally

Published in:
Journal of Experimental Medicine. 2015 Oct 19;212(11):1783-91

ABSTRACT

Disruption of the intestinal epithelial barrier allows bacterial translocation and predisposes to destructive inflammation. To ensure proper barrier composition, crypt-residing stem cells continuously proliferate and replenish all intestinal epithelial cells within days. As a consequence of this high mitotic activity, mucosal surfaces are frequently targeted by anti-cancer therapies, leading to dose-limiting side effects. The cellular mechanisms that control tissue protection and mucosal healing in response to intestinal damage remain poorly understood. Type 3 innate lymphoid cells (ILC3s) are regulators of homeostasis and tissue responses to infection at mucosal surfaces. We now demonstrate that ILC3s are required for epithelial activation and proliferation in response to small intestinal tissue damage induced by the chemotherapeutic agent methotrexate. Multiple subsets of ILC3 are activated after intestinal tissue damage and in the absence of ILC3s epithelial activation is lost, correlating with increased pathology and severe damage to the intestinal crypts. Using ILC3-deficient Lgr5 reporter mice we show that maintenance of intestinal stem cells after damage is severely impaired in the absence of ILC3s or the ILC3 signature cytokine IL-22. These data unveil a novel function of ILC3s in limiting tissue damage by preserving tissue-specific stem cells..

INTRODUCTION

The intestinal epithelium combines efficient uptake of nutrients and water with providing a physical barrier between the intestinal microbiota and our body[1]. Damage sustained by intestinal epithelial cells needs to be swiftly and efficiently repaired to prevent inappropriate immune responses to commensal bacteria. Intestinal damage is an early event in the development of both Graft-versus-Host disease (GvHD)[2] and alimentary mucositis[3] and a driver of bacterial translocation and T cell activation in inflammatory bowel disease (IBD)[4].

A major pathway involved in the intestinal epithelial response to damage is the activation of Stat3, which is expressed along the crypt-villus axis of the intestinal epithelium[5,6]. Phosphorylated Stat3 translocates to the nucleus and activates genes involved in proliferation, survival and mucosal defense[7–9]. Mutations in *STAT3* have been identified as susceptibility factors for inflammatory bowel disease (IBD)[7,10,11] and in mice, upon DSS-induced colitis, epithelial Stat3 is required for mucosal wound healing[9].

Intestinal regeneration depends on the continuous differentiation of epithelial cells from crypt residing intestinal stem cells (ISCs)[12–14]. Even though multiple intestinal progenitor cells have been described, the best-characterized population are the Lgr5 expressing cells that reside at the crypt bottom, interspersed with Paneth cells. These stem cells have the ability to give rise to all intestin

al epithelial cells *ex vivo*[15]. Similar to its role in differentiated epithelial cells, Stat3 activation is also an important pathway for survival of intestinal epithelial stem cells[16].

Type 3 innate lymphoid cells (ILC3s) are innate immune cells that reside in the lamina propria of both the small and large intestines and are involved in tissue homeostasis, early defense against enteric pathogens and containment of microbiota[17,18]. In the intestines, multiple ILC3 subsets exist, two of which can be distinguished by mutual exclusive expression of the natural cytotoxicity receptor NKp46 and the chemokine receptor CCR6[19,20]. Most Nkp46$^+$ ILC3s are found dispersed throughout the lamina propria, a localization that depends on the expression of CXCR6[21]. In contrast, the majority of CCR6$^+$ ILC3s are located in close proximity to the intestinal crypts, in anatomically defined sites known as cryptopatches[22]. Recent findings indicated that under inflammatory conditions, such as experimental GvHD, ILC3s can interact with the epithelial stem cells in the crypts, protecting them from T cell-mediated killing[23].

The well-known ability of ILC3s to condition the local microenvironment, the close proximity of ILC3s to intestinal crypts and the ability of ILC3s to communicate with epithelial stem cells led us to hypothesize that ILC3s are involved in directing intestinal epithelial responses to tissue damage. Using the Methotrexate (MTX)-model of small intestinal damage we now show that ILC3s are activated immediately after MTX administration, leading to a rapid activation of epithelial Stat3 and maintenance of intestinal stem cells. Our data reveal a novel function for ILC3s as organizers of the intestinal epithelial response to tissue damage through activation of epithelial cells and maintenance of ISCs and suggest that ILC3s might in future be therapeutically harnessed to prevent stem cell loss during chemotherapy.

MATERIALS AND METHODS

Mice. C57BL/6, RORγt$^{-/-}$, Rag1$^{-/-}$, Ncr1$^{-/-}$ (Gazit et al., 2006) and Lgr5-eGFP mice were bred in the animal facility of the Erasmus University Medical Center Rotterdam. Animal experiments were approved by the Animal Ethics Committee of the Erasmus MC and performed in accordance with institutional guidelines. Age and gender-matched littermates were used whenever possible.

Thy1^{+} cells were depleted using anti-Thy1 antibodies (clone YTS154, provided by Herman Waldmann, Cambridge) or isotype controls (a-Phytochrome AFRC MAC5.1). Antibodies were diluted in saline and mice were injected i.p. with 200μg every other day, for 2 weeks.

Monoclonal antibodies. EpCAM-1 (G8.8 Biolegend); CD45 (30F11, Invitrogen); Lin-biotin (eBioscience): CD19 (1D3), CD3 (145-2C11), CD11c (N418), CD11b (M1/70), Gr1 (RB6-8C5); Streptavidin (Biolegend), NK1.1 (PK136, eBioscience); CD127 (A7R34, eBioscience); CD117 (2B8, BD), NKp46 (2941.4, eBioscience); CCR6 (29-2L17, Biolegend)

Methotrexate. 8-12 weeks old mice were injected i.p. with 120mg/kg MTX (PCH) at day-1 and with 60mg/kg at day 0. Body weight was monitored daily and tissues were collected at day 1 and day 4 after the last MTX injection.

Cytokine neutralization. 150μg of anti-IL-22 antibody (8E11, kind gift from W. Ouyang, Genentech Inc.) or mouse IgG1 isotype control (MOPC-21, BioXcell) were administered i.p to Lgr5-eGFP mice every 2 days, starting 5 days before the first MTX dose, until day 2 after the last MTX dose.
Rag1$^{-/-}$ mice were treated with 1 mg of anti-IFNγ (XMG 1.2) or IgG1 isotype control (GL113) together with the first dose of MTX at day -1 and with 0.5 mg on day 0 and day 1.

Radiation chimeras. 8 weeks old Lgr5-eGFP mice were irradiated at 9Gy and subsequently reconstituted by i.v injection of 1-2.10^{6} bone marrow cells from either WT or RORγt$^{-/-}$ mice. Mice were under antibiotic water for 2 weeks after bone marrow transplantation. To eliminate radio-resistant ILC3s, 2 weeks after reconstitution, Lgr5-eGFP chimeras received 5 i.p. injections with 200μg of anti-Thy1 antibody (YTS154, provided by Herman Waldmann, Cambridge) during two weeks. Four weeks after Thy1 depletion, Lgr5-eGFP chimeras were exposed to MTX.

Crypt isolation. Isolation of intestinal crypts was performed as previously described (Sato et al., 2009). Briefly, isolated small intestines were opened longitudinally and washed with cold PBS. Tissues were cut into 5mm pieces and subsequently washed by mechanical pipetting with cold PBS until supernatant was clear. Tissues were incubated with EDTA (2mM) in PBS at 4°C for 30 min. Tissues were then washed several times with cold PBS and suspended

by vigorous pipetting. Crypt-enriched sediments were passed through a 70µm cell strainer and centrifuge at 600 rpm for 3 min to separate the crypts from single cells. Crypts were incubated with 1 ml of TrypLE Express (Gibco) at 37°C for 10-15 min until crypt dissociation was observed. Single cell suspensions were stained with conjugated antibodies and analyzed for the expression of GFP by flow cytometry (FACS CantoII, BD).

Histology. Small intestinal tissue pieces (5 mm) were fixed in 4% PFA and embedded in paraffin. Four-µm sections were deparaffinized and stained with hematoxylin (Vector Laboratories) and eosin (Sigma-Aldrich). For Ki67 and pStat3 detection endogenous peroxidases were blocked and antigen retrieval was achieved by microwave treatment in citrate buffer (10mM, pH 6.0). Prior to staining, Fc receptors were blocked in blocking solution (Blocking endogenous peroxidase: 1% periodic acid in deionized water for 20 min; blocking FC receptors: 10% normal mouse serum; Tris buffer (10 mM), EDTA (5 mM), NaCl (0.15 M), gelatine (0.25%) and Tween-20 (0.05%), pH 8.0). Tissue sections were incubated overnight at 4°C with rat Ki67 monoclonal antibody (MIB-5, Dako) or rabbit pStat3 antibody (D3A7, Cell signaling). Immunoreactions were detected using biotinylated donkey anti-rat and goat-anti-rabbit (Vector Laboratories) and incubated with the Vectastin ABC Elite Kit (Vector Laboratories) and 3,3'-diaminobenzidine tetrahydrochloride (Sigma-Aldrich). Sections were counterstained with hematoxylin.

Both the analysis of pathology and $Ki67^+$ cells was performed blinded by at least two independent analysts. Pathology score was obtained as previously described (de Koning et al., 2006) and Ki67-expressing cells were counted in 5 to 12 crypts per section. Measurement of pStat3 intensity in IEC from sections was determined using HistoQuest software (TissueGnostics).

Explant cultures. Isolated small intestine was opened longitudinally and cleaned with cold PBS. A piece of 1 cm length was cultured in RPMI with 10% FCS and 1% P/S at 37°C for 24 hours. Protein content of supernatants was determined by enzyme-linked immunosorbent assay (eBioscience) and absorbance was measured at 450 nm using Victor X4 (Perkin Elmer). Protein content of the supernatants was calculated relative to tissue weight.

Isolation of lamina propria lymphocytes. Isolated small intestine was opened longitudinally and washed with cold HBSS containing Hepes (15 mM), pH 7.2. Tissues were cut in 1 cm pieces and incubated in HBSS buffer containing 10% FBS, Hepes (15 mM), EDTA (5 mM) and DTT (1mM) (pH 7.2) at 37°C, two times for 20 min to remove epithelium and intraepithelial lymphocytes. The tissues were digested with Collagenase VIII (100U/ml, Sigma) in RPMI containing 10% FBS, Hepes (15 mM), P/S (100U/ml) and DTT (1mM) (pH7.2) at 37°C in a shaker, two times for 1 hour. Supernatants were passed through a 70µm cell strainer and

washed in cold HBSS. Pellets were suspended in 90% percoll, overlaid with 40% percoll and centrifuge at 1800rpm for 20 min to allow separation of mononuclear cells by density gradient. Interphase was washed and stained with conjugated antibodies. Lamina propria lymphocytes were analyzed by flow cytometry (Facs ARIAIII, BD) and ILC3s were sorted as $CD45^{+}Lin^{-}NK1.1^{-}CD127^{+}CD117^{+}CCR6^{+/-}NKp46^{+/-}$. See supplemental Figure 1 (Figure S1) for full gating strategy.

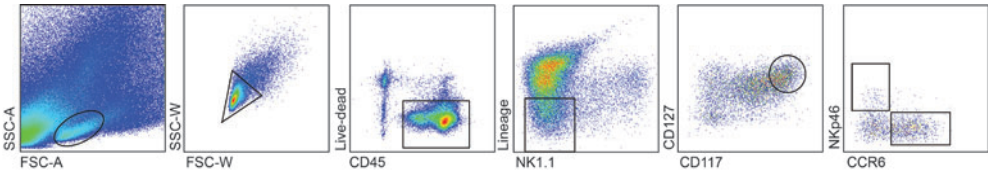

Figure S1: FACS-Gate-strategy for intestinal ILC3 subsets.
Small intestinal lamina propria lymphocyte cell suspensions from wild-type mice at steady-state were analyzed by Flow Cytometry and $NKp46^{+}$ ILC3s and $CCR6^{+}$ ILC3s were gated as indicated (including lymphocyte gate (CD45+ cells); excluding duplets, dead cells (L/D), Lin^{+} cells (CD19, CD3, CD11c, CD11b, Gr1) and NK cells (NK1.1); and analyzing NKp46 and CCR6 expression within $CD117^{+}$ $CD127^{+}$ cells).

Transcript analysis. RNA was extracted using the NucleoSpin RNA XS kit (Machery Nagel). RNA from sorted cells was amplified according to the manufacturer's protocol (Ovation PicoSL WTA System V2, NuGen). For quantitative PCR, a Neviti Thermal Cycler (Applied Biosystems) and DyNAmo Flash SYBR Green qPCR kit (Finnzymes) were used, with the addition of $MgCl_2$ to a final concentration of 4 mM. All reactions were done in duplicate and are normalized to the expression of Gapdh. Relative expression was calculated by the cycling threshold (CT) method as $2^{-\Delta CT}$. The primers sequences can be found in Table 1 (see below).

Table 1. Primer sequences

Gene	***Forward Primer***	***Reverse Primer***
Gapdh	TCAACGGCACAGTCAAG	GCTCCACCCTTCAAGTG
Socs3	GGAGCCCCTTTGTAGACT	CGGGAAACTTGCTGTG
Il22	CTCCCC CAGTCAGACAG	CAATCGCCTTGATCTCTC
Csf2 (Gm-csf)	GACCCGCCTGAAGATATT	ATCCGCATAGGTGGT AAC T
Tnf (Tnfa)	GGGGGCTTCCAGAACT	GGGCCATAGAACTGATGAG
Ncr1 (NKp46)	CCCCCTGAAACTGGTAGTA	GTGGCAGTCTTCAGTTGG
Il17	CTTGGCGCAAAAGTGA	TTGCTGGATGAGAACAGAA
Ifng	CAAAAGGATGGTGACATGA	GGGTTGTTGACCTCAAACT
Rorc	GTGGGGACAAGTCATCTG	CGGCCAAACTTGACAG
Ltb	ACGTCGGGTTGAGAAGA	GGATGTGGAGGCTAGATTC
Bax	AAGGCCCTGTGCACTAA	GAGGCGGTGAGGACTC
Bcl2l1 (Bclxl)	CGTGGCCTTTTTCTCC	GGCTGCTGCATTGTTC
Wnt5a	CGTGGACGCTAGAGAAAG	AGCCAGACACTCCATGAC

Statistical analysis. Samples were analyzed using unpaired Mann-Whitney test. P values < 0.05 were considered significant. Data are shown as mean ± SEM.

RESULTS AND DISCUSSION

To study tissue damage responses in the small intestine, where most ILC3s reside, we exposed mice to MTX, an anti-metabolite that inhibits folic acid metabolism and targets cells in S-phase[24]. MTX application is a well-established, self-resolving model of small intestinal damage ideally suited to dissect epithelial responses to sterile insult[25–27]. Upon MTX administration, mice lost weight until day 4, after which they fully recovered by day 7 **(Figure 1A)**. This rapid weight loss correlated with intestinal pathology, which peaked as early as day 1 after the last MTX injection and subsequently stabilized at day 4 **(Figure 1B)** before recovering by day 7 (not shown). Pathological examination of the small intestine showed villus flattening and crypt hyperplasia with an overall loss of epithelial architecture **(Figure 1C)**.

To visualize damage responses by epithelial cells we assessed the number of cycling crypt cells, a measure of regenerative capacity. $Ki67^+$ crypt cells were reduced at day 1 but returned to baseline levels by day 4 **(Figures 1D-E)**. Conversely, transcripts for the regeneration-associated Wnt family member *Wnt5a*[28] were increased early after damage **(Figure 1F)**. Phosphorylation of Stat3 in intestinal epithelial cells (IECs) plays a central role in mucosal wound healing[8]. Stat3 phosphorylation was induced early after MTX application, peaking at day 1 **(Figure 1G)**. Four days after the last MTX injection, the phosphorylation of Stat3 had returned to baseline **(Figure 1G)**. These data show that MTX-induced small intestinal damage induces rapid and transient epithelial activation followed by regeneration.

Immediate MTX-induced pathology has been mainly attributed to direct effects on intestinal epithelial cells, leading to epithelial cell-intrinsic responses to tissue damage[27]. To determine whether the restoration of cycling crypt cells and the phosphorylation of Stat3 are indeed epithelial cell intrinsic or whether immune cells are involved, we administered MTX to $Rag1^{-/-}$ mice that lack adaptive immunity and to $Rag1^{-/-}$ mice pre-treated with Thy1-depleting antibodies to eradicate innate immune cell subsets. $Rag1^{-/-}$ mice treated with isotype control antibodies showed normal restauration of the cycling crypt compartment at day 4 **(Figures 2A-B)** and normal phosphorylation of Stat3 at day 1 after MTX **(Figures 2C)**, confirming that adaptive immune cells are dispensable for these responses **(Figure 1E)**. In contrast, depletion of $Thy1^+$ cells in $Rag1^{-/-}$ mice strongly reduced the recovery of cycling cells at day 4 **(Figure 2A-B)** and impaired Stat3 phosphorylation in IECs in response to tissue damage **(Figure 2C)**. To validate the reduced Stat3 phosphorylation we quantified the intensity of pStat3 staining on tissue sections using semi-automated analysis and found a significant reduction in pStat3 intensity at day 1 after the last MTX administration **(Figure 2D)**. In addition, transcript analysis of total ileum revealed a reduction in levels of the Stat3 target gene *Socs3*, indicative of reduced Stat3 signaling **(Figure 2E)**. Of note, pStat3 positive hematopoietic cells were found in the lamina propria of both control $Rag1^{-/-}$ and Thy1-depleted $Rag1^{-/-}$ mice **(Figure 2C)**, suggesting differential regulation of Stat3 activation

in epithelial and hematopoietic cells. In conclusion, these experiments establish that restoration of the proliferating crypt cell compartment and epithelial phosphorylation of Stat3 after tissue damage are not epithelial cell intrinsic responses but require the presence of Thy1^{+} cells.

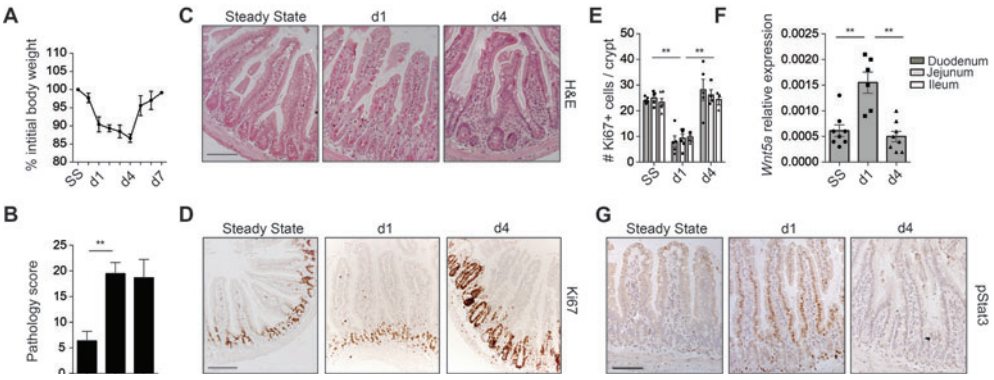

Figure 1. Epithelial responses to MTX. (A) Weight curve of wild-type mice treated with MTX. (B) MTX-induced pathology as described in materials and methods. (C) Representative H&E staining and (D) immunostaining of Ki67 in ileal sections at the indicated time points. (E) Number of KI67^{+} cells per crypt at indicated time points. (F) Transcript analysis of *Wnt5a* in Ileal tissues. (G) Representative immunostaining of pStat3 in ileal sections at indicated time points. (A-C and G: 2-4 independent experiment, N>5 per time point; D-F: 2 independent experiment, N= 2-3 per time point). *, P<0.05; **, P<0.01. Bars: 50µm.

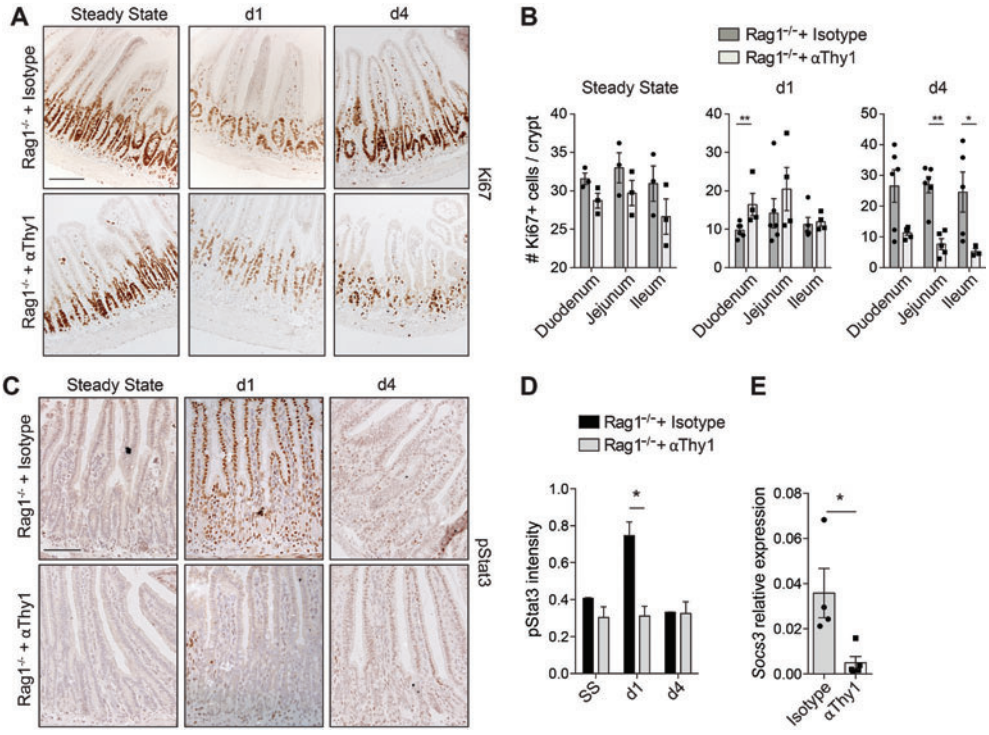

Figure 2. Epithelial responses to tissue damage depend on Thy1+ cells. (A) Representative immunostaining of Ki67 in isotype and anti-Thy1 treated Rag1$^{-/-}$ mice and (B) number of Ki67^{+} cells per crypt at indicated time points. (C) Immunostaining of pStat3 in isotype and anti-Thy1 treated Rag1$^{-/-}$ mice. (D) pStat3 intensity in ileal sections at the indicated time points. (E) *Socs3* transcript levels relative to *Gapdh* from ileum at day 1 after MTX (2 independent experiments, N=2-5 per time point) *, P<0.05; **, P<0.01. Bars, 50µm.

ILC3s are activated in response to intestinal tissue damage

The finding that phosphorylation of epithelial Stat3 depends on Thy1$^+$ cells led us to hypothesize that Thy1$^+$ ILC3s are involved in the intestinal response to MTX-induced tissue damage. To determine whether ILC3s are activated in response to intestinal damage, CCR6$^+$ and NKp46$^+$ lamina propria ILC3s were analyzed for expression of activation-associated transcripts at 1 day after the last MTX injection **(Figure 3A and B)**. Compared to homeostasis, CCR6$^+$ ILC3s maintained transcription of *Ltb*, *Rorc*, *Ifng*, *Il22* and *Csf2*, but showed increased transcription of *Tnf* and *Il17a* **(Figure 3A)**. NKp46$^+$ ILC3s significantly increased transcription of *Ltb*, *Rorc*, *Il22*, *Ifng*, *Csf2* and *Tnf* **(Figure 3B)**. These data show that in response to intestinal tissue damage, both NKp46$^+$ and CCR6$^+$ ILC3s are activated, albeit in a differential manner. IFNγ-secreting ILC3s have been implicated in intestinal pathology[29] and we therefore assessed the contribution of this ILC3-derived cytokine to MTX-induced damage by neutralizing IFNγ in Rag1$^{-/-}$ mice. After exposure to MTX, intestinal pathology was similar in Rag1$^{-/-}$ mice treated with either neutralizing IFNγ antibodies or isotype controls, suggesting that IFNγ is not critical for pathology in this model **(Figure 3C)**. In line with the activation of ILC3s at the cytokine level, we also noted that expression of NKp46 was increased on ILC3 at day 1 after insult. This increased expression was apparent both at the protein **(Figure 3D)** and transcript level **(Figure 3E)**. We next exposed Ncr1$^{-/-}$ and littermate controls to MTX in order to determine whether absence of NKp46 influences MTX-induced pathology. However, the overall pathology in Ncr1$^{-/-}$ mice did not differ from the Ncr1$^{+/-}$ littermate controls, arguing against an essential role of NKp46 in response to MTX **(Figure 3F)**. To confirm the transcription of the ILC3 activation-associated cytokines in an *in vivo* setting we analyzed the intestines of Rag1$^{-/-}$ mice in the presence or absence of Thy1$^+$ cells. Transcript analysis of total ileum, or protein analysis after overnight ileal explant cultures clearly showed that the presence of Thy1$^+$ cells was essential for generation of transcripts for *Csf2*, *Tnf*, *Il22*, *Ltb* and *Ifng* **(Figure 3G)**, as well as protein for both IL-22 and GM-CSF **(Figure 3H)** in response to intestinal tissue damage.

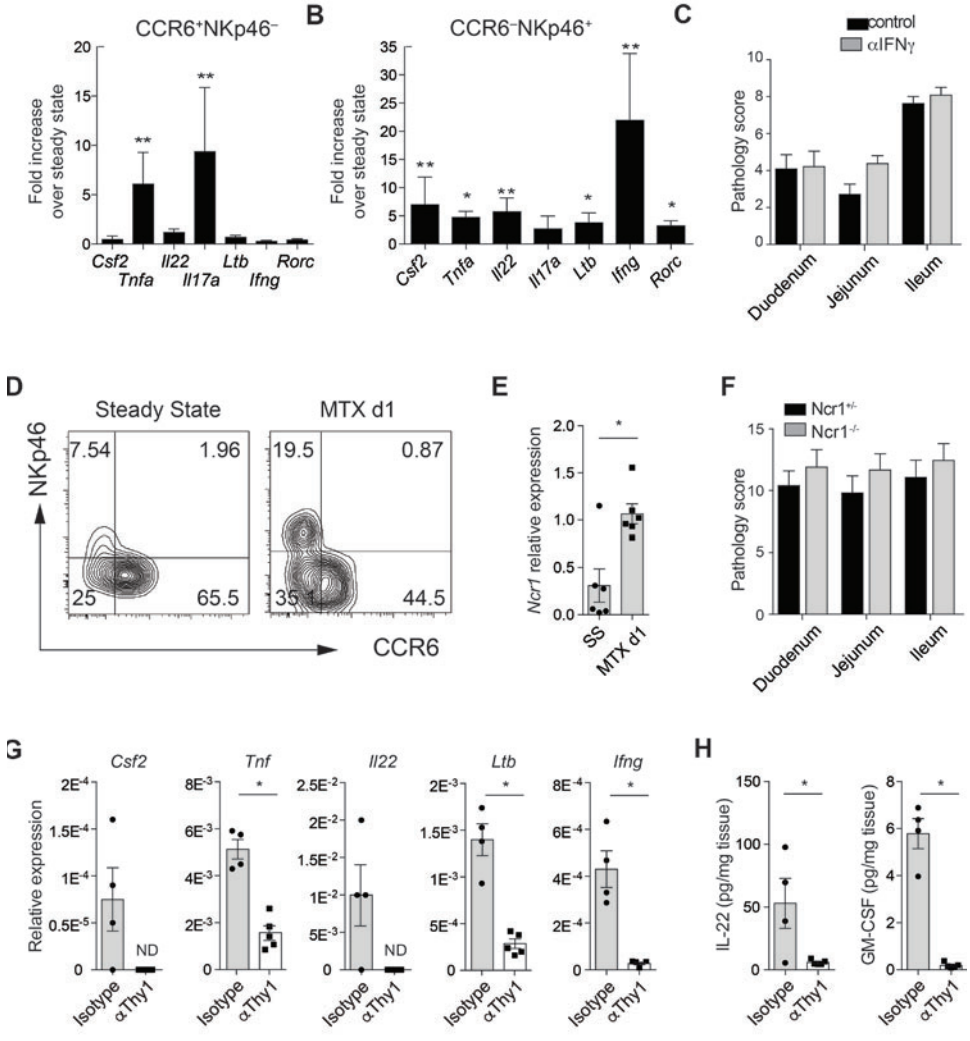

Figure 3. ILC3s are activated upon MTX-induced damage. Fold induction of indicated transcripts relative to steady-state of lamina propria (A) CCR6^{+}NKp46^{-}ILC3 and (B) CCR6^{-}NKp46^{+} ILC3, at day 1 after MTX. (C) Pathology score at day 4 after MTX of ileum of Rag1$^{-/-}$ mice treated with neutralizing IFNγ or isotype control antibodies. (D) Representative flow cytometry plot of NKp46 and CCR6 expression on lamina propria ILC3 at steady state and day 1 after MTX. (E) Transcript levels of *Ncr1* relative to *Gapdh* from sorted CCR6^{-}NKp46^{+} ILC3. (F) Pathology score at day 4 after MTX of ileum of Ncr1$^{+/-}$ or Ncr1$^{-/-}$ mice. (G) Transcriptional analyses of indicated genes relative to *Gapdh* from ileum of isotype control or Thy1-depleted Rag1$^{-/-}$ mice at day 1 after MTX. (H) Protein levels of IL-22 and GM-CSF after overnight ileal explant cultures isolated at day 1 after MTX. (A, B, D, E: 4-6 independent experiments, N=5-7 per time point; C, F: 2 independent experiment, N= 2-4 per group; G, H: 2 independent experiments, N=2-3 per group) *, P<0.05; **, P<0.01. ND, not detected.

ILC3 deficiency aggravates MTX-induced damage

Depletion of Thy1^{+} cells diminished regeneration of crypt cells and activation of epithelial Stat3 in response to MTX and ILC3s were activated early after tissue damage. However, because Thy1 antibodies do not specifically target ILC3s we next exposed ILC3-deficient RORγt$^{-/-}$ mice to MTX to confirm that ILC3s are responsible for the observed damage-associated epithelial responses. RORγt$^{-/-}$ mice showed impaired recovery of the cycling crypt compartment at day 4 after MTX **(Figures 4A-B)** and intestinal epithelial cells in RORγt$^{-/-}$ mice did not show phosphorylation of Stat3 in response to tissue damage **(Figure 4C)**. Consequently, Stat3 signaling was reduced as evidenced by lower levels of *Socs3* transcripts **(Figure 4D)**. In contrast, induction of *Wnt5a* transcription was independent of ILC3 and occurred normal in RORγt-/- mice **(Figure 4E)**.

Histological analysis of the small intestines of MTX-exposed RORγt$^{-/-}$ mice revealed a slight increase in overall pathology at day 4 after MTX **(Figure 4F)**. The differences in overall pathology between WT and RORγt$^{-/-}$ mice did not reach statistical significance, even though there seemed to be a trend towards increased of pathology in RORγt$^{-/-}$ mice at day 4 **(Figure 4G)**.

To understand this trend, we performed differential pathology scoring on intestinal villus and crypt compartments. This revealed a significant increase in the damage sustained by the small intestinal crypts in RORγt$^{-/-}$ mice compared to control mice **(Figure 4H)**. The extent of crypt epithelial flattening, the presence of crypt abscesses and the eventual loss of crypts were all significantly increased in the absence of RORγt **(Figure 4I)**. Survival of epithelial cells in response to tissue damage is regulated by the balance between several pro- and anti-apoptotic molecules[30]. To assess whether this balance was shifted in the absence of RORγt we determined transcript levels of the pro-apoptotic gene *Bax* and the anti-apoptotic gene *Bcl2l1* (BclXL) in ileum **(Figure 3G)**. In RORγt$^{-/-}$ mice, one day after MTX, the *Bax*-*Bcl2l1* ratio was significantly increased, indicating a shift towards a more pro-apoptotic program in the absence of ILC3s.

Combined, these data suggest that the absence of RORγt^{+} ILC3s augments tissue damage to the stem cell-containing intestinal crypts in response to MTX.

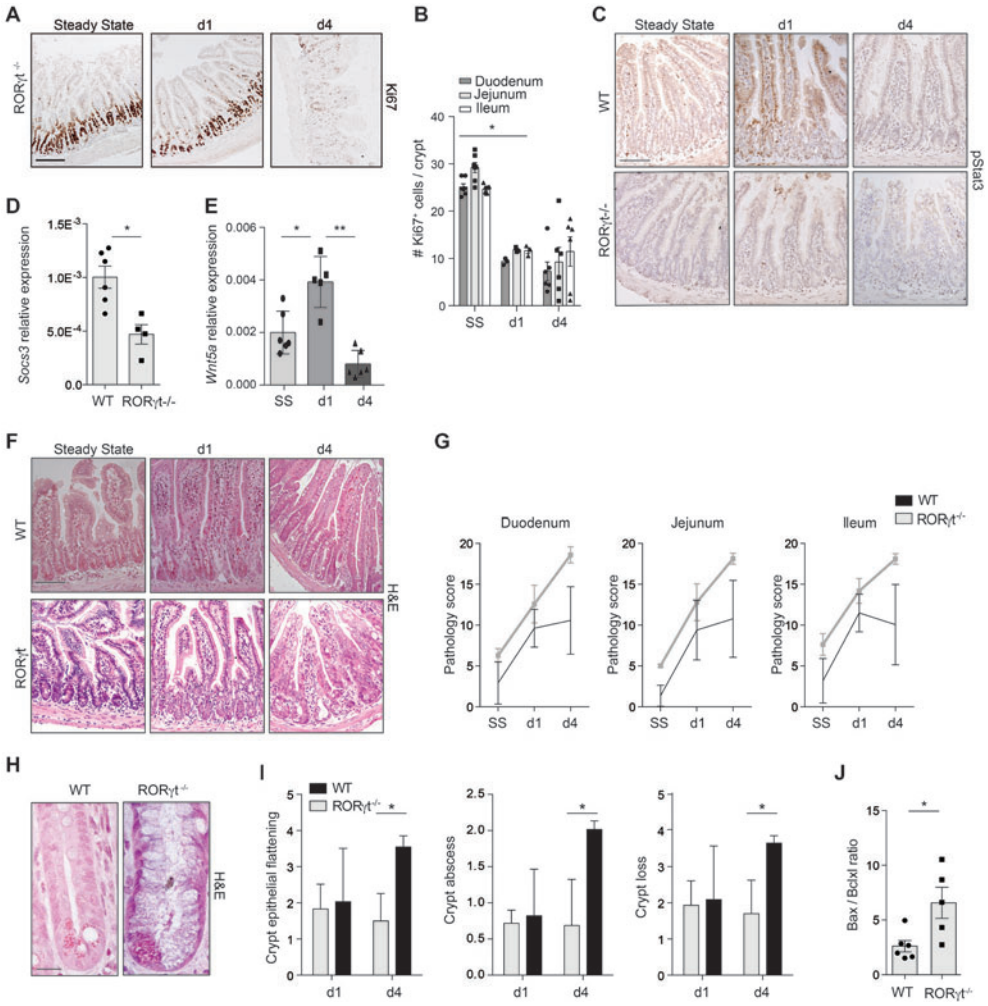

Figure 4. Absence of RORγt augments crypt damage after MTX. (A) Ki67 in ileum sections of RORγt$^{-/-}$ mice at indicated time points. (B) Number of Ki67^{+} cells in crypts of RORγt$^{-/-}$ mice at indicated time points. (C) pStat3 in ileum sections from WT and RORγt$^{-/-}$ mice at indicated time points. (D) *Socs3* transcripts relative to *Gapdh* from ileum of WT and RORγt$^{-/-}$ mice at day 1 after MTX. (E) *Wnt5a* transcripts from ileum of RORγt$^{-/-}$ mice at indicated time points. (F) Representative H&E staining of ileal sections at the indicated time points. (G) MTX-induced small intestinal damage in WT and RORγt$^{-/-}$ mice as specified in materials and methods. (H) Representative high-power magnification of ileal crypts of WT and RORγt$^{-/-}$ mice 4 days after MTX. (I) Crypt damage in WT and RORγt$^{-/-}$ mice at day 1 and day 4. (J) Ratio between *Bax* and *Bcl2l1* transcript levels in ileum of WT and RORγt$^{-/-}$ mice at day 1 after MTX. (A, B: 2 independent experiments, N=3-4 per group; C, D, F-I: 2-4 independent experiments, N=2-5 per group; E, J: 2 independent experiments, N=2-3 per group) *, P<0.05 **, P<0.01. Bars, 50μm (A, C and F), 10μm (H).

ILC3s preserve intestinal stem cells after tissue damage

A prerequisite for epithelial regeneration is the presence of crypt-residing ISCs[31]. Since RORγt$^{-/-}$ mice exposed to MTX had increased crypt pathology and reduced crypt proliferation, we investigated the fate of Lgr5^{+} ISCs in response to MTX. In order to determine whether Lgr5^{+} ISCs are sensitive to MTX, we exposed Lgr5-eGFP reporter mice to MTX and assessed the percentage of GFP^{+} cells in purified crypts of duodenum, jejunum and ileum at several time points post treatment **(Figure 5A)**. Lgr5^{+} ISCs numbers declined directly after treatment, indicating that ISCs were targeted by MTX. Stem cell recovery started after day 4 and numbers normalized by day 6 **(Figure 5A)**. To investigate the role of RORγt-expressing ILC3s in epithelial stem cell maintenance, we generated radiation bone-marrow chimeras by transferring either wild type or RORγt-deficient bone marrow into lethally irradiated Lgr5-eGFP recipient mice. To eliminate host-derived radio-resistant ILC3s, both groups were treated with depleting anti-Thy1 antibodies. Such RORγt$^{-/-}$-Lgr5-eGFP chimeric mice provide a model to study GFP-labeled Lgr5^{+} ISCs in the absence of RORγt^{+} hematopoietic cells. In response to MTX, RORγt$^{-/-}$-Lgr5-eGFP chimeric mice developed increased intestinal pathology compared to WT chimeric mice **(Figure 5B and C)** as characterized by crypt epithelial flattening, crypt abscesses and crypt loss **(Figure 5D)**, resembling the pathology in RORγt-deficient mice. To determine the effect of absence of RORγt^{+} lymphocytes on ISCs we purified small intestinal crypts from RORγt sufficient and deficient chimeric mice. At steady state, the percentages of Lgr5-eGFP^{+} cells were comparable between both groups **(Figure 5E)**. At day 4 after MTX, flow cytometric analyses revealed a significant reduction in the percentage of Lgr5-eGFP^{+} ISCs within the EpCAM-1^{+} crypt epithelial cell fraction **(Figure 5F)**. This reduction in Lgr5^{+} ISCs occurred along the entire length of the small intestine. In duodenum, jejunum and ileum Lgr5^{+} ISCs were reduced by 68% (68.3 ±3.1), 71% (71.2±1.4) and 52% (52.1±8.1) respectively **(Figure 5G)**, highlighting the importance of RORγt^{+} ILC3s as guardians of intestinal stem cells after damage.

IL-22 is an ILC3 signature cytokine involved in communication between ILC3s and crypt epithelial cells[23] and is transcribed after MTX-induced damage. To determine whether IL-22 mechanistically links ILC3s to stem cell maintenance after damage we used antibodies to neutralize this cytokine during MTX treatment. IL-22 blockade led to a significant loss of stem cell maintenance in the duodenum, while ISC numbers in jejunum and ileum were less affected **(Figure 5J-K)**. These data indicate that IL-22 is one of the factors involved in stem cell maintenance after tissue damage.

Collectively our findings reveal that ILC3s preserve organ-specific stem cells in response to tissue insult. MTX application evokes a rapid and transient activation of epithelial Stat3, followed by epithelial regeneration in a Thy1^{+}RORγt^{+} cell-dependent manner. Multiple subsets of ILC3s respond to intestinal tissue damage and absence of ILC3s aggravates pathology in intestinal crypts. Importantly, we could show that the maintenance of intestinal stem cells after cytotoxic therapy is regulated by ILC3s and that mechanistically, IL-22 is one of the

effector molecules involved. Our findings thus highlight a previously unappreciated feature of ILC3s in coordinating epithelial responses to tissue damage in the small intestine. Their location in close proximity to the crypts and their resistance to chemo- and radiotherapy-induced cell death put ILC3s in the ideal position to minimize tissue damage after cytotoxic insult and controlling ILC3 responses might hold the key to designing future therapeutic strategies aimed at minimizing intestinal damage in patients undergoing anti-cancer therapies.

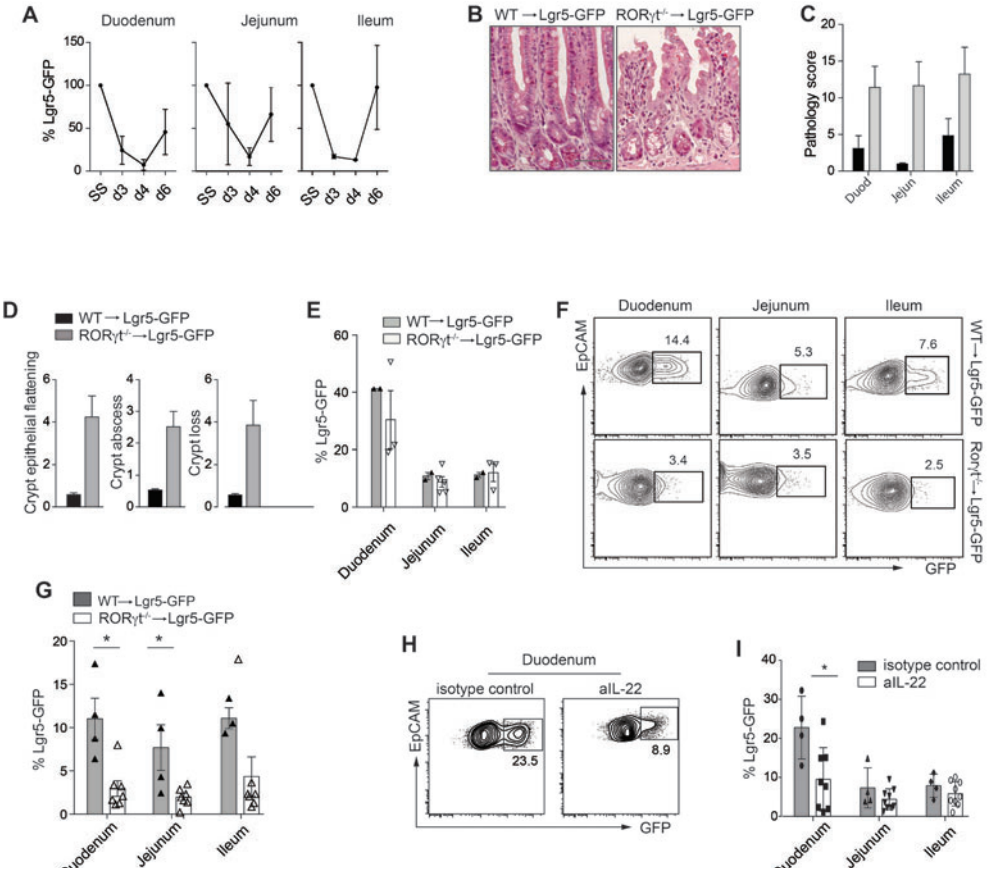

Figure 5. ILC3s preserve intestinal stem cells after MTX-induced damage. (A) Percentage of GFP$^+$ stem cells within EpCAM1$^+$ cells from purified intestinal crypts at the indicated time points. (B) Representative H&E staining of ileal sections of WT and RORγt$^{-/-}$ chimeras at day 4 after MTX. (C) Small intestinal damage in WT and RORγt$^{-/-}$ chimeras at day 4 after MTX as described in materials and methods. (D) Crypt pathology score. (E) Frequency of GFP$^+$ cells from WT and RORγt$^{-/-}$ chimeras at homeostasis. (F) Representative plots of purified crypts of WT and RORγt$^{-/-}$ chimeras at day 4 after MTX. Numbers adjacent to outlined areas indicate percent of EpCAM$^+$Lgr5-eGFP$^+$ cells. (G) Frequency of GFP$^+$ cells from WT and RORγt$^{-/-}$ chimeras at day 4 after MTX. (H) Representative plots of purified duodenal crypts at day 4 after MTX of Lgr5-eGFP mice treated with aIL-22 or control antibodies (I) Frequency of GFP$^+$ cells at day 4 after MTX from Lgr5-eGFP mice treated with aIL-22 or control antibodies (A: 2 independent experiments, N=2 per group; B-D, F, G: 2 independent experiments with 2-4 mice per group; E: 2 independent experiments, WT: N=1 per group, KO: N=1-3 per group; H, I: 2 independent experiments, 2-5 mice per group); *, P<0.05. Bars, 50μm

ACKNOWLEDGEMENTS

We are grateful to Reina Mebius (Amsterdam) and Ivo Touw (Rotterdam) for critical reading of the manuscript. Ncr1$^{gfp/gfp}$ mice were a kind gift from Ofer Mandelboim (Jerusalem, Israel) and neutralizing IL-22 antibody was a kind gift from Wenjun Ouyang (Genentech Inc.). This work was supported by ZonMW Innovative Research Incentives Vidi grant #91710377 to T.C. and by the People Program (Marie Curie Actions) of the European Union's Seventh Framework Program FP7/2007-2013 under REA grant agreement no. 289720. The authors declare no competing financial interests.

REFERENCES

1. Peterson, L. W. & Artis, D. Intestinal epithelial cells: regulators of barrier function and immune homeostasis. *Nat. Rev. Immunol.* **14,** 141–153 (2014).
2. Reddy, P. & Ferrara, J. L. M. Immunobiology of acute graft-versus-host disease. *Blood Rev.* **17,** 187–194 (2003).
3. Sonis, S. T. Pathobiology of mucositis. *Seminars in Oncology Nursing* **20,** 11–15 (2004).
4. Salim, S. Y. & Söderholm, J. D. Importance of disrupted intestinal barrier in inflammatory bowel diseases. *Inflammatory Bowel Diseases* **17,** 362–381 (2011).
5. Grivennikov, S. *et al.* IL-6 and Stat3 Are Required for Survival of Intestinal Epithelial Cells and Development of Colitis-Associated Cancer. *Cancer Cell* **15,** 103–113 (2009).
6. Heneghan, A. F., Pierre, J. F. & Kudsk, K. A. JAK-STAT and intestinal mucosal immunology. *Gut Microbes* **5,** 1–8 (2014).
7. Bollrath, J. *et al.* gp130-Mediated Stat3 Activation in Enterocytes Regulates Cell Survival and Cell-Cycle Progression during Colitis-Associated Tumorigenesis. *Cancer Cell* **15,** 91–102 (2009).
8. Ernst, M., Thiem, S., Nguyen, P. M., Eissmann, M. & Putoczki, T. L. Epithelial gp130/Stat3 functions: An intestinal signaling node in health and disease. *Seminars in Immunology* **26,** 29–37 (2014).
9. Pickert, G. *et al.* STAT3 links IL-22 signaling in intestinal epithelial cells to mucosal wound healing. *J. Exp. Med.* **206,** 1465–72 (2009).
10. Anderson, C. A. *et al.* Meta-analysis identifies 29 additional ulcerative colitis risk loci, increasing the number of confirmed associations to 47. *Nat. Genet.* **43,** 246–252 (2011).
11. Demaria, M., Misale, S., Giorgi, C., Miano, V., Camporeale, A., Campisi, J., Pinton, P. & Poli, V. STAT3 can serve as a hit in the process of malignant transformation of primary cells. *Cell Death Differ.* **19,** 1390–1397 (2012).
12. Gunther, C., Neumann, H., Neurath, M. F. & Becker, C. Apoptosis, necrosis and necroptosis: cell death regulation in the intestinal epithelium. *Gut* 1062–1071 (2012).
13. Potten, C. S., Al-Barwari, S. E. & Searle, J. Differential Radiation Response Amongst Proliferating Epithelial Cells. *Cell Prolif.* **11,** 149–160 (1978).
14. Ritsma, L., Ellenbroek, S. I. J., Zomer, A., Snippert, H. J., de Sauvage, F. J., Simons, B. D., Clevers, H. & van Rheenen, J. Intestinal crypt homeostasis revealed at single-stem-cell level by in vivo live imaging. *Nature* **507,** 362–365 (2014).
15. Sato, T. *et al.* Single Lgr5 stem cells build crypt-villus structures in vitro without a mesenchymal niche. *Nature* **459,** 262–5 (2009).
16. Matthews, J. R., Sansom, O. J. & Clarke, A. R. Absolute requirement for STAT3 function in small-intestine crypt stem cell survival. *Cell Death Differ.* **18,** 1934–1943 (2011).
17. Artis, D. & Spits, H. The biology of innate lymphoid cells. *Nature* **517,** 293–301 (2015).
18. Spits, H. & Cupedo, T. Innate Lymphoid Cells: Emerging Insights in Development, Lineage Relationships, and Function. *Annu. Rev. Immunol.* **30,** 647–675 (2012).
19. Reynders, A. *et al.* Identity, regulation and in vivo function of gut NKp46+RORgammat+ and NKp46+RORgammat- lymphoid cells. *EMBO J* **30,** 2934–2947 (2011).
20. Sawa, S., Cherrier, M., Lochner, M., Satoh-Takayama, N., Fehling, H. J., Langa, F., Di Santo, J. P. & Eberl, G. Lineage Relationship Analysis of ROR t+ Innate Lymphoid Cells. *Science (80-.).* **330,** 665–9 (2010).
21. Satoh-Takayama, N., Serafini, N., Verrier, T., Rekiki, A., Renauld, J. C., Frankel, G. & DiSanto, J. P. The chemokine receptor CXCR6 controls the functional topography of interleukin-22 producing intestinal innate lymphoid cells. *Immunity* **41,** 776–788 (2014).

22. Kanamori, Y., Ishimaru, K., Nanno, M., Maki, K., Ikuta, K., Nariuchi, H. & Ishikawa, H. Identification of novel lymphoid tissues in murine intestinal mucosa where clusters of c-kit+ IL-7R+ Thy1+ lympho-hemopoietic progenitors develop. *J. Exp. Med.* **184,** 1449–1459 (1996).

23. Hanash, A. M. *et al.* Interleukin-22 protects intestinal stem cells from immune- mediated tissue damage and regulates sensitivity to graft vs. host disease. *Immunity* **37,** 339–350 (2012).

24. Visentin, M., Zhao, R. & Goldman, I. D. The Antifolates. *Hematology/Oncology Clinics of North America* **26,** 629–648 (2012).

25. de Koning, B. A. E. *et al.* Contributions of mucosal immune cells to methotrexate-induced mucositis. *Int. Immunol.* **18,** 941–949 (2006).

26. Frank, M., Hennenberg, E. M., Eyking, a., Runzi, M., Gerken, G., Scott, P., Parkhill, J., Walker, a. W. & Cario, E. TLR Signaling Modulates Side Effects of Anticancer Therapy in the Small Intestine. *J. Immunol.* **194,** 1983–1995 (2015).

27. Verburg, M., Renes, I. B., Van Nispen, D. J. P. M., Ferdinandusse, S., Jorritsma, M., Büller, H. A., Einerhand, A. W. C. & Dekker, J. Specific responses in rat small intestinal epithelial mRNA expression and protein levels during chemotherapeutic damage and regeneration. *J. Histochem. Cytochem.* **50,** 1525–1536 (2002).

28. Miyoshi, H. *et al.* Wnt5a Potentiates TGF- Signaling to Promote Colonic Crypt Regeneration After Tissue Injury. *Science (80-.).* **338,** 108–13 (2012).

29. Klose, C. S. N. *et al.* A T-bet gradient controls the fate and function of CCR6−RORγt+ innate lymphoid cells. *Nature* **494,** 261–265 (2013).

30. Vereecke, L., Beyaert, R. & van Loo, G. Enterocyte death and intestinal barrier maintenance in homeostasis and disease. *Trends in Molecular Medicine* **17,** 584–593 (2011).

31. Potten, C. S. A comprehensive study of the radiobiological response of the murine (BDF1) small intestine. *International Journal of Radiation Biology* **58,** 925–973 (1990).

3

GROUP 3 INNATE LYMPHOID CELLS DIRECT YAP1-MEDIATED REGENERATION OF INTESTINAL CRYPTS AFTER TISSUE DAMAGE

Mónica Romera-Hernández[1], Patricia Aparicio-Domingo[1], Julien J. Karrich[1], Ferry Cornelissen[1], Natalie Papazian[1], Remco M. Hoogenboezem[1], Janneke N. Samsom[2] and Tom Cupedo[1]

[1]Department of Hematology, Erasmus University Medical Center, Rotterdam, The Netherlands
[2]Department of Pediatrics, Division of Gastroenterology, Erasmus University Medical Center, Rotterdam, The Netherlands

Manuscript in preparation

ABSTRACT

Intestinal injury provokes an epithelial response aimed at rapidly restoring the intestinal barrier by proliferation and differentiation of epithelial stem cells contained within the small intestinal crypts. Intestinal repair was long thought of as an epithelial-autonomous process, yet recently we identified a role for group 3 innate lymphoid cells (ILC3s) in crypt regeneration after stem cell damage. Here, using IL-22-deficient mice, IL-22 neutralizing antibodies and Stat3 inhibition we show that IL-22 is dispensable for ISC proliferation and intestinal regeneration following stem cell injury. Based on these findings we hypothesized that ILC3s modulate damage-driven stem cell-specific signaling pathways independently of IL-22. To identify ILC3-regulated ISCs responses upon injury we generated ILC3-deficient Lgr5-reporter mice, induced stem cell damage and analyzed transcriptional changes in Lgr5^{hi} ISCs by RNA-sequencing. In ILC3-deficient mice, Yap1-induced stem cell reprograming, which is essential for crypt regeneration, is blunted: Lgr5^{hi} ISCs fail to downregulate Wnt and Notch signaling and become unable to regulate their stemness versus secretory cell differentiation gene programs. Finally, we identify IL-6/IL-11 as a possible mechanism controlling Yap1 induction in crypt epithelial cells. In sum, our findings reveal an important role for ILC3s in controlling the evolutionary conserved Yap1 pathway of crypt regeneration, highlighting a previously unappreciated layer of epithelial regulation dependent on cells of the innate immune system.

INTRODUCTION

The mucosa of the gastrointestinal tract (GI) provides a physical barrier that separates the luminal content of the intestine from the underlying immune system. Any discontinuity in the epithelial barrier can lead to bacterial translocation and elicits an immune response, concomitantly resulting in further epithelial injury. Therefore, maintenance of the epithelial barrier is of critical importance.

Innate lymphoid cells (ILCs) are well known for their role in epithelial homeostasis and innate immunity. Recently, we identified group 3 ILCs (ILC3s) as architects of tissue damage responses after experimental chemo-therapy. Intestinal ILC3s are strategically localized in anatomically well-defined structures called cryptopatches, positioned directly adjacent to epithelial crypts. In the crypts of Lieberkühn, intestinal epithelial stem cells (ISCs) are responsible for the continuous replenishment of the epithelial barrier. ISCs give rise to rapidly dividing transit-amplifying (TA) cells[1], from which six different lineages of mature epithelial cells derive: absorptive enterocytes, goblet cells, Paneth cells, microfold (M) cells, Tuft cells and enteroendocrine cells[2,3].

ILC3s are required for the maintenance of Lgr5^{+} ISC frequencies during *in vivo* regenerative responses in a model of methotrexate (MTX)-induced small intestinal damage[4]. Interleukin-22 (IL-22), produced by ILC3s, is one of the factors involved in controlling Lgr5^{+} ISCs after damage but also after murine allogenic bone marrow transplantation (BMT)[5]. In addition, absence of ILC3s leads to a loss of proliferative cells in the crypts during the recovery phase, precluding normal tissue repair. The underlying mechanisms for ILC3-dependent intestinal regeneration remain unidentified.

Epithelial intrinsic and extrinsic mechanisms regulate ISC self-renewal and differentiation of daughter cells. In particular, the Wnt and Notch signaling pathways are important for stem cell proliferation and differentiation[6–8]. At the bottom of the crypts, Wnt and Notch ligands promote ISC proliferation and suppress differentiation[9,10,11]. Loss of Notch activity in progenitor cells shifts differentiation towards secretory rather than absorptive cell fate specification[12,13]. Besides these master regulators of ISC function, bone morphogenic protein (BMP), Hedgehog, Ephrin, JAK/STAT1, PTEN, AKT and PI3K signaling pathways are all involved in the regulation of ISC function[12,14–17].

Here, we set out to identify the mechanisms of intestinal regeneration controlled by ILC3s. We show that IL-22 signaling is dispensable for crypt recovery but that in the absence of ILC3s, Lgr5^{+} ISCs fail to activate regenerative Yap1 signaling, a critical pathway involved in early stem cell responses upon injury. Our findings highlight a previously unappreciated layer of epithelial regulation by cells of the innate immune system.

MATERIALS AND METHODS

Mice. C57BL/6, RORγt-GFP, IL-22$^{-/-}$, Lgr5-GFP-IRES-creERT2 (Lgr5-GFP) and Lgr5-GFP/RORγt-GFP mice were bred in the animal facility of the Erasmus University Medical Center Rotterdam. Animal experiments were approved by the relevant authorities and procedures were performed in accordance with institutional guidelines. Age and gender-matched littermates were used whenever possible.

Methotrexate (MTX). 8-12 weeks old mice were injected i.p. with 120mg/kg MTX (PCH) at day-1 and with 60mg/kg at day 0. Tissues were collected at day 1 and day 4 after the last MTX injection.

Cytokine neutralization. 150μg of anti-IL-22 antibody (8E11, Genentech) or mouse IgG1 isotype control (MOPC-21, BioXcell) were administered i.p to Lgr5-GFP$^{+/-}$ mice every 2 days, starting 4 days before the first MTX dose, until day 2 after the last MTX dose. 200μg of anti-IL-6 antibody (MP5, BioXcell) or Rat IgG isotype control (GL113, BioXcell) were administered i.p to WT mice at day-1 and day 0 for MTX d1 analysis and at day-1, day 0 and day 2 for MTX d4 analysis.

Drug administration. Stattic (Sigma) was injected at MTX d-1 and MTX d0 at 0.5mg/ml dissolved in 2.5% DMSO. Control mice were injected with 2.5% DMSO. Verteporfin (Selleckchhem) and PP2 (Sigma) were administered at MTX d-1 and MTX d0 for analysis at MTX d1. One extra dose at MTX d1 was given to mice that where sacrificed at MTX d4. Verteporfin was dissolved at a final concentration of 10mg/injection and PP2 at 1mg/injection. Both were dissolved in 10% DMSO. Control mice received 10% DMSO. LMT-28 was dissolved in pure ethanol and was diluted 5x with saline and injected i.p at a dose of 20mg/kg per mouse, on the same day as the first injection of MTX. Control mice were given the same quantity in volume of saline containing 20% of pure ethanol.

Crypt isolation. Isolation of intestinal crypts was performed as previously described[18]. Briefly, isolated small intestines were opened longitudinally and washed with cold PBS. Tissues were cut into 5mm pieces and subsequently washed by mechanical pipetting with cold PBS until supernatant was clear. Tissues were incubated with EDTA (2mM) in PBS at 4°C for 30 min. Tissues were then washed with several times with cold PBS and suspended by vigorous shacking. Crypt-enriched sediments were passed through a 70μm cell strainer and centrifuge at 200g for 2 min to separate the crypts from single cells. Crypts were incubated with 1 ml of TrypLE Express (Gibco) + Dnase I (Merk Millipore) at 37°C for 10-15min until crypt dissociation was observed. Single cell suspensions were washed with Advanced DMEM/F12 media (ThermoFisher) and filtered through 40um cell strainer and stained with conjugated antibodies. Samples were analyzed by FACS ARIAIII, BD.

Antibodies. Monoclonal antibodies used for flow cytometry were: CD45 (MCD4517; LifeTechnologies), CD19-bio (1D3; eBioscience), B220-bio (RA3-6B2; eBioscience), CD11c-bio (N418; eBioscience), CD11b-bio (M1/70; BioLegend), Gr1-bio (RB6-8C5; eBioscience), CD3 (145-2C11; BD), CD90.2 (30H12; BioLegend), NK1.1 (PK136; eBioscience), CD127 (A7R34, eBioscience), CD117 (2B8; Biolegend), NKp46 (29A1.4; eBioscience), CCR6 (29-2L17; BioLegend). EpCAM-1 (G8.8; BioLegend); CD45 (30F11; Invitrogen), CD24 (M1/69; BioLegend), CD31 (390; BioLegend), Ter119 (TER-119; BioLegend).
Antibodies used for paraffin immunostaining were: rat anti-mouse Ki67 monoclonal antibody (MIB-5, Dako), Rabbit anti-mouse Yap1 antibody (D8H1X, Cell signaling), Rabbit anti-mouse ChgA (NB120-15160, Novus).

Flow cytometry and cell sorting. Cells were incubated with Zombie Aqua Fixable Viability dye (BioLegend) prior to staining or 7AAD (Beckman coulter) before acquisition, depending on the staining panel. Fc block was performed by incubation with normal mouse serum and rat-anti-mouse CD16/CD32 (2.4G2; BD). All stainings were performed in PBS containing 2% heat-inactivated fetal calf serum (FCS) at 4°C. Labelled cells were analyzed using FACS LSRII (BD Biosciences) and data processed with Flow software (Flow, LLC).

RNA sequencing. cDNA was prepared using SMARTer Ultra Low RNA kit (Clontech Laboratories) for Illumina Sequencing following the manufacturer's protocol. The Agilent 2100 Bio-analyzer and the High Sensitivity DNA kit were applied to determine the quantity and quality of the cDNA production. Amplified cDNA was further processed according to TruSeq Sample Preparation v.2 Guide (Illumina) and paired end-sequenced (2x75bp) on the HiSeq 2500 (Illumina). Demultiplexing was performed using CASAVA software (Illumina) and the adaptor sequences were trimmed with Cutadapt (http://code.google.com/p/cutadapt/). Alignments against the mouse genome (mm10) and analysis of differential expressed genes were performed with DESeq2 in the R environment on the raw fragment counts extracted from the BAM files by HTSeq-count[19]. Cufflinks software was used to calculate the number of fragments per kilobase of exon per million fragments mapped (FPKM) for each gene. Principle component analysis was performed on the fragment counts using the R environment. Finally, gene set enrichment analysis (GSEA, Broad Institute) was performed on the FPKM values using the curated C2 collection of gene sets within MSigDB[20].

Histology. Small intestinal tissue pieces (5mm) or Swiss rolls were fixed in 4% PFA (4h, RT), washed in 70% ethanol and embedded in paraffin. Four-µm sections were deparaffinized and stained with hematoxylin (Vector Laboratories) and eosin (Sigma-Aldrich). For Ki67, Yap1 and ChgA detection, endogenous peroxidases were blocked in 1% periodic acid in deionized water for 20 min, and antigen retrieval was achieved by microwave treatment in citrate

buffer (10mM, pH 6.0). Prior to staining, Fc receptors were blocked in 10% normal mouse serum and 10% of normal serum matching the same host species in which the secondary antibody is raised, 10 mM Tris buffer, 5 mM EDTA, 0.15 M NaCl, 0.25% gelatin, and 0.05% Tween-20 (pH 8.0). Tissue sections were incubated overnight at 4°C with primary antibodies in PBS supplemented with 2% normal mouse serum. Immunoreactions were detected using biotinylated donkey anti-rat (Dako) and goat-anti-rabbit (Vector Laboratories) and incubated with the Vectastin ABC Elite Kit (Vector Laboratories) and 3,3'-diaminobenzidine tetrahydrochloride (Sigma-Aldrich). Sections were counterstained with hematoxylin. The analysis of pathology, $Ki67^+$ cells and Yap1 localization were performed blinded by at least two independent analysts. Pathology was scored as previously described[21] and Ki67-expressing cells were counted in 7 to 15 crypts per section. Pictures were taken with a Leica DFC350 FX microscope.

Isolation of lamina propria lymphocytes. Isolated small intestine was opened longitudinally and washed with cold HBSS containing Hepes (15 mM), pH 7.2. Tissues were cut in 1 cm pieces and incubated in HBSS buffer containing 10% FBS, 15 mM Hepes, 5 mM EDTA, and 1 mM DTT (pH 7.2) at 37°C two times for 20 min to remove epithelium and intraepithelial lymphocytes. The tissues were digested with Collagenase VIII (100U/ml, Sigma) in RPMI containing 10% FCS, 15 mM Hepes, 100 U/ml Penicillin-Streptomycin, and 1 mM DTT, pH 7.2, at 37°C in a shaker, two times for 1 hour. Supernatants were passed through a 70µm cell strainer and washed in cold HBSS. Pellets were suspended in 90% Percoll (GE Healthcare), overlaid with 40% Percoll and centrifuge at 1800rpm for 20 min to allow separation of mononuclear cells (MNC) by density gradient. Interphase was washed and stained with conjugated antibodies.

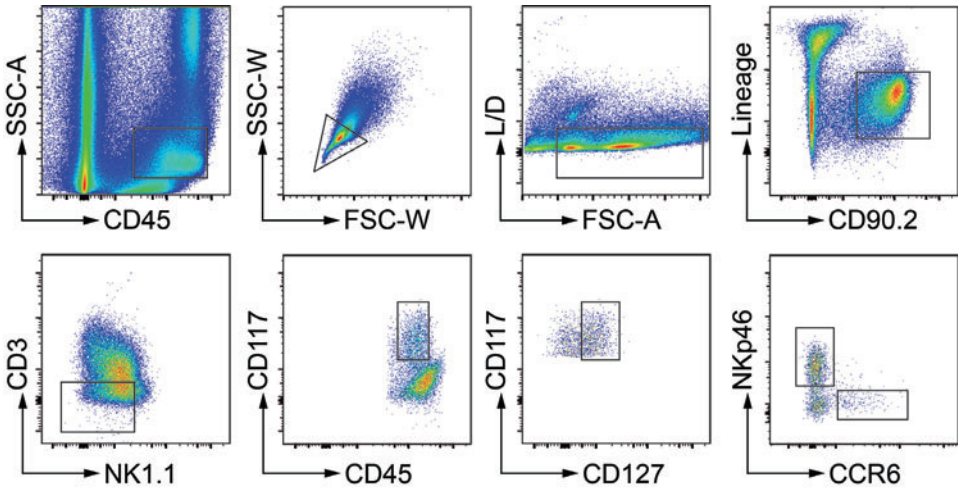

ILC3 FACS-Sort analysis: Lamina propria lymphocytes were analyzed by flow cytometry (FACS ARIAIII, BD) and CCR6^{+} ILC3s were sorted as indicated.

Transcript analysis. RNA was extracted using the NucleoSpin RNA XS kit (Machery Nagel). RNA from sorted cells was amplified according to the manufacturer's protocol (Ovation PicoSL WTA System V2, NuGen). For quantitative PCR, a Neviti Thermal Cycler (Applied Biosystems) and SensiFAST SYBR Lo-Rox kit (BioLine) were used were used, with the addition of $MgCl_2$ to a final concentration of 4 mM. All reactions were done in duplicate and normalized to the expression of *Gapdh*. Relative expression was calculated by the cycling threshold (CT) method as $2^{-\Delta CT}$. The primers sequences can be found in Table 1 (see below).

Table S1. Primer sequences

Gene	***Forward Primer***	***Reverse primer***
Reg3b	GCCTGATGCTCTTATCTC	AAGGCATAGCAGTAGGAG
Defa5	CCACAAAACAGATGAAGAGAC	TCTTTTGCAGCCTCTTATTC
Reg3g	CCATCTTCACGTAGCAGC	CAAGATGTCCTGAGGGC
Gapdh	TCAACGGCACAGTCAAG	GCTCCACCCTTCAAGTG

Statistical analysis. Samples were analyzed using unpaired Mann-Whitney test. p values < 0.05 were considered significant. Data are shown as mean ± SEM.

RESULTS

MTX-induced pathology and regeneration depend on RORγt^{+} ILC3s but are not controlled by IL-22

In order to investigate the importance of ILC3-derived IL-22 to intestinal regeneration after damage, we exposed IL-22-deficient mice to MTX and compared this to the response in ILC3-deficient RORγt$^{-/-}$ mice. Four days after the last MTX injection, general pathology and specific crypt pathology were increased in RORγt$^{-/-}$ mice compared to littermate controls, whereas in IL-22$^{-/-}$ mice MTX-induced intestinal pathology was similar to that of littermate controls **(Figure 1a-c)**. Ki67 immunostaining revealed a strong reduction in the number of proliferating cells in small intestinal crypts of RORγt$^{-/-}$ mice but not of IL-22$^{-/-}$ mice, indicating that crypt regeneration is dependent on ILC3 presence, but independent of IL-22 **(Figure 1d)**. To substantiate these findings in additional models, we neutralized IL-22 or its downstream signaling molecule STAT3 in Lgr5-GFP$^{+/-}$ mice during MTX treatment. In these two models, we could assess both the maintenance of stem cells as well as the induction of crypt proliferation. Neutralization of IL-22 or STAT3 reduced *Reg3g* transcripts, indicating effective inhibition of IL-22 signaling in the crypt compartment **(Figure S1)**. Quantification of stem cell frequencies by flow cytometry four days after MTX confirmed the importance of IL-22 and STAT3 signaling for stem cell maintenance **(Figure 1f,h)**. In contrast, the number of Ki67^{+} cells was unaltered after neutralization of IL-22 or STAT3 **(Figure 1e,g)**. These data show that crypt regeneration and stem cell maintenance after MTX-induced damage are differentially regulated by ILC3s and that regeneration occurs in an IL-22 independent manner.

Figure 1: MTX-induced pathology and regeneration depend on RORγt^{+} ILC3s but are not controlled by IL-22. **(a)** Representative H&E staining of duodenal sections from RORγt$^{+/+}$, RORγt$^{-/-}$, IL-22$^{+/-}$ and IL-22$^{-/-}$ mice four days after MTX treatment. **(b)** Lamina propria/villi and **(c)** crypt pathology scores after MTX-induced tissue damage in RORγt$^{+/+}$, RORγt$^{-/-}$, IL-22$^{+/-}$ and IL-22$^{-/-}$ mice. **(d)** Representative Ki67 immunostaining and number of Ki67+ cells in small intestinal crypts from RORγt$^{+/+}$, RORγt$^{-/-}$, IL-22$^{+/-}$ and IL-22$^{-/-}$ mice four days after MTX treatment. **(e)** Representative Ki67 immunostaining and number of Ki67^{+} cells in duodenal crypts four days after MTX in Lgr5-GFP$^{+/-}$ mice treated with anti-IL-22 antibodies or isotype controls. **(f)** Representative FACS plots and frequency of Lgr5-GFP^{+} cells in duodenal crypt-derived cell suspensions four days after MTX from Lgr5-GFP$^{+/-}$ mice treated with anti-IL-22 antibodies or Isotype controls. **(g)** Representative Ki67 immunostaining and number of Ki67+ cells in duodenal crypts four days after MTX in Lgr5-GFP$^{+/-}$ mice treated with Stattic or DMSO control. or **(h)** Representative FACS plots and frequency of Lgr5-GFP^{+} cells in duodenal crypt-derived cell suspensions four days after MTX from Lgr5-GFP$^{+/-}$ mice treated with Stattic or DMSO control. Numbers adjacent to outlined areas indicate percent of Lgr5-GFP^{+} cells within Live(+) CD45(-) Ter119(-) CD31(-) EpCAM(+) cells. Mann-Whitney test *p<0.01; **p<0.001; non-significant (not indicated). Scale bars: 50μm (a,d,f,j); n=4-8 per group.

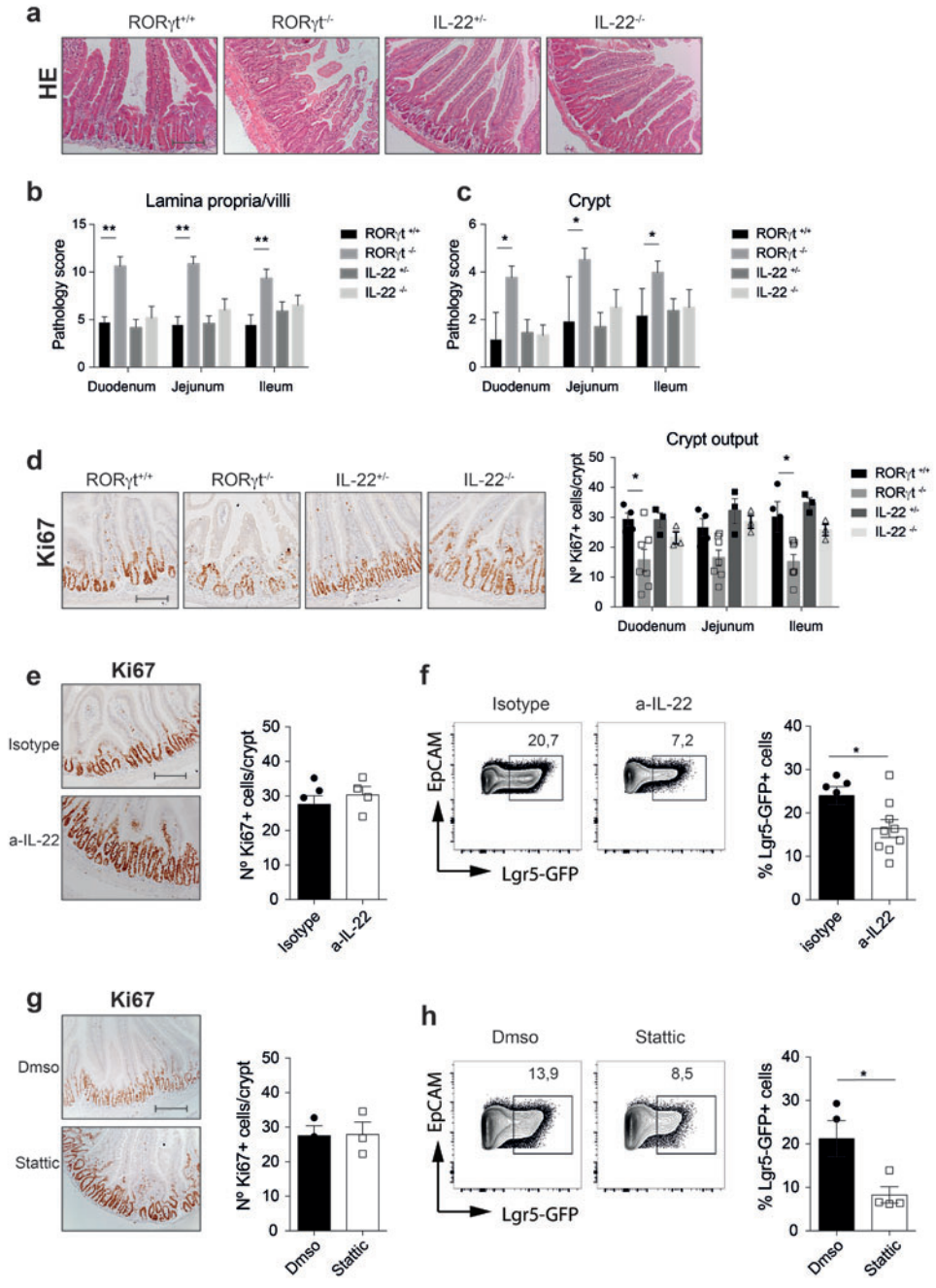
a
RORγt+/+
RORγt-/-
IL-22+/-
IL-22-/-
HE
b
Lamina propria/villi
Pathology score
Duodenum
Jejunum
Ileum
RORγt +/+
RORγt -/-
IL-22 +/-
IL-22 -/-
c
Crypt
d
Ki67
Crypt output
Nº Ki67+ cells/crypt
e
Isotype
a-IL-22
f
20,7
7,2
EpCAM
Lgr5-GFP
% Lgr5-GFP+ cells
g
Dmso
Stattic
h
13,9
8,5

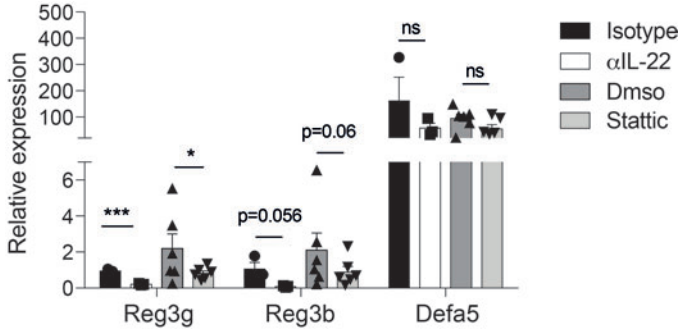

Figure S1: STAT3-target gene expression upon IL-22 neutralization and STAT3 inhibition. *Reg3g*, *Reg3b* and *Defa5* mRNA transcript expression relative to *Gapdh* in total crypts from Lgr5-GFP$^{+/-}$ mice after isotype, anti-IL-22, DMSO or Stattic treatment four days after MTX. Mann-Whitney test *p<0.05 and ***p<0.001; non-significant (ns); n=3-5 mice per group.

Intestinal damage induces a Yap1-driven regenerative response in stem cells

After damage, regeneration of ISCs is driven by evolutionarily conserved repair-promoting pathways that control stem cell survival, proliferation and differentiation. To identify the repair pathways relevant for regeneration after MTX-induced small intestinal injury we performed kinetic analysis of the stem cell transcriptome by RNA sequencing of Lgr5-GFP^{hi} intestinal stem cells at steady-state, one and four days after MTX. Principal component analysis (PCA) clearly demonstrated that the ISC gene expression signature after damage was significantly altered compared to steady-state (SS) **(Figure 2a).** Analysis of differentially expressed genes showed that 729 genes were significantly upregulated (adjusted p value <0.01) at day 1 after MTX compared to steady-state, whereas 692 genes were downregulated. Moreover, 532 genes were upregulated at day 4 after MTX compared to steady-state, and 282 genes were downregulated. 128 transcripts were upregulated both at one and four days after MTX and 142 transcripts were downregulated at both the indicated time points **(Figure 2b).** Yap1 is an effector molecule of the Hippo pathway, an evolutionarily conserved signaling pathway with key roles in regeneration after injury. Yap1 is a transcriptional co-activator of TEAD transcription factors, which control a gene-expression program that stimulates cell proliferation and differentiation. We identified strong upregulation of Yap1 target genes at MTX d1, including *Gprc5a*, *Tnfrsf12a*, *Areg*, *Il1rn* and *Clu*, indicating increased Yap1 activity early after MTX-induced epithelial injury. The majority of Yap1 target genes were still upregulated four days after MTX treatment, with the exception of *Tnfrsf12a* **(Figure 2c).** Yap1 can drive regeneration by temporal repression of Wnt signaling. One day after MTX treatment, Wnt target genes, such as *Axin2*, *Aqp4*, *Lgr5*, *Olfm4*, *Sp5*, *Ephb3* and *Ephb4* were downregulated. Similarly, four days after MTX treatment, all of these Wnt targets, except for *Ephb3* were still downregulated when compared to steady-state conditions **(Figure 2d)**. This suggests that Yap1 suppresses Wnt signaling, in line with previous reports[22]. Stem cell differentiation is associated with inhibition of Notch signaling, and transcription of the Notch target gene *Hes1* was downregulated in Lgr5-GFP^{hi} ISCs one and four days after MTX **(Figure S2a)**. In line with *Hes1*-mediated inhibition of *Atoh1*, *Atoh1* transcription increased at MTX day 4 **(Figure S2a)**. Expression of the receptor *Notch1* decreased after MTX treatment, whereas Notch ligands *Jagged-1, Dll1* and *Dll4* were not significantly altered upon MTX treatment **(Figure S2a).** Besides preserving stemness, Notch also determines cell fate decisions during differentiation. In order to gain further insights into the differentiation of stem cells towards different lineages during the immediate response to MTX we analyzed changes in transcription of genes associated with stemness or epithelial lineage specification. Transcripts associated with Lgr5^{+} intestinal stem cells, i.e. *Ascl2*, *Prom1* and *Kitl* were significantly downregulated at MTX d1, and *Ascl2* and *Kitl* further decreased at MTX d4 **(Figure 2e)**. Mex3a labels a slowly cycling subpopulation of Lgr5^{+} ISCs that help promoting regeneration following toxic insults. In our analysis, *Mex3a* target gene was detected at low levels within Lgr5-GFP^{hi} ISCs and its transcription was unchanged by MTX **(Figure 2e)**. Finally, the expression of other stem cell genes that mark reserve stem cell populations with important roles in epithelial

regeneration after injury were not changed during MTX, with the exception of *Lrig1,* which was downregulated one day after MTX (**Figure S2d)**. These results indicate that Lgr5^{+} ISCs are not differentially expressing genes characteristic to the reserve ISC population. Genes characteristic of differentiated enteroendocrine cells, such as *Neurog3* and *Nkx2-2* were detected at low levels in Lgr5-GFP^{hi} cells at steady-state but significantly increased one and four days after MTX **(Figure 2f)**. Other genes associated with enteroendocrine cells, such as *Chga*, *Sct*, *Ffar4*, *Reg4*, *Cldn4*, *Klf4* and *Guca2a* were induced four days after MTX **(Figure 2f)**. Paneth cell genes, such as *Lyz1*, *Xbp1*, *Reg3g*, *Defa21*, *Defa26*, *Wnt3*, *Spdef*, *Ccl6*, *Kit* and *Gfi1* and Goblet cell genes *Muc2*, *Spink4*, *RetnIIb*, *Agr2*, *Tff3* and *Hgfac* were all upregulated four days after MTX **(Figure S2e,f)**. In addition, flow cytometric analysis of small intestinal crypts revealed that the percentage of enteroendocrine cells increased one day after MTX and returned to steady-state frequencies at MTX day 4, whereas Paneth cell frequencies did not significantly change **(Figure 2g).** *Alpi*, a signature gene of terminally differentiated absorptive enterocytes remained constant during MTX (data not shown). Collectively, these results indicate that Lgr5-GFP^{hi} ISCs initiate differentiation towards the secretory cell lineage but not to the enterocyte lineage after MTX-induced stem cell damage, but likely loose GFP before terminal differentiation. Finally, we also observed an increase in the expression of *Bax, Ccnd1*, *Cdkn1a* and *Pcna* and a reduction of Bcl2l11, Cdkn1b and Ki67 after MTX, thus suggesting an alteration in the regulation of apoptosis and proliferation of Lgr5-GFP^{hi} ISCs. Although the apoptotic activator Bax was increased one day after MTX, another gene inducing apoptosis, Bcl2l11 decreased its expression after MTX. Thus, staining cleaved Casp3 is necessary to formally quantify whether apoptosis is increased in crypts after MTX treatment. Regarding proliferation, the increase in Pcna could reflect changes in chromatin remodeling, although protein quantification, in particular that of cyclin-dependent kinases are essential to understand how MTX alters Lgr5^{+} ISCs cell cycle during regeneration. Taken together, these results demonstrate that Lgr5-GFP^{hi} ISCs activate Yap1 in response to MTX-induced damage, concomitant to a repression of the Wnt signaling pathway. The ISC transcriptional signature is repressed after MTX while secretory cell-associated genes are upregulated, coinciding with an increased frequency of enteroendocrine cells in small intestinal crypts.

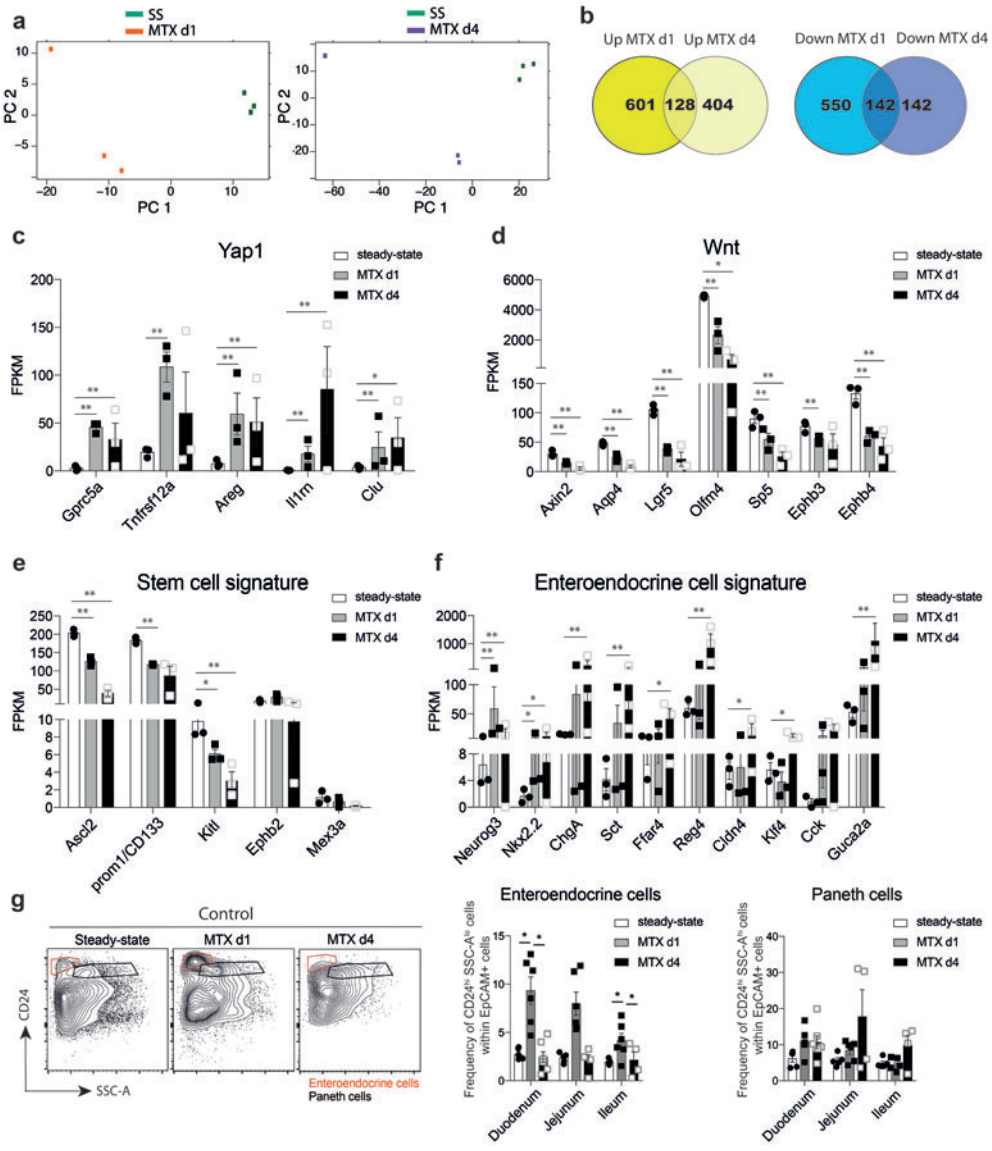

Figure 2: MTX-induced regeneration is initiated by Yap1 induction in intestinal crypts. (a) PCA plot of Lgr5-GFP^{hi}-expressing cells at steady-state (SS) and one day after MTX (MTX d1) (n=3) (left) or at steady-state and four days after MTX (MTX d4) (right). **(b)** Venn diagrams plotting the relationship between transcripts with upregulated (up) or downregulated (down) expression when comparing Lgr5-GFP^{hi} cells at MTX d1 vs SS and MTX d4 vs SS (DESeq2 analysis of count data, adjusted p value < 0.01). **(c)** FPKM values at SS, MTX d1 and MTX d4 of a selected group of (c) Yap1 target genes and **(d)** Wnt target genes. **(e)** Changes in transcripts involved in stem cell identity or **(f)** enteroendocrine cell identity. **(g)** Representative FACS plots and percentages of small intestinal crypt-derived cell suspensions at the indicated time points. Gated CD24^{hi} SSC-A^{lo}-expressing cells correspond to enteroendocrine cells and CD24^{hi} SSC-A^{hi}-expressing cells to Paneth cells and were gated as Live(+) CD45(-) Ter119(-) CD31(-) EpCAM(+) Lgr5-GFP(-) cells. FPKM values are plotted for transcripts that have statistically significant Log$_2$fold change (DESeq2 analysis of count data) with ** adjusted p value <0,01, * adjusted p value <0.05 or non-significant (not indicated); n=3 per group (e-i). Mann-Whitney test *p value< 0.01 (g); n=3-6 per group (g).

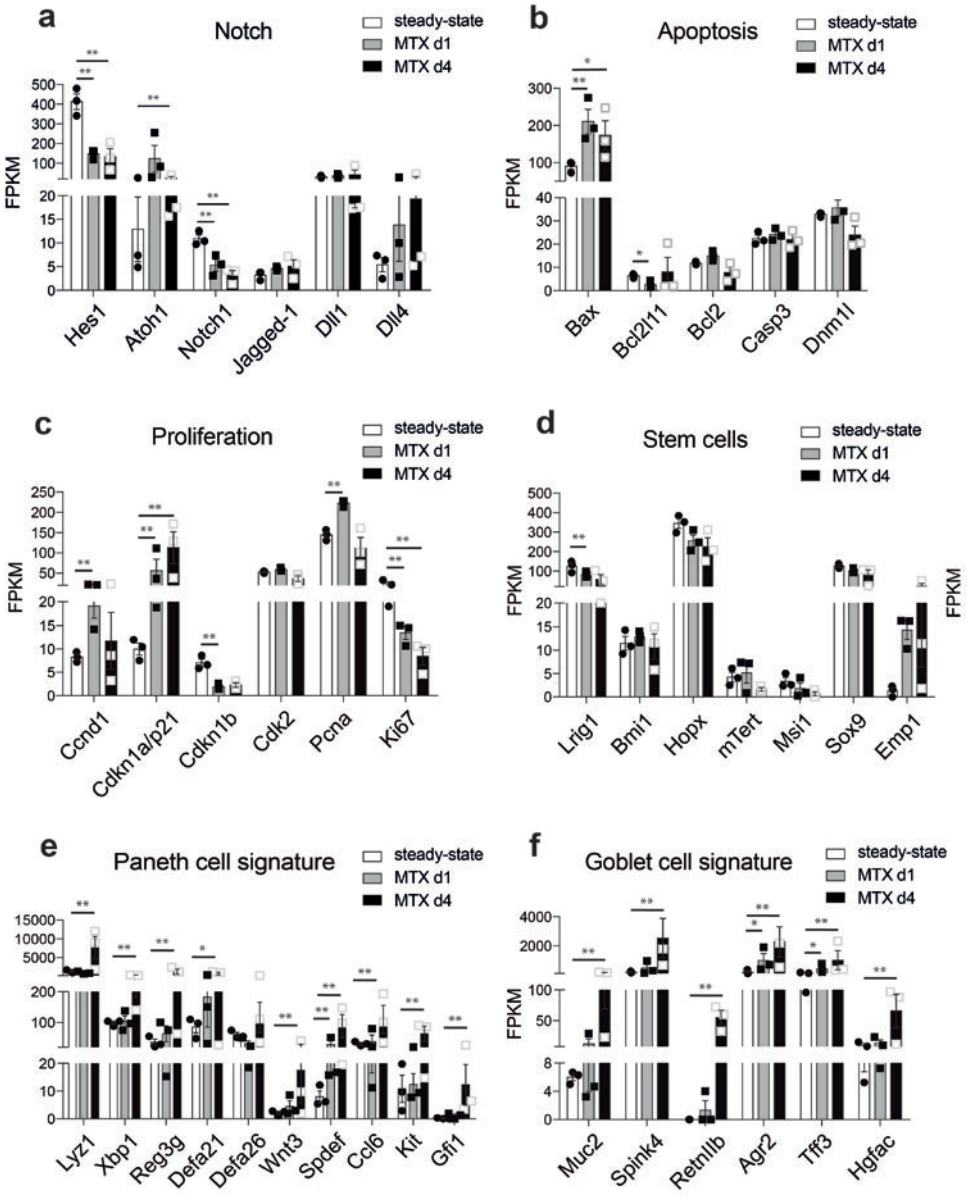

Figure S2: MTX treatment affects Notch signaling in Lgr5-GFP^{hi} stem cells, modulate apoptosis and proliferation and induces Paneth- and Goblet- cell gene signatures. FPKM values at SS, MTX d1 and MTX d4 of a selected group of genes with important function in **(a)** Notch signaling, **(b)** apoptosis and **(c)** proliferation. FPKM values at SS, MTX d1 and MTX d4 of gene expression profiles characteristic fo r **(d)** stem cells, **(e)** Paneth cells and **(f)** Goblet cells. FPKM values are plotted for transcripts that have statistically significant Log_2fold change (DESeq2 analysis of count data) with ** adjusted p value <0,01, * adjusted p value <0.05 or non-significant (not indicated); n=3 per group.

Inhibition of Yap1 aggravates MTX-induced pathology and impairs regeneration

Yap1-TEAD interactions can be inhibited by the FDA-approved drug Verteporfin. To determine the importance of Yap1 activation on intestinal regeneration we cultured crypt-derived organoids in vitro treated them with Verteporfin in the presence or absence of MTX. Upon inhibition of Yap1-TEAD interactions, organoids collapsed after 48h independently of MTX **(Figure 3a),** suggesting that the organoid system reflects the regenerative behavior of epithelial stem cells and that Yap1 is important during epithelial remodeling. To test whether Yap1 signaling is needed for intestinal crypt regeneration *in vivo* we blocked Yap1-TEAD interactions during MTX treatment. We observed that four days after MTX, inhibition of Yap1 signaling lead to a general increase in pathology **(Figure 3b)**. This increased pathology was mainly caused by a disruption of the stem cell compartment in the intestinal crypts **(Figure 3c)**. Ki67 immunostaining revealed a decrease in the number of proliferating cells four days after MTX in mice treated with Verteporfin compared to controls **(Figure 3d).** Altogether, this demonstrate that Yap1 activation is a critical event in intestinal crypt regeneration and proliferation after injury.

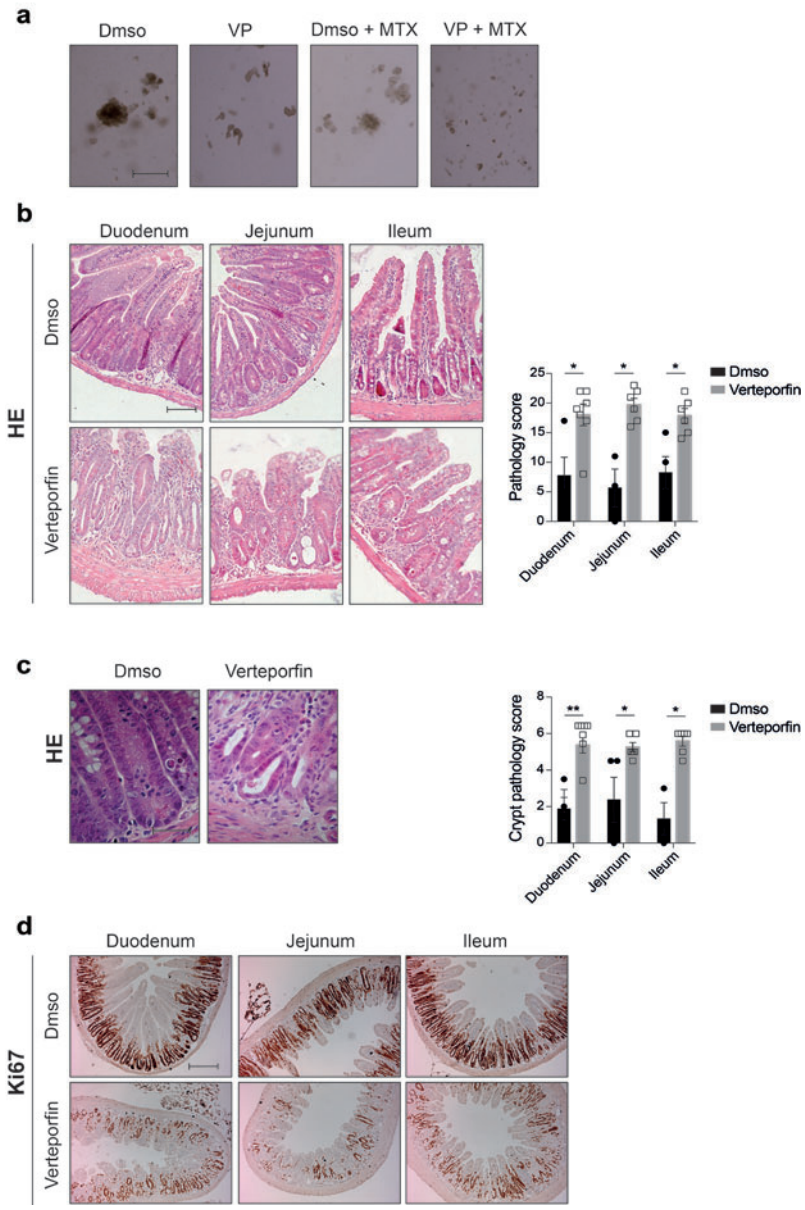

Figure 3: Inhibition of Yap1-mediated transcription aggravates MTX-induced pathology and impairs regeneration. **(a)** Crypt-derived organoids treated with DMSO, Verteporfin, DMSO and MTX or Verteporfin and MTX for 48h. **(b)** Representative H&E staining at MTX d4 of small intestinal sections of WT mice treated with DMSO (top) and Verteporfin (bottom) and the corresponding Intestinal pathology scores. **(c)** Representative H&E staining at MTX d4 of duodenal crypts of WT mice treated with DMSO and Verteporfin (right) and the corresponding crypt pathology score of the different parts of the small intestine. **(d)** Representative Ki67 immunostaining at MTX d4 of small intestinal sections of WT mice treated with DMSO (top) and Verteporfin (bottom). Mann-Whitney test **p<0.01; *p<0.05; non-significant (not indicated). Scale bars: 50µm (a), 20µm (c), 10µm (d), 100µm (e); n=5-8 per group (a-d); n=3 per group (g).

Yap1-induced reprogramming of intestinal stem cells during regeneration is ILC3-dependent

To test whether ILC3s are controlling activation of Yap1 following intestinal damage, we used Lgr5-GFP$^{+/-}$ mice crossed to ILC3-deficient RORγt$^{-/-}$ mice. We performed RNA sequencing on Lgr5-GFP^{hi}-expressing ISCs purified from freshly isolated crypts at steady-state conditions and in response to MTX-induced damage. Principal component analysis (PCA) revealed that Lgr5-GFP^{hi} ISCs display a remarkable divergent gene expression signature in the presence or absence of RORγt^{+} cells one day after MTX, whereas this difference was absent four days after MTX **(Figure 4a).** DESeq2 analysis of transcripts from Lgr5-GFP^{hi} ISCs from RORγt$^{+/+}$ mice compared to RORγt$^{-/-}$ mice revealed 177 genes differentially expressed one day after MTX, and 37 genes four days after MTX **(Table 1)**. Moreover, comparing the ISC transcriptome at one day after MTX versus the steady-state condition, control Lgr5-GFP^{hi} ISCs showed 1421 genes differentially expressed, in contrast to only 126 genes in Lgr5-GFP^{hi} ISCs from RORγt$^{-/-}$. Similarly, four days after MTX, control Lgr5-GFP^{hi} ISCs showed 816 genes differentially expressed, while RORγt$^{-/-}$ Lgr5-GFP^{hi} ISCs only showed 3 genes with statistically significant differential expression **(Table 2)**. Only 94 genes were common at MTX d1 and 2 genes at MTX d4 between control and RORγt$^{-/-}$ Lgr5-GFP^{hi} ISCs **(Figure 4b)**. Focusing on Yap1 signaling we identified Yap1-target genes *Edn1* and *Cyr61* as significantly decreased in control and not changed in RORγt-/- ISCs. *Clu*, *Tnfrsf12a*, *Areg*, *Tinagl1* and *Gprc5a* were increased in controls but remained unaltered in RORγt-/- mice in response to MTX-induced damage **(Figure 4c)**. Lgr5-GFP^{hi} ISCs in control mice showed a relevant downregulation of Wnt-target genes but these were unchanged in RORγt$^{-/-}$ mice **(Figure 4d)**. Similarly, genes with important function in the Notch pathway were also not regulated during MTX in RORγt$^{-/-}$ mice **(Figure S4a)**.

In non-stimulated epithelial cells, Yap1 remains in the cytoplasm and undergoes proteosomal degradation, as a result of phosphorylation of inhibitory serine residues by Lats1/2 kinases. In the absence of Lats1/2 kinases or the activators Mst1/2, dephosphorylated Yap1 translocates into the nucleus to activate TEAD and its downstream transcription. To analyze the localization of YAP1 protein in homeostasis and after MTX-induced tissue damage, we stained tissue sections with anti-YAP1 antibody. In crypts, YAP1 was localized in the nuclei of epithelial cells, in contrast to cytoplasmatic staining observed in villus cells. Histological analysis of intestinal crypts revealed an increase of nuclear Yap1 one day after MTX-mediated damage in RORγt$^{+/+}$ but not in RORγt$^{-/-}$ **(Figure 4e).** The percentage of crypts with induced YAP1 were significantly reduced in RORγt$^{-/-}$ mice one day after MTX **(Figure 4e)**. In conclusion, Yap1 induction in Lgr5-GFP^{hi} cells after injury, and concurrent alterations in Wnt and Notch signaling pathways, only occur in the presence of RORγt^{+} cells.

Transcripts associated with ISC identity, such as *Ascl2*, *Kitl* and *Prom1* were not downregulated in RORγt$^{-/-}$ mice **(Figure 4f)** in contrast to controls. Other stem cell genes were also regulated differently between controls and RORγt$^{-/-}$ ISCs **(Figure S4b)**. Finally, genes associated with the secretory lineage, including enteroendocrine, Paneth and Goblet

cells, were inversely regulated in RORγt$^{-/-}$ ISCs compared to controls **(Figure 4g and S4c,d).** Interestingly, *Chga* and *Ccl6* were significantly downregulated in the absence of ILC3s. Since enteroendocrine cells were increased in control crypts after MTX-induced tissue damage (Figure 2g) and genes associated with differentiation towards the secretory lineages were not induced in Lgr5-GFP^{hi} ISCs in the absence of RORγt, we analyzed the frequencies of enteroendocrine cells at steady-state and one day after MTX by flow cytometry in the absence of ILC3s. This revealed that in RORγt$^{-/-}$ mice, enteroendocrine cell frequencies were not increased in response to damage **(Figure 4h)**.

In sum, these findings indicate that ILC3s regulate Yap1 signaling in Lgr5-GFP^{hi} intestinal stem cells after damage, allowing for downregulation of Wnt signaling and modulation of differentiation programs.

Table 1

Control vs RORγt$^{-/-}$			
MTX d1		MTX d4	
Up	Down	Up	Down
77	100	22	15
177		**37**	

Number of differentially expressed genes in Lgr5-GFP^{hi} ISCs from Lgr5/RORγt$^{+/+}$ (control) and Lgr5/RORγt$^{-/-}$ mice at MTX d1 and MTX d4. Up stands for positive Log_2Fold change values, meaning higher gene expression levels in control, whereas Down represents negative Log_2Fold change values, indicating lower gene expression levels in control. DESeq2 analysis with adjusted p values < 0.01.

Table 2

Steady-State vs MTX d1				**Steady-State vs MTX d4**			
Control		RORγt$^{-/-}$		Control		RORγt$^{-/-}$	
Up	Down	Up	Down	Up	Down	Up	Down
729	692	72	54	532	284	1	2
1421		**126**		**816**		**3**	

Number of differentially expressed genes one or four days after MTX versus steady-state in Lgr5-GFP^{hi} ISCs from Lgr5/RORγt$^{+/+}$ (control) and Lgr5/RORγt$^{-/-}$ mice. Up stands for positive Log_2Fold change values, meaning increased values after MTX compared to steady-state, whereas Down represents negative Log_2Fold change values, indicating a repression in gene expression levels. DESeq2 analysis with adjusted p values < 0.01.

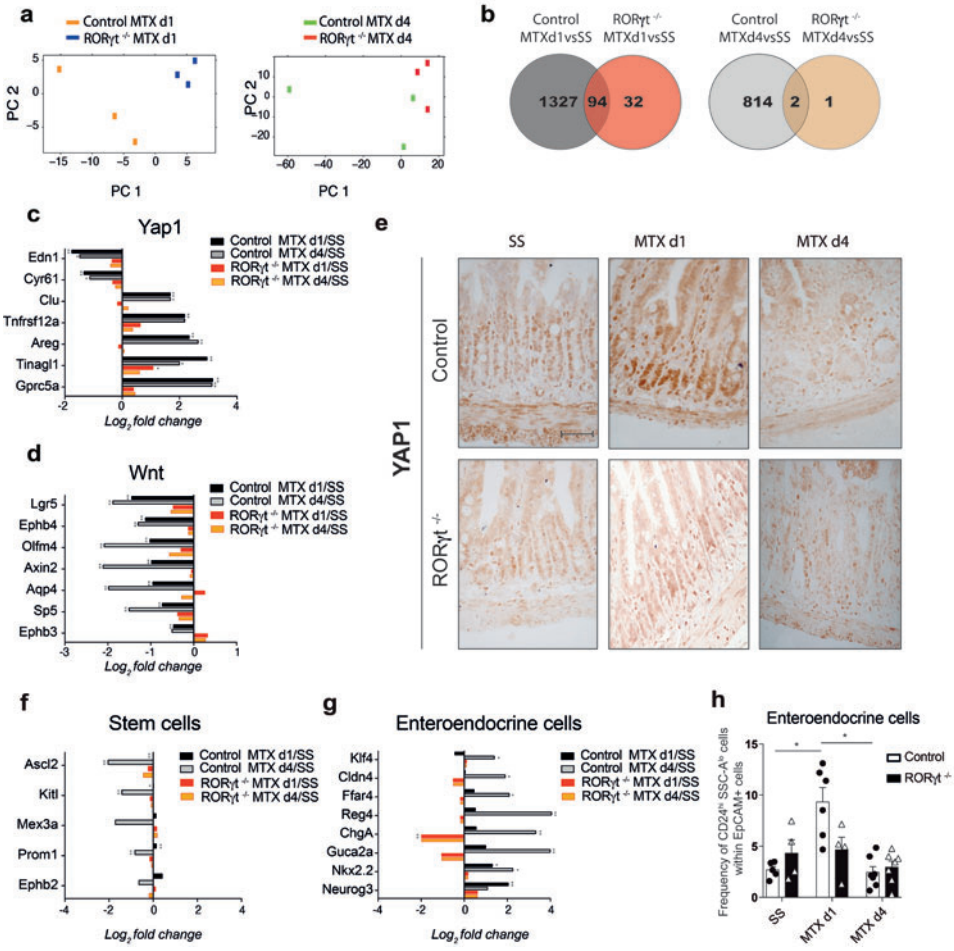

Figure 4: Yap1-induced reprogramming of Lgr5-GFP^{hi} intestinal stem cells during regeneration is ILC3-dependent. **(a)** PCA plot of Lgr5-GFP^{hi}-expressing cells from RORγt$^{+/+}$ control mice and RORγt$^{-/-}$ mice at MTX d1 (n=3) (right) or at MTX d4 (n=3) (left). **(b)** Venn diagrams plotting the relationship between transcripts from Lgr5-GFP^{hi}-expressing cells in control or RORγt$^{-/-}$ ISCs when comparing MTX d1 or MTX d4 versus SS. **(c)** Log_2 fold change values for transcripts that correspond to Yap1 and **(d)** Wnt target genes from Lgr5-GFP^{hi}-expressing cells comparing MTX d1 versus SS (black and red bars) or MTX d4 versus SS (grey and orange bars) from controls (black and grey) and RORγt$^{-/-}$ mice (red and orange). **(e)** Representative Yap1 immunostaining of duodenal sections from control and RORγt$^{-/-}$ mice at the indicated time points during MTX treatment and quantification of the percentage of crypts with Yap1^{+} cells from control or RORγt$^{-/-}$ mice at one day after MTX. **(f)** Log_2 fold change values for transcripts that correspond to gene signatures defining stem cells and **(g)** enteroendocrine cells from Lgr5-GFP^{hi}-expressing cells comparing MTX d1 versus SS (black and red bars) or MTX d4 versus SS (grey and orange bars) from controls (black and grey) and RORγt$^{-/-}$ mice (red and orange). **(h)** Percentages of enteroendocrine cells in duodenal crypt-derived cell suspensions at the indicated time points from controls and RORγt$^{-/-}$ mice. Enteroendocrine cells were gated as Live(+) CD45(-) Ter119(-) CD31(-) EpCAM(+) Lgr5-GFP(-) cells CD24^{hi} SSC-A^{lo}. Log_2 fold change (DESeq2 analysis of count data) with ** adjusted p value <0,01, * adjusted p value <0.05 or non-significant (not indicated) (c,d,f,g); Scale bars: 20µm (e); Mann-Whitney test *p<0.01; non-significant (not indicated) (h). n=3 per group (a-d; f,g); n=4-8 per group (e,h)

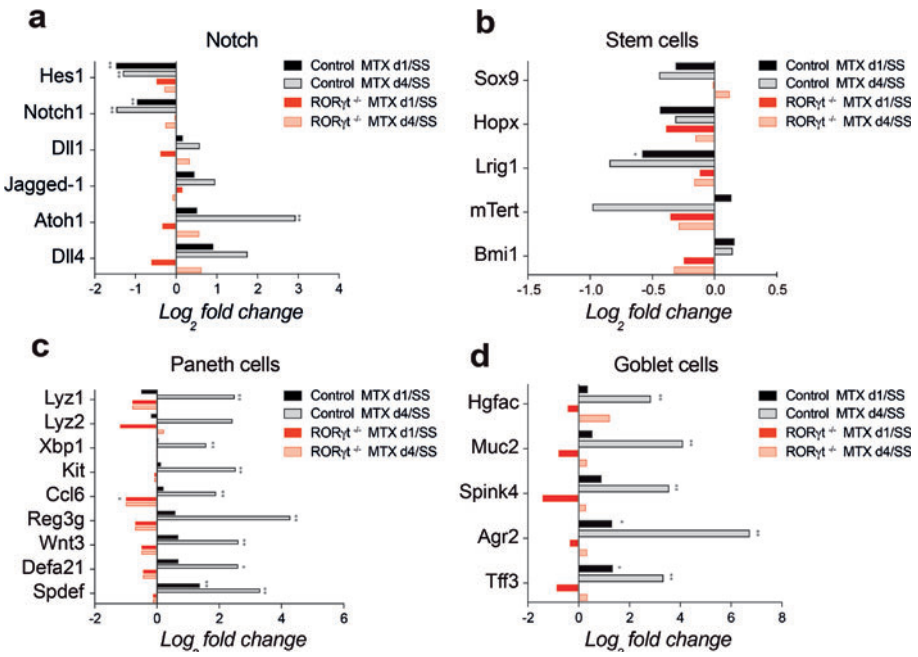

Figure S4: Differential gene expression analysis of stem and secretory cell signatures and conserved signaling pathways important for intestinal stem cell function. (a) Log_2 fold change values corresponding to the expression of a selected group of genes defining stem cells, Paneth and Goblet cells in Lgr5-GFP^{hi}-expressing cells at MTX d1 or MTX d4 versus SS from RORγt$^{+/+}$ control mice (black and grey bars, respectively) and MTX d1 or MTX d4 versus SS from RORγt$^{-/-}$ mice (red and orange bars, respectively). Log_2 fold change values were obtained by DESeq2 analysis of count data with ** adjusted p value <0,01, * adjusted p value <0.05 or not significant (not indicated); n=3 per group.

Activation of Yap1 signaling in intestinal crypts is independent of IL-22

To assess a possible role for IL-22 in Yap1 activation in intestinal crypts after damage we performed YAP1 immunostaining in IL-22-deficient mice and littermate controls. In the absence of IL-22, induction of YAP1 at one day after MTX was comparable to controls **(Figure S5a).** To exclude confounding effects of the prolonged absence of IL-22, we tested whether short-term neutralization of IL-22 or the downstream effector STAT3 are involved in YAP1 nuclear localization after injury. To do so, we used neutralizing antibodies against IL-22 and blocked STAT3 signaling by administering Stattic during MTX treatment. In both conditions, YAP1 localized to the nuclei one day after MTX **(Figure 5b and Figure S5b)**, thus confirming that Yap1 induction during regeneration is regulated independently of IL-22 and STAT3 signaling. As a positive control, we found decreased Reg3g and Reg3b transcripts in total crypts one day after MTX after anti-IL-22 blocking antibody treatment **(Figure 5b)**. Then, we performed RNA sequencing of Lgr5-GFP^{hi} intestinal stem cells one day after MTX in the presence of *in vivo* administration of isotype or neutralizing antibodies to IL-22. FPKM values for Yap1, Wnt and Notch signaling pathways, as well as markers characteristics for ISC signature or differentiated cells showed no significant differences between the isotype or anti-IL-22-treated mice **(Figure 5c-f, Figure 5Sc-f)**. Relative quantification of enteroendocrine cells in

duodenal crypts after IL-22 neutralization confirmed that IL-22 is dispensable for secretory cell specification **(Figure 5g)**. These data indicate that the IL-22/STAT3 axis is dispensable for Yap1-mediated regeneration and that IL-22 is not a major mechanism driving intestinal stem cell regeneration early after MTX-induced tissue damage.

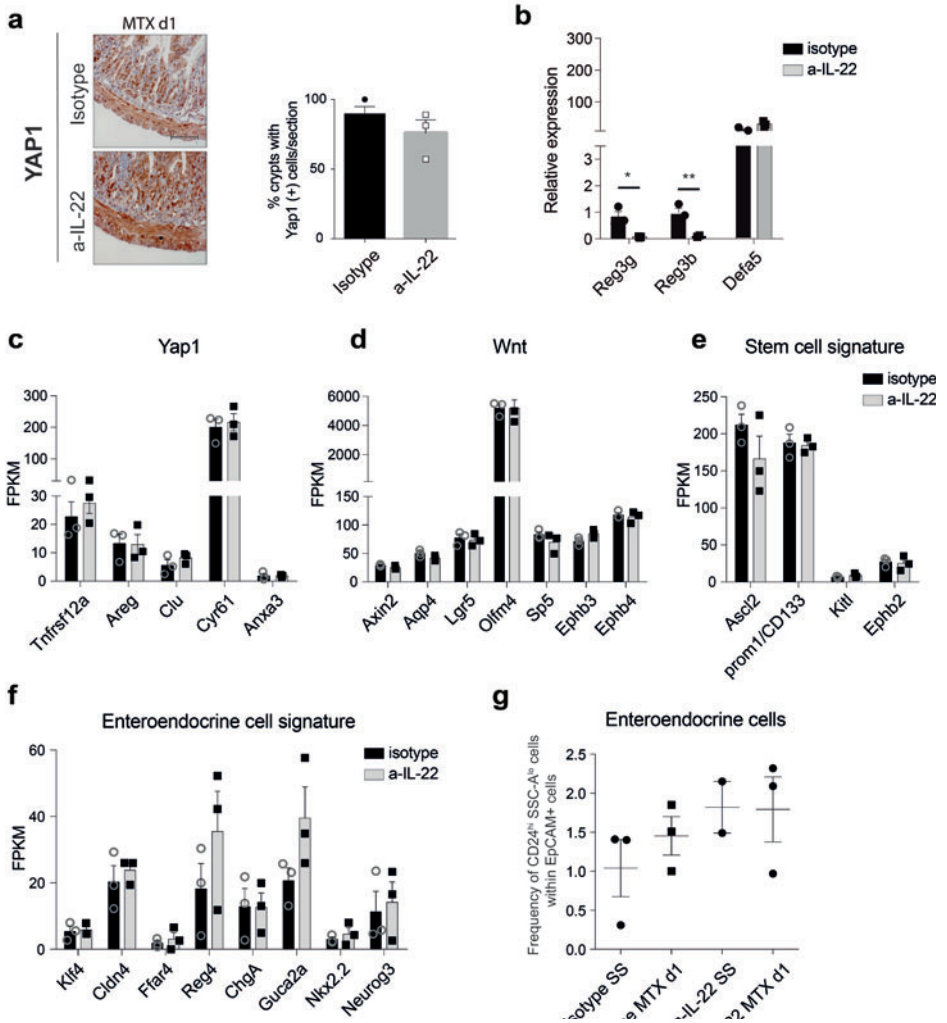

Figure 5: Activation of Yap1 signaling in intestinal crypts is independent of IL-22. (a) Representative Yap1 immunostaining and quantification of crypts with Yap1^{+} cells in duodenal sections from Lgr5-GFP$^{+/-}$ mice treated with isotype or anti-IL-22 antibodies. **(b)** *Reg3g*, *Reg3b* and *Defa5* transcript levels relative to *Gapdh* expression in duodenal crypts from isotype or a-IL-22 treated mice at one day after MTX. **(c)** FPKM values of Lgr5-GFP^{hi}-expressing intestinal stem cells for a selected group of genes with important function in Yap1 and **(d)** Wnt, **(e)** as well as genes identifying intestinal stem cells and **(f)** enteroendocrine cells. **(g)** Percentages of enteroendocrine cells in duodenal crypt-derived cell suspensions at the indicated time points (ss: steady-state, MTX d1: one day after MTX) from isotype vs a-IL-22-treated mice. Enteroendocrine cells were gated as Live(+) CD45(-) Ter119(-) CD31(-) EpCAM(+) Lgr5-GFP(-) cells CD24^{hi} SSC-A^{lo} cells. Scale bars: 40µm (a). n=3 per group. FPKM values are plotted for transcripts that have statistically significant Log_2fold change (DESeq2 analysis of count data). Unpaired T test **p<0.01; *p<0.05 (b). Mann-Whitney test *p<0.01; non-significant (not indicated) (a, g).

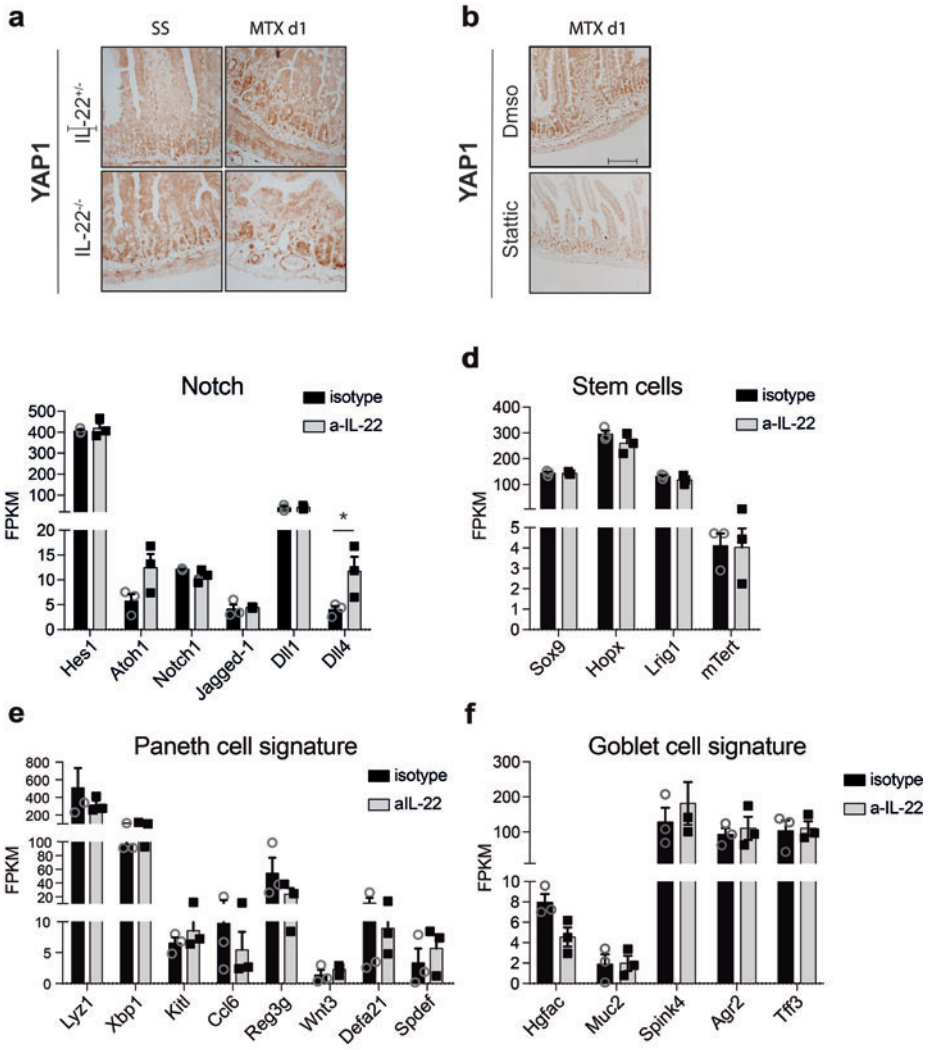

Figure S5: Epithelial cell gene signatures after IL-22 neutralization. (a) Representative Yap1 immunostaining of duodenal sections from IL-22$^{+/-}$ mice and IL-22$^{-/-}$ mice at the indicated time points. **(b)** Representative Yap1 immunostaining of duodenal sections from DMSO or Stattic treated WT mice at one day after MTX. **(c)** FPKM values of Lgr5-GFP^{hi}-expressing intestinal stem cells for a selected group of genes with important function in Notch signaling and characteristic gene expression profile for **(d)** stem cells, **(e)** Paneth cells and **(f)** Goblet cells. FPKM values are plotted for transcripts that have statistically significant Log_2fold change (DESeq2 analysis of count data) with ** adjusted p value <0,01, * adjusted p value <0.05 or non-significant (not indicated). n=3 per group.

Src kinase inhibition impairs Yap1-mediated crypt regeneration

Yap1 can be activated by signaling though the IL-6 family receptor Gp130, in a manner dependent on downstream activation of Src family kinases (SFKs) Src and Yes, independently of STAT3. We set out to determine whether Src family kinase signaling is needed for Yap1 activation in intestinal regeneration after MTX-induced tissue damage. We administered the Src inhibitor PP2 to WT mice to inactivate Src kinases downstream of gp130 signaling. PP2 treatment recapitulated the pathology observed after Yap1 inhibition by Verteporfin at four days after MTX treatment **(Figure 6a)**. Inhibition of Src kinase family members *in vivo* lead to increased total and crypt pathology **(Figure 6b,c)**. Moreover, we interrogated the role of gp130-Src in Yap1-induced proliferation during the regenerative response to MTX-induced pathology. Ki67 immunostaining revealed that inhibition of Src family kinase signaling induced a decrease in proliferation when compared to controls and an impairment of Yap1 induction **(Figure 6d,e).** Overall, we demonstrate that Src family kinase signaling is essential for Yap1 activation and epithelial regeneration and proliferation after injury.

Intestinal regeneration induced by ILC3s involves IL-11-mediated activation of Yap1

ILC3 presence is essential for Yap1 activation after damage, which depends on signaling via Src family kinases. To identify an ILC3-dependent Gp130 activating signal controlling Yap1 activation and intestinal regeneration we aimed at defining the transcription of Gp130-associating receptors by Lgr5^{+} ISCs and transcription of cytokines using Gp130 for signaling in ILC3s. Lgr5-GFP^{hi} intestinal stem cells transcribed gp130 and il11ra1, as well as lower levels of il6ra **(Figure 6f)**. To determine transcription of Gp130 activating cytokines by small intestinal ILC3s we isolated cryptopatch-enriched CCR6^{+} ILC3 and analyzed their transcriptome by RNA-sequencing. CCR6^{+} ILC3s transcribed *IL-6*, *Osm*, *Clcf1* and *Lif* at one day after MTX **(Figure 6g).** Both IL-6 and IL-11 have been implicated in intestinal regeneration. To determine the relative contributions of these two cytokines we used neutralizing antibodies for IL-6 and a small molecule inhibitor of Gp130 homodimerization that inhibits signaling via both IL-6 and IL-11 (LMT-28). Inhibition of IL-6 induced no statistically significant differences in crypt pathology or proliferation four days after MTX **(Figure S6a,b)**. Similarly, the percentage of crypts with Yap1(+) cells were not reduced after IL-6 neutralization **(Figure 6h)**. Based on these data, we conclude that it is unlikely that ILC3-derived IL-6 is an essential mediator of Yap1 activation after MTX-induced small intestinal tissue damage, and suggests an involvement of L-11 signaling. To test this, we made use of a small molecule inhibitor of Gp130 homodimerization that inhibits signaling via both IL-6 and IL-11 (LMT-28). LMT-28 was administered together with the first injection of MTX and it led to a reduction of crypts with activated Yap1(+) cells at one day after MTX **(Figure 6i)**, although crypt pathology and proliferation four days after MTX were not significantly increased after LMT-28 blockade.

These data identify the IL-6/IL-11 pathway controlled by cryptopatch ILC3s as a dominant inducer of Yap1-driven regeneration during the early response to tissue damage.

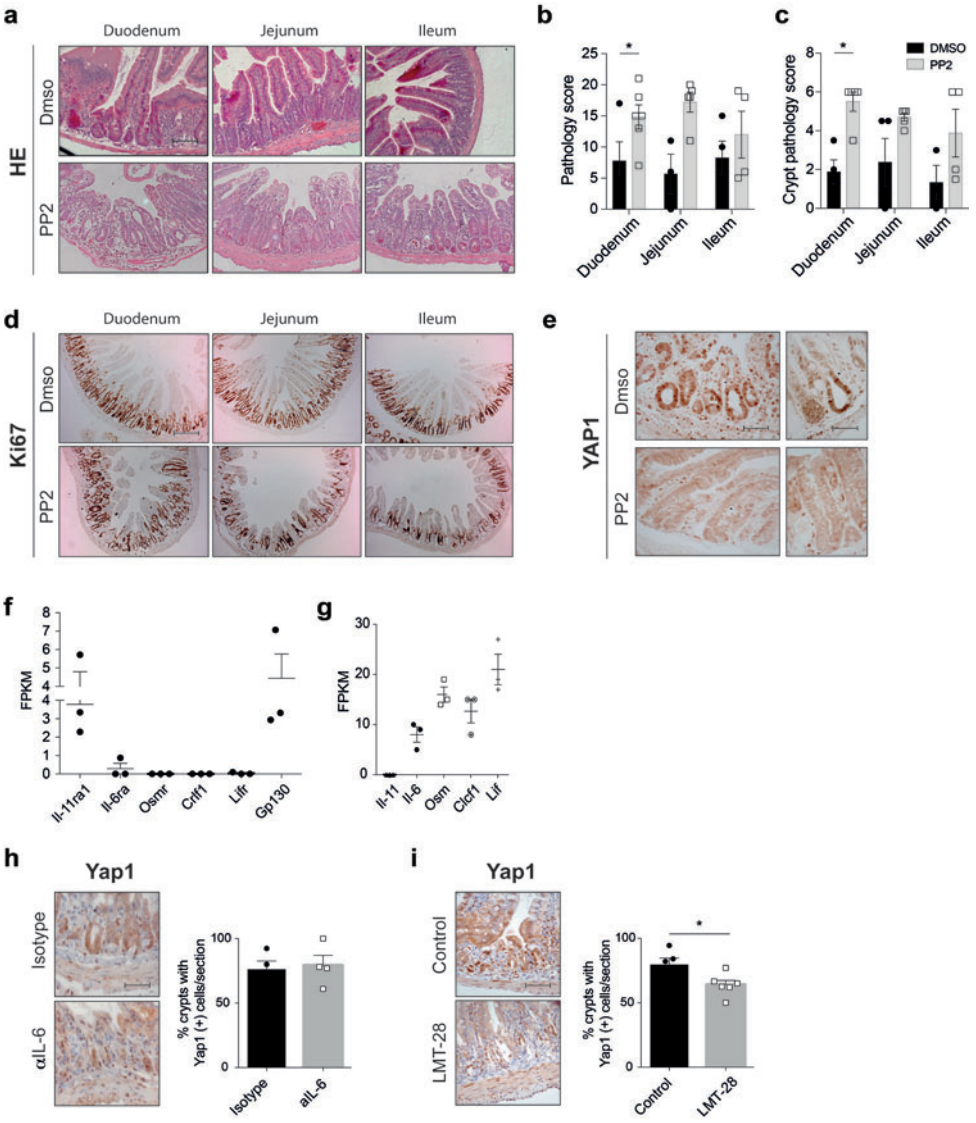

Figure 6: Inhibition of Src axis impairs Yap1-mediated crypt regeneration. (a) Representative H&E staining at MTX d4 of small intestinal sections of WT mice treated with Dmso (top) or PP2 (bottom). **(b)** Intestinal pathology at MTX d4 of WT mice treated with DMSO or PP2. **(c)** Crypt pathology at MTX d4 of WT mice treated with DMSO or PP2. **(d)** Representative Ki67 immunostaining at MTX d4 of small intestinal sections of WT mice treated with DMSO (top) or PP2 (bottom). **(e)** Representative Yap1 immunostaining of duodenal sections at MTX d1 of WT mice treated with DMSO (top) or PP2 (bottom). **(f)** FPKM values of Gp130 and Gp130 co-receptors expressed on Lgr5-GFP^{hi} stem cells at MTX d1. **(g)** FPKM values of Gp130 ligands expressed on cryptopatch CCR6^{+} ILC3s at MTX d1. Representative YAP1 immunostaining and percentage of crypts with Yap1^{+} cells at MTXd1 of duodenal intestinal sections of WT mice treated with **(h)** isotype or a-IL-6 antibodies and **(i)** control or LMT-28 compound. Scale bars: 50µm (a), 20µm (d); 80µm (left) and 100µm (right) (e), 80µm (h,i). Mann-Whitney test *p<0.01 and not statistically significant (not indicated) (b,c). Unpaired T test *p<0.05 and not statistically significant (not indicated) (h,i). n=4-6 per group (a-e; h-i); n=3 (f,g).

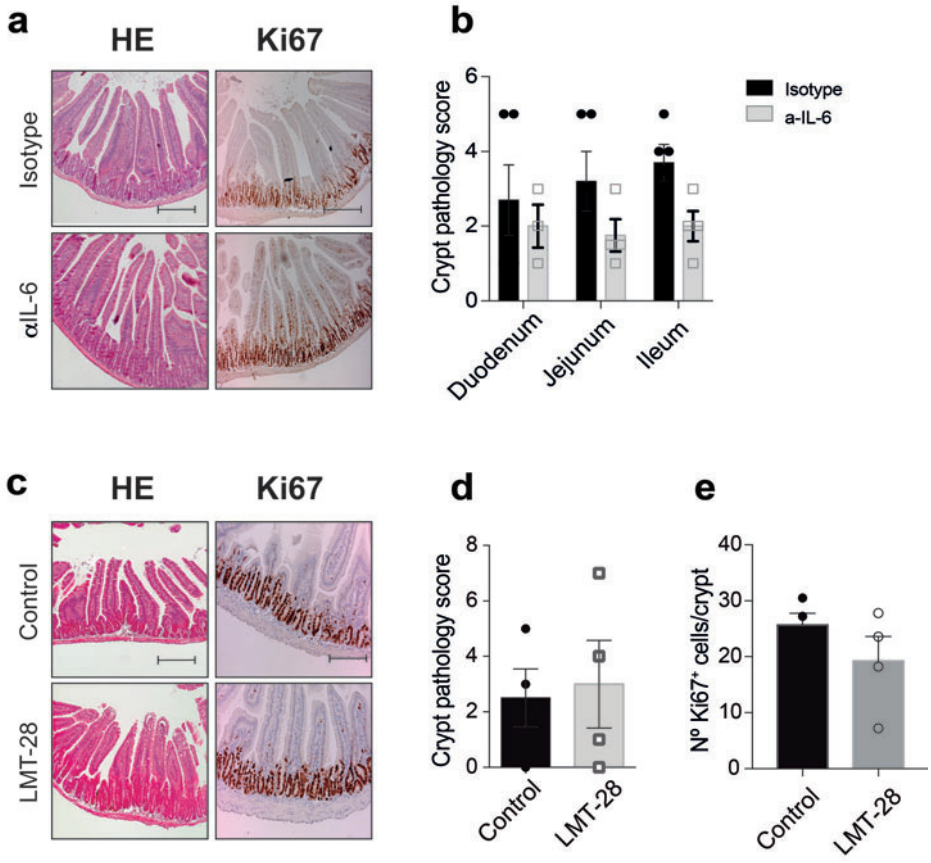

Figure S6: Inhibition of IL-6/IL-11 early during MTX does not alter crypt pathology and proliferation. Representative H&E staining and Ki67 immunostaining at MTX d4 of small intestinal sections of WT mice treated with **(a)** isotype or neutralizing a-IL-6 antibodies and **(c)** control or LMT-28 compound. Intestinal crypt pathology at MTX d4 of WT mice treated with **(b)** isotype or neutralizing a-IL-6 antibodies and **(d)** control or LMT-28 compound. **(e)** Representative Ki67 immunostaining and number of $Ki67^+$ cells in duodenal crypts from WT mice treated with control or LMT-28 four days after MTX. Scale bars: 20µm (a,c). Mann-Whitney test: not statistically significant (not indicated). n=3-4 mice per group.

DISCUSSION

Disruption of the epithelial barrier requires rapid repair to prevent bacterial translocation and subsequent activation of the intestinal immune system, potentially causing further tissue damage. As a result of the high division rate of intestinal epithelial stem cells, these cells are often targeted as side effect of chemo- or radio-therapies for cancer. Mucositis resulting from barrier disruption and subsequent immune cell activation is a common toxicity associated with cancer treatments.

Alterations in conserved signalling pathways in stem cells have been identified in inflammatory bowel disease and intestinal cancers. ISCs integrate various environmental signals to control self-renewal, maintenance and differentiation, all essential for integrity of the mucosal barrier. Important signals controlling stem cell function are derived from immune cells, mesenchymal cells and the enteric nervous system, which together form the ISC niche.

The ISC niche provides Wnt, Notch and epidermal growth factor (EGF) signals to support $Lgr5^+$ crypt base columnar ISCs and to ensure normal epithelial maintenance. However, little is known about the cells that regulate regeneration of the ISC compartment after tissue damage. Here we identified a unique feature of group 3 innate lymphoid cells (ILC3s) in driving ISC regulatory pathways during regeneration after chemotherapy-induced small intestinal damage. Hence, the identification of specific molecules produced by these cells may serve as effective therapeutic approaches for GI disorders by stimulating stem cell function indirectly.

The IL-22/STAT3 axis drives ISC proliferation and protection from allogeneic T cells during experimental GVHD. Expression of the IL-22 receptor is restricted to non-hematopoietic cells[23,24]. Radio-resistant ILC3s are a major source of IL-22 in the intestine and that after stem cell transplantation IL-22 protects and stimulates epithelial regeneration in both the thymus and the small intestine[25,26]. These findings suggest an important role for ILC3s in reducing ISC loss and intestinal pathology and mortality during experimental Graft versus Host disease (GVHD). In addition, ILC3s can stimulate growth of small intestinal organoids in an IL-22-dependent fashion by directly driving $Lgr5^+$ ISC expansion[27].

In this study, we interrogated the *in vivo* function of small intestinal ILC3s and ILC3-derived factors in the regulation of conserved signalling pathways in Lgr5-expressing stem cells in response to MTX-induced epithelial damage. First, we unravelled two distinct mechanisms controlling $Lgr5^+$ ISC maintenance and proliferation. The IL-22 - STAT3 signalling pathway is required for the preservation of ISCs after MTX treatment while, in contrast, IL-22 deficiency or neutralization, or STAT3 inhibition, did not affect the proliferative response observed during the regenerative phase after tissue damage. These data led us to hypothesize that ILC3s controlled ISC proliferation and differentiation through IL-22 independent mechanisms.

Through a combination of RNA sequencing of Lgr5^{hi}-expressing ISCs in the absence of ILC3s and *in vivo* blocking experiments, we revealed that activation of the Yap1 pathway, which occurred one day after MTX treatment was strongly deregulated in the absence of ILC3s. Consistent with the RNA sequencing data, Yap1 protein localisation in the nuclei of crypt cells was also reduced in RORγt-deficient mice after MTX.

Although Yap1 is not essential for normal intestinal homeostasis, its activity is essential for intestinal regeneration after injury. In the intestine, endogenous Yap1 is restricted to the stem cell niche at the bottom of the crypt[28], suggesting an association with ISC regulation. In line with these results, several studies suggest that Yap1 regulates intestinal tissue regeneration by increasing ISC proliferation. IEC-specific conditional knockout of Yap1 induces loss of crypts 2-5 days after DSS-induced colitis and reduces crypt proliferation after whole body irradiation[29]. Furthermore, Yap1 reprograms ISCs 2-4 days after ionizing radiation[22]. On one hand, Yap1 induction leads to the expression of Notch ligands and receptors, which maintains proliferation of ISCs and TA cells, whereas inhibits the generation of secretory and absorptive cell types[30]. On the other hand, Yap1 transiently suppresses Wnt signalling and activates EGFR pathway in the first few days of the regeneration phase[22]. Later during regeneration, hyperproliferation is critical to regain the number of damaged epithelial cells and this is controlled by increasing Wnt signalling[31,32].

Here we show that immediately following MTX-induced damage, Yap1 induction in Lgr5^{+} ISCs coincides with robust inhibition of Wnt-target genes and genes of the "stem cell" signature, and an increase of transcripts acquired during secretory cell differentiation. However, this normal loss of "stem cell" transcripts or the engagement of the "differentiation" program did not occur in the absence of ILC3s, thus indicating that reprogramming of Lgr5^{+} ISCs by Yap1 depends on presence of ILC3s.

In order to investigate the importance of Yap1 for proliferation of the epithelium we inhibited the Yap1-TEAD interactions, which activate gene transcription, by using Verteporfin and found that crypt pathology was increased after inhibition of Yap1 signalling. Furthermore, blockage of Yap1 signalling also led to a reduction of crypt proliferation, demonstrating the function of Yap1 in ISC-driven regeneration upon injury.

ILC3s respond quickly to environmental cues by producing cytokines, in particular IL-22. Interestingly, Yap1 induction was not affected by IL-22-deficiency or neutralization, nor STAT3 inhibition, signifying that ILC3s control Yap1 signalling via an IL-22 independent mechanism.

It is known that the stimulation of ligand dependent Gp130 signalling, in particular by IL-6, IL-11 or LIF, leads to Src-dependent Yap1 activation upon epithelial barrier destruction[30]. In agreement with this, our results derived from *in vivo* Src inhibition, revealed an involvement of Src activation in Yap1-driven regeneration during MTX-induced tissue damage.

Based on our data we propose two possible regulatory pathways by which Yap1 mediates intestinal regeneration. We show that Lgr5^{+} ISCs transcribed Gp130 and il11ra1. Conversely, ILC3s express transcripts for the Gp130 binding cytokine IL-6. However, IL-6 neutralization *in vivo* led to normal intestinal epithelial remodelling after MTX-induced pathology, implying for a possible role of IL-11 in inducing Yap1, which was strengthen with the results observed by blocking both the IL-6 and IL-11 binding to Gp130 by using LMT-28. IL-6/IL-11 signaling early neutralization in response to MTX is essential for Yap1 induction. The contribution of these cytokines to crypt pathology and proliferation need to be assessed by blocking with LMT-28 during a longer period of time.

Our studies reveal that Yap1 reprogramming of Lgr5^{+} ISCs is controlled by innate lymphoid cells, adding a new layer of regulation and linking inflammation to regeneration. This work sheds light on mucosal immunology and intestinal stem cell biology and highlights the immune system as a critical modulator of intestinal stem cell function. Taking a dual-network view, that is integrating extrinsic cues by innate lymphoid cells to modulate cellular outcomes in ISCs, will undoubtedly provide insights that will lead to more adequate tissue healing treatments in a large variety of intestinal diseases.

REFERENCES

1. Arnout Schepers, H. C. Wnt Signaling, Stem Cells, and Cancer of the Gastrointestinal Tract. *Cold Spring Harb Perspect Biol* 385–505 (2014).
2. Sancho, E., Batlle, E. & Clevers, H. Live and let die in the intestinal epithelium. *Current Opinion in Cell Biology* **15,** 763–770 (2003).
3. Schonhoff, S. E., Giel-Moloney, M. & Leiter, A. B. Minireview: Development and differentiation of gut endocrine cells. *Endocrinology* **145,** 2639–2644 (2004).
4. Aparicio-Domingo, P. *et al.* Type 3 innate lymphoid cells maintain intestinal epithelial stem cells after tissue damage. *J. Exp. Med.* **212,** 1783–91 (2015).
5. Lindemans, C. A. *et al.* Interleukin-22 promotes intestinal-stem-cell-mediated epithelial regeneration. *Nature* **528,** 560–564 (2015).
6. Collu, G. M., Hidalgo-Sastre, A. & Brennan, K. Wnt-Notch signalling crosstalk in development and disease. *Cellular and Molecular Life Sciences* **71,** 3553–3567 (2014).
7. Igawa, D., Sakai, M. & Savan, R. An unexpected discovery of two interferon gamma-like genes along with interleukin (IL)-22 and -26 from teleost: IL-22 and -26 genes have been described for the first time outside mammals. *Mol. Immunol.* **43,** 999–1009 (2006).
8. Korinek, V., Barker, N., Moerer, P., van Donselaar, E., Huls, G., Peters, P. J. & Clevers, H. Depletion of epithelial stem-cell compartments in the small intestine of mice lacking Tcf-4. *Nat. Genet.* **19,** 379–383 (1998).
9. Smith, N. R., Davies, P. S., Silk, A. D. & Wong, M. H. Epithelial and mesenchymal contribution to the niche: A safeguard for intestinal stem cell homeostasis. *Gastroenterology* **143,** 1426–1430 (2012).
10. Pinto, D., Gregorieff, A., Begthel, H. & Clevers, H. Canonical Wnt signals are essential for homeostasis of the intestinal epithelium. *Genes Dev.* **17,** 1709–1713 (2003).
11. Pellegrinet, L. *et al.* Dll1- and Dll4-mediated notch signaling are required for homeostasis of intestinal stem cells. *Gastroenterology* **140,** 1230–1240 (2011).
12. van der Flier, L. G. & Clevers, H. Stem Cells, Self-Renewal, and Differentiation in the Intestinal Epithelium. *Annu. Rev. Physiol.* **71,** 241–260 (2009).
13. Crosnier, C., Stamataki, D. & Lewis, J. Organizing cell renewal in the intestine: stem cells, signals and combinatorial control. *Nat. Rev. Genet.* **7,** 349–59 (2006).
14. Beebe, K., Lee, W. C. & Micchelli, C. A. JAK/STAT signaling coordinates stem cell proliferation and multilineage differentiation in the Drosophila intestinal stem cell lineage. *Dev. Biol.* **338,** 28–37 (2010).
15. Mazerbourg, S. *et al.* Leucine-rich repeat-containing, G protein-coupled receptor 4 null mice exhibit intrauterine growth retardation associated with embryonic and perinatal lethality. *Mol Endocrinol* **18,** 2241–2254 (2004).
16. Jin, Y., Patel, P. H., Kohlmaier, A., Pavlovic, B., Zhang, C. & Edgar, B. A. Intestinal Stem Cell Pool Regulation in Drosophila. *Stem Cell Reports* **8,** 4–12 (2017).
17. Scoville, D. H., Sato, T., He, X. C. & Li, L. Current View: Intestinal Stem Cells and Signaling. *Gastroenterology* **134,** 849–864 (2008).
18. Barker, N. *et al.* Lgr5+ve Stem Cells Drive Self-Renewal in the Stomach and Build Long-Lived Gastric Units In Vitro. *Cell Stem Cell* **6,** 25–36 (2010).
19. Gröschel, S. *et al.* A single oncogenic enhancer rearrangement causes concomitant EVI1 and GATA2 deregulation in Leukemia. *Cell* **157,** 369–381 (2014).
20. Subramanian, A. *et al.* Gene set enrichment analysis: a knowledge-based approach for interpreting genome-wide expression profiles. *Proc. Natl. Acad. Sci. U. S. A.* **102,** 15545–50 (2005).

21. de Koning, B. A. E. *et al.* Contributions of mucosal immune cells to methotrexate-induced mucositis. *Int. Immunol.* **18,** 941–949 (2006).
22. Gregorieff, A., Liu, Y., Inanlou, M. R., Khomchuk, Y. & Wrana, J. L. Yap-dependent reprogramming of Lgr5+ stem cells drives intestinal regeneration and cancer. *Nature* **526,** 715–8 (2015).
23. Naik, S. H. *et al.* Cutting edge: generation of splenic CD8+ and CD8- dendritic cell equivalents in Fms-like tyrosine kinase 3 ligand bone marrow cultures. *J. Immunol.* **174,** 6592–6597 (2005).
24. Wolk, K., Kunz, S., Witte, E., Friedrich, M., Asadullah, K. & Sabat, R. IL-22 increases the innate immunity of tissues. *Immunity* **21,** 241–254 (2004).
25. Hanash, A. M. *et al.* Interleukin-22 protects intestinal stem cells from immune- mediated tissue damage and regulates sensitivity to graft vs. host disease. *Immunity* **37,** 339–350 (2012).
26. Dudakov, J. A. *et al.* Interleukin-22 Drives Endogenous Thymic Regeneration in Mice. *Science (80-.).* **336,** 91–95 (2012).
27. Lindemans, C. A. *et al.* Interleukin-22 Promotes Intestinal Stem Cell-Mediated Epithelial Regeneration. *Nature* **528,** 560–564 (2015).
28. Camargo, F. D., Gokhale, S., Johnnidis, J. B., Fu, D., Bell, G. W., Jaenisch, R. & Brummelkamp, T. R. YAP1 Increases Organ Size and Expands Undifferentiated Progenitor Cells. *Curr. Biol.* **17,** 2054–2060 (2007).
29. Cai, J., Zhang, N. & Zheng, Y. The Hippo signaling pathway restricts the oncogenic potential of an intestinal regeneration program The Hippo signaling pathway restricts the oncogenic potential of an intestinal regeneration program. 2383–2388 (2010).
30. Taniguchi, K. *et al.* A gp130-Src-YAP Module Links Inflammation to Epithelial Regeneration. *Nature* **519,** 57–62 (2015).
31. Ashton, G. H. *et al.* Focal Adhesion Kinase is required for intestinal regeneration and tumorigenesis downstream of Wnt/c-Myc signaling. *Dev. Cell* **19,** 259–269 (2010).
32. Karin, M. & Clevers, H. Reparative inflammation takes charge of tissue regeneration. *Nature* **5 2 9,** 307–315 (2016).

4

INTESTINAL EPITHELIAL STEM CELL HOMEOSTASIS IS ALTERED IN THE ABSENCE OF GROUP 3 INNATE LYMPHOID CELLS

Mónica Romera-Hernández[1], Patricia Aparicio-Domingo[1], Julien J. Karrich[1], Ferry Cornelissen[1], Natalie Papazian[1], Janneke N. Samsom[2] and Tom Cupedo[1]

[1]Department of Hematology, Erasmus University Medical Center, Rotterdam, The Netherlands
[2]Department of Pediatrics, Division of Gastroenterology, Erasmus University Medical Center, Rotterdam, The Netherlands

Manuscript in preparation

ABSTRACT

ILC3s are essential for normal regeneration of Lgr5^{+} intestinal stem cells (ISCs) after MTX-induced damage, independently of IL-22. However, whether presence of ILC3s or IL-22 influences the intestinal stem cell niche under homeostatic conditions remains unknown. Here we set out to analyze crypt composition and stem cell homeostasis in the absence of ILC3 or IL-22. Small intestinal crypts showed mild abnormalities in RORγt$^{-/-}$ but not in in IL-22$^{-/-}$ mice, suggesting that crypt integrity was controlled in an ILC3-dependent yet IL-22 independent manner. Transcript analysis of Reg family genes in crypt cells revealed that transcription of *Reg4* was regulated by ILC3s in an IL-22-independent fashion. Since *Reg4* has been detected in a rare subtype of damage-activated stem cells we hypothesized that ILC3s could control the stem cell pool. To test this hypothesis, we examined the composition and transcriptome of cells within the Lgr5-GFP gate. This revealed an increase in Lgr5^{+} cells with an enteroendocrine cell phenotype in the absence of ILC3s. When mice were exposed to MTX, enteroendocrine-like Lgr5^{+} cells expanded, indicating that these cells contribute to the physiological crypt response to tissue stress. Strikingly, the recruitment of enteroendocrine-like Lgr5^{+} cells was completely absent in RORγt$^{-/-}$ mice. Our data demonstrate that ILC3s contribute to the homeostatic and damage-induced recruitment of Lgr5^{+} ISC resembling enteroendocrine cells.

INTRODUCTION

The intestine is colonized by commensal microbiota and is a primary entry site for pathogenic microorganisms. ILC3s reside in the intestinal lamina propria and are important in regulating epithelial barrier function. ILC3s can produce cytokines that directly instruct epithelial cells and consequently shape microbial diversity[1], but also interact with adaptive immune cells to promote tolerance and prevent bacteria-driven inflammation[2].

Continuous regeneration of the epithelial lining of the small intestine (SI) relies on multipotent ISC that differentiate into cycling progenitor cells (transient-amplifying (TA) cells) that differentiate while migrating upwards to the villi. Small cycling ISC located at the base of the crypts, also termed crypt base columnar cells (CBCs), express Lgr5 and generate all epithelial cell types in the intestinal epithelium, i.e. absorptive enterocytes and secretory cells, including Paneth cells, Goblet cells, enteroendocrine cells and Tuft cells[3,4].

As discussed in Chapter 3, ILC3s drive regenerative epithelial responses by regulating evolutionary conserved signaling pathways in Lgr5$^+$ intestinal stem cells (ISCs) after damage inflicted by methotrexate (MTX). However, little is known about the contribution of ILC3s to the homeostatic regulation of ISC functioning and possible downstream consequences for intestinal homeostasis. It is intriguing that a subset of ILC3s, which expresses CCR6, reside in cryptopatches directly adjacent to the crypts that contain ISCs and Paneth cells[5]. ILC3s are an important source of IL-22[6], which acts mainly on epithelial cells and mesenchymal stromal cells, and constitutes an important mechanism by which immune cells instruct the function of epithelial cells[7]. For example, ILC3-derived IL-22 has been linked to the production of Reg3 proteins by PC[8,9]. PC are located intermingled with Lgr5$^+$ ISCs at the crypt bottom. They provide niche factors to ISC and have important roles in innate immunity by regulating microbial density and in the protection of nearby stem cells[10]. In addition, IL-22 induces membrane-bound mucins and can regulate Goblet cell (GC) hyperplasia to attain spatial segregation of commensal bacteria and the intestinal barrier[11]. Finally, IL-22 also can act on Lgr5$^+$ ISCs directly, as evidenced by activation of STAT3 in organoid cultures[12].

There is emerging data supporting the concept that the ISC compartment is comprised of multiple subtypes of ISCs, some rapidly cycling, others quiescent and more damage resistant. The functional relationship between these ISC populations during homeostasis and regeneration and their exact location within the crypt remain controversial. One type of intestinal stem cell are located at the bottom of the crypts in both the small and large intestine and are known as “crypt base columnar cells or CBCs[3,13]. They are characterized by the expression of the Wnt target gene Lgr5/GPR49 and continuously proliferating. Such a high proliferation rate renders Lgr5$^+$ ISCs vulnerable to genotoxic damage[14]. Interestingly, de novo generation of Lgr5-expressing cells is essential for regeneration after radiation injury[15]. This notwithstanding, the intestine displays a remarkable capacity to recover from genotoxic insults that target cycling cells, suggesting the existence of reserve stem cells with

a relatively quiescent state. Numerous studies reported the existence of additional stem cells molecularly distinct to the Lgr5^{+} CBCs, located at the + 4 position and expressing markers such as Bmi1, mTert, Lrig1 or Hopx[16–20]. Whereas Lgr5^{+} CBCs are completely dispensable for tissue maintenance under homeostatic conditions, the reserve Hopx/Bmi1-CreER-marked cells (that largely overlap with each other) seems to be required for tissue fidelity and maintenance of normal crypt-villus architecture [21,22]. However, because Hopx and Bmi1 mRNA can be found in non-stem cells throughout the crypt, the specific function of each stem cell type remains unknown[16–18,21,23]. Emerging concepts among quiescent populations have included their mobilization upon tissue injury or upon CBC loss and possession of secretory progenitor features.

Enterocyte-lineage precursor progenitors can become stem cells during intestinal regeneration[24]. Similarly, recent data suggest that subsets of secretory enteroendocrine cells (EE) can act as reserve stem cells and replace rapidly cycling Lgr5^{+} ISC after injury or with age, by acquiring stem cell properties. For example, a subset of post-mitotic (non-proliferating) EE cells marked by Chromogranin A (ChgA) and Lgr5 has been identified at the crypt-base of the mouse intestine and has the capacity to give rise to all differentiated epithelial cells in vivo and in vitro. These cells were negative for Ki67 but expressed CD133, DCAMKL-1, Neurogenin 3 and multiple endocrine hormones[14,25–28].

An important unresolved question is whether ILC3s and ILC3-derived IL-22 influence intestinal stem cell proliferation, differentiation and gene-expression networks under steady-state conditions *in vivo*.

Therefore, we analyzed intestinal morphology in RORγt-deficient mice and found alterations of the crypt compartment, mainly characterized by epithelial flattening and crypt loss. We demonstrate that ILC3s instruct crypt epithelial cells via IL-22 dependent and independent mechanisms, both in Paneth cells and in other crypt epithelial cells. In addition, our data strongly suggests an interaction between ILC3s and Notch signaling in stem cells and progenitor cells, and finally we present a novel theory on the importance of ILC3s in the regulation of the ISC pool, mainly formed by Lgr5^{hi} ISCs that can be replaced by Lgr5^{lo} secretory progenitors reacquiring stem cell properties. We propose that the recruitment of Lgr5^{lo} stem cells is increased in the absence of ILC3s to serve as functional clonogenic stem cell population under stress conditions.

MATERIALS AND METHODS

Mice. C57BL/6, RORγt-GFP, IL-22$^{-/-}$, Lgr5-GFP-IRES-creERT2 (Lgr5-GFP), Lgr5-GFP/RORγt-GFP mice were bred in the animal facility of the Erasmus University Medical Center Rotterdam. Animal experiments were approved by the relevant authorities and procedures were performed in accordance with institutional guidelines. Age and gender-matched littermates were used whenever possible.

Methotrexate. 8-12 weeks old mice were injected i.p. with 120mg/kg MTX (PCH) at day-1 and with 60mg/kg at day 0. Tissues were collected at day 1 and day 4 after the last MTX injection.

Cytokine neutralization. 150μg of anti-IL-22 antibody (8E11, Genentech) or mouse IgG1 isotype control (MOPC-21, BioXcell) were administered i.p to Lgr5-GFP$^{+/-}$ mice every 2 days, starting 4 days before the first MTX dose, until day 2 after the last MTX dose.

Crypt isolation. Isolation of intestinal crypts was performed as previously described (Sato et al., 2009). Briefly, isolated small intestines were opened longitudinally and washed with cold PBS. Tissues were cut into 5mm pieces and subsequently washed by mechanical pipetting with cold PBS until supernatant was clear. Tissues were incubated with EDTA (2mM) in PBS at 4°C for 30 min. Tissues were then washed several times with cold PBS and suspended by vigorous shacking. Crypt-enriched sediments were passed through a 70μm cell strainer and centrifuge at 200g for 2 min to separate the crypts from single cells. Crypts were incubated with 1 ml of TrypLE Express (Gibco) + Dnase I (Calbiochem) at 37°C for 10-15min until crypt dissociation was observed. Single cell suspensions were filtered through 40um cell strainer and stained with conjugated antibodies. Samples were analyzed by FACS ARIAIII (BD Biosciences).

Organoid culture. Small intestinal crypts were counted and 1000 crypts were plated per well in a pre-warmed 24-well plate in a drop of 50μl of Matrigel (Corning). After solidification at 37°C, crypts embedded in matrigel were overlaid with 500μl of Advanced DMEM/F12 medium (ThermoFischer) with Hepes, Glutamax (ThermoFischer) and Pen/Strep, supplemented with 1x N2(ThermoFischer), 1x B27 (ThermoFisher), Noggin-1 (PeproTech), EGF (R&D Systems) and human-Rspo1 conditioned medium. Factors were refreshed every two days and the entire medium was changed every four days. Organoids were visualized and counted by using a microscope.

Antibodies. For flow cytometry: monoclonal antibodies were EpCAM-1 (G8.8; BioLegend); CD45 (30F11; Invitrogen); CD24 (MI/69; BioLegend), CD31 (390; BioLegend), Ter119 (Ter-

119; BioLegend), ckit (2B8; BioLegend) For paraffin immunostaining: Rat Ki67 monoclonal antibody (MIB-5, Dako) and polyclonal Rabbit ChgA antibody (NB120-15160, Novus).

Flow cytometry and cell sorting. Fc receptors were blocked by pre-incubation with normal mouse serum and rat-anti mouse CD16/CD32 (2.4G2; BD). All stainings were performed in PBS containing 2% heat-inactivated fetal calf serum (FCS) in the dark and at 4°C. Cells were incubated with 7AAD (Beckman Coulter) to exclude dead cells. Stained cells were analyzed using FACS LSRII (BD Biosciences) or FACS ARIAIII (BD Biosciences) and data processed with FlowJo software (FlowJo, LLC).

RNA sequencing. cDNA was prepared using SMARTer Ultra Low RNA kit (Clontech Laboratories) for Illumina Sequencing following the manufacturer's protocol. The Agilent 2100 Bio-analyzer and the High Sensitivity DNA kit were applied to determine the quantity and quality of the cDNA production. Amplified cDNA was further processed according to TruSeq Sample Preparation v.2 Guide (Illumina) and paired end-sequenced (2x75bp) on the HiSeq 2500 (Illumina). Demultiplexing was performed using CASAVA software (Illumina) and the adaptor sequences were trimmed with Cutadapt (http://code.google.com/p/cutadapt/). Alignments against the mouse genome (mm10) and analysis of differential expressed genes were performed with $DESeq_2$ in the R environment on the raw fragment counts extracted from the BAM files by HTSeq-count[29]. Cufflinks software was used to calculate the number of fragments per kilobase of exon per million fragments mapped (FPKM) for each gene. Principle component analysis was performed on the fragment counts using the R environment. Finally, gene set enrichment analysis (GSEA, Broad Institute) was performed on the FPKM values using the curated C2 collection of gene sets within MSigDB[30].

Histology. Small intestinal tissue pieces (5mm) or Swiss rolls were fixed in 4% PFA (4h, RT), washed in 70% ethanol and embedded in paraffin. Four-µm sections were deparaffinized and stained with hematoxylin (Vector Laboratories) and eosin (Sigma-Aldrich). For Ki67, Yap1 and ChgA detection, endogenous peroxidases were blocked in 1% periodic acid in deionized water for 20 min, and antigen retrieval was achieved by microwave treatment in citrate buffer (10mM, pH 6.0). Prior to staining, Fc receptors were blocked in 10% normal mouse serum, 10 mM Tris buffer, 5 mM EDTA, 0.15 M NaCl, 0.25% gelatin, and 0.05% Tween-20 (pH 8.0). Tissue sections were incubated overnight at 4°C with primary antibodies. Immunoreactions were detected using biotinylated donkey anti-rat and goat-anti-rabbit (Vector Laboratories) and incubated with the Vectastin ABC Elite Kit (Vector Laboratories) and 3,3'-diaminobenzidine tetrahydrochloride (Sigma-Aldrich). Sections were counterstained with hematoxylin. The analysis of pathology, Ki67 and ChgA positivity were performed blinded by at least two independent analysts. Pathology was scored as previously described[31] and ChgA-expressing cells were counted in 7 to 15 crypts and/or villi per section. Pictures were taken with a Leica DFC350 FX microscope.

Transcript analysis. RNA was extracted using the NucleoSpin RNA XS kit (Machery Nagel). RNA from sorted cells was amplified according to the manufacturer's protocol (Ovation PicoSL WTA System V2, NuGen). For quantitative PCR, a Neviti Thermal Cycler (Applied Biosystems) and SensiFAST SYBR Lo-Rox kit (BioLine) were used, with the addition of $MgCl_2$ to a final concentration of 4 mM. All reactions were done in duplicate and normalized to the expression of *Gapdh*. Relative expression was calculated by the cycling threshold (CT) method as $2^{-\Delta CT}$. The primers sequences can be found in Table S1 (see below).

Table S1: Primer sequences

Gene	Forward Primer	Reverse Primer
Reg3g	CCATCTTCACGTAGCAGC	CAAGATGTCCTGAGGGC
Reg4	GGAAGCCAGTGTCATATCA	CCTTGGGGTTCATCTCA
Lyz1	GATGGCTACCGTGGTGT	CACCCATGCTCGAATG
Lgr5	GGGGGTGTGAGAATGTCT	AGGGCCTTCAGGTCTTC
Hes1	GCGAAGGGCAAGAATAA	TCGGGTCTGTGCTGAG
Ccnd1	GCACAACGCACTTTCTTT	GGTGGCCCTCAGATGT
Atoh1	TGGACGCTTTGCACTT	AGTGGGGGGAAAACTCT
Dll1	GGAGGACGATGTTCAGATAA	CGGCACAGGTAAGAGTTG
Gapdh	TCAACGGCACAGTCAAG	GCTCCACCCTTCAAGTG

Statistical analysis. Samples were analyzed using unpaired Mann-Whitney test. P values < 0.05 were considered significant. Data are shown as mean ± SEM.

RESULTS

RORγt-deficiency alters the homeostasis of intestinal crypts

In order to assess whether ILC3s have a role in maintaining intestinal homeostasis, we analyzed H&E stained sections of small intestine from RORγt-deficient mice and littermate controls. We used a scoring scheme for intestinal morphology and pathology that evaluates distinct features of the epithelium and the lamina propria, such as the length of the villi and their integrity, the structure of the lamina propria, the number of infiltrating cells and the degree of bleeding. It also comprised several parameters related to the appearance of the stem cell-containing crypt compartment including degree of crypt loss, crypt abscesses and crypt epithelial flattening. This detailed morphological assessment revealed the presence of intestinal alterations in the absence of ILC3s when compared to littermate controls **(Figure 1a-d)**. Interestingly, the pathological changes were mainly alterations in crypt morphology **(Figure 1d)**, indicating that absence of ILC3s alters the stem cell niche. Importantly, the histology scores are significantly lower compared to true pathological situations such as MTX application (Chapter 2 and 3). To substantiate these findings, we analyzed transcript levels of total small intestinal crypts and found a significant increase in the epithelial stress related transcripts *Tnf* and *Qa1* **(Figure 1e)**. Since a key function of intestinal crypts is to generate proliferative TA cells, we analyzed the number of proliferating crypt cells in RORγt-/- and control mice. The number of dividing crypt cells in both RORγt-deficient and controls mice were similar **(Figure 1f)**, showing that ILC3 absence does not alter steady-state crypt output. Finally, we examined the *in vitro* regenerative capacity of *ex vivo* isolated small intestinal crypts from RORγt-deficient mice and controls, by assessing their ability to form intestinal organoids. The efficiency of seeding was similar (data not shown) as was the average number of mature organoids that grew per well **(Figure 1g)**. Together these data suggest that RORγt-deficient mice have alterations affecting the crypt compartment yet retain normal crypt output and regenerative capacity in vitro.

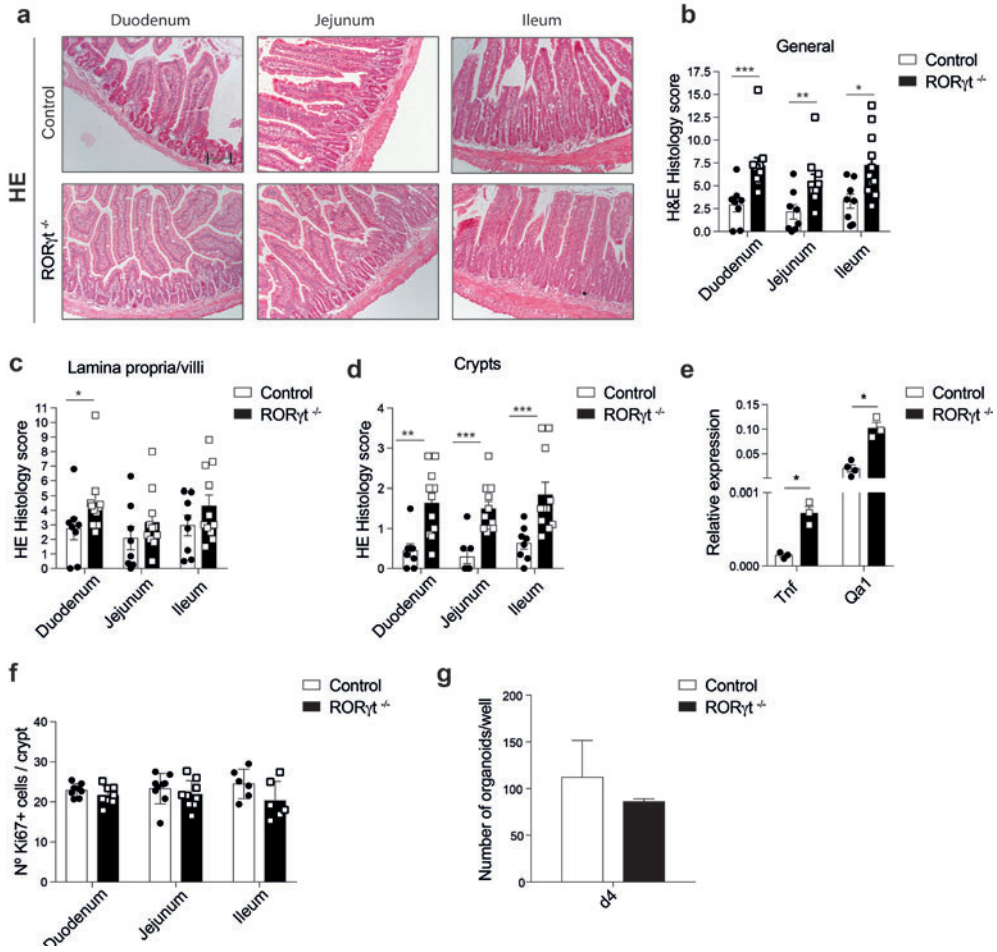

Figure 1: RORγt-deficiency alters the homeostasis of intestinal crypts. (a) Representative H&E staining of small intestinal sections from RORγt$^{+/+}$ (control) and RORγt$^{-/-}$ mice. **(b)** General small intestinal histology score or **(c)** specific Lamina propria/villi histology score or **(d)** specific crypt histology score in RORγt$^{+/+}$ (control) and RORγt$^{-/-}$ mice. **(e)** *Tnf* and *Qa1* transcript levels relative to *Gapdh in total crypts* expressed as fold change of RORγt$^{-/-}$ versus RORγt$^{+/+}$ controls. **(f)** Number of Ki67^{+} cells in small intestinal crypts from RORγt$^{+/+}$ (control) and RORγt$^{-/-}$ mice. **(g)** Average number of organoids in each well four days after culturing total small intestinal crypts isolated from RORγt$^{+/+}$ (control) and RORγt$^{-/-}$ intestines. * p<0.05, **p<0.01; ***p<0.001 Scale bars: 50µm; n=8-10 per group (a-e), n=3 per group (f) and n=2-3 per group (g).

Deficiency in IL-22 does not lead to altered homeostasis of the small intestine

The only ILC3-derived factor that has been linked to stem cell function is IL-22[12,32,33]. To gain insight into the role of ILC3-derived IL-22 in intestinal crypt homeostasis we evaluated histological alterations in the intestinal stem cell niche in IL-22-deficient mice. Intriguingly, IL-22-deficient mice did not recapitulate the altered features observed in RORγt-deficient mice and had normal intestinal morphology compared to control mice **(Figure 2a-d)**. In line with this, crypt output **(Figure 2e)** and in vitro stem cell regeneration in organoid cultures from IL-22-/- small intestinal crypts were not affected **(Figure 2f)**. Collectively, these results indicate that ILC3s regulate small intestinal homeostasis independent of IL-22.

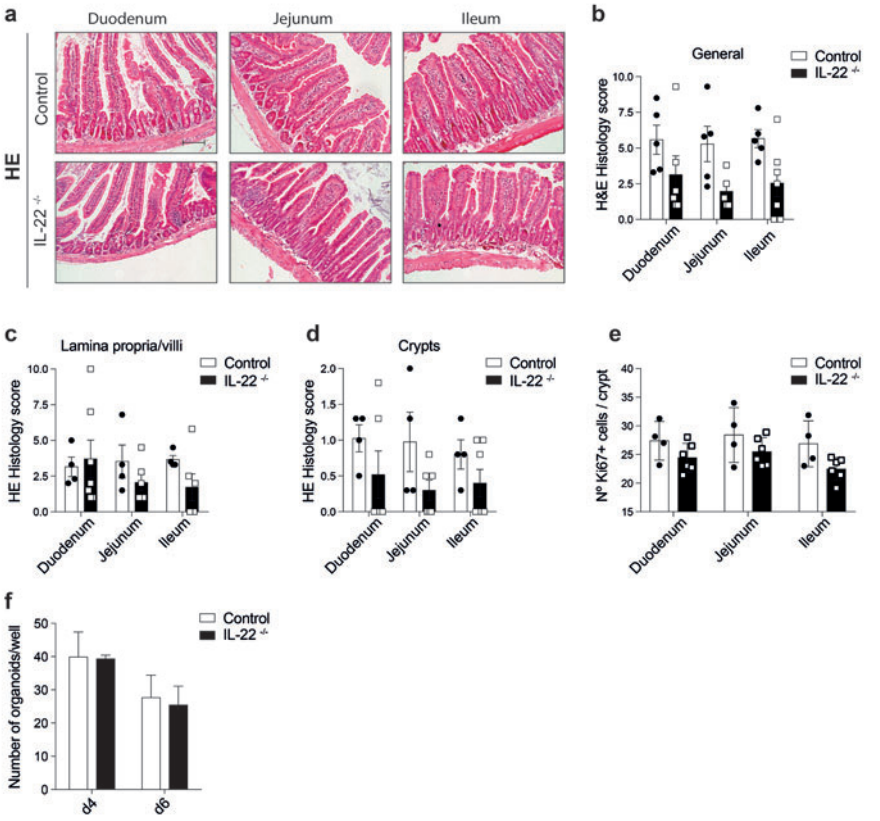

Figure 2: IL-22-deficiency does not recapitulate RORγt-deficiency. (a) Representative H&E staining in small intestinal sections from IL-22$^{+/-}$ (control) and IL-22$^{-/-}$ mice. **(b)** General or **(c)** Lamina propria/villi or **(d)** crypt H&E histological scores in IL-22$^{+/-}$ (control) and IL-22$^{-/-}$ mice. **(e)** Number of Ki67^{+} cells in small intestinal crypts from IL-22$^{+/-}$ (control) and IL-22$^{-/-}$ mice. **(f)** Average of the number of organoids in each well at day 4 (d4) and 6 (d6) after culturing total small intestinal crypts isolated from IL-22$^{+/-}$ (control) and IL-22$^{-/-}$ intestines. * p<0.05, **p<0.01; Scale bars: 50µm; n=4-6 per group (a-e), n=3-6 per group (f).

Transcript analysis in small intestinal crypts reveals ILC3-crypt crosstalk

Safeguarding the proliferative Lgr5^{+} stem cell compartment at the bottom of the crypts is crucial to provide a continuous source of TA cells to form the epithelial barrier and maintain mucosal defense mechanisms. We aimed at identifying the ILC3-dependend changes in intestinal crypt functionality that are independent of IL-22. Since all differentiated enterocytes are derived from crypt progenitors, we tested whether the presence or absence of ILC3s or IL-22 resulted in differences in the composition of small intestinal crypts at steady-state. In crypts of Lgr5-GFP reporter mice, all Lgr5-GFP^{+} ISCs express intermediate levels of the cell adhesion molecule CD24 **(Figure 3a)**. Hence, we used intermediate CD24 levels (CD24^{med}) to define a crypt cell subset that is enriched for Lgr5^{+} ISCs in wild-type B6 (WT), RORγt$^{-/-}$ and IL-22$^{-/-}$ mice. In addition, we quantified frequencies of enteroendocrine cells (EE; CD24^{hi} SSC-A^{lo}) and Paneth cells (PC; CD24^{hi} SSC-A^{hi}) in small intestinal crypts by flow cytometry **(Figure 3b)**. We did not observe significant changes in frequencies of these three main cellular subsets in absence of ILC3s or IL-22 **(Figure 3c)**. Next, we tested whether the frequency of Lgr5-GFP^{+} cells at steady-state was controlled by IL-22. To assess this, we treated Lgr5-GFP$^{+/-}$ reporter mice with neutralizing antibodies against IL-22 or with isotype controls every two days during a 6-day period. Subsequently, we isolated intestinal crypt cells and analyzed percentages of Lgr5^{+} ISCs and of the other cell subsets present in the crypts. Again, we did not detect changes in frequency of any of the aforementioned populations **(Figure 3d)**. Even though the frequency of PC was not altered by the absence of RORγt or IL-22, their function could still be influenced. We therefore purified PC from RORγt$^{-/-}$ or IL-22$^{-/-}$ mice. As expected, *Reg3g* transcript levels were significantly reduced in both RORγt$^{-/-}$ and IL-22$^{-/-}$ PC when compared to WT controls **(Figure 3e)**. This is in line with the strong correlation between ILC3-derived IL-22 and antimicrobial protein production in epithelial cells. In contrast, transcript levels of *Reg4,* a marker of both PC and EE cells[34] as well as a rare population of ISC[35], was increased in PC from RORγt$^{-/-}$ mice but not in IL-22$^{-/-}$ PC **(Figure 3e).**

Next, we set out to determine changes in ISC markers and genes important for ISC function in the CD24^{med} population. We analyzed the expression of the stem cell marker *Lgr5* and the Notch-target gene *Hes1.* The Notch-target gene *Hes1* was significantly lower transcribed in CD24^{med}-expressing cells from both RORγt- and IL-22-deficient crypts **(Figure 3f)**, suggesting differentiation towards the secretory cell lineage. Altogether, these analyses identify subtle ILC3-dependent changes in PC transcripts and suggest an impairment in Notch signaling within crypt epithelial cells enriched for ISCs.

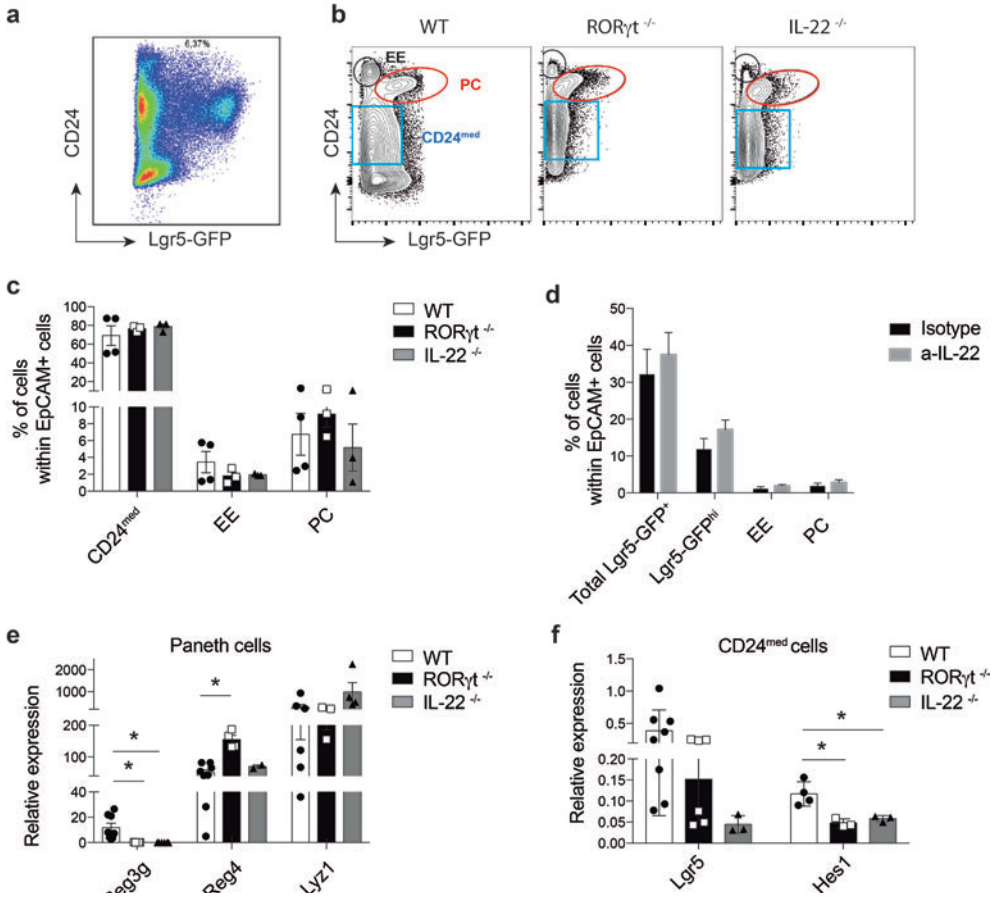

Figure 3: Sorted crypt cell populations from RORγt$^{-/-}$ and IL-22$^{-/-}$ reveal differences in stem cell and Paneth cell markers. (a) Representative FACS plots of duodenal crypts from Lgr5-GFP$^{+/-}$ reporter mice. **(b)** Representative FACS plots of total small intestinal crypts from WT, RORγt$^{-/-}$ and IL-22$^{-/-}$ mice. **(c)** Frequency of CD24^{med}-expressing cells, enteroendocrine cells (EE) and Paneth cells (PC) from WT, RORγt$^{-/-}$ and IL-22$^{-/-}$ small intestinal crypts. **(d)** Frequency of total Lgr5-GFP-expressing cells, Lgr5-GFP^{hi}-expressing cells, enteroendocrine cells and Paneth cells within EpCAM^{+} crypt cells from Lgr5-GFP$^{+/-}$ reporter mice treated with isotype or anti-IL-22 antibodies. **(e)** *Reg3g, Reg4* and *Lyz1* transcripts relative to *Gapdh* in sort-purified Paneth cells from WT, RORγt$^{-/-}$ and IL-22$^{-/-}$ mice. **(f)** *Lgr5* and *Hes1* transcripts relative to *Gapdh* in sort-purified CD24^{med}-expressing cells from WT, RORγt$^{-/-}$ and IL-22$^{-/-}$ mice. * p<0.05, **p<0.01; n=3-4 per group.

The Lgr5^{+} ISC pool contains higher frequencies of CD24^{hi} SSC-A^{lo} cells in the absence of ILC3s

To assess the effects of ILC3 absence on Lgr5^{+} ISCs directly, we analyzed ISCs from Lgr5-GFP/ RORγt$^{-/-}$ mice and control mice. Frequencies of total Lgr5-GFP^{+} cells as well as Lgr5-GFP^{hi} and Lgr5-GFP^{int} cells within total EpCAM-1^{+} crypt cells in duodenum, jejunum and ileum were determined by flow cytometry **(Figure 4a, left panels)**. In line with published reports, duodenal crypt fractions from control mice contained the highest frequency of Lgr5-GFP-expressing cells **(Figure 4b,c)**. RORγt$^{-/-}$ crypts showed similar percentages of total Lgr5-GFP^{+} stem cells and Lgr5-GFP^{hi}-expressing ISCs when compared to RORγt$^{+/+}$ and RORγt$^{+/-}$ mice **(Figure 4b,c)**. We next analyzed genes involved in stem cell function within total Lgr5-GFP-expressing cells of small intestinal crypts from RORγt$^{+/-}$ and RORγt$^{-/-}$ mice. Genes involved in Notch signaling, such as *Hes1*, *Atoh1* and *Dll1* were transcribed at similar levels in Lgr5^{+} ISCs from either RORγt$^{+/-}$ or RORγt$^{-/-}$ mice **(Figure 4d)**. *Lgr5* transcript levels seemed slightly lower in Lgr5^{+} ISCs from RORγt-/- crypts, although this did not reach statistical significance. In accordance with our findings that proliferation of crypt cells in the absence of ILC3s was unaltered, Lgr5^{+} ISCs expressed similar levels of the regulator of cyclin-dependent kinase, *Ccnd1*, which is required for cell cycle G1/S transition. Together these analyses revealed no gross alterations in molecular or cellular make-up of the stem cell pool in the absence of ILC3s. Since we detected alterations in the EE-lineage/stem cell-associated marker *Reg4* in PC, we also analyzed transcription of *Reg4* in Lgr5-GFP^{+} ISC. Similar to our findings in PC, *Reg4* was increased in purified Lgr5-GFP^{+} ISCs from RORγt$^{-/-}$ compared to RORγt$^{+/-}$ mice **(Figure 4d).** This prompted us to investigate the contribution of phenotypic enteroendocrine lineage cells (CD24^{hi} SSC-A^{lo}) to the Lgr5-GFP^{hi} and Lgr5-GFP^{int} cell populations by flow cytometry **(Figure 4e)**. Compared to control crypts, RORγt$^{-/-}$ duodenal crypts contained increased frequencies of CD24^{hi} SSC-A^{lo} cells that co-expressed GFP **(Figure 4e).** This was the case for cells expressing Lgr5-GFP at both high **(Figure 4e)** or intermediate levels **(Figure 4f)**. In sum, these results suggest that the composition of the Lgr5^{+} ISC pool in the absence of ILC3s is altered, and contains a higher proportion of cells displaying a bilineage phenotype with features of both enteroendocrine cells (CD24hi SSC-A^{lo} and Reg4^{+}) and ISCs (Lgr5-GFP, Hes1, Atoh1).

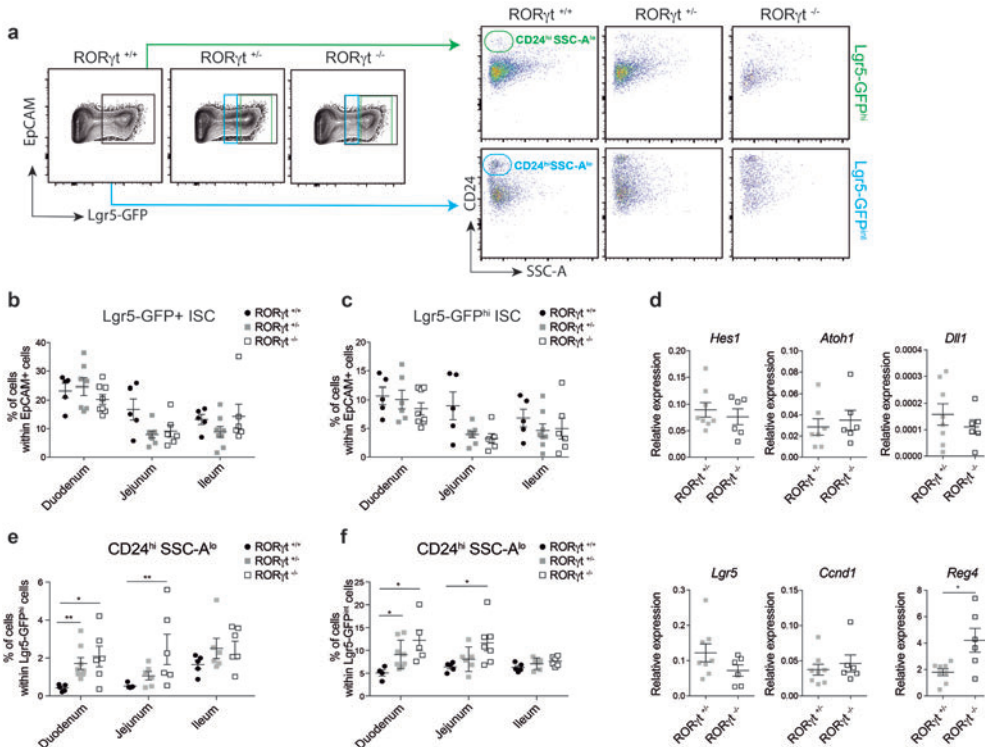

Figure 4: Composition of small intestinal crypts is not impaired in the absence of RORγt⁺ cells. (a) Representative FACS plots of duodenal crypt-derived cell suspensions from Lgr5-GFP/RORγt$^{+/+}$, Lgr5-GFP/RORγt$^{+/-}$ and Lgr5-GFP/RORγt$^{-/-}$ mice. Outlined areas indicate gates for total Lgr5-GFP^{+}, Lgr5-GFP^{hi} cells and Lgr5-GFP^{int} within CD45(-) Ter119(-) CD31(-) EpCAM(+) 7AAD(-) cells and CD24^{hi} SSC-A^{lo} cells within Lgr5-GFP^{hi} (top panel) and Lgr5-GFP^{int} cells (bottom panel). **(b)** Frequency of total Lgr5-GFP^{+} and **(c)** Lgr5-GFP^{hi} cells from Lgr5-GFP/RORγt$^{+/+}$, Lgr5-GFP/RORγt$^{+/-}$ and Lgr5-GFP/RORγt$^{-/-}$ small intestinal crypts. **(d)** Transcript analysis relative to *Gapdh* in total Lgr5-GFP^{+} cells from RORγt$^{+/-}$ and RORγt$^{-/-}$ small intestinal crypts. *p<0.01; **p<0.001; n=3-8 per group.

Lgr5-GFP^{hi} ISCs express secretory lineage transcripts in the absence of ILC3s

We considered two possible scenarios to explain the presence of Lgr5-GFP-expressing cells with an EE cell phenotype in the absence of ILC3s. One possibility is that in RORγt$^{-/-}$ mice, Lgr5^{+} ISCs differentiate towards the EE lineage faster than in RORγt$^{+/+}$ mice, generating EE cells that have terminated Lgr5 transcription but still contain GFP protein. An alternative explanation is that Lgr5-GFP^{int} cells that are differentiating along the EE lineage, dedifferentiate to become Lgr5-GFP^{hi} cells. In order to gather evidence for either of these scenarios we analyzed Lgr5-GFP^{hi} ISC from RORγt$^{+/+}$ (control) and RORγt$^{-/-}$ duodenal crypts by RNA sequencing. In the absence of RORγt, only a small number of genes were differentially expressed in Lgr5^{hi} ISCs and in line with this high degree of similarity, PCA revealed a poor segregation between control Lgr5-GFP^{hi} ISCs and Lgr5-GFP^{hi} from RORγt$^{-/-}$ ISCs **(Figure 5a)**. Further analysis showed a statistically significant downregulation of 23 genes and an upregulation of 38 genes in Lgr5-GFP^{hi} from RORγt$^{-/-}$ crypts when compared to control cells. First, we established the expression of genes involved in controlling stemness, to determine if co-expression of GFP and EE genes is caused by residual GFP presence in differentiated EE cells. GFP^{hi} cells from RORγt-/- mice had lower transcript levels of *Lgr5*, *Aqp4* and *Tnfrsf19* **(Figure 5b)**, yet when we analyzed additional genes associated with either CBCs with +4 quiescent stem cells, this revealed unaltered transcription of these genes in the absence of ILC3s. This indicates that the GFP^{hi} cells in RORγt$^{-/-}$ mice still express a full array of stem cell genes. Subsequently we focused on genes associated with mature EE cells, in support of a scenario entailing dedifferentiation of maturing cells. Interestingly, in the absence of ILC3s, Lgr5-GFP^{hi} cells were enriched for EE cell-associated genes, such as *Cck*, *Guca2a*, *Chga* and Chgb; and other genes characteristic of secretory cells like *Reg4*, *Defa21*, *Defa26*, *Scin*, *Spink4*, *Tff3* and *Muc2* **(Figure 5c)**. The increase in EE genes was not due to altered EE cell differentiation, as no significant changes were observed in the number of mature ChgA+ enteroendocrine cells in villi or crypts in the absence of ILC3s **(Figure 5d,e)**. In sum, Lgr5-GPF^{hi} ISCs in the absence of ILC3s co-express secretory genes and stem cell genes, which suggests that these might be originating from Lgr5-GFP^{int} EE precursors.

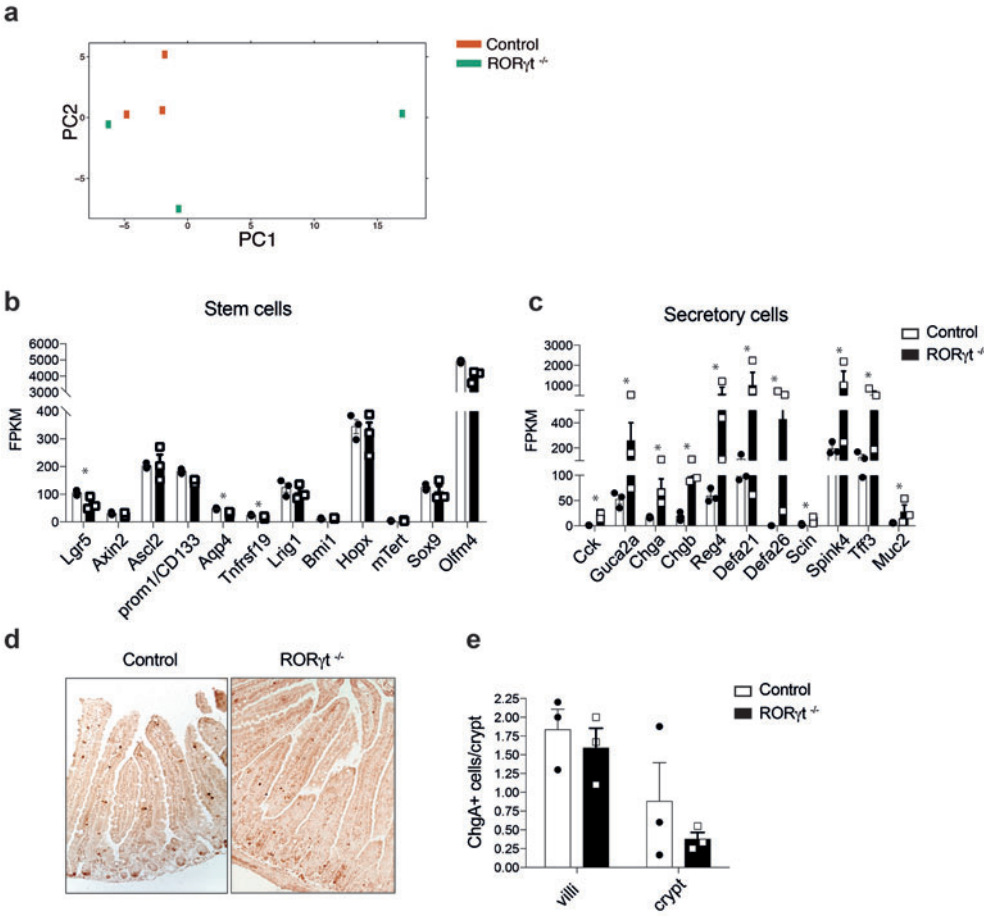

Figure 5: Lgr5-GFP^{hi} ISC express high levels of secretory transcripts. (a) PCA plot of Lgr5-GFP^{hi} cells at steady-state (SS) from Lgr5-GFP/RORγt$^{+/+}$ (control) and Lgr5-GFP/RORγt$^{-/-}$ mice. **(b)** FPKM values of a selected group of genes associated with stem cells and **(c)** secretory cells in Lgr5-GFP/RORγt$^{+/+}$ (control) and Lgr5-GFP/RORγt$^{-/-}$ Lgr5-GFP^{hi} cells. **(d)** Representative ChgA immunostaining of duodenal sections and **(e)** quantification of ChgA^{+} cells from Lgr5-GFP/RORγt$^{+/+}$ and Lgr5-GFP/RORγt$^{-/-}$ mice at steady-state. *p<0.01. n=3 per group.

ILC3s contribute to the differentiation of Lgr5^{+} cells into secretory cells after MTX

Dedifferentiation of EE-lineage cells to replenish lost Lgr5^{+} ISCs has been reported in response to intestinal damage. To determine whether this also happens in response to MTX, and whether this is altered in the absence of ILC3s we exposed RORγt$^{+/+}$ and RORγt$^{-/-}$ Lgr5-GFP reporter mice to MTX. Within the Lgr5-GFP^{hi} **(Figure 6a)** and Lgr5-GFP^{int} **(Figure 6b)** ISC populations, the frequency of cells displaying the EE-lineage phenotype (GFP^{+} CD24^{hi} SSC-A^{lo}) increased in response to MTX induced damage in control mice. In ILC3-deficient mice, steady-state frequencies of GFP^{+} EE-lineage cells were increased **(Figure 6a)**, but in contrast to control mice, the enrichment of EE-lineage GFP^{+} cells in response to tissue damage was completely abrogated **(Figure 6b)**. This is in line with the RNA profiling we performed and discussed in chapter 3. In control mice, GFP^{+} cells are enriched for EE-lineage genes at day 1 after MTX, while this enrichment is absent in GFP^{+} cells from ILC3-deficient mice **(Figure 6c)**. To determine whether the lack of IL-22 in RORγt$^{-/-}$ mice is responsible for this phenotype, we neutralized IL-22 in Lgr5-GFP$^{+/-}$ mice. In response to damage and compared to steady-state conditions, the recruitment of Lgr5-GFP^{+} cells with the EE-like phenotype was similar to ILC3-deficiency, indicating that IL-22 is partially involved **(Figure 6d,e)**. In sum, these data suggest that the increase in phenotypically bilineage progenitor cells is part of the tissue response to damage, and that this accumulation is regulated by ILC3, in part through IL-22.

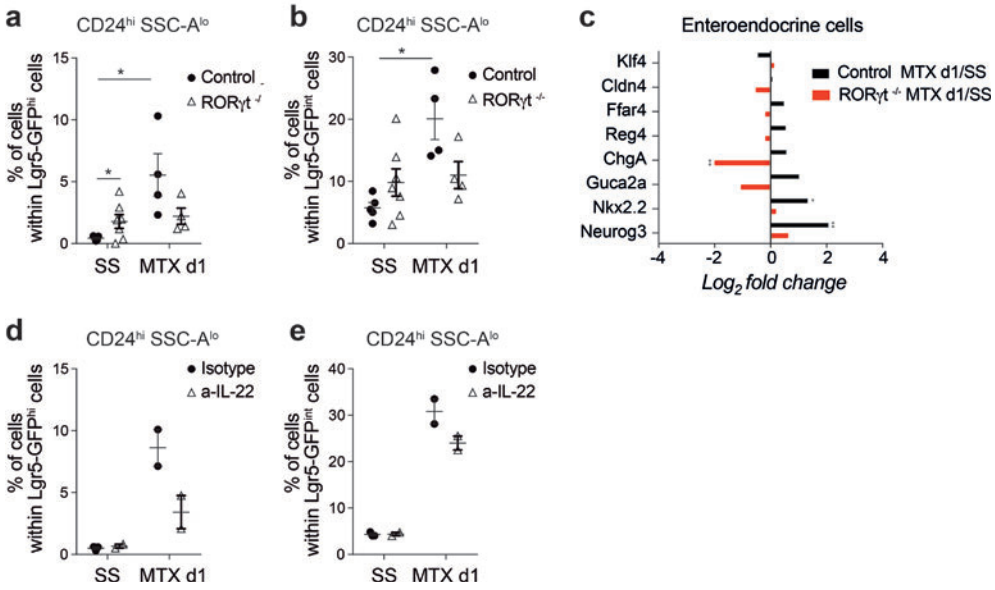

Figure 6: RORγt-deficiency alters the Lgr5^{+} ISC pool in response to MTX. (a) Frequency of CD24^{hi} SSC-A^{lo} cells within Lgr5-GFP^{hi} and **(b)** Lgr5-GFP^{int} cells in duodenal crypts of RORγt$^{+/+}$ (Control) and RORγt$^{-/-}$ mice at SS and MTX d1. **(c)** Log_2fold change values for transcripts that correspond to genes required during enteroendocrince cell differentiation expressed by Lgr5-GFP^{hi} cells comparing MTX d1 versus SS from Lgr5-GFP/RORγt$^{+/+}$ controls (black bars) and Lgr5-GFP/RORγt-/- mice (red bars). FPKM values are plotted for transcripts that have statistically significant Log_2fold change (DESeq2 analysis of count data) with p value <0,01 or ns (non-significant). Frequency of CD24^{hi} SSC-A^{lo} cells within **(d)** Lgr5-GFP^{hi} and **(e)** Lgr5-GFP^{int} cells in duodenal crypts of Lgr5-GFP$^{+/-}$ mice treated with isotype or anti-IL-22 and harvested at SS and MTX d1. *p<0.01; **p<0.001; *** p<0.0001; n=3-10 per group.

DISCUSSION

Small intestinal ILC3s reside in cryptopatches directly adjacent to the crypts that contain stem cells. ILC3s contribute to epithelial renewal in response to damage[12,32,33]. The cellular and molecular mechanisms by which ILC3s control stem cell behavior under homeostatic conditions and after injury are yet to be fully elucidated. Here we show that in the absence of ILC3s the crypts of the small intestine have an altered architecture. Furthermore, we provide evidence for regulation of *Hes1*-expressing crypt epithelial stem by ILC3s. The reduced levels of *Hes1* mRNA expression in crypt cells in the absence of ILC3s suggests a shift in cell fate decisions towards secretory cell types at the expense of the absorptive lineage, similar to Hes1 deficient mice[36]. In agreement with this, RORγt-deficient crypts harbor higher percentages of CD24^{hi} SSC-A^{lo} cells within the Lgr5-GFP^{hi}- or Lgr5-GFP^{int}- expressing cells. In fact, the Lgr5-GFP^{hi} cells from RORγt$^{-/-}$ were enriched for transcripts characteristic of enteroendocrine cells (*Cck, Guca2, CghA, ChgB, Reg4*), expressed lower transcripts for the stem cell genes *Lgr5*, *Aqp4* and *Tnfrsf19* but similar levels of *Axin2*, *Ascl2*, *Ephb2* and *Lrig1*, among others stem cell genes. However, frequencies of Lgr5-GFP^{hi} ISCs and mature epithelial cell types, such as enteroendocrine and Paneth cells were unaltered in the absence of RORγt under homeostatic conditions. Together these data suggest that in the absence of ILC3s, secretory precursor cells expressing intermediate levels of Lgr5 are continuously recruited into the Lgr5-GFP^{hi} ISC pool to maintain normal crypt output, raising the possibility that survival or function of Lgr5-GFP^{hi} ISCs is affected in the absence of ILC3s. To gain further insight into this possibility, double-immunostaining for secretory and stem cell markers, such as ChgA and Lgr5 would be essential, as well as further investigation to specifically identify proliferative cells crypt cells in the absence of ILC3s. Moreover, it is fundamental to validate the efficiency of organoid formation for Lgr5-GFP^{hi} ISCs from ILC3-deficient or sufficient mice as an *ex vivo* measurement of their regenerative potential.

The role of IL-22 in regulation of the intestinal stem cell pool under homeostatic conditions is still incompletely understood. IL-22 deficiency does not result in major changes in small intestinal architecture and we could not detect any pathology in the crypt compartment. Accordingly, the presence of ILC3s, although IL-22 deficient, seems sufficient for maintenance of crypt homeostasis. IL-22$^{-/-}$ Paneth cells had no detectable transcript levels of *Reg3g*, confirming previous reports on the importance of IL-22 in supporting antimicrobial functionality of epithelial cells[8,9]. Differences in the antimicrobial response in the epithelium directly influence the microbiota, hence it would be interesting to investigate whether the differences observed in RORγt$^{-/-}$ and IL-22$^{-/-}$ mice are explained by distinct microbiota communities. Antibiotic treatment to modulate the microbiota would allow the investigation of epithelial responses in the presence of reduced microbiota. In our current study, the vast majority of experiments were conducted by using littermate controls for RORγt$^{-/-}$ and Lgr5-GFP$^{+/-}$ mice treated with neutralizing anti-IL-22 antibodies,

thus reducing microbiota-dependent effects. Inhibiting IL-22 for a short period of time is sufficient to decrease *Reg3g* and *Reg3b* in total small intestinal crypts (data not shown) but does not reduce Lgr5-GFP^{+} cell frequencies nor increase EE-lineage Lgr5-GFP^{+} cells in the small intestinal crypts at steady-state. One interesting follow-up experiment would be to neutralize IL-22 for longer periods of time to assess the molecular mechanisms by which IL-22 precisely regulates Lgr5-expressing cells *in vivo*.

Interestingly, we found that whereas the frequency of Lgr5-GFP^{hi} cells one day after MTX is reduced, a cell subset co-expressing Lgr5-GFP and a phenotype resembling enteroendocrine cells was increased. These cells acquired secretory cell transcripts and maintained the expression of some stem cell genes. All together this suggests that subsets of Lgr5-expressing cells are recruited during injury and contribute to progeny. Strikingly, this regulation was completely absent in RORγt-deficient Lgr5-expressing cells, suggesting a possible contribution from ILC3s to plasticity of the stem cell pool and the induction of differentiation. As a follow up, determining the identity, molecular functions of cell subsets within the Lgr5-GFP^{int} and Lgr5-GFP^{hi} cells related to tissue homeostasis and regeneration would be highly interesting, in particular to determine which populations of stem cells proliferate during injury. Beyond the recognition of specific populations of crypt cells, focus must be placed on identifying the mechanisms by which cellular transformation of resting crypt cells into cycling intestinal stem cells is established.

This study contributes to current views on how innate lymphoid cells regulate crypt homeostasis and the activation of intestinal epithelial cells to allow regeneration upon damage to the Lgr5^{+} stem cell population. Ultimately, this could aid in identifying novel therapeutic strategies to modulate intestinal epithelial regeneration during intestinal inflammation or after damage sustained from anti-cancer therapies.

REFERENCES

1. Peterson, L. W. & Artis, D. Intestinal epithelial cells: regulators of barrier function and immune homeostasis. *Nat. Rev. Immunol.* **14,** 141–153 (2014).
2. Qiu, Ju; Heller, Jennifer J; Guo, Xiaohuan; Zong-ming E Chen, K. F., Yang-Xin Fu, and L. Z., Qiu, J., Heller, J. J., Guo, X., Chen, Z. E. M. E., Fish, K., Fu, Y.-X. X. & Zhou, L. The Aryl Hydrocarbon Receptor Regulates Gut Immunity through Modulation of Innate Lymphoid Cells. *Immunity* **36,** 92–104 (2012).
3. Barker, N. *et al.* Identification of stem cells in small intestine and colon by marker gene Lgr5. *Nature* **449,** 1003–1007 (2007).
4. Sato, T. *et al.* Growing Self-Organizing Mini-Guts from a Single Intestinal Stem Cell: Mechanism and Applications. *Science (80-.).* **340,** (2013).
5. Lügering, A., Ross, M., Sieker, M., Heidemann, J., Williams, I. R., Domschke, W. & Kucharzik, T. CCR6 identifies lymphoid tissue inducer cells within cryptopatches. *Clin. Exp. Immunol.* **160,** 440–449 (2010).
6. Ouyang, W., Kolls, J. K. & Zheng, Y. The Biological Functions of T Helper 17 Cell Effector Cytokines in Inflammation. *Immunity* **28,** 454–467 (2008).
7. Wolk, K., Witte, E., Witte, K., Warszawska, K. & Sabat, R. Biology of interleukin-22. *Seminars in Immunopathology* **32,** 17–31 (2010).
8. Kolls, J. K., McCray, P. B. & Chan, Y. R. Cytokine-mediated regulation of antimicrobial proteins. *Nat. Rev. Immunol.* **8,** 829–835 (2008).
9. Zheng, Y. *et al.* Interleukin-22 mediates early host defense against attaching and effacing bacterial pathogens. *Nat. Med.* **14,** 282–9 (2008).
10. Sato, T. *et al.* Paneth cells constitute the niche for Lgr5 stem cells in intestinal crypts. *Nature* **469,** 415–418 (2011).
11. Turner, J. E., Stockinger, B. & Helmby, H. IL-22 Mediates Goblet Cell Hyperplasia and Worm Expulsion in Intestinal Helminth Infection. *PLoS Pathog.* **9,** 1–7 (2013).
12. Lindemans, C. A. *et al.* Interleukin-22 promotes intestinal-stem-cell-mediated epithelial regeneration. *Nature* **528,** 560–564 (2015).
13. Muñoz, J. *et al.* The Lgr5 intestinal stem cell signature: robust expression of proposed quiescent '+4' cell markers. *EMBO J.* **31,** 3079–3091 (2012).
14. Tao, S. *et al.* Wnt activity and basal niche position sensitize intestinal stem and progenitor cells to DNA damage. *EMBO J.* **34,** 624–40 (2015).
15. Metcalfe, C., Kljavin, N. M., Ybarra, R. & De Sauvage, F. J. Lgr5+ stem cells are indispensable for radiation-induced intestinal regeneration. *Cell Stem Cell* **14,** 149–159 (2014).
16. Montgomery, R. K. *et al.* Mouse telomerase reverse transcriptase (mTert) expression marks slowly cycling intestinal stem cells. *Proc. Natl. Acad. Sci. U. S. A.* **108,** 179–184 (2011).
17. Powell, A. E. *et al.* The pan-ErbB negative regulator Irig1 is an intestinal stem cell marker that functions as a tumor suppressor. *Cell* **149,** 146–158 (2012).
18. Takeda, N., Jain, R., LeBoeuf, M. R., Wang, Q., Lu, M. M. & Epstein, J. A. Interconversion between intestinal stem cell populations in distinct niches. *Science* **334,** 1420–1424 (2011).
19. Yan, K., Chia, L., Li, X. & Ootani, A. The intestinal stem cell markers Bmi1 and Lgr5 identify two functionally distinct populations. *Proc. Natl. Acad. Sci. U. S. A.* **109,** 466–471 (2012).
20. Li, N., Nakauka-Ddamba, A., Tobias, J., Jensen, S. T. & Lengner, C. J. Mouse Label-Retaining Cells Are Molecularly and Functionally Distinct From Reserve Intestinal Stem Cells. *Gastroenterology* **151,** 298–310. e7 (2016).

21. Sangiorgi, E. & Capecchi, M. R. Bmi1 is expressed in vivo in intestinal stem cells. *Nat. Genet.* **40,** 915–20 (2008).

22. Tian, H., Biehs, B., Warming, S., Leong, K. G., Rangell, L., Klein, O. D. & de Sauvage, F. J. A reserve stem cell population in small intestine renders Lgr5-positive cells dispensable. *Nature* **478,** 255–9 (2011).

23. Wong, V. W. Y. *et al.* Lrig1 controls intestinal stem-cell homeostasis by negative regulation of ErbB signalling. *Nat. Cell Biol.* **14,** 401–8 (2012).

24. Tetteh, P. W. *et al.* Replacement of Lost Lgr5-Positive Stem Cells through Plasticity of Their Enterocyte-Lineage Daughters. *Cell Stem Cell* **18,** 203–213 (2016).

25. Yoshitatsu Sei, Xinping Lu, Alice Liou, Xilin Zhao, S. A. W., Sei, Y., Lu, X., Liou, A., Zhao, X. & Wank, S. A. A stem cell marker-expressing subset of enteroendocrine cells resides at the crypt base in the small intestine. *Am J Physiol Gastrointest Liver Physiol* **300,** 345–356 (2011).

26. Yan, K., Chia, L. & Li, X. The intestinal stem cell markers Bmi1 and Lgr5 identify two functionally distinct populations. *Pnas* **109,** 466–471 (2012).

27. Yan, K. S. *et al.* Intestinal Enteroendocrine Lineage Cells Possess Homeostatic and Injury-Inducible Stem Cell Activity. *Cell Stem Cell* **21,** 78–90.e6 (2017).

28. Jadhav, U., Saxena, M., O'Neill, N. K., Saadatpour, A., Yuan, G. C., Herbert, Z., Murata, K. & Shivdasani, R. A. Dynamic Reorganization of Chromatin Accessibility Signatures during Dedifferentiation of Secretory Precursors into Lgr5+ Intestinal Stem Cells. *Cell Stem Cell* (2016).

29. Gröschel, S. *et al.* A single oncogenic enhancer rearrangement causes concomitant EVI1 and GATA2 deregulation in Leukemia. *Cell* **157,** 369–381 (2014).

30. Subramanian, A. *et al.* Gene set enrichment analysis: a knowledge-based approach for interpreting genome-wide expression profiles. *Proc. Natl. Acad. Sci. U. S. A.* **102,** 15545–50 (2005).

31. de Koning, B. A. E. *et al.* Contributions of mucosal immune cells to methotrexate-induced mucositis. *Int. Immunol.* **18,** 941–949 (2006).

32. Hanash, A. M. *et al.* Interleukin-22 Protects Intestinal Stem Cells from Immune-Mediated Tissue Damage and Regulates Sensitivity to Graft versus Host Disease. *Immunity* **37,** 339–350 (2012).

33. Aparicio-Domingo, P. *et al.* Type 3 innate lymphoid cells maintain intestinal epithelial stem cells after tissue damage. *J. Exp. Med.* **212,** 1783–91 (2015).

34. Sasaki, N. *et al.* Reg4+ deep crypt secretory cells function as epithelial niche for Lgr5+ stem cells in colon. *Proc. Natl. Acad. Sci. U. S. A.* 1607327113- (2016).

35. Grün, D., Lyubimova, A., Kester, L., Wiebrands, K., Basak, O., Sasaki, N., Clevers, H. & van Oudenaarden, A. Single-cell messenger RNA sequencing reveals rare intestinal cell types. *Nature* **525,** 251–5 (2015).

36. Jensen, J. *et al.* Control of endodermal endocrine development by Hes-1. *Nat. Genet.* **24,** 36–44 (2000).

5

DENDRITIC CELLS ASSOCIATE WITH GROUP 3 INNATE LYMPHOID CELLS TO CONTROL INTESTINAL REGENERATION

Mónica Romera-Hernández[1], Julien J. Karrich[1], Patricia Aparicio-Domingo, Ferry Cornelissen[1], Natalie Papazian[1], Louis Boon[2], Janneke N. Samsom[3] and Tom Cupedo[1]

[1]Department of Hematology, Erasmus University Medical Center, Rotterdam, The Netherlands
[2]Bioceros B.V., Utrecht, The Netherlands
[3]Department of Pediatrics, Division of Gastroenterology, Erasmus University Medical Center, Rotterdam, The Netherlands

Manuscript in preparation

ABSTRACT

In the small intestine (SI), CCR6$^+$ group 3 innate lymphoid cells (ILC3) cluster together with CD11c$^+$ dendritic cells (DCs) in small intestinal solitary lymphoid tissues (SILTs). The simplest SILT structures are called cryptopatches (CP) and locate near the stem cell-containing crypts. The innate function of SILTs under homeostatic conditions is still unknown. We hypothesized that SILTs act as innate control centers where ILC3 and DC interact and translate environmental cues into homeostatic and regenerative responses in the small intestinal crypts. Because of the important role of DCs in sensing and modulating ILC3 functions, we first asked whether DCs contribute to ILC3-mediated regenerative responses after MTX-induced tissue damage. Depletion of CD11c$^+$ cells during MTX treatment resulted in impaired proliferation of small intestinal crypts, indicating that CD11c$^+$ cells contribute to epithelial responses during regeneration after damage, although the mechanisms underlying these processes remain elusive. Next, we aimed at identifying specifically dendritic cells that cluster in SILTs together with ILC3. Immunohistochemistry, in vitro assays and RNA sequencing allowed for a classification of SILT-DCs as CD11c$^+$ MHCII$^+$ CD11b$^-$ CD103$^-$ Plet1$^+$ cells, expressing high levels of *IL23a, IL1b* and *Il22ra1* transcripts, factors capable of regulating ILC3 function. Altogether, this work characterizes a novel DC population that uniquely locate in SILTs, closely associating with ILC3s and able to regulate ILC3. It suggests that SILT-DCs can sense epithelial damage responses and contribute to tissue regeneration.

INTRODUCTION

The mucosal immune system needs to protect the single layer of epithelial cells which is largely exposed to foreign antigens, commensal bacteria and pathogens. Key immune cells central to this process are dendritic cells (DCs), a heterogeneous family of innate leukocytes with an exceptional ability to balance tolerogenic and effector immune responses to enteric antigens, allowing for a symbiotic system between the microbiome and their host.

Our earlier results have delineated how group 3 innate lymphoid cells (ILC3s) in cryptopatches (CP) are able to induce intestinal epithelial stem cell (ISC) regeneration, yet the mechanisms leading to ILC3 activation remain elusive. Due to their capabilities of sense the environment and their positioning in CP, we hypothesized that during epithelial stem cell damage, DCs are in charge of triggering ILC3-mediated tissue repair.

Classical DCs are found diffused in the intestinal lamina propria (LP), in gut-associated lymphoid tissue (GALT) including Peyer's Patches (PPs) and solitary isolated lymphoid follicles (SILTs), and in intestinal draining LNs such as the mesenteric LNs (MLNs)[1,2]. DCs induce tolerance by presenting harmless antigens (derived from commensal bacteria and dietary components) to naïve T cells and initiate adaptive immunity against pathogenic microbes.

Multiple intestinal DC subsets have recently been classified in the murine gut and associated lymphoid tissues by the expression of distinct surface markers. DCs are defined by the expression of CD11c and MHCII while being negative for CD64. In addition, the integrins CD103 and CD11b define four major populations of conventional DCs in the LP of the murine small bowel[3,4]. Double positive DCs expressing $CD103^+CD11b^+$ drive Th17 and Th2 cell differentiation in intestine-draining MLNs[3,5,6]. Single $CD103^+CD11b^-$ cells ($CD24^+$ $XCR1^+$ $CD8\alpha^+$) have a predominant function in cross-presentation to $CD8^+$ T cells and induction of Th1 responses[7,8]. Another subset of DCs, the $CD103^-CD11b^+$ cells are able of inducing both Th17 and Th1 responses[4]. And finally, the double negative $CD11b^-CD103^-$ cells is a largely unexplored DC subset that is believed to locate in GALT, as it is virtually absent in RORγt-deficient mice, which lack PP and SILTs.

Besides their role in T cell differentiation DCs also have the ability to ILC3s to maintain epithelial integrity. Interactions between IL-23-expressing DCs with IL-22-expressing ILC3s are essential to induce the expression of *RegIII* and *S100a* family of epithelial genes, critical for steady-state epithelial protective functions[9,10]. During pathogen challenge, IL-22 production by ILC3s is regulated by $LT\beta R^+$ DCs[11] clustered in lymphoid follicles. Interestingly, there is evidence that DC positioning within the intestinal mucosa dictates compartmentalization of ILC3 subsets. For instance, DCs expressing CXCL16 retain $NKp46^+$ ILC3 in the LP due to their expression of the ligand CXCR6[12,13]. In addition, DCs also localize in SILTs with an ILC3 population that express CXCR5, CCR6 and CCR7[14,15].

SILTs develop after birth and contain CP and isolated lymphoid follicles (ILFs). Both structures are developmentally dependent on ILC3s[16,17] and on $LT\alpha_1\beta_2$-$LT\beta R$[18] interactions with mesenchymal stromal cells, as evidenced by their absence in RORγt-deficient mice and $LT\alpha^{-/-}$ and $LT\beta R^{-/-}$ mice.

CP are defined as small aggregates of cells mainly composed of CCR6$^+$ ILC3, DCs and non-hematopoietic stromal cells. CP function is incompletely understood. Their localization in the subepithelial space of the murine gut, and our findings on the importance of ILC3s and CP in epithelial regeneration suggests that CP are important for immune-epithelial crosstalk to ensure epithelial barrier function.

In this chapter, we aimed at identifying DC subsets co-localized with CCR6$^+$ ILC3 in SILTs in order to test whether a crosstalk between DCs and ILC3s takes place in anatomically defined locations within the small intestine (SI) and its relevance during epithelial crypt homeostasis and regeneration after MTX-induced tissue damage.

MATERIALS AND METHODS

Mice. C57BL/6, CD11c-DTR, RORγt-GFP and hCD2-GFPmice were bred in the animal facility of the Erasmus University Medical Center Rotterdam. Animal experiments were approved by the relevant authorities and procedures were performed in accordance with institutional guidelines. Age and gender-matched littermates were used whenever possible. $Csf2^{-/-}$ mice were bred at Icahn School of Medicine at Mount Sinai Hess Center for Science and Medicine (New York) and samples were kindly provided by Arthur Mortha from The Merad Laboratory.

Methotrexate (MTX). 8-12 weeks old mice were injected i.p. with 120mg/kg MTX (PCH) at day-1 and with 60mg/kg at day 0. Tissues were collected at day 1 and day 4 after the last MTX injection.

CD11c depletion. 100ng of diphtheria toxin (DT) and either phosphate-buffered saline (PBS) or saline were administered i.p to CD11c-$DTR^{+/-}$ mice. When DT was combined with MTX, DT was injected at day -2, followed by two consecutive i.p injections of MTX on day -1 and day 0. CD11c depletion was validated 24-72h after DT administration, both in the lamina propria as well as in mesenteric lymph nodes.

SILT enrichment. Microdissection of solitary intestinal lymphoid tissues was performed manually with biopsy punch needles (Luer strub adaptor blunt needles; Access Technologies) from hCD2-GFP small intestinal fragments exposed to a stereoscopic microscope. SILTs were collected in PBS + 2% FCS and kept on ice until further processing. SILTs were digested by Liberase I (Roche) and Dnase I (Calbiochem) at 37°C for 15 min on a magnetic stirrer. Cells were washed and filtered through a 100um cell strainer.

Generation and *in vitro* stimulation of splenic or BMDC. Spleen were excised into small pieces and placed onto a strainer attached to a 50ML conical tube. Spleen fragments were pressed through the strainer using the plunger end of a syringe. Cells were washed with PBS and centrifuged. Supernatant was resuspended in 2m of lysing solution to lyse red blood cells (IOTEST; Beckman Coulter). Cells were washed in PBS and $CD11c^{+}$ cells were enriched by using MACS Cell Separation beads (Milteny Biotec). BMDC were generated from bone marrow suspensions harvested from 8 to 12 weeks old C57BL/6 mice. Briefly, bone marrow was flushed from femurs and tibias, passed through a 100 μm mesh to remove fibrous tissue, and red blood cells were lysed using IOTEST lysis solution (Beckman Coulter). Cells were cultured at $0.3x10^6$ cells/ml in IMDM medium (GIBCO BRL) supplemented with 10% FCS, 2 mM glutamine, 50 μM β2-mercaptoethanol, 100 IU/ml penicillin, 100 μg/ml streptomycin and 20 ng/ml Granulocyte-macrophage colony-stimulating factor (GM–CSF; X63 supernatant).[14] On days 3 and 6, fresh GM-CSF-containing medium was added. Floating

differentiated BMDC were isolated at day 7 and separated from plate-adherent macrophages, and used for further experiment. BMDC purity was determined by flow cytometry and was consistently over 60%. For *in vitro* stimulations, $1x10^6$ splenic DCs or BMDC were cultured overnight in the presence of 20ng/ml GM-CSF (X63 supernatant) or left untreated.

Immunohistochemistry. Tissues were frozen in Tissue-Tek O.C.T compound (Sakura Finetek Europe B.V.) and stored at -80°C. Six µm cryosections were fixed for 5 min in ice-cold acetone and air-dried for 10 min, and subsequently blocked with 5% normal mouse serum and 5% normal donkey serum for 15 min. Sections were incubated with primary antibody Rat anti-Plet-1 (1D4, Bioceros B.V.) and biotinylated Hamster anti-CD11c (N418, Ebioscience) or CD103 (M290, BD Biosciences) for 1 h at room temperature, followed by a 30min incubation with secondary donkey anti-rat labeled with AlexaFluor-488 (Molecular Probes) or streptavidin labeled with AlexaFluor-594 (Molecular Probes). Sections were embedded in Pro-long Gold with DAPI (Invitrogen) and analyzed on a Leica DMRXA.

Antibodies. Monoclonal antibodies used for flow cytometry were: CD45 (30-F11, BioLegend), CD11c (N418; BioLegend), CD11b (M1/70; eBioscience), CD103 (M290; BD Biosciences), MHCII (MD/114.15.2; BioLegend), Plet1 (1D4; Bioceros B.V.), CD8a (45-6.7; eBioscience), B220 (RA3-6B2; BD), CD64 (X54.5/7.1; BioLegend); Intracellular staining of IRF8 (V36YWCH; eBioscience) was performed following the BD Biosciences Transcription Factor staining kit protocol; CD45 (MCD4517; LifeTechnologies), CD19-bio (1D3; eBioscience), B220-bio (RA3-6B2; eBioscience), CD11c-bio (N418; eBioscience), CD11b-bio (M1/70; BioLegend), Gr1-bio (RB6-8C5; eBioscience), CD3 (145-2C11; BD), CD90.2 (30H12; BioLegend), NK1.1 (PK136; eBioscience), CD127 (A7R34, eBioscience), CD117 (2B8; Biolegend), NKp46 (29A1.4; eBioscience), CCR6 (29-2L17; BioLegend).
Antibodies used for paraffin immunostaining were: rat anti-mouse Ki67 monoclonal antibody (MIB-5, Dako).

Flow cytometry and cell sorting. Cells were incubated with Zombie Aqua Fixable Viability (BioLegend) prior to staining. Cells were pre-incubated with normal mouse serum, normal donkey serum and normal rat serum (Jacksonimmuno). Fc block was performed by incubation with CD16/CD32 (553142; BD). All stainings were performed in PBS containing 2% heat-inactivated fetal calf serum (FCS) at 4°C. Stained cells were analyzed using FACS LSRII (BD Biosciences) and data processed with FlowJo software (FlowJo, LLC).

RNA sequencing. cDNA was prepared using SMARTer Ultra Low RNA kit (Clontech Laboratories) for Illumina Sequencing following the manufacturer's protocol. The Agilent 2100 Bio-analyzer and the High Sensitivity DNA kit were applied to determine the quantity and quality of the cDNA production. Amplified cDNA was further processed according to TruSeq Sample Preparation v.2 Guide (Illumina) and paired end-sequenced (2x75bp) on the HiSeq 2500 (Illumina). Demultiplexing was performed using CASAVA software (Illumina) and

the adaptor sequences were trimmed with Cutadapt (http://code.google.com/p/cutadapt/). Alignments against the mouse genome (mm10) and analysis of differential expressed genes were performed with $DESeq_2$ in the R environment on the raw fragment counts extracted from the BAM files by HTSeq-count[19]. Cufflinks software was used to calculate the number of fragments per kilobase of exon per million fragments mapped (FPKM) for each gene. Principle component analysis was performed on the fragment counts using the R environment. Finally, gene set enrichment analysis (GSEA, Broad Institute) was performed on the FPKM values using the curated C2 collection of gene sets within MSigDB[20].

Histology. Small intestinal tissue pieces (5mm) were fixed in 4% PFA (4h, RT), washed in 70% ethanol and embedded in paraffin. Four-µm sections were deparaffinized. For Ki67 detection, endogenous peroxidases were blocked in 1% periodic acid in deionized water for 20 min, and antigen retrieval was achieved by microwave treatment in citrate buffer (10mM, pH 6.0). Prior to staining, Fc receptors were blocked in 10% normal mouse serum and 10% of normal serum matching the same species in which the secondary antibody is raised, 10 mM Tris buffer, 5 mM EDTA, 0.15 M NaCl, 0.25% gelatin, and 0.05% Tween-20 (pH 8.0). Tissue sections were incubated overnight at 4°C with primary antibodies in PBS supplemented with 2% of normal mouse serum. Immunoreactions were detected using biotinylated donkey anti-rat (Vector Laboratories) and incubated with the Vectastin ABC Elite Kit (Vector Laboratories) and 3,3'-diaminobenzidine tetrahydrochloride (Sigma-Aldrich). Sections were counterstained with hematoxylin. $Ki67^+$ cells were analyzed in a blinded manner in 7 to 15 crypts per section by at least two independent analysts. Pictures were taken with a Leica DFC350 FX microscope.

Isolation of lamina propria lymphocytes. Isolated small intestine was opened longitudinally and washed with cold HBSS containing Hepes (15 mM), pH 7.2. Tissues were cut in 1 cm pieces and incubated in HBSS buffer containing 10% FBS, 15 mM Hepes, 5 mM EDTA, and 1 mM DTT (pH 7.2) at 37°C two times for 20 min to remove epithelium and intraepithelial lymphocytes. The tissues were digested with Collagenase VIII (100U/ml, Sigma) in RPMI containing 10% FCS, 15 mM Hepes, 100 U/ml Penicillin-Streptomycin, and 1 mM DTT, pH 7.2, at 37°C in a shaker, two times for 1 hour. Supernatants were passed through a 70µm cell strainer and washed in cold HBSS. Pellets were suspended in 90% Percoll (GE Healthcare), overlaid with 40% Percoll and centrifuge at 1800rpm for 20 min to allow separation of mononuclear cells (MNC) by density gradient. Interphase was washed, stained with the fixable viability dye Zombie Aqua Dye (BioLegend) to distinguish live cells, incubated with normal serums and CD16/CD32 Fc-block (553142, BD Biosciences), and stained with biotinylated or conjugated antibodies. Lamina propria lymphocytes were filtered through 40µm cell strainers previous to flow cytometry analysis (FACS ARIAIII, BD). Percentages of DCs and ILC3s were analyzed following the gating strategy shown below for DCs and in Materials and Methods chapter 3 for ILC3s.

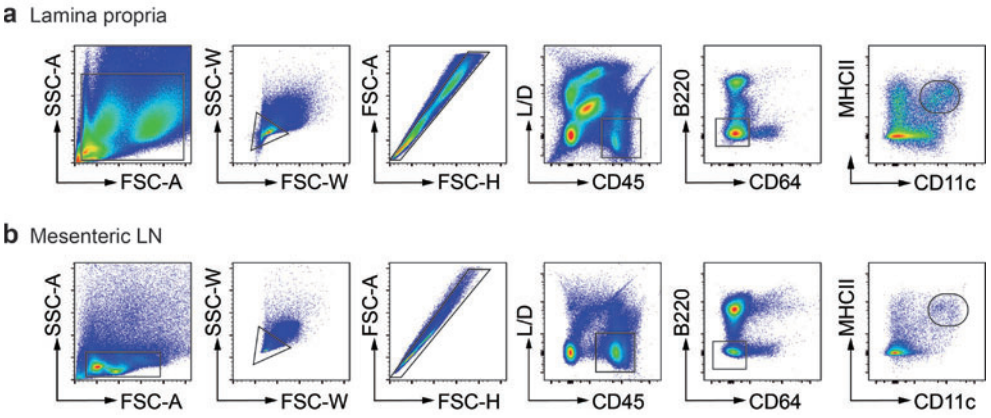

Figure S1: FACS-Gate-strategy for DC subsets in the mesenteric lymph nodes and small intestinal lamina propria. Small intestinal lamina propria lymphocyte cell suspensions from wild-type mice at steady-state were analyzed by Flow Cytometry and MHCII$^+$ CD11c$^+$ DCs were gated as indicated (including lymphocyte gate (CD45$^+$ cells); excluding duplets, dead cells (L/D), B cells (B220) and macrophages (CD64).

Enzymatic digestion of lymph nodes from individual mice. Mesenteric lymph nodes (MLNs) were dissected and pierced into small pieces. These were incubated in 2ml of PBS containing 2% FCS, Liberase I (Roche) and Dnase I (Calbiochem) for 15min at 37°C, stirring. After 15min, the lymph node fragments were gently aspired and expired using a 1ml pipette, which disrupted the capsule and released most leukocytes. Cells were washed with 10ml PBS 2% FCS, filtered through a 100µm cell strainer, assessed for viability using trypan blue and kept on ice until further process.

Transcript analysis. RNA was extracted using the NucleoSpin RNA XS kit (Machery Nagel). RNA from sorted cells was amplified according to the manufacturer's protocol (Ovation PicoSL WTA System V2, NuGen). For quantitative PCR, a Neviti Thermal Cycler (Applied Biosystems) and SensiFAST SYBR Lo-Rox kit (BioLine) were used, with the addition of $MgCl_2$ to a final concentration of 4 mM. All reactions were done in duplicate and normalized to the expression of *Gapdh*. Relative expression was calculated by the cycling threshold (CT) method as $2^{-\Delta CT}$. The primers sequences can be found in Table S1 (see below)

Table S1: Primer sequences

Gene	*Forward Primer*	*Reverse Primer*
Gapdh	TCAACGGCACAGTCAAG	GCTCCACCCTTCAAGTG
Il22	CTCCCCCAGTCAGACAG	CAATCGCCTTGATCTCTC
Plet1	CGTGGTCCTTGATAACATCT	TCACGGCACTGACTGAA

Statistical analysis. Samples were analyzed using unpaired Mann-Whitney test. P values < 0.05 were considered significant. Data are shown as mean ± SEM.

RESULTS

CD11c$^+$ cells contribute to proliferation of crypt cells after MTX-induced tissue damage

The presence of ILC3 and CP is essential for restoration of crypt output after MTX-induced stem cell damage. We hypothesize that the CD11c$^+$ CP-DCs are involved in this immune cell-driven tissue repair by sensing tissue damage. To investigate whether CD11c$^+$ cells in general contribute to tissue regeneration after tissue damage in the SI, we depleted all CD11c$^+$ mononuclear phagocytes using CD11c-DTR$^{+/-}$ mice before treating these animals with MTX i.p. First, we verified the efficacy of the depletion of CD11c$^+$ cells in the lamina propria (LP) and in the mesenteric lymph nodes (MLNs) 24, 48 and 72h after a single dose of diphtheria toxin (DT) in CD11c-DTR$^{+/-}$ mice and compared to PBS control injection **(Figure 1a, b)**. One single dose of DT lead to a specific and efficient depletion of CD11c$^+$ cells in both the LP and MLNs **(Figure 1a, b)**. After 72h the frequencies of CD11c$^+$ cells slightly increased, likely reflecting newly formed CD11c$^+$ cells that have differentiated in these tissues after being recruited from bone marrow-derived progenitors. This strategy allowed us to further investigate whether CD11c$^+$ cell depletion led to a defect in crypt regeneration after MTX treatment, hypothesizing that CD11c$^+$ cells and ILC3s in cryptopatches are required to modulate crypt epithelial cell responses after injury. We next induced intestinal damage with MTX in mice lacking CD11c$^+$ cells. Tissue sections were evaluated for crypt output by enumerating Ki67$^+$ cells per crypt. In the absence of CD11c$^+$ cells, crypt output at day 4 after MTX treatment was significantly reduced compared to PBS treated mice **(Figure 1 c,d).** This indicated that intestinal CD11c$^+$ cells are involved in the regeneration of the small intestinal epithelium after MTX-induced small intestinal damage.

We assessed whether CD11c$^+$ cell depletion affected SILT-ILC3s by analyzing LP CCR6$^+$ ILC3s from CD11c-DTR$^{+/-}$ mice treated with DT or PBS at steady-state. First, we determined the frequencies of CCR6$^+$ILC3s within the LP of the SI and found to be unchanged **(Figure 1e)**. Second, we analyzed the level of expression of the signature cytokine IL-22. CD11c$^+$ cell depletion slightly decreased *Il22* transcripts from CCR6$^+$ ILC3s at steady-state, demonstrating that CD11c$^+$ cell depletion disrupts ILC3 function is SILTs **(Figure 1f).**

These findings show that CD11c$^+$ cells contribute to small intestinal epithelial crypt proliferation after MTX.

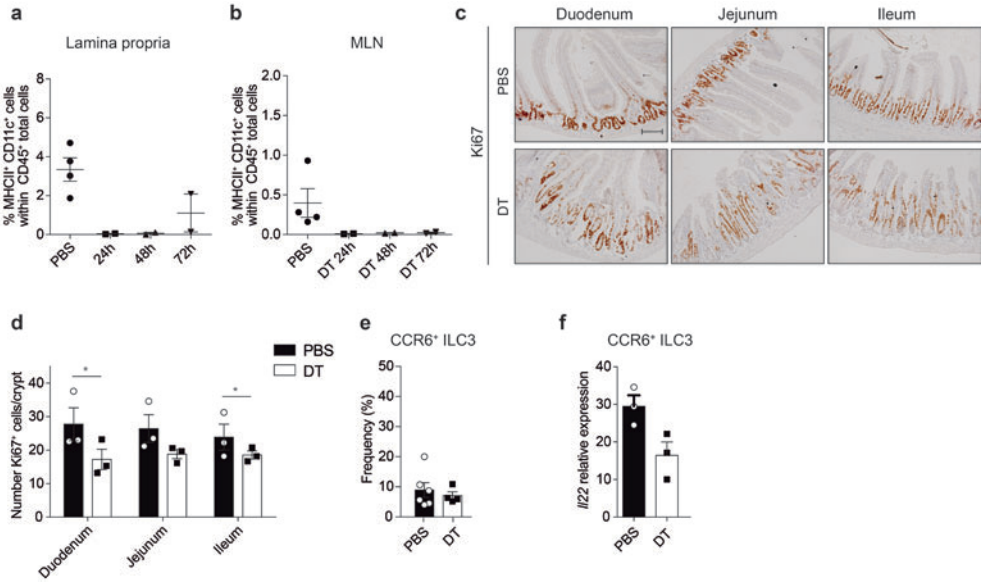

Figure 1: Depletion of CD11c$^+$ cells during MTX treatment decreased the proliferative response of the epithelium in the small intestinal crypts. (a) Frequency of CD11c$^+$ MHCII$^+$ DCs in lamina propria and **(b)** in mesenteric lymph nodes (MLN) CD11c-DTR$^{+/-}$ mice 24h, 48h and 72h after treatment with one single dose of diphtheria toxin (DT) or PBS. **(c)** Representative Ki67 immunostaining of paraffin embedded small intestinal tissues from DT- or PBS-treated CD11c-DTR$^{+/-}$ mice four days after MTX treatment. **(d)** Number of Ki67$^+$ cells in small intestinal crypts from DT- or PBS- treated CD11c-DTR$^{+/-}$ mice four days after MTX treatment. **(e)** Frequency of CCR6$^+$ ILC3 in small intestinal lamina propria from PBS or DT-treated CD11c-DTR$^{+/-}$ mice. **(f)** *Il22* transcript levels relative to *Gapdh* in CCR6$^+$ ILC3 isolated from small intestinal lamina propria from PBS or DT-treated CD11c-DTR$^{+/-}$ mice. *p<0,05. Scale bar (50µm). n=3-6.

CD11c$^+$ cells in SILTs are CD11b$^-$ CD103$^-$ DCs and partly express Plet1

In order to investigate whether CP-DCs are the relevant DC population controlling epithelial regeneration we aimed at identifying the subset of DCs that reside in SILTs. Staining of intestinal sections containing SILTs with several mononuclear phagocyte (MNP) markers identified CD11c$^+$ cells that lacked CD103 but expressed Plet1 **(Figure 2a)**. We have previously identified Plet1 as a marker for intestinal CD103$^+$ CD11b$^+$ migratory DCs. To confirm the specific CP localization of CD103$^-$ Plet1$^+$ DCs we first analyzed their presence in SILT-deficient RORγt$^{-/-}$ mice. This revealed that CD103$^-$ Plet1$^+$ DCs were almost absent in RORγt$^{-/-}$ mice **(Figure 2b,c)**, indicating that the deficiency in SILTs leads to the absence of Plet1-expressing SILT-DCs. Next, we made use of hCD2-GFP$^+$ reporter mice in which SILTs can be micro dissected using a stereomicroscope due to high expression of hCD2-GFP in ILC3 and B cells. Comparing cell suspensions derived from micro dissected GFP$^+$ SILT regions or GFP$^-$ non-SILT lamina propria regions showed that CD103$^-$ Plet1$^+$ DCs were only present in GFP$^+$ SILT tissue and absent from non-SILT lamina propria **(Figure 2d,e)**. Based on these findings we felt confident in using the CD103$^+$ Plet1$^-$ phenotype to isolate CP-DCs and perform phenotypic analyses. LP fractions from total SI were isolated and we used CD64 and B220 to exclude macrophages and B cells, and gated as CD11c$^+$ MHCII$^+$ cells, to define DCs. We plotted total DCs based on CD103 and CD11b and show that even though the vast majority of Plet1$^+$ DCs are CD11b$^+$CD103$^+$ there is another small subset of CD11b$^-$CD103$^-$Plet1$^+$ DCs **(Figure 2f)**. As in Figure 2b, we identified 4 subsets of DCs based on the expression of CD103 and Plet1 **(Figure 2g)**. CD103$^-$ Plet1$^+$ cells were further examined for the expression of CD11b, CD8α and IRF8 **(Figure 2g)** and were found to be negative. Next, signifying that SILT-DCs are comprised within the double negative CD103 and CD11b DC subset. In accordance to these findings and previous published studies, RORγt$^{-/-}$ mice showed decreased frequencies of the double negative CD103 and CD11b DC subset **(Figure 2h,i)**. Collectively, these findings identify CD11c$^+$ CD11b$^-$ CD103$^-$ Plet1$^+$ DCs as SILT-resident cells.

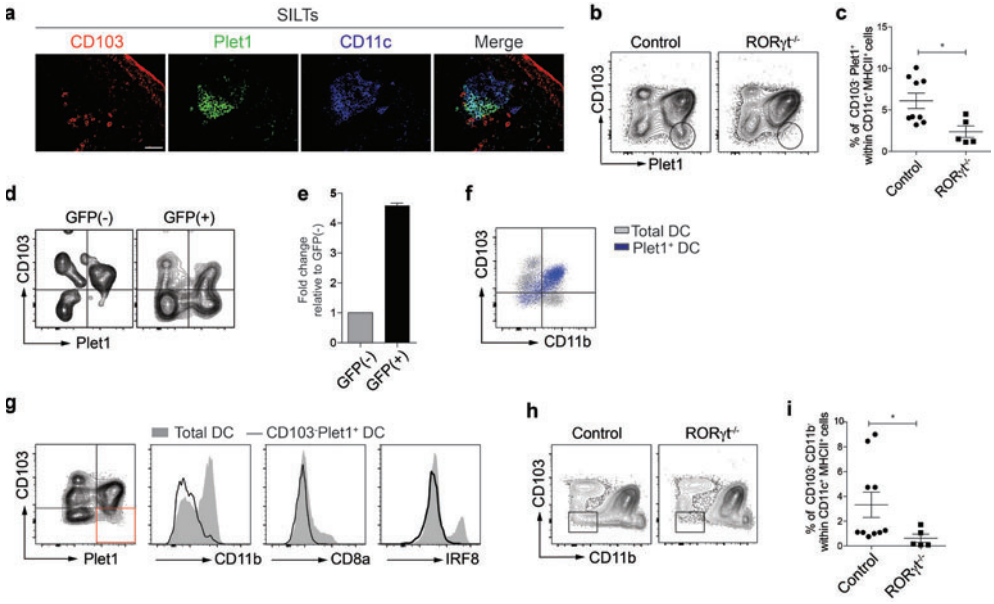

Figure 2: SILT-DCs are CD11b$^-$ CD103$^-$ Plet1$^+$ cells. (a) Representative immunofluorescence of small solitary intestinal lymphoid tissues (SILTs) labelled with CD103 (red), Plet1 (green) and CD11c (blue) **(b)** Representative FACS plots from SI LP of RORγt$^{+/+}$ and RORγt$^{-/-}$ mice gated on CD45$^+$CD64$^-$B220$^-$CD11c$^+$MHCII$^+$LiveDead$^-$ cells. **(c)** Frequency of CD103$^-$Plet1$^+$ DCs from RORγt$^{+/+}$ and RORγt$^{+/-}$ mice (control) compared to RORγt$^{-/-}$ mice gated as in **(b)**. **(d)** Representative FACS plots of GFP$^-$ and GFP$^+$ micro dissected tissues from hCD2-GFP$^+$ mice. **(e)** Increase in CD103$^-$Plet1$^+$ DCs in GFP$^+$ micro dissected tissues from hCD2-GFP$^+$ mice compared to GFP-negative LP tissue. **(f)** Representative FACS plots from LP cell suspensions showing total DCs (CD45$^+$CD64$^-$B220$^-$CD11c$^+$MHCII$^+$LiveDead$^-$ in grey) and Plet1$^+$ DCs (CD45$^+$CD64$^-$B220$^-$CD11c$^+$MHCII$^+$LiveDead$^-$Plet1$^+$ in blue). **(g)** Representative FACS plots from SI LP cells gated on CD45$^+$CD64$^-$B220$^-$CD11c$^+$MHCII$^+$LiveDead$^-$ cells. Histograms show expression of indicated markers in total DCs (grey filled histograms) and CD103$^-$Plet1$^-$ cells (black line histograms). **(h)** Representative FACS plots from SI LP cell suspensions from RORγt$^{+/+}$ and RORγt$^{-/-}$ mice gated on CD45$^+$CD64$^-$B220$^-$ CD11c$^+$ MHCII$^+$ cells, as DC gate. **(i)** Frequency of CD103$^-$CD11b$^-$ DCs from RORγt$^{+/+}$ and RORγt$^{-/-}$ mice within total DC population. *p<0,05. Scale bar (200 µm). n=3-6.

Plet1 can be regulated by CSF2

Interestingly, TLR/Myd88-dependent IL-1β production in tissue resident MNPs has been reported to be essential for CSF2 production by ILC3, the major source of CSF2 in the small and large intestine. Because ILC3 cluster in SILTs with $CD11b^+$ $CD103^-$ $Plet1^+$ DCs that transcribe the GM-CSF receptor, we assessed whether CSF2 has any effect in the regulation of Plet1 expression. Indeed, spleen-derived DCs treated with CSF2 over night (ON) notably upregulated Plet1 transcript levels **(Figure 3a)**. The induction of Plet1 in spleen-derived DCs was also apparent on the protein level. After ON culture with CSF2, spleen-derived DCs increased Plet1 protein expression **(Figure 3b)**. In order to confirm these findings, we analyzed $Csf2^{-/-}$ mice and found that Plet1 transcript levels were almost undetectable in total ileum, as compared to littermate controls **(Figure 3c)**. Altogether, these data suggest that Plet1 is induced in SILT-DCs by ILC3-derived CSF2 production.

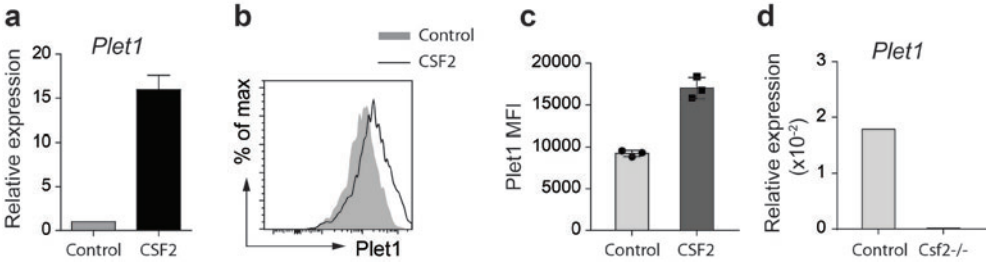

Figure 3: Plet1 expression is induced by CSF2. (a) *Plet1* transcript levels relative to *Gapdh* in splenic $CD11c^+$ DCs treated overnight with CSF2 (20ng/ml; X63 supernatant) versus non-treated (control). **(b)** Plet1 expression in bone marrow-derived DCs treated overnight with CSF2 20ng/ml; X63 supernatant) versus non-treated (control), shown in histogram and as mean fluorescence intensity. **(c)** *Plet1* transcript levels relative to *Gapdh* in ileum from $Csf2^{-/-}$ and littermate controls under homeostatic conditions. n=3-6.

Transcriptome of SILT-DCs implies regulation of ILC3 function

To further characterize SILT-DCs, we performed RNA sequencing of SI LP CD103$^-$ Plet1$^+$ DC and compared their transcriptome with that of CD11b$^+$ CD103$^+$ DCs, as this population also expresses Plet1. PCA analysis showed distinct clustering, indicating differential transcriptomes in these two populations **(Figure 4a)**. 1089 transcripts were significantly up-regulated in SILT-DCs when compared with CD11b$^+$ CD103$^+$ DCs, whereas 786 transcripts were found to be down-regulated **(Figure 4b)**. Despite the fact that CD11b$^-$ CD103$^-$ cells derive from pre-DC precursors and require Flt3L for their development, the transcription factor requirements during the development and function of this DC subset are still unclear. As approximately 60-80% of Plet1$^+$ DCs are contained within CD11b$^-$ CD103$^-$ DN population (data not shown), we focused our analyses on expression of genes associated with: 1- DC development from precursor cells, 2-DC or macrophage identity, 3- microbes-interacting molecules, 4- cell activation/maturation and 5- cytokine expression. We found that SILT-DCs express lower levels of *Batf3* and *Irf4*, which are essential for CD103$^+$ DC development **(Figure 4c)**. *Id2* expression was similar between the two DC subset analyzed. However, SILT-DCs expressed higher levels of *Notch2* and *Irf8*, which have also been associated with CD11b$^+$ CD103$^+$ and CD11b$^-$ CD103$^+$ DCs, respectively **(Figure 4c)**. Likewise, SILT-DCs expressed *Csf1r* and *Csf2r* **(Figure 4c)**. In addition, RNA sequencing showed additional genes that were highly enriched in SILT-DCs, such as *Lyz2* and *CD24a* **(Figure 4d)**. In contrast, SILT-DCs were negative for *Xcr1* and *CD8a*, indicating that they are not related to lymphoid tissue resident CD103$^+$ CD11b$^-$ CD8α^+ DCs, which play important roles in cross-presentation. As expected, SILT-DCs were virtually negative for monocyte or macrophage markers, such as *Ly6c1*, *Cx3cr1* and *Fcgr1* **(Figure 3e)**. Furthermore, SILT-DCs were enriched for *Dxd21*, *Dxd3*, *Tlr5*, *Tlr8* and *Irak4*, whereas they lacked *Tlr4* and *Tlr7* expression. This observation suggests that SILT-DCs are able to sense various pathogen-associated antigens and induce innate immunity **(Figure 4g)**. SILT-DCs also expressed high levels of *Ccr7* **(Figure 4g)**, which indicates that SILT-DCs might be able to migrate to gut-draining lymph nodes. Nonetheless, CD80, CD86 and CD40 were transcribed at similar levels in SILT-DCs and CD11b$^+$ CD103$^+$ DCs, indicating that the activation state under steady-state conditions is similar between these two cell types **(Figure 4g)**. Strikingly, SILT-DCs were enriched for transcripts encoding *Il23a* and *Il22ra2*, suggesting the potential to modulate ILC3 **(Figure 4h)**. Other cytokines expressed by SILT-DC were *Il6* and *Il1b*, while *Il10* and *Csf1* were absent. These findings suggest that SILT-DCs possess the machinery to sense environmental changes and to influence ILC3 activation.

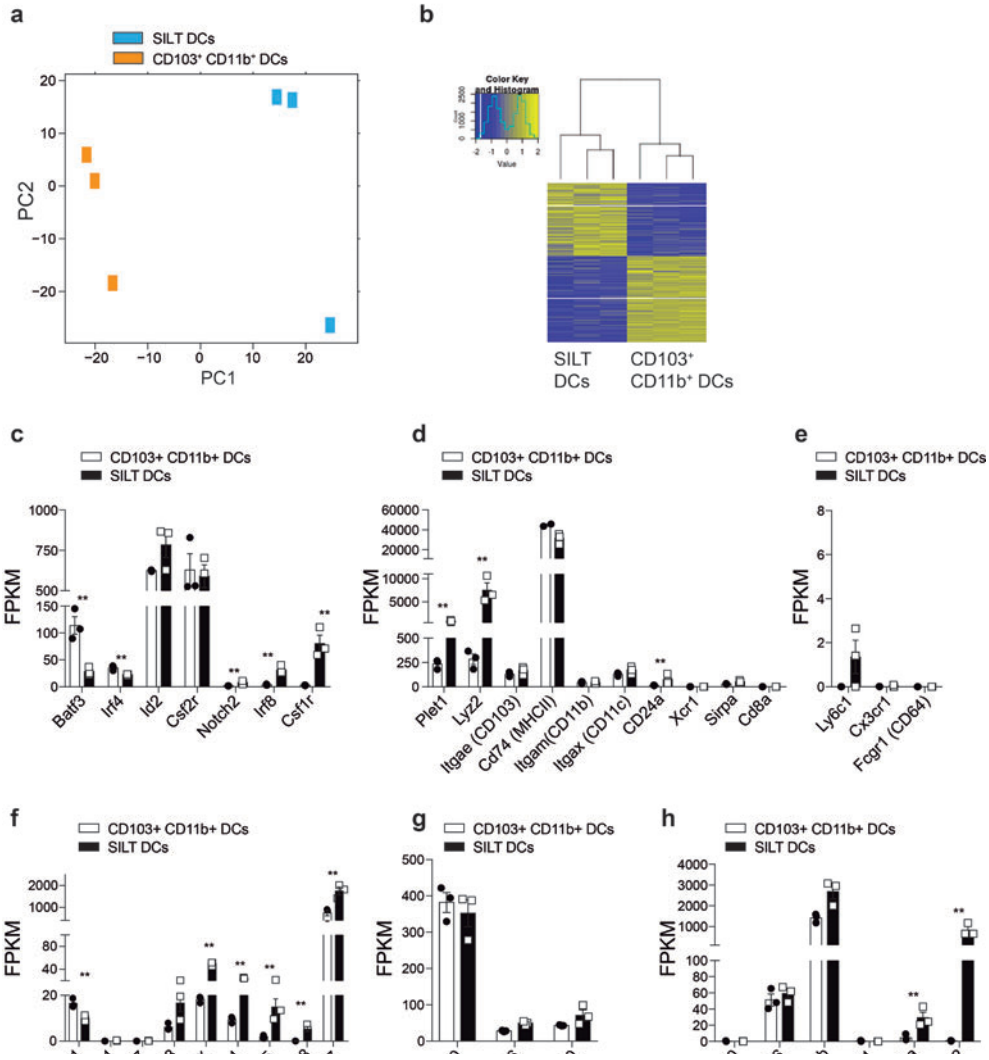

Figure 4: CD103⁻Plet1⁺ DC population comprises SILT-DCs. **(a)** PCA plot of SI LP CD103⁻Plet1⁺ cells (SILT-DCs) and CD11b⁺CD103⁺ DCs under steady-state. **(b)** Heat-map of $DESeq_2$ analysis of RNA sequencing count data of SI LP CD103⁻Plet1⁺ cells (SILT-DCs) and CD11b⁺CD103⁺ DCs under steady-state. Blue colors represent the genes with low expression values whereas yellow colors represent the genes with high expression values. **(c-g)** FPKM values of RNA transcripts corresponding to genes with important function in **(c)** DC development, **(d)** phenotypic DC subsets classification, **(e)** monocyte/macrophage identity, **(f)** pathogen-associated molecular pattern receptors and helicases, **(g)** DC activation markers, and **(h)** cytokines. FPKM values plotted for transcripts that have statistically significant Log2fold change ($DESeq_2$ analysis of count data; p value <0,01 (**) or non-significant (not indicated)). n=3 per group.

SILT-DCs migrate to gut-draining lymph nodes in response to MTX-induced tissue damage

Because CD11c$^+$ cells were required for crypt epithelial proliferation during MTX-tissue damage, and we identified a specific subset of DCs that locates in cryptopatches in close association with ILC3, we set out to investigate the responses of SILT-DCs after MTX treatment. We performed RNA sequencing of SI LP SILT-DCs at steady-state (SS) and one day after MTX (MTX d1) in control mice. Again, PCA component analysis showed distinct clustering, indicating that changes in gene expression occur in SILT-DCs in response to MTX-induced stem cell damage **(Figure 5a,b)**. In particular, 18 genes were significantly downregulated and 35 up-regulated (data not shown). Genes associated with DC maturation and migration, such as *Marcksl1*, *Tagln2* and *Ccr7*, were increased in response to MTX, and the immature DC marker *DC-Sign* was downregulated **(Figure 5c)**. In addition, the negative regulator of DC immunogenicity Dab2 was significantly up-regulated, whereas Fabp5 gene, with important for DC function and T cell priming was increased after MTX **(Figure 5d)**. However, there was no change in the activation-associated co-stimulatory molecules *Cd80*, *Cd86* and *Cd40* **(Figure 5e)** indicating absence of overt DC activation in SILTs. Since we observed increased transcription of *Ccr7*, we hypothesized that SILT-DCs might emigrate from the SILTs upon maturation. To test this hypothesis, we quantified the frequencies of CD103$^-$ Plet1$^+$ DCs within CD11c$^+$ MHCII$^+$ total DCs in small intestine-draining MLN and found a significant increase in phenotypic SILT-DCs after MTX-induced tissue injury **(Figure 5f)**. Further experiments are in progress to fully demonstrate that SILT-DCs are able to migrate to lymph nodes and to elucidate their possible function within the LN.

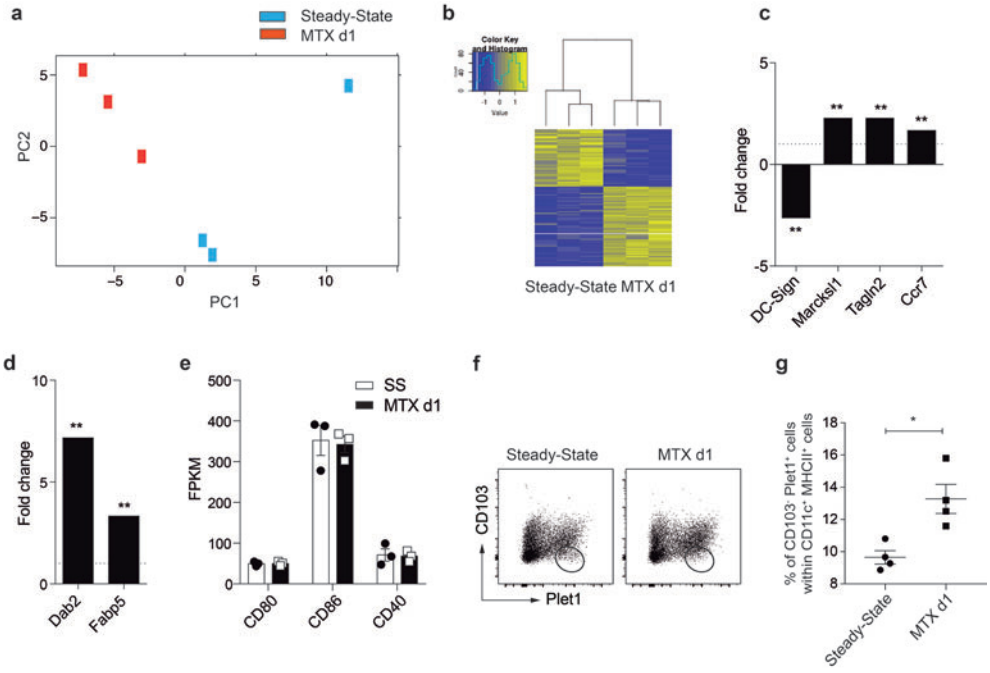

Figure 5: SILT-DCs respond to MTX-induced tissue damage by maturation and migration to MLNs. (a) PCA plot of SI LP CD103$^-$Plet1$^+$ cells (SILT-DCs) at steady-state (SS) and one day after MTX (MTX d1) (n=3). **(b)** Heat-map of DESeq$_2$ analysis of RNA sequencing count data of SILT-DCs SS and MTX d1. Blue colors represent the genes with low expression values whereas yellow colors represent the genes with high expression values. **(c)** Gene expression fold change calculated from DESeq$_2$ analysis comparing SILT-DCs at MTX d1 versus SS for DC maturation markers and **(d)** immune-regulatory molecules. Positive values represent up-regulation of expression in response to MTX-induced damage, whereas negative values represent down-regulated genes after MTX. **(e)** FPKM values of RNA transcripts corresponding to genes with important function in DC activation and **(f)** Representative FACS plots for DC frequencies in the MLN of wild type mice at steady-state and one day after MTX. **(g)** Frequency of DC subsets within CD11c$^+$ MHCII$^+$ expressing cells in MLN at the indicated time points. **p<0.01, *p<0.05. n=3 per group.

DISCUSSION

Previously we identified an important role for ILC3s in regeneration of intestinal epithelial cells after tissue damage. Here we propose that this innate immune cell-driven tissue healing depends on dendritic cells (DCs) that locate in anatomically defined locations, directly underlying the intestinal epithelial barrier. The overall aim of this study was to unravel the identity of SILT-DCs and to establish their role in epithelial repair.

We hypothesize that tissue damage is sensed by dendritic cells that subsequently interact with ILC3s in SILTs and trigger immune cell-driven tissue regeneration. To test the importance of dendritic cells during epithelial responses to injury we induced crypt epithelial damage by MTX in an experimental model of conditional $CD11c^+$ cell depletion. In the absence of these sensing cells, tissue regeneration by means of crypt proliferative capacity was severely affected. CD11c is expressed in DCs but also in some subsets of macrophages, therefore a more specific deletion method, such as Zbtb46-Cre mice, would help to define which population of cells is driving epithelial responses after tissue damage. In addition, it is of importance to investigate whether DCs directly affect signaling pathways in crypt epithelial cells after sensing tissue damage. Ablation of AhR in $CD11c^+$ cells leads to alterations in Wnt signaling pathway, resulting in biased epithelial differentiation to the Goblet cell lineage, which increases severity of DSS-induced colitis[21]. To determine whether similar mechanisms are operational in SILT-DC interactions with epithelial cells co-cultures of SILT-DCs or whole cryptopatches together with epithelial crypts in organoids would questioned to be performed. As an alternative, transfer of DCs or DC progenitors in the absence of ILC3 could demonstrate whether DCs can induce tissue repair directly independently of ILC3s.

More studies are needed to understand the heterogeneity and relationship between $CD103^-$ $CD11b^-$ DC subsets present in the lamina propria of the small intestine. It is unclear whether $Plet1^+$ SILT-DCs are either absent in ILC3-deficient mice or that these cells lack the interactions with ILC3s needed for Plet1 expression. However, the decreased frequency in $CD103^-$ $CD11b^-$ DCs in $ROR\gamma t^{-/-}$ mice suggests that SILT-DCs are only present when their cryptopatches are formed.

The association of SILT-DCs as $Plet1^+$ $CD103^-$ $CD11c^+$ DCs allowed for the first time the isolation of these cells from total lamina propria. Transcriptomic analysis of SILT-DCs revealed transcription of cytokines involved in ILC3 modulation, such as *Il23*, *Il1b* and *Il22ra1*, and showed that DC-expressing Plet1 express *Csf2r*. This suggests bi-directional crosstalk with Csf2-producing ILC3s, likely occurring in cryptopatches.

An important subject that requires further investigation is what developmental pathways and transcription factor requirements are critical for SILT-DC development, in order to fully elucidate whether SILT-DCs are DC precursors or an intermediate state during DC development. This could be achieved by analyzing KO mice of lineage determining transcription factors, such as IRF4 or IRF8.

Furthermore, specific targeted deletion of SILT-DCs is key to unraveling the mechanisms by which this specific subset of DC modulate ILC3 function. So far, Lyz2-Cre mice may be useful for Cre-lox studies, although the identification of more specific markers expressed on SILT-DCs would still be required.

Our identification and characterization of a DC subset that specifically locates in SILTs open new strategies to investigate molecular mechanisms that translate intestinal damage into immune-cell driven tissue repair. SILT-DCs express a range of receptors capable of sensing microbial patterns and cell damage. Especially TLR5 is of interest as ligation of this receptor on dendritic cells can stimulate production of IL-23, important for ILC3 activation[22]. There is also evidence that DCs can phagocyte apoptotic epithelial cells and migrate to T cell areas in MLN to induce tolerance[23–25], although no special attention has been given to $CD103^-$ $CD11b^-$ DC subsets in these studies. Together, we suggest that once damage is sensed, DCs activate ILC3s in cryptopatches. It will be important to investigate the signals and effector molecules that drive immune cell-driven tissue repair. Also, it is of interest to further address SILT-DC migration. By using intra-vital imaging of cryptopatches it would be plausible to understand whether tissue repair is associated with egress of DCs from cryptopatches.

Our work could open novel opportunities for enhancing mucosal healing via targeting cryptopatch immune cells, aimed at reducing intestinal epithelial damage, which is a common, dose-limiting side effect of anti-cancer treatments and an important risk factor for graft-versus-host disease. In addition, it could improve mucosal healing in patients suffering from inflammatory bowel disease or other chronic inflammatory disorders, in which impaired tissue regeneration fuels the pathological anti-microbial response characteristic for these diseases.

REFERENCES

1. Iwasaki, A. Mucosal Dendritic Cells. *Annu. Rev. Imunol.* **25,** 381–418 (2007).
2. Smith, P. D., Ochsenbauer-Jambor, C. & Smythies, L. E. Intestinal macrophages: Unique effector cells of the innate immune system. *Immunological Reviews* **206,** 149–159 (2005).
3. Persson, E. *et al.* IRF4 Transcription-Factor-Dependent CD103+CD11b+ Dendritic Cells Drive Mucosal T Helper 17 Cell Differentiation. *Immunity* **38,** 958–969 (2013).
4. Cerovic, V., Houston, S. A., Scott, C. L., Aumeunier, A., Yrlid, U., Mowat, A. M. & Milling, S. W. F. Intestinal CD103− dendritic cells migrate in lymph and prime effector T cells. *Mucosal Immunol.* **6,** 104–113 (2013).
5. Scott, C. L. *et al.* CCR2(+)CD103(-) intestinal dendritic cells develop from DC-committed precursors and induce interleukin-17 production by T cells. *Mucosal Immunol.* **8,** 327–339 (2014).
6. Mayer, J. U., Demiri, M., Agace, W. W., MacDonald, A. S., Svensson-Frej, M. & Milling, S. W. Different populations of CD11b+ dendritic cells drive Th2 responses in the small intestine and colon. *Nat. Commun.* **8,** 15820 (2017).
7. Luda, K. M. *et al.* IRF8 Transcription-Factor-Dependent Classical Dendritic Cells Are Essential for Intestinal T Cell Homeostasis. *Immunity* **44,** 860–874 (2016).
8. Cerovic, V. *et al.* Lymph-borne CD8α+ dendritic cells are uniquely able to cross-prime CD8+ T cells with antigen acquired from intestinal epithelial cells. *Mucosal Immunol.* **8,** 38–48 (2015).
9. Satoh-Takayama, N. *et al.* Microbial Flora Drives Interleukin 22 Production in Intestinal NKp46+ Cells that Provide Innate Mucosal Immune Defense. *Immunity* **29,** 958–970 (2008).
10. Sanos, S. L., Bui, V. L., Mortha, A., Oberle, K., Heners, C., Johner, C. & Diefenbach, A. RORgammat and commensal microflora are required for the differentiation of mucosal interleukin 22-producing NKp46+ cells. *Nat. Immunol.* **10,** 83–91 (2009).
11. Tumanov, A. V., Koroleva, E. P., Guo, X., Wang, Y., Kruglov, A., Nedospasov, S. & Fu, Y. X. Lymphotoxin controls the IL-22 protection pathway in gut innate lymphoid cells during mucosal pathogen challenge. *Cell Host Microbe* **10,** 44–53 (2011).
12. Satoh-Takayama, N., Serafini, N., Verrier, T., Rekiki, A., Renauld, J. C., Frankel, G. & DiSanto, J. P. The chemokine receptor CXCR6 controls the functional topography of interleukin-22 producing intestinal innate lymphoid cells. *Immunity* **41,** 776–788 (2014).
13. Chea, S., Possot, C., Perchet, T., Petit, M., Cumano, A. & Golub, R. CXCR6 Expression Is Important for Retention and Circulation of ILC Precursors. *Mediators Inflamm.* **2015,** (2015).
14. Hepworth, M. R. & Sonnenberg, G. F. Regulation of the adaptive immune system by innate lymphoid cells. *Current Opinion in Immunology* **27,** 75–82 (2014).
15. Mackley, E. C. *et al.* CCR7-dependent trafficking of RORγ+ ILCs creates a unique microenvironment within mucosal draining lymph nodes. *Nat. Commun.* **6,** 5862 (2015).
16. Eberl, G. & Littman, D. R. Thymic origin of intestinal alphabeta T cells revealed by fate mapping of RORgammat+ cells. *Science* **305,** 248–51 (2004).
17. Eberl, G., Marmon, S., Sunshine, M. J., Rennert, P. D., Choi, Y. & Littman, D. R. An essential function for the nuclear receptor RORgt in the generation of fetal lymphoid tissue inducer cells. *Nat. Immunol.* **5,** 64–73 (2003).
18. Taylor, R. T., Lügering, A., Newell, K. A. & Williams, I. R. Intestinal cryptopatch formation in mice requires lymphotoxin alpha and the lymphotoxin beta receptor. *J. Immunol. (Baltimore, Md 1950)* **173,** 7183–7189 (2004).
19. Gröschel, S. *et al.* A single oncogenic enhancer rearrangement causes concomitant EVI1 and GATA2 deregulation in Leukemia. *Cell* **157,** 369–381 (2014).

20. Subramanian, A. *et al.* Gene set enrichment analysis: a knowledge-based approach for interpreting genome-wide expression profiles. *Proc. Natl. Acad. Sci. U. S. A.* **102,** 15545–50 (2005).

21. Chng, S. H., Kundu, P., Dominguez-Brauer, C., Teo, W. L., Kawajiri, K., Fujii-Kuriyama, Y., Mak, T. W. & Pettersson, S. Ablating the aryl hydrocarbon receptor (AhR) in CD11c+ cells perturbs intestinal epithelium development and intestinal immunity. *Sci. Rep.* **6,** 23820 (2016).

22. Kinnebrew, M. A., Buffie, C. G., Diehl, G. E., Zenewicz, L. A., Leiner, I., Hohl, T. M., Flavell, R. A., Littman, D. R. & Pamer, E. G. Interleukin 23 Production by Intestinal CD103 +CD11b + Dendritic Cells in Response to Bacterial Flagellin Enhances Mucosal Innate Immune Defense. *Immunity* **36,** 276–287 (2012).

23. Cummings, R. J. *et al.* Different tissue phagocytes sample apoptotic cells to direct distinct homeostasis programs. *Nature* **539,** 565–569 (2016).

24. Huang, F. P., Platt, N., Wykes, M., Major, J. R., Powell, T. J., Jenkins, C. D. & MacPherson, G. G. A discrete subpopulation of dendritic cells transports apoptotic intestinal epithelial cells to T cell areas of mesenteric lymph nodes. *J. Exp. Med.* **191,** 435–444 (2000).

25. Steinman, R. M., Turley, S., Mellman, I. & Inaba, K. The Induction of Tolerance by Dendritic Cells That Have Captured Apoptotic Cells. *J. Exp. Med* **191,** 411–416 (2000).

6

GENERAL DISCUSSION

SUMMARY

The overall goal of this thesis was to underpin the role of Group 3 Innate Lymphoid cells (ILC3s) during small intestinal epithelial regeneration. We addressed the function of ILC3s in an experimental murine model of small intestinal damage based on the administration of the chemotherapeutic agent methotrexate (MTX), which targets highly proliferative epithelial cells, leading to epithelial barrier disruption. Our findings highlight that ILC3s are essential to induce a transient activation of STAT3 in the epithelium and to ensure the preservation of $Lgr5^+$ intestinal stem cells (ISCs) following MTX-induced tissue damage. The absence of ILC3-driven epithelial responses leads to a failure to recover the proliferative capacity of small intestinal crypts and causes augmented intestinal pathology, indicating that cryptopatch ILC3s are critical for tissue repair. In order to decipher ILC3-dependent mechanisms underlying $Lgr5^+$ ISC maintenance and crypt proliferation, we investigated the involvement of the ILC3-derived cytokine IL-22, based on its reported functions regulating epithelial cell functions. We found that IL-22 contributes to maintenance of $Lgr5^+$ ISCs, but its absence does not lead to defects in crypt regeneration, substantiating the existence of alternative mechanisms controlling epithelial responses after damage. $Lgr5^+$ ISCs from RORγt-deficient mice also fail to upregulate the regenerative YAP1 signaling pathway, which we showed to be crucial for crypt proliferation after MTX-induced damage. YAP1-mediated tissue repair is dependent on the gp130-Src axis and our results suggest that ILC3 control of YAP1 signaling in $Lgr5^+$ ISCs likely occurs indirectly via another cell type. We propose that ILC3-derived cytokines can induce IL-11 production in intestinal stromal cells, which in turn would orchestrate stem cell responses to tissue damage. We could also show that $ROR\gamma t^{-/-}$ mice have an altered stem cell niche at homeostasis, characterized by an overrepresentation of $Lgr5^+$ ISCs expressing enteroendocrine-like markers, closely resembling a reserve ISC population that is induced after MTX in control mice. This suggests that the absence of cryptopatches and ILC3s translates into increased recruitment of the reserve ISC population at steady-state, probably due to an alteration in $Lgr5^+$ ISC cell function. Finally, we investigated whether ILC3s in cryptopatches require interactions with mononuclear phagocytes to induce epithelial regeneration after damage. $CD11c^+$ cells contributed to crypt proliferation following MTX administration, and we subsequently characterized $CD11c^+$ cells co-localizing with ILC3s in solitary lymphoid follicles and found that they transcribe high levels of *IL-23*, *IL-1b* and *IL-22bp*, which may regulate ILC3 function. Altogether, this thesis untangles the importance of innate immune cells in driving epithelial responses to tissue damage and underscores the mechanisms by which ILC3s fine-tune stem cell responses to ensure epithelial regeneration, likely together with stromal cells and myeloid cells in cryptopatches (Figure 1 and 2).

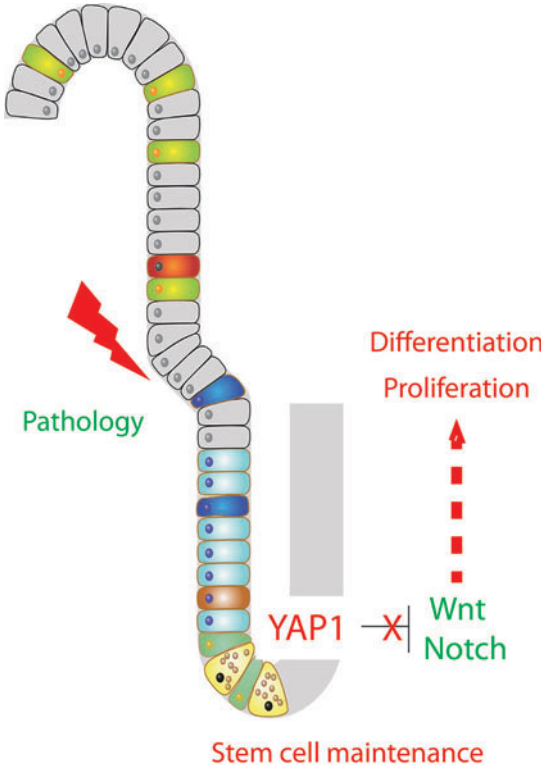

Figure 1: Failure in tissue regeneration in the absence of ILC3s. Lgr5^{+} stem cells after damage are unable to induce Yap1 signaling in ROR$\gamma t^{-/-}$. Proliferation and differentiation of epithelial cells is impaired and tissue pathology is worsen in the absence of ILC3s and after IL-11 blockage.

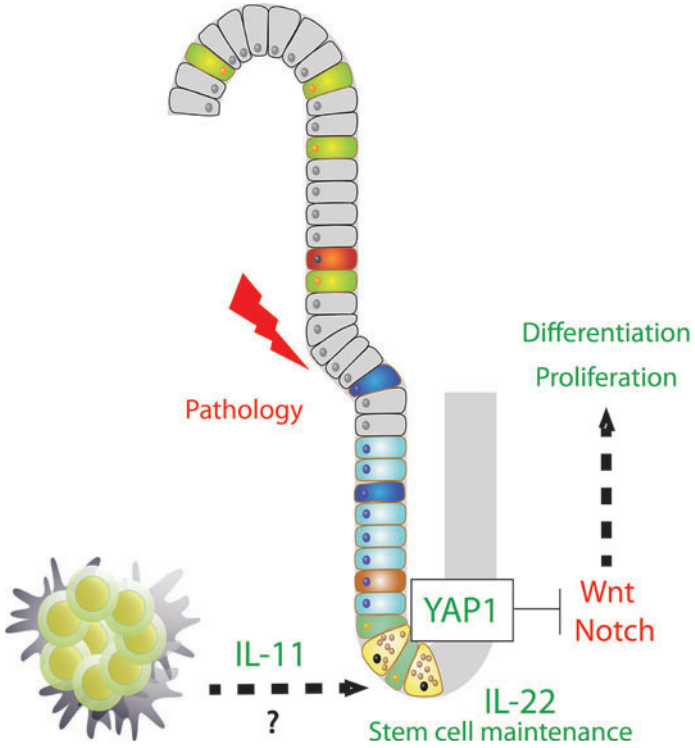

Figure 2: ILC3s in lymphoid tissues drive Yap1-induced small intestinal epithelial regeneration. The presence of ILC3s in the small intestinal lamina propria is essential for epithelial regeneration via activation of Yap1 signlaing in stem cells in a IL-11 dependent fashion. Yap1 induction in $Lgr5^{+}$ stem cells after tissue damage drives regeneration by modulating proliferation and differentiation of epithelial cells through modulation of Wnt/Notch signaling pathways.

The family of innate immune cells

Our body is in constant contact with environmental factors. Epithelial barriers, such as the skin and the gut epithelium, represent the first line of defense against these potentially harmful factors. In the gut mucosa, immune cells reinforce the epithelial barrier and induce tolerance against food or commensal bacteria. Among these immune cells, a recently discovered type of lymphocytes, innate lymphoid cells or ILCs, orchestrates immune responses and maintains tissue homeostasis[1–3]. Unlike T and B lymphocytes, ILCs do not express rearranged-antigen recognition receptors. As such, their activation and expansion are not driven by specific antigens, but rather by signals released by the tissue microenvironment. ILCs come in three types, ILC1s, ILC2s and ILC3s[4]. ILC3s interact with dendritic cells to maintain epithelial barrier integrity. DCs secrete IL-23 upon pathogen challenge and stimulate ILC3s to make IL-22[5,6]. This is amplified via the LT$\alpha\beta_2$-LTβR signaling pathway[7] . In turn, IL-22 activates the epithelium to produce antimicrobial peptides and mucins that kill bacteria directly[6,8]. In addition, epithelial cells can also produce IL-23 and induce IL-22 production in a LTβR-dependent manner during intestinal injury caused by DSS[9].

ILC3s also interact with macrophages to establish tolerance towards the commensal microbiota. Antigen from gut bacteria induces the inflammatory cytokine IL-1β in LysM$^+$ mononuclear phagocytes, which in turn induces the production of GM-CSF by ILC3s. GM-CSF signals back to mononuclear phagocytes to enhance retinoic acid, which promotes the differentiation of regulatory T cells (Tregs)[10]. Tregs are essential in maintaining tolerance towards the commensal microbiota[11–14]. ILC2s contribute to responses against helminths. These parasitic worms secrete enzymes that digest the mucus and cause massive enterocyte cell death. Epithelial cells sense the danger signals released by the dying cells and produce alarmins, such as IL-25, IL-33 and TSLP. In response to alarmins, ILC2s make IL-13 that increases mucus production from Goblet cells[15,16] and sends activated dendritic cells to the MLN where they can prime effector T cells[17]. ILC2s also produce IL-5 that attracts eosinophils and mast cells and induces intestinal muscle contractions[18]. Together these actions result in the expulsion of worms from the gut. In addition, after IL-33 stimulation, ILC2s make Areg, which is important for tissue repair following worm clearance[19]. However, ILCs can also contribute to tissue pathology. ILC1s which secrete the inflammatory cytokine IFNγ and ILC3s, which can acquire the ability to make IFNγ during chronic inflammation are increased in inflammatory bowel disease, such as ulcerative colitis and Crohn's disease and contribute to gut pathology[20,21]. As such, ILCs participate in various aspects of immunity, from maintenance of barrier, tolerance against commensals and immune responses against pathogens to pathology-associated with chronic inflammation.

Group 3 Innate Lymphoid cells and intestinal epithelial regeneration

A role for ILC3s in the regeneration of epithelial tissues has only recently started to be appreciated. ILC3s contribute to skin wound healing[22], thymic epithelial cell restoration after insult[23] and intestinal stem cell protection in graft-versus-host disease[24]. In this thesis, we aimed at elucidating whether ILC3s contribute to intestinal epithelial barrier repair in the absence of inflammation. Barrier disruption can occur during radio- or chemo- therapies to reduce tumor growth. Anti-cancer drugs also target highly proliferative intestinal epithelial cells, which are crucial for epithelial self-renewal. As a result, epithelial damage is a dose-limiting side effect of commonly used anti-cancer therapies. Thus, understanding the precise mechanisms leading to mucosal repair and deciphering methods to enhance repair after damage could improve the efficiency of current anti-cancer treatments.

Different subsets of ILC3s have been identified within the small intestine, including lamina propria NKp46$^+$ ILC3s and cryptopatch CCR6$^+$ ILC3s. In particular, we envisioned that cryptopatch ILC3s, clustered near the epithelial crypts, could modulate intestinal stem cells to enhance regeneration.

The intestinal stem cell niche during epithelial regeneration

Intestinal epithelial regeneration relies on intestinal stem cells, which have a high index of mitosis and are able to self-renew and differentiate to all differentiated epithelial cells that form the epithelial barrier, every 3-5 days. During homeostasis, the intestinal epithelium is already in constant remodeling but after damage, auxiliary programs are engaged to restitute the damaged epithelium. It is known that defective control of intestinal stem cell proliferation can predispose for tumor development. Thus, it is of crucial importance to understand the mechanisms underlying intestinal stem cell regulation. Intestinal stem cell regulation has long been considered a largely epithelial cell-intrinsic process. However, it is now firmly established that other cell types, in particular mesenchymal or endothelial cells[25–27], enteric neurons[28] and group 3 innate lymphoid cells[29] (this thesis) can regulate intestinal stem cell function.

To date, different population of intestinal stem cells have been identified. Under homeostatic conditions, proliferating Lgr5$^+$ columnar base crypt cells (CBCs) give rise to progeny that differentiates into all distinct epithelium cell lineages while migrating upward to the villi. In response to Lgr5$^+$ stem cell ablation, different crypt epithelial cell types reacquire stem cell characteristics and dedifferentiate into Lgr5$^+$ CBCs. The cells that can contribute to regenerate the epithelium after injury include Bmi1-GFP$^+$ cells, Prox1$^+$ cells, enteroendocrine/Paneth cell precursors and goblet cell precursors[30–34]. The actual understanding holds that lineage-specified mature cells can revert into ISCs when native ISCs are depleted. Although insights into cells with the potential to regenerate the epithelium during damage is increasing, little is known on the cellular and molecular mechanisms that influence these processes.

ILC3s protect Lgr5^{+} CBC protection from alloreactive T cells after bone marrow transplantation. ILC3s are activated in response to pre-transplant conditioning and function in an IL-22-dependent manner. Accordingly, ILC3-derived IL-22 is critical to reduced susceptibility to experimental GI GVHD after transplantation[24].

This thesis evaluates the role of ILC3s in small intestinal regeneration and the most important results are discussed below. In general, our work provides novel insights into the mechanisms leading to immune cell-driven tissue repair.

Do ILC3s regulate the intestinal epithelium (villi *vs* crypts) and by which mechanisms?

To interrogate the role of ILC3s in epithelial regeneration, we use the well-established model of acute small intestinal tissue damage induced by the cytostatic drug MTX[29]. High-dose MTX causes selective small intestinal enteropathy in mice as a result of the inhibition of the DHFR enzyme, essential for the conversion of folic acid into thymidylate and purines. In a series of experiments, we demonstrate that ILC3s are necessary to induce a number of responses after causing damage in the intestinal epithelium:

ILC3s and STAT3 activation in villi and crypt epithelial cells

In chapter 2, we use ILC3-deficient mice, generated either by depleting Thy1 positive cells in Rag1$^{-/-}$ mice or through genetic deletion of RORγt$^{-/-}$ to demonstrate a role for ILC3s in transient activation of epithelial cells in response to MTX. Epithelial activation is evidenced by STAT3 phosphorylation, in line with a critical role for STAT3 signaling during mucosal wound healing[35]. STAT3 is phosphorylated one day after MTX administration, when the peak of damage occurs, which indicates that epithelial responses are induced very rapidly after cytostatic treatments. Transcription of STAT3 target genes is also impaired in the absence of ILC3s, although the biological functions induced after activation of STAT3 signaling remain to be determined. First, it would be necessary to assess the phenotype of the pSTAT3^{+} epithelial cells after MTX to establish which cell type is responding to tissue damage and then look at their specific function. To do so, a combination of different surface and intracellular markers should be used to specifically differentiate enterocytes (alkaline phosphatase enzyme Alpi), goblet cells (Periodic Schiff staining), tuft cells (DCKL-1[36]) and enteroendocrine cells (Claudin-4[37]). Importantly, epithelial specific functional parameters should be assessed as well, such as the absorptive capacity or the production of the mucus protein Muc2, antimicrobial peptides, or cytokines and hormones. Once the epithelial cell subsets that activate STAT3 after damage have been identified, transcription of genes associated with survival and apoptosis should be assessed. Finally, DNA damage responses and barrier permeability (tight junctions) are other aspects that could be influenced by STAT3 activation. DNA damage responses can be evaluated by quantification of nuclear γH2AX foci and the expression of ATM and ATR proteins. The permeability of the epithelium is tested by Dextran-FITC translocation.

Another question that is still unresolved is the identity of the ILC3-dependent mediator or mediators that lead to STAT3 phosphorylation in epithelial cells. One hypothesis is that IL-22 induces pSTAT3, as we found that NKp46^{+} ILC3s increase IL-22 transcription one day after MTX. To elucidate the role of this cytokine, pSTAT3 intensity should be quantified in IL-22 neutralized mice vs isotype-treated mice as well as in IL-22$^{-/-}$ mice. However, it is still possible that other cytokines contribute to pSTAT3 activation, like IL-6, CLCF1, OSM and LIF, produced in both subsets of ILC3s (data not shown). Other possibilities are that other stimuli activate STAT3, such as epidermal growth factors, or, perhaps most likely, a combination of multiple signals.

Additionally, myeloid cells can also activate STAT3. IL-6 and OSM are known cytokines activating STAT3. However, classical IL-6 signaling is dispensable for normal colonic epithelial proliferation and repair after DSS-induced colitis[38]. Similarly, we show that IL-6 is not critical to induce Yap1 activation in crypt cells of the small intestine. Despite the fact that OSM has been reported to contribute to hematopoiesis and bone, heart and liver regeneration, its function in intestinal remodeling is incompletely understood.

Finally, it would be very interesting to decipher the specific downstream gene programs that are induced by each STAT3-activating cytokine, and whether these differ from one cell type to another. IL-22-induced STAT3 phosphorylation in Lgr5^{+} CBCs mediates stem cell proliferation in culture[39], while in Paneth cells, IL-22 signaling and STAT3 activation induces antimicrobial peptide production [40].

ILC3s and crypt proliferation and pathology

ILC3s are critical for crypt intestinal epithelial regeneration after MTX-induced damage. In wild-type mice, one day after MTX, proliferation in the crypts is reduced and this coincides with the peak of pathology, as characterized by crypt epithelial flattening, crypt loss and crypt abscesses. Four days after damage, crypt proliferation is back to steady state levels in wildtype mice, while the proliferation in the crypts is severely reduced in ILC3-defiicent RORγt$^{-/-}$ mice. Together with significantly worse pathology this suggests that proliferation is critical to alleviate pathological symptoms. Nevertheless, whether intestinal pathology is associated with a failure in crypt regeneration will need to be formally proven.

Defective proliferation or increased severity of tissue damage is not observed after neutralization of IL-22, STAT3 or IL-6 (chapter 3). In addition, blocking IL-6 and IL-11 binding to gp130 with LMT28 did not lead to differences in crypt output after MTX, which together suggests that crypt proliferation is controlled via several gp130- and STAT3- activators, and that it cannot be inhibited by only blocking one or two mediators. Alternatively, proliferation could also be regulated through various signaling pathways in addition to gp130, such as Wnt, Notch, BMP, EGF.

During homeostasis, *in vitro* crypt proliferation and stem cell growth potential is not altered in organoids grown from mice lacking ILC3s or IL-22. However, alterations in the

crypt compartment resembling low-grade intestinal pathology were observed only in RORγt$^{-/-}$ but not IL-22$^{-/-}$ mice (Chapter 4), suggesting important functions for additional ILC3-derived cytokines in the regulation of crypt epithelial integrity at basal conditions.

Finally, during MTX, depletion of CD11c^{+} cells leads to a decrease in crypt output, indicating that CD11c^{+} cells are also important in regulating epithelial regeneration (Chapter 5). Whether this is a direct effect or indirect via activation of ILC3s or other cell types is not known yet. RORγt$^{-/-}$ mice also have reduced numbers of the specific CD11c^{+} cell subset that we think interact with ILC3s, therefore it is not a good model to address this. Co-cultures with CD11c^{+} cells and/or ILC3s with organoids to assess their contribution to epithelial regeneration should be employed to address these questions.

ILC3s and Lgr5^{+} CBCs

One important question that arises from our work is whether proliferation of the crypts in response to injury depends on Lgr5^{+} CBCs. On the one hand, our data shows that the loss of Lgr5^{+} CBCs caused by blocking IL-22 or STAT3 signaling does not translate in reduced proliferation (Chapter 3), suggesting that stem cell survival and proliferation are two independent processes regulated in different ways. However, the timing of IL-22 or STAT3 signaling block could influence this discrepancy. On the other hand, the lack of correlation between CBCs and crypt proliferation could be explained by the presence of additional stem cell populations that take over after injury and are driving proliferation in the absence of Lgr5^{+} CBCs, as supported by previous published reports[30,41–43]. It might also be possible that *de novo* generation of Lgr5^{+} CBCs is critical to maintain proliferation and differentiation during epithelial remodeling. Finally, many different progenitors or transit amplifying cells exist in crypts that contribute to crypt proliferation in response to distinct signaling molecules, which reflects the complexity of the crypt stem cell niche.

We show that by blocking IL-22, Lgr5^{+} CBC loss in duodenum was significantly increased in response to MTX, indicating that IL-22 regulates Lgr5^{+} CBC maintenance (Chapter 2 and 3). In addition, by blocking STAT3 signaling by using Stattic, we confirm that IL-22 and STAT3 contribute to the maintenance of Lgr5^{+} CBCs (Chapter 3). This is in line with the expansion of the stem cell compartment in *in vitro* organoids after stimulation with recombinant IL-22[39]. However, blocking cytokine signaling or administering recombinant cytokines *in vivo* or *in vitro* has several inherent limitations, such as their life-time in circulation and dose-dependent and tissue-specific effects. Therefore, we cannot exclude that additional cytokines produced by ILC3s are involved in the maintenance of Lgr5^{+} CBCs.

ILC3-driven Yap1 regenerative pathway

Our data convincingly show the requirement of ILC3 presence for regulation of the evolutionary conserved stem cell signaling pathways Wnt, Notch and Yap1 in Lgr5^{+} CBCs in response to MTX (Chapter 3). Only in the presence of ILC3s, Lgr5^{+} CBCs downregulate

expression of genes downstream of Wnt signaling, coinciding with a loss of stem cell identity. This reprogramming of Lgr5$^+$ ISCs by Yap1-mediated transient inhibition of Wnt signaling is in line with a recently published report on epithelial responses to radiation-induced intestinal damage[44]. In addition, ILC3 presence allows for Lgr5$^+$ CBC downregulation of Notch1 receptor and Hes1 transcription while increasing the expression of genes associated with secretory cells. This is in contrast with villin-specific Yap1$^{-/-}$ mice in which radiation damage induces inhibition of Paneth cell formation. This is likely explained by the fact that while strongly reduced, Yap1 is not completely absent in mice lacking ILC3s.

We show that in response to MTX-induced injury, the Yap1 signaling pathway is crucial for crypt epithelial proliferation (Chapter 3). In the absence of Yap1 regulation, intestinal pathology becomes more severe, especially in the crypt compartment. This is in agreement with previous reports that highlighted the importance of Yap1 in crypt epithelial regeneration after DSS or irradiation[44–46]. Our experiments in which we blocked Yap1 activity with Verteporfin are not specific to the intestinal epithelium as they are performed by administering the drug i.p. Although treatment of organoids with verteporfin clearly shows that Yap1 in epithelial cells is indispensable for cell viability, additional effects of non-epithelial Yap1$^+$ cells *in vivo* cannot be ruled out.

We have also shown that IL-22 blocking does not affect Yap1 activation in the crypts and we do not observe differences in Yap1-, Wnt-, Notch1-mediated transcription in Lgr5$^+$ CBCs purified after MTX in IL-22 neutralized mice. Analysis of Yap1 in IL-22-deficient mice will be important to unequivocally show that Yap1 signaling is regulated in an IL22-independent manner. In line with this, IL-22 transcription is not induced in cryptopatch ILC3s following MTX damage. While organoid systems would seem attractive to directly test Yap1 activation by IL-22, this would require the optimization of the organoid cell culture in a soft matrix, as high matrix stiffness is able to activate Yap1 and drive stem cell expansion[47]. This could be achieved in low density collagen or hydrogels. Altogether, IL-22 seems to be partially involved in intestinal regeneration, contributing to the preservation of Lgr5$^+$ CBCs but not to crypt proliferation and intestinal regeneration after MTX. It is an interesting question to investigate the role of IL-22 in different populations of stem and progenitor cells, as YAP1 may induce different epithelial cell type-specific signaling pathways during homeostasis and regeneration.

Because Yap1 can be induced via gp130 activators, independently of STAT3 via Src family kinases, we blocked Src family kinases with PP2 and were able to show reduced proliferation, reduced Yap1 activation and increased pathology, indicating that Src activation is important in tissue remodeling and that Yap1 is activated in accordance with previously reported results[48].

Lgr5$^+$ CBCs expressed high levels of transcripts encoding *gp130* and *il11ra1*, and low levels of *Il6ra1*. Because cryptopatch ILC3s expressed *Il-6* but not *Il-11*, we blocked IL-6 during MTX-induced tissue damage and found that pathology, proliferation and Yap1 activation

were not affected. By blocking IL-11 and IL-6 binding to gp130 with LMT28 but not blocking IL-6 alone, Yap1^{+} cells in crypts were significantly reduced. This series of experiments can be interpreted as either a contribution of both IL-6 and IL-11 to synergistically induce Yap1 signaling, but IL-11 being sufficient if IL-6 is absent. The role of ILC3s in Yap1 induction would then be via an indirect mechanism through mesenchymal or epithelial cell-derived IL-11. It is therefore important to investigate whether in RORγt$^{-/-}$ mice there is a reduction of IL-11 and if so, to decipher the source of IL-11 in response to intestinal injury.

Are myeloid cells involved in ILC3-driven epithelial regeneration?

Mononuclear phagocytes, including dendritic cells (DCs) and macrophages have well-stablished roles in controlling production of IL-22 and GM-CSF by ILC3s in the gut[8,10,49,50]. However, the exact cell type and the location of the interactions between mononuclear phagocytes and ILC3s is still under debate. This thesis includes a detail description of a subset of dendritic cells that are found in solitarily intestinal lymphoid follicles (SILTs) together with ILC3s (Chapter 5). These cells are negative for macrophages markers, but express the dendritic cell markers CD11c and MHCII. By analyzing CD103 and CD11b, which aid in classifying distinct DC subsets in small intestinal lamina propria, cells in cryptopatches are negative for both CD103 and CD11b, and thus are part of the poorly characterized double-negative DC population. SILT-DCs are characterized by their expression of Plet1 and LysM and possess a unique transcriptome associated with ILC3 function, including high levels of transcription of *Il-23*, *il1β* and *il22bp* genes. A subject of further research is their contribution to epithelial regeneration after tissue damage. To assess this, strategies to specifically deplete SILT-DCs need to be generated. Important questions that remain to be assessed are whether SILT-DCs respond to microbial-derived antigens during homeostasis and in response to damage and whether they migrate to lymph nodes to interact with lymph node ILCs or induce adaptive T cell responses.

Why are ILC3s needed to control epithelial cell responses?

The findings described in this thesis, showing that the presence of ILC3s in cryptopatches is essential to drive Yap1-mediated intestinal tissue regeneration after damage, let us to propose that cryptopatches have emerged in mammals in order to regulate the magnitude of the regenerative response by amplifying signaling pathways important for epithelial stem cell function. In addition, the specific contribution of ILC3 subsets to intestinal regeneration remain unknown, and models of specific depletion of ILC3s are still lacking.

We have demonstrated that the use of the chemotherapeutic drug MTX in mice allows studying Lgr5^{+} stem cell injury and regeneration, and it is suitable to interrogate the role of ILC3s in small intestinal epithelial cell responses. It would be of great interest to develop different models of intestinal injury to validate our results. A possible strategy would be the use of 5-Fluorouracil to induce intestinal mucositis or the exposure of mice to high doses of

gamma-irradiation, known to induce DNA damage and deplete Lgr5$^+$ intestinal stem cells[51]. DSS-induced colitis would be a model to study ILC3 function in colonic tissue repair.

Beyond the scope of this thesis, but still highly interesting, it is the identification of the epithelial stem cell population responsible for regeneration.

In addition, studying cryptopatches during intestinal regeneration is needed to understand their function during non-infectious inflammation. A Ccl19-Cre-YFP crossed with RosaiDTR is a transgenic mouse model that allows inducible depletion of CCL19-YFP$^+$ stromal cells present in cryptopatches during intestinal regeneration, and could be used to prove whether cryptopatches are sites from where epithelial responses are orchestrated.

Finally, in order to completely understand ILC3-induced tissue repair it is important to investigate how the response is shut down after tissue regeneration has been accomplished. To do this, ILC3 maintenance and survival after activation should be investigated, such as analyzing cellular and molecular inhibitory pathways that lead to functional ILC3 arrest.

Do ILC3s mediate epithelial stem cell regeneration in other tissues?

Innate lymphoid cells expressing RORγt, IL-7 and producing IL-17A/F have been reported in the liver and expand after adenovirus and LCMV infection. IL-17 signaling is important to create a cytokine milieu critical for priming T cell responses in viral hepatitis[52]. Also, ILCs have been shown to protect against acute hepatitis[53,54] but can also mediate hepatic fibrosis[55]. In addition, stroma-derived Yap1 signaling also plays an important role in hepatic cell regeneration[56,57], thus studying ILC3 contribution in hepatic epithelial regeneration is interesting. Similarly, tissues such as the kidney[58], skin or hair follicles[59], corneal epithelium[60] and lung pulmonary alveoli and bronchi[61] contain Lgr5$^+$ stem cells and can contain ILC3s upon injury. These tissues could be used to assess whether ILC3-driven tissue regeneration is a feature that goes beyond the intestine and impacts additional peripheral organs.

What is the long-term outlook derived from this research?

Improving tissue repair in patients that suffer from intestinal pathologies is highly relevant, in particular in inflammatory bowel disease (IBD) and in graft-versus-host disease (GvHD) following hematopoietic stem cell transplantation. The ultimate goal of treatment strategies will be to suppress pathogenic immune cells and activate immune cell-driven tissue repair.

It would be necessary to unravel the signals that regulate immune-cell driven tissue repair in cryptopatches. One hypothesis is that cryptopatches exist as sites where protective immune reactions are mounted, similar to lymph nodes. For that, dendritic cells might sense tissue damage and migrate to cryptopatches to activate innate lymphoid cells. Subsequently, innate lymphoid cells and stromal cells might interact and this could be essential for the organization of the organ and the proper course of the locally activated immune response.

Having identified the phenotype of dendritic cells that locate in cryptopatches and their essential role in cryptopatch-driven intestinal repair, the next step is to identify the

mechanisms by which these cells get in contact with innate lymphoid cells and activate them. To study their migration in the tissue, intra-vital imaging of the intestines will be necessary. In parallel, in vitro and in vivo experiments could help to elucidate the signals that are necessary for dendritic cells to sense damage and to activate innate lymphoid cells. Dendritic cells could be analyzed after stimulation with damage-associated or microbial-derived molecules both in vitro and in vivo. In addition, it will be relevant to determine whether dendritic cells and innate lymphoid cells require cell-to-cell contact or soluble molecules are produced and signal through membrane-bound receptors. Finally, the candidate molecules, will be also need to be tested both in vitro and in vivo.

For clinical translation, three main strategies could be explored: one is to engineer dendritic cells or innate lymphoid cells for adoptive cell transfer; another possibility is to administer molecules that activate cryptopatch responses and induce tissue repair; or to target intestinal epithelial stem cells directly to enhance repair.

In conclusion, experiments based on my research could provide a future rationale design of clinical strategies aimed at improving mucosal healing by enhancing intestinal crypt regeneration.

REFERENCES

1. Tumanov, A. V., Koroleva, E. P., Guo, X., Wang, Y., Kruglov, A., Nedospasov, S. & Fu, Y. X. Lymphotoxin controls the IL-22 protection pathway in gut innate lymphoid cells during mucosal pathogen challenge. *Cell Host Microbe* **10,** 44–53 (2011).
2. Withers, D. R. *et al.* Transient inhibition of ROR-γt therapeutically limits intestinal inflammation by reducing TH17 cells and preserving group 3 innate lymphoid cells. *Nat. Med.* **22,** 319–323 (2016).
3. Giacomin, P. R. *et al.* Epithelial-intrinsic IKKα expression regulates group 3 innate lymphoid cell responses and antibacterial immunity. *J. Exp. Med.* **212,** 1513–28 (2015).
4. Mortha, A., Chudnovskiy, A., Hashimoto, D., Bogunovic, M., Spencer, S. P., Belkaid, Y. & Merad, M. Microbiota-dependent crosstalk between macrophages and ILC3 promotes intestinal homeostasis. *Science (80-.).* **343,** 1249288–1249288 (2014).
5. Pearson, C. *et al.* ILC3 GM-CSF production and mobilisation orchestrate acute intestinal inflammation. *Elife* **5,** 1–21 (2016).
6. Hepworth, M. R. *et al.* Immune tolerance. Group 3 innate lymphoid cells mediate intestinal selection of commensal bacteria-specific $CD4^+$ T cells. TL - 348. *Science* **348 VN-,** 1031–1035 (2015).
7. Spits, H. *et al.* Innate lymphoid cells--a proposal for uniform nomenclature. *Nat. Rev. Immunol.* **13,** 145–9 (2013).
8. Balzola, F., Bernstein, C., Ho, G. T. & Lees, C. Innate lymphoid cells drive interleukin-23-dependent innate intestinal pathology: Commentary. *Inflammatory Bowel Disease Monitor* **11,** 79 (2010).
9. Chen, L. *et al.* IL-23 activates innate lymphoid cells to promote neonatal intestinal pathology. *Mucosal Immunol.* **8,** 390–402 (2015).
10. Klein Wolterink, R. G. J., Serafini, N., van Nimwegen, M., Vosshenrich, C. A. J., de Bruijn, M. J. W., Fonseca Pereira, D., Veiga Fernandes, H., Hendriks, R. W. & Di Santo, J. P. Essential, dose-dependent role for the transcription factor Gata3 in the development of IL-5+ and IL-13+ type 2 innate lymphoid cells. *Proc. Natl. Acad. Sci.* **110,** 10240–10245 (2013).
11. Zheng, Y. *et al.* Interleukin-22 mediates early host defense against attaching and effacing bacterial pathogens. *Nat. Med.* **14,** 282–9 (2008).
12. Kinnebrew, M. A., Buffie, C. G., Diehl, G. E., Zenewicz, L. A., Leiner, I., Hohl, T. M., Flavell, R. A., Littman, D. R. & Pamer, E. G. Interleukin 23 Production by Intestinal CD103 +CD11b + Dendritic Cells in Response to Bacterial Flagellin Enhances Mucosal Innate Immune Defense. *Immunity* **36,** 276–287 (2012).
13. Macho-Fernandez, E., Koroleva, E. P., Spencer, C. M., Tighe, M., Torrado, E., Cooper, A. M., Fu, Y.-X. & Tumanov, A. V. Lymphotoxin beta receptor signaling limits mucosal damage through driving IL-23 production by epithelial cells. *Mucosal Immunol.* **8,** 403–413 (2015).
14. Atarashi, K. *et al.* Induction of Colonic Regulatory T Cells by Indigenous Clostridium Species. *Science (80-.).* **331,** 337–341 (2011).
15. Smith, P. M., Howitt, M. R., Panikov, N., Michaud, M., Gallini, C. A., Bohlooly-Y, M., Glickman, J. N. & Garrett, W. S. The Microbial Metabolites, Short-Chain Fatty Acids, Regulate Colonic Treg Cell Homeostasis. *Science (80-.).* **341,** 569–573 (2013).
16. Furusawa, Y. *et al.* Commensal microbe-derived butyrate induces the differentiation of colonic regulatory T cells. *Nature* **504,** 446–450 (2013).
17. Arpaia, N. *et al.* Metabolites produced by commensal bacteria promote peripheral regulatory T-cell generation. *Nature* **504,** 451–455 (2013).
18. Neill, D. R. *et al.* Nuocytes represent a new innate effector leukocyte that mediates type-2 immunity. *Nature* **464,** 1367–1370 (2010).

19. Moro, K. *et al.* Innate production of TH2 cytokines by adipose tissue-associated c-Kit+Sca-1+ lymphoid cells. *Nature* **463,** 540–544 (2010).
20. Oliphant, C. J. *et al.* MHCII-mediated dialog between group 2 innate lymphoid cells and CD4+ T cells potentiates type 2 immunity and promotes parasitic helminth expulsion. *Immunity* **41,** 283–295 (2014).
21. Nussbaum, J. C. *et al.* Type 2 innate lymphoid cells control eosinophil homeostasis. *Nature* **502,** 245–248 (2013).
22. Monticelli, L. A., Osborne, L. C., Noti, M., Tran, S. V., Zaiss, D. M. W. & Artis, D. IL-33 promotes an innate immune pathway of intestinal tissue protection dependent on amphiregulin–EGFR interactions. *Proc. Natl. Acad. Sci.* **112,** 10762–10767 (2015).
23. Bernink, J. H. *et al.* Human type 1 innate lymphoid cells accumulate in inflamed mucosal tissues. *Nat. Immunol.* **14,** 221–229 (2013).
24. Geremia, A., Arancibia-Cárcamo, C. V, Fleming, M. P. P., Rust, N., Singh, B., Mortensen, N. J., Travis, S. P. L. & Powrie, F. IL-23–responsive innate lymphoid cells are increased in inflammatory bowel disease. *J. Exp. Med.* **208,** 1127–1133 (2011).
25. Li, Z. *et al.* Epidermal Notch1 recruits RORγ+ group 3 innate lymphoid cells to orchestrate normal skin repair. *Nat. Commun.* **7,** 11394 (2016).
26. Dudakov, J. A. *et al.* Interleukin-22 Drives Endogenous Thymic Regeneration in Mice. *Science (80-.).* **336,** 91–95 (2012).
27. Hanash, A. M. *et al.* Interleukin-22 protects intestinal stem cells from immune- mediated tissue damage and regulates sensitivity to graft vs. host disease. *Immunity* **37,** 339–350 (2012).
28. Kabiri, Z. *et al.* Stroma provides an intestinal stem cell niche in the absence of epithelial Wnts. *Development* **141,** 2206–2215 (2014).
29. Gong, W. *et al.* Mesenchymal stem cells stimulate intestinal stem cells to repair radiation-induced intestinal injury. *Cell Death Dis.* **7,** e2387 (2016).
30. Chang, P. Y., Jin, X., Jiang, Y. Y., Wang, L. X., Liu, Y. J. & Wang, J. Mensenchymal stem cells can delay radiation-induced crypt death: impact on intestinal CD44+ fragments. *Cell Tissue Res.* **364,** 331–344 (2016).
31. Ibiza, S. *et al.* Glial-cell-derived neuroregulators control type 3 innate lymphoid cells and gut defence. *Nature* **535,** 440–443 (2016).
32. Aparicio-Domingo, P. *et al.* Type 3 innate lymphoid cells maintain intestinal epithelial stem cells after tissue damage. *J. Exp. Med.* **212,** 1783–91 (2015).
33. Tetteh, P. W. *et al.* Replacement of Lost Lgr5-Positive Stem Cells through Plasticity of Their Enterocyte-Lineage Daughters. *Cell Stem Cell* **18,** 203–213 (2016).
34. Buczacki, S. J. A., Zecchini, H. I., Nicholson, A. M., Russell, R., Vermeulen, L., Kemp, R. & Winton, D. J. Intestinal label-retaining cells are secretory precursors expressing Lgr5. *Nature* **495,** 65–9 (2013).
35. van Es, J. H. *et al.* Dll1+ secretory progenitor cells revert to stem cells upon crypt damage. *Nat. Cell Biol.* **14,** 1099–104 (2012).
36. Yan, K. S. *et al.* Intestinal Enteroendocrine Lineage Cells Possess Homeostatic and Injury-Inducible Stem Cell Activity. *Cell Stem Cell* **21,** 78–90.e6 (2017).
37. Jadhav, U., Saxena, M., O'Neill, N. K., Saadatpour, A., Yuan, G. C., Herbert, Z., Murata, K. & Shivdasani, R. A. Dynamic Reorganization of Chromatin Accessibility Signatures during Dedifferentiation of Secretory Precursors into Lgr5+ Intestinal Stem Cells. *Cell Stem Cell* **21,** 65–77.e5 (2017).
38. Bollrath, J. *et al.* gp130-Mediated Stat3 Activation in Enterocytes Regulates Cell Survival and Cell-Cycle Progression during Colitis-Associated Tumorigenesis. *Cancer Cell* **15,** 91–102 (2009).
39. Middelhoff, M., Westphalen, C. B., Hayakawa, Y., Yan, K. S., Gershon, M. D., Wang, T. C. & Quante, M. Dclk1-expressing tuft cells: Critical modulators of the intestinal niche? *Am. J. Physiol. - Gastrointest. Liver Physiol.* ajpgi.00073.2017 (2017).

40. Hamazaki, Y. Enteroendocrine cells are specifically marked by cell surface expression of claudin-4 in mouse small intestine. *PLoS One* (2014).
41. Lindemans, C. A. *et al.* Interleukin-22 promotes intestinal-stem-cell-mediated epithelial regeneration. *Nature* **528,** 560–564 (2015).
42. Aden, K. *et al.* Classic IL-6R signalling is dispensable for intestinal epithelial proliferation and repair. *Oncogenesis* **5,** e270 (2016).
43. Sonnenberg, G. F. & Artis, D. Innate lymphoid cells in the initiation, regulation and resolution of inflammation. *Nat. Med.* **21,** 698–708 (2015).
44. Gregorieff, A., Liu, Y., Inanlou, M. R., Khomchuk, Y. & Wrana, J. L. Yap-dependent reprogramming of Lgr5+ stem cells drives intestinal regeneration and cancer. *Nature* **526,** 715–8 (2015).
45. Juan, W. C. & Hong, W. Targeting the Hippo signaling pathway for tissue regeneration and cancer therapy. *Genes* **7,** (2016).
46. Hong, A. W., Meng, Z. & Guan, K.-L. The Hippo pathway in intestinal regeneration and disease. *Nat. Rev. Gastroenterol. Hepatol.* **13,** 324–337 (2016).
47. Gjorevski, N., Sachs, N., Manfrin, A., Giger, S., Bragina, M. E., Ordóñez-Morán, P., Clevers, H. & Lutolf, M. P. Designer matrices for intestinal stem cell and organoid culture. *Nature* **539,** 560–564 (2016).
48. Taniguchi, K. *et al.* A gp130-Src-YAP Module Links Inflammation to Epithelial Regeneration. *Nature* **519,** 57–62 (2015).
49. West, N. R. *et al.* Oncostatin M drives intestinal inflammation and predicts response to tumor necrosis factor–neutralizing therapy in patients with inflammatory bowel disease. *Nat. Med.* (2017).
50. Longman, R. S. *et al.* CX_3CR1^+ mononuclear phagocytes support colitis-associated innate lymphoid cell production of IL-22. *J. Exp. Med.* **211,** 1571–83 (2014).
51. Balzola, F., Cullen, G., Ho, G. T., Hoentjen, F. & Russell, R. K. IL-22BP is regulated by the inflammasome and modulates tumorigenesis in the intestine. *Inflammatory Bowel Disease Monitor* **13,** 108–109 (2013).
52. Potten, C. S., Al-Barwari, S. E. & Searle, J. Differential Radiation Response Amongst Proliferating Epithelial Cells. *Cell Prolif.* **11,** 149–160 (1978).
53. Goyal, N., Rana, A., Ahlawat, A., Bijjem, K. R. V. & Kumar, P. Animal models of inflammatory bowel disease: A review. *Inflammopharmacology* **22,** 219–233 (2014).
54. Korneychuk, N., Meresse, B. & Cerf-Bensussan, N. Lessons from rodent models in celiac disease. *Mucosal Immunol.* **8,** 18–28 (2015).
55. Bouziat, R. *et al.* Reovirus infection triggers inflammatory responses to dietary antigens and development of celiac disease. *Science (80-.).* **356,** 44–50 (2017).
56. Jie, Z., Liang, Y., Hou, L., Dong, C., Iwakura, Y., Soong, L., Cong, Y. & Sun, J. Intrahepatic Innate Lymphoid Cells Secrete IL-17A and IL-17F That Are Crucial for T Cell Priming in Viral Infection. **J. Immunol. 192,** 3289–3300 (2014).
57. Liang, Y., Jie, Z., Hou, L., Aguilar-Valenzuela, R., Vu, D., Soong, L. & Sun, J. IL-33 Induces Nuocytes and Modulates Liver Injury in Viral Hepatitis. **J. Immunol. 190,** 5666–5675 (2013).
58. Matsumoto, A. **et al.** IL-22-Producing RORγt-Dependent Innate Lymphoid Cells Play a Novel Protective Role in Murine Acute Hepatitis. **PLoS One 8,** (2013).
59. Mchedlidze, T. **et al.** Interleukin-33-dependent innate lymphoid cells mediate hepatic fibrosis. **Immunity 39,** 357–371 (2013).
60. Camargo, F. D., Gokhale, S., Johnnidis, J. B., Fu, D., Bell, G. W., Jaenisch, R. & Brummelkamp, T. R. YAP1 Increases Organ Size and Expands Undifferentiated Progenitor Cells. **Curr. Biol. 17,** 2054–2060 (2007).
61. Swiderska-Syn, M., Xie, G., Michelotti, G. A., Jewell, M. L., Premont, R. T., Syn, W. K. & Diehl, A. M. Hedgehog regulates yes-associated protein 1 in regenerating mouse liver. **Hepatology 64,** 232–244 (2016).

62. Kato, S., Matsubara, M., Matsuo, T., Mohri, Y., Kazama, I., Hatano, R., Umezawa, A. & Nishimori, K. Leucine-rich repeat-containing G protein-coupled receptor-4 (LGR4, Gpr48) is essential for renal development in mice. **Nephron - Exp. Nephrol. 104,** (2006).

63. Jaks, V., Barker, N., Kasper, M., van Es, J. H., Snippert, H. J., Clevers, H. & Toftgård, R. Lgr5 marks cycling, yet long-lived, hair follicle stem cells. **Nat. Genet. 40,** 1291–1299 (2008).

64. Curcio, C., Lanzini, M., Calienno, R., Mastropasqua, R. & Marchini, G. The expression of LGR5 in healthy human stem cell niches and its modulation in inflamed conditions. **Mol. Vis. 21,** 644–8 (2015).

65. Zhang, X. **et al.** Lgr5-positive cells in the lung and their clinical significance in patients with lung adenocarcinoma. **Mol. Clin. Oncol. 5,** 283–288 (2016).

A

ADDENDUM

LIST OF ABBREVIATIONS

ILCs: innate lymphoid cells
ILC1s: Group 1 innate lymphoid cells
ILC2s: Group 2 innate lymphoid cells
ILC3s: Group 3 innate lymphoid cells
ILCregs: Regulatory innate lymphoid cells
GvHD: graft-versus host disease
DCs: Dendritic cells
NK: Natural Killer (cells)
GI: gastrointestinal
SI: small intestine
GALT: gut-associated lymphoid follicles
LP: lamina propria
BM: bone-marrow
PPs: Peyer Patches
CPs: Cryptopatches
SILTs: Solitary intestinal lymphoid tissues
ILFs: Intestinal lymphoid follicles
LNs: lymph nodes
MLNs: mesenteric lymph nodes
TH: T helper (cells)
Th17: T helper 17 (cells)
Th2: T helper 2 (cells)
Tregs: Regulatory T (cells)
LTi: lymphoid tissue inducer (cells)
LTin: lymphoid tissue initiator
LTo: lymphoid tissue organizer
TLR: toll-like receptor
CLPs: common lymphoid progenitors
CHILPs: common helper Innate Lymphoid Cell progenitor
AhR: aryl hydrocarbon receptor
SAA: serum amyloid protein
SFG: segmented filamentous bacteria
HLA-DR: Human Leukocyte Antigen – antigen D Related
RA: retinoic acid
ISCs: intestinal stem cells
TA: transit-amplifying (cells)
CBCs: crypt base columnar (cells)

MNP: mononuclear phagocytes
NCR: natural cytotoxicity receptor
Lgr5: leucine-rich repeat-containing G-protein coupled receptor 5
RORγ: RAR-related orphan receptor gamma
Plet1: placenta-expressed transcript 1 protein
ECM: extracellular matrix
HSCT: hematopoietic stem cell transplantation
BMT: bone marrow transfer
TBI: total body irradiation
SL-TBI: single slow dose total body irradiation
IBD: inflammatory bowel disease
DHFR: dihydrofolate reductase
MTX: methotrexate
DSS: dextran sulfate sodium
SS: steady-state
IECs: intestinal epithelial cells
STAT3: signal transducer and activator of transcription 3
YAP1: yes-associated protein 1
EGF: epidermal growth factor
BMP: bone morphogenetic protein
Ihh: indian hedgehog
GC: Goblet cell
PC: Paneth cell
EE: Enteroendocrine cell
DT: diphtheria toxin
DMSO: dimethyl sulfoxide
i.p: intraperitoneal

ENGLISH SUMMARY

t aimed at unraveling which functions of the intestinal epithelium are regulated by ILC3s and which cellular and molecular mechanisms are involved in such crosstalk. Second, we also aimed to decipher whether ILC3-driven tissue repair is controlled from solitary intestinal lymphoid tissues (SILTs) and whether dendritic cells (DCs) play a role in ILC3 activation during these processes.

Chapter 1 provides an overview of the current knowledge on innate lymphoid cells (ILCs) and extends to different aspects of ILC biology: development, migration, classification and plasticity of the different described subsets of ILCs and their effector functions.

In **chapter 2**, we demonstrated in an experimental model of chemotherapy-induced small intestinal damage that the presence of ILC3s in cryptopatches are necessary for the preservation of intestinal stem cells, the activation and proliferation of the epithelium and the resolution of pathology. This model of small intestinal damage resembles the development of mucositis, often seen in patients as a side effect of cancer treatments. We showed that the ILC3s are critical for the activation of STAT3 signaling pathway in epithelial cells transiently after methothrexate (MTX) administration. Although control mice developed intestinal pathology, crypt proliferation was restored four days after the MTX treatment. Mice deficient on ILC3s showed increased pathology and strongly reduced crypt proliferation during the regenerative phase after MTX. We also showed that IL-22 is involved in the preservation of $Lgr5^{+}$ ISCs after tissue damage.

We further investigated which features of intestinal stem cells were directly modulated by ILC3-derived IL-22 in response to epithelial insult in **chapter 3**. By blocking IL-22 and STAT3 downstream of the IL-22 receptor we found that while IL-22 was critical to maintain ISC frequencies, IL-22 absence did not impact the recovery of proliferative crypts upon injury. To identify defects in crypt renewal in the absence of ILC3s and SILTs we generated ILC3-deficient ISC-reporter mice and analyzed ISCs by RNA-sequencing. This revealed that SILTs are essential for the initiation of the evolutionary conserved epithelial regeneration pathway Yap1 in ISCs, which enhanced enteroendocrine cell differentiation. We could show that the cytokines IL-11 and IL-6 are involved in Yap1-driven intestinal regeneration after damage. This revealed a previously unacknowledged layer of immune cell-mediated control of epithelial tissue repair.

In **chapter 4** we examined whether the impaired intestinal regenerative response after MTX in mice lacking ILC3s was a consequence of defective epithelial function at steady-state. We noted regularly alterations in the crypt compartment of $ROR\gamma t^{-/-}$ mice at steady-state: crypt epithelial flattening, crypt loss, increased expression of stress/inflammatory-associated genes and an accumulation of enteroendocrine-like ISCs. This mirrored a situation seen after administration of MTX, suggesting low-grade tissue injury in the absence of SILTs. RNA sequencing of ISC revealed an enrichment of secretory markers, which strongly

resembled the phenotype of a reserve stem cell population recently described to reacquire stem cell properties and drive regeneration in response to injury. This chapter proposes a model in which ILC3s in SILTS contribute to the regulation of the ISC pool under homeostatic conditions.

We next investigated whether intestinal DCs were involved in ILC3-driven tissue repair in **chapter 5**. We hypothesized that DCs, that can sense signals from penetrating bacteria or stress-induced molecules in the crypts, would activate ILC3s to drive tissue repair. Indeed, when we depleted $CD11c^{+}$ cells during tissue damage, crypt epithelial cells showed decreased proliferation and the mice developed increased intestinal pathology. We then further set out to characterize the subset of DCs interacting with ILC3s in SILTS to drive tissue remodeling. Immunohistochemical analysis, SILT micro-dissection and transcriptional profiling of intestinal DC subsets revealed that $CD103^{-}$ $Plet1^{+}$ DCs are present in SILTs and possess an ILC3-associated transcriptional profile. Furthermore, SILT-DCs expressed a selective range of toll-like receptors, which in response to epithelial barrier disruption could be important for recognition of molecules in the crypts and subsequent translation of these signals into ILC3s activation.

Finally, **chapter 6** provides a general discussion of the most relevant findings described in this thesis, places them in a broader perspective and address future experiments needed to progress this research.

In sum, we have uncovered a novel pathway controlling epithelial regeneration after chemotherapy-induced small intestinal epithelial injury, which is immune-cell driven. I believe that unraveling the mechanisms that drive ILC3-mediated tissue repair from SILTs can help to understand what the function of these organs are in tissue repair. Our findings suggest that SILTs are anatomical sites from where innate immune cells orchestrate epithelial homeostasis and tissue remodeling, thus proposing ILC3s as new clinically relevant targets to improve mucosal healing in inflammatory conditions or during anti-cancer treatments.

NEDERLANDSE SAMENVATTING (DUTCH SUMMERY)

Het doel van dit proefschrift was om inzicht te verkrijgen in de rol van groep 3 innate lymfoïde cellen (ILC3s) in functie van het darm epitheel tijdens homeostase en weefselherstel. Het in dit proefschrift beschreven werk richtte zich op het ontrafelen van de functies van het darmepitheel die door ILC3s worden gereguleerd en het identificeren van de cellulaire en moleculaire mechanismen betrokken bij de communicatie tussen ILC3 en het darmepitheel. Tevens wilden we het belang van solitaire intestinaal lymfoïde weefsel (SILT) en dendritische cellen (DCs) bepalen voor het herstel van darmschade door ILC3.

Hoofdstuk 1 geeft een overzicht van de huidige kennis over innate lymfoïde cellen (ILCs) en behandeld verschillende aspecten van de ILC-biologie: ontwikkeling, migratie, classificatie en plasticiteit van de verschillende subsets van ILCs en hun effector functies.

In **hoofdstuk 2** hebben we in een experimenteel model van chemotherapie geïnduceerde beschadiging van de dunne darm aangetoond dat de aanwezigheid van ILC3s in cryptopatches noodzakelijk is voor het behoud van darm stamcellen, de activatie en proliferatie van het epitheel en het repareren van de schade. Dit model van schade aan de dunne darm heeft overeenkomsten met de ontwikkeling van mucositis, een vorm van ontsteking aan de darmmucosa (slijmvliezen) die vaak optreedt als bijwerking van kankerbehandelingen zoals bestraling en chemotherapie. In dit model hebben we kunnen aantonen dat ILC3s van cruciaal belang zijn voor de activering van de STAT3-signaalroute in epitheelcellen, na schade door toediening van het cytostaticum methothrexaat (MTX). Controle muizen darm schade ontwikkelden, maar de proliferatie van de darmcrypten was vier dagen na de toediening van MTX weer hersteld. Muizen die deficiënt waren voor ILC3s toonden verhoogde darm pathologie en een sterk verminderde proliferatie van de darmcrypten tijdens de regeneratieve fase. We konden tevens aantonen dat het cytokine IL-22 betrokken was bij het behoud van de $Lgr5^{+}$ darm stamcellen na weefselschade.

In **hoofdstuk 3** onderzochten we welke functies van darm stamcellen direct gereguleerd worden door ILC3-geproduceerd IL-22 als reactie op epitheelschade. Door verschillende onderdelen van de IL-22/STAT3 signalering te blokkeren, ontdekten we dat IL-22 essentieel is om darm stamcellen te behouden. Echter, de afwezigheid van IL-22 had geen invloed op het herstel van delende cellen in darmcrypten na schade. Om de defecten in crypt herstel te kunnen identificeren in afwezigheid van zowel ILC3s en SILTs, hebben we ILC3-deficiente muizen gegenereerd waarin darm stamcellen geïdentificeerd en geïsoleerd kunnen worden. Van deze dieren hebben we de darm stamcellen geïsoleerd en gekarakteriseerd door het uitlezen van hun RNA-transcriptie, een maat voor gen expressie. Dit onthulde dat SILTs essentieel zijn voor de activatie van de Yap1 epitheliale regeneratie route in darm stamcellen. De activatie van deze Yap1 signaalroute leidde tot verhoogde differentiatie van entero-endocriene cellen. Tevens hebben we kunnen aantonen dat de cytokines IL-11 en IL-6 betrokken waren bij het door de Yap1 signaalroute aangestuurde darmherstel na

schade. Deze controle van darm epitheliale cellen door cellen van het immuun systeem was nooit eerder beschreven.

Zoals hierboven beschreven trad er na toediening van MTX bij muizen zonder ILC3s een verstoorde darm reparatie op. In **hoofdstuk 4** hebben we bepaald of dit een gevolg was van defecte epitheliale functies in de gezonde weefsels door de afwezigheid van ILC3s. We vonden dat er veranderingen waren in het crypt-compartiment van muizen zonder ILC3, ook in de afwezigheid van darmschade. Deze veranderingen bestonden onder andere uit crypt-epitheelafvlakking, een verhoogde expressie van stress en ontstekings genen, en een accumulatie van entero-endocrien-achtige darm stamcellen. Dit weerspiegelde een situatie die, in mindere mate, ook waargenomen werd na toediening van MTX, wat zou kunnen wijzen op laaggradige weefselschade bij afwezigheid van SILTs. RNA-transcriptie analyse van darm stamcellen onthulde een verrijking van genen geassocieerd met bij secretoire epitheel cellen. Dit leek op het fenotype van een recentelijk beschreven reserve stamcel populatie die stamcel eigenschappen kan her-activeren en zodoende bijdragen aan weefselherstel. In dit hoofdstuk wordt dan ook een model voorgesteld waarin ILC3s in SILTs bijdragen aan de regulatie van darm stamcellen onder homeostatische omstandigheden.

Tenslotte hebben we in **hoofdstuk 5** onderzocht of dendritische cellen in de darm betrokken waren bij ILC3-gedreven weefselherstel. Onze hypothese was dat dendritische cellen, die signalen van darmbacteriën of van gestreste cellen in de crypten kunnen detecteren, ILC3s activeren om weefselherstel aan te sturen. Inderdaad, toen we $CD11c^+$ dendritische cellen voor het induceren van darm schade verwijderden, vertoonden crypt epitheel cellen verminderde proliferatie en ontwikkelden deze muizen ernstigere darm schade. Vervolgens hebben we de subset van dendritische cellen die communiceren met ILC3s in SILTs gekarakteriseerd. Immunohistochemische analyses, SILT-microdissecties en expressie profileringen van darm dendritische cel-subsets onthulden dat CD103-$Plet1^+$ dendritische cellen aanwezig zijn in SILTs en dat deze cellen genen tot expressie brengen die ILC3 functie kunnen beinvloeden. Verder brachten SILT-dendritische cellen een selectief aantal Toll-like receptoren tot expressie, die in reactie op epitheliale barrière-verstoring belangrijk zouden kunnen zijn voor de herkenning van moleculen afkomstig van bacteriën of beschadigde epitheel cellen. Dendritische cellen zouden deze signalen zodanig kunnen verwerken dat ze leiden to activatie van ILC3s.

Tenslotte bevat **hoofdstuk 6** een algemene discussie over de meest relevante bevindingen beschreven in dit proefschrift, plaatst het deze bevindingen in een breder perspectief en gaat het in op toekomstige experimenten die nodig zijn om dit onderzoek te vervolgen.

Samengevat hebben we een nieuwe route ontdekt die epitheliale regeneratie reguleert na chemotherapie-geïnduceerde beschadiging van de dunne darm, aangestuurd door immuun cellen. Het ontrafelen van de mechanismen die zorgen voor ILC3-gemedieerd weefselherstel vanuit SILTs kan helpen om te begrijpen wat de functie van deze organen is in de darm. Onze bevindingen suggereren dat SILTs anatomische locaties zijn van waaruit

immuun cellen de homeostase van het epitheel en het herstel van het weefsel controleren. ILC3s zouden daarom in de toekomst wellicht klinisch gemanipuleerd kunnen worden om herstel van darm schade tijdens chronische ontstekingen of tijdens behandeling van kanker te verbeteren.

CURRICULUM VITAE

Mónica Romera Hernández was born in Berga, Barcelona (Spain) in 1989. After studying Science and Technology at IES Guillem de Berguedà high school she obtain her cum laude diploma and she gained access to Universitat Autònoma de Barcelona, where she conducted a licentiate program in Biotechnology. In 2011, she was awarded with a Junior Research Fellowship within the Europe's Erasmus Exchange Programme in order to perform an internship at a foreign university and finalize her university degree. She completed one-year research project at the Department of Immunohematology at Leiden Universiteit Medisch Centre, under the supervision of Frits Koning. Her project focused on the characterization of aberrant intraepithelial lymphocyte subsets originating in Refractory Celiac Disease Type II patients and the study of the developmental capacity of these cells isolated from the intestine and the thymus. In September 2012, after she graduated in Barcelona, she was appointed as PhD candidate in the research group of Dr. Tom Cupedo at the Department of Hematology at the Erasmus MC. Until December 2015, she was part of the STROMA ITN, a Marie Curie ITN (Initial Training Network) under the European Commission's 7th Framework Programme for research and coordinated by Dr. Mark Coles and Prof.dr. Paul Kaye at the Centre for Immunology and Infection, University of York. She was trained to investigate stromal cells and the infrastructure of the immune system and collaborated with industrial and academic partners to gain further experience in the field. During her doctoral training, she studied intestinal homeostasis and remodelling after injury, with a special focus on unrevealing the mechanisms by which innate lymphoid cells regulate intestinal epithelial stem cell behavior, thus contributing to tissue regeneration. The ultimate goal of her research is to improve mucosal healing in patients who suffer from intestinal inflammatory disorders.

Honors:

Selected to present in the Bright Sparks session at the Dutch Society of Immunology, 50th Anniversary Annual Meeting. December 2015.

Selected to present in the Rising Stars session at the International Congress of Mucosal Immunology. July 2017, Washington DC.

LIST OF PUBLICATIONS

1. Integrin-Alpha IIb Identifies Murine Lymph Node Lymphatic Endothelial Cells Responsive to RANKL. Cordeiro OG, Chypre M, Brouard N, Rauber S, Alloush F, **Romera-Hernandez M**, Bénézech C, Li Z, Eckly A, Coles MC, Rot A, Yagita H, Léon C, Ludewig B, Cupedo T, Lanza F, Mueller CG.
PLoS One. 2016 Mar 24;11(3):e0151848. doi: 10.1371/journal.pone.0151848. eCollection 2016.

2. Interleukin-22 promotes intestinal-stem-cell-mediated epithelial regeneration. Lindemans CA, Calafiore M, Mertelsmann AM, O'Connor MH, Dudakov JA, Jenq RR, Velardi E, Young LF, Smith OM, Lawrence G, Ivanov JA, Fu YY, Takashima S, Hua G, Martin ML, O'Rourke KP, Lo YH, Mokry M, **Romera-Hernandez M**, Cupedo T, Dow L, Nieuwenhuis EE, Shroyer NF, Liu C, Kolesnick R, van den Brink MRM, Hanash AM.
Nature. 2015 Dec 24;528(7583):560-564. doi: 10.1038/nature16460. Epub 2015 Dec 9.

3. Type 3 innate lymphoid cells maintain intestinal epithelial stem cells after tissue damage. Aparicio-Domingo P, **Romera-Hernandez M**, Karrich JJ, Cornelissen F, Papazian N, Lindenbergh-Kortleve DJ, Butler JA, Boon L, Coles MC, Samsom JN, Cupedo T.
J Exp Med. 2015 Oct 19;212(11):1783-91. doi: 10.1084/jem.20150318. Epub 2015 Sep 21.

4. Tertiary lymphoid Structures in Rheumatoid Arthritis: NF-kB-Inducing Kinase-Positive Endothelial Cells as Central Players. Noort AR, van Zoest KP, van Baarsen LG, Maracle CX, Helder B, Papazian N, **Romera-Hernandez M**, Tak PP, Cupedo T, Tas SW.
Am J Pathol. 2015 Jul;185(7):1935-43. doi: 10.1016/j.ajpath.2015.03.012. Epub 2015 May 9.

5. Damage control: Rorgt+ innate lymphoid cells in tissue regeneration. **Romera-Hernandez M**, Aparicio-Domingo P, Cupedo T.
Curr Opin Immunol. 2013 Apr;25(2):156-60. doi: 10.1016/j.coi.2013.01.007. Epub 2013 Feb 19. Review.

PhD PORTFOLIO

Name PhD student: **M. Romera-Hernández**	Promotor:
Erasmus MC Department: **Hematology**	**Prof.Dr. J.J. Cornelissen**
Research School: **Molecular Medicine**	Supervisor:
PhD Period: **August 2012 - March 2017**	**Dr. T. Cupedo**

1. PhD Training

	Year	ECTS
General courses		
• Laboratory Animal Science (Art.9).	2013	4.2
• Imaging course.	2013	4
• Infection, autoimmunity and lymphoma course.	2014	4
In-depth courses and workshops		
• Photoshop and Illustrator CS6 Workshop.	2013	0.3
• The Microscopic Image Analysis course.	2014	4
• Galaxy for NGS.	2017	2.5
Scientific meetings Department of Hematology		
• Work discussions.	2012-2017	10
• Erasmus Hematology Lectures.	2012-2017	2.5
• PhD lunch with seminar speaker.	2012-2017	2.5
• AIO/PostDoc meetings.	2012-2016	2
• Literature discussions.	2012-2017	7.5
(Inter)national conferences		
• T cell consortium meetings.	2012- 2017	2.5
• Annual Molecular Medicine Day. (2x)	2013, 2015	0.6
• Symposium & Masterclass on Mucosal Immunology. (2x)	2013-2015	1
• International Congress of Mucosal Immunology. (2x)	2015, 2017	1.4
• EMBO Conference on innate lymphoid cells. (2x)	2014, 2016	1.4
• International Lymphoid Tissue Meeting. (2x)	2013, 2017	1.4
• Nederlandse Vereniging voor Immunologie (NVVI) annual meetings.	2012-2107	2.5
• NVVI Lunteren Symposium.	2014	0.3

	Year	ECTS
Presentations		
• AIO/PostDoc meeting. (Oral, 2x)	2012-2016	2
• Journal Club. (Oral, 6x)	2012-2017	7.5
• Workdiscussion. (Oral, 10x)	2012-2017	4.5
• Annual Molecular Medicine Day. (Poster 2x)	2013, 2015	1
• Symposium & Masterclass on Mucosal Immunology. (Oral 2x)	2013-2015	2
• International Congress of Mucosal Immunology. (Oral 2x)	2015, 2017	2
• EMBO Conference on innate lymphoid cells. (Oral 1x, Poster 1x)	2014, 2016	2
• International Lymphoid Tissue Meeting. (Poster 2x)	2013, 2017	2
• Nederlandse Vereniging voor Immunologie (NVVI) annual meetings. (Poster 3x, Oral 3x)	2012-2107	6
• NVVI Lunteren Symposium. (Poster)	2014	1
2. Teaching		
Supervising practicals		
• Organization of PhD lunch with seminar speaker.	2012-2017	0.2
Supervising Master's theses		
• Master Student Infection & Immunity. (2x)	2014, 2015	6
3. Total		90.8

ACKNOWLEDGEMENTS

First of all, I would like to thank all the people who have supported me taking this very important step in my career as a PhD student at the Erasmus Medical Center. I have learnt a lot and enjoyed every single challenge that I have encountered during this time. You all have made those years unforgettable!

Prof.dr. I.P Touw, Prof.dr. R.E Mebius and Prof.dr. F. Koning, thank you for the critical reading of the manuscript, suggestions and for being part of the scientific committee.

I would like to thank my promotor Prof.dr. J.J Cornelissen to critically read the manuscript and guide my research project since the beginning with his comments during work discussions. I thank you for teaching me how important is our fundamental research to be applied in the clinical setting. Your advice has helped me to be more rigorous in all my scientific disseminations.

To Dr. Tom Cupedo, thanks so much for your great guidance and mentoring as my co-promotor and supervisor. Without your courage and love for science, all this work would not have happened, but not only this, you gave me the keys to continue being a scientist. I acknowledge your creative thinking and positivity through everything we faced during this period. I am extremely thankful to you for being always there, so approachable and full of ideas. I hope we can discuss science for many more years, it will always be a pleasure!

I want to specially thank Dr. Janneke Samsom for sharing all your knowledge in science, not only about mucosal immunology but also on how to approach our research questions. I have learnt so much from you! Thanks for teaching me great organizational skills and how to convey science into a crystal-clear message.

I cannot be more grateful to any other person in the lab rather than to Natalie. You know it, without you everyone is lost in the lab! Thanks so much for your vitality and strength during all these difficult experiments. Our beginning was hard but I know now that I was a child. Thanks for making me grow as a person next to you. Honestly, I will always have your coco-chocolate sweets as a memory of your special soul.

Patricia, mil gracias por todo lo que me enseñaste. Sin ti no hubiera sido capaz de inyectar a miles de ratones ni a desayunar con intestinos. Qué buenos momentos pasamos y cuánto los eché de menos cuando te marchaste! I am really grateful to you, for supporting me in the initiation of my project and to let me contribute so closely to yours. Thanks for all the enjoyable moments and to still be there as my advisor in difficult decisions.

Oh là là Julien-Jamal Karrich, I appreciate you so much! I know it is not needed to say, but you are a great scientist!!! I always listened to you and was impressed by your bright ideas and learned so much from your skill hands in the lab. Also, thanks for your patience, your care and to make me smile during stressful moments. You gave rays of sun in the office and left a special footprint in my heart. Thanks again for trusting me as a scientist as well as including me in your party agenda. I hope you keep all the fun moments to forget the "good price" of bikes and roller skates!

To Ferry, thanks so much for teaching me the importance of being so precise in the lab. I learnt a lot and I will keep on doing it, I promise you! I appreciate so much your willingness to help and I thank you for sharing with me your great experience and your time involved in my project. I am happy for the new turn in your career and I wish you all the best.

And to Niels, even though we did not have a lot of time to know each other better, I enjoyed you a lot! I would like to thank you for sharing your different perspective in science and to encourage me so much. It will be a great pleasure to travel in Canada together! I will be waiting…

I am especially thankful to Dicky for showing me everything about immuno-histochemistry. Thanks to find the time to look at my slides, to advise me in getting better results and to motivate me when I was staining so many slides. Thanks for letting me your space and forgive me when I made some mistakes. Like that, it was easier and always enjoyable.

Of course, a special thank you to my girl colleagues in the 15th… Lea, Sharon, Sandrine and Linda, it has been a great pleasure to meet you and share experiences in the lab and outside. Thanks for your input during work discussions and your support through all these years. I enjoyed a lot our borrel activities and will always remember our trips to congresses. Luckily, we will have the chance to discover other parts of the world together, even though it is mostly in the hotel (but with a spa)! Finally, I would like to congratulate all the other members of Janneke's group for your work! You are the best!

Thanks to Rogier M. Reijmers and Jurre Y. Siegers who were in the lab when I started, helped me a lot the first days and for all these well enjoyed Belgian beers!
I would not like to forget the students that have spent some time in Tom's group as they have also contributed to my training: Anusha, Agustín, Nora, Vilma and Winnie. Thanks for your help and good luck in the next steps in your career!

I am also thankful to Eric Braakman, Elwin, Mariette, Jess and Amiet for sharing your

knowledge with me during work discussions and helping me with machines, reagents and protocols in the lab.

Thank you very much to prof.dr. Mark Raaijmakers for his critical feedback and suggestions during lab meetings. I also would like to thank the former and actual members of his group, Noemi, Adrián, Si, Ping and Keane, as they have been a great support to me, both in the scientific path but also in my personal life.

I also would like to take the time to thank all the group leaders Rudd Delwel, Mojca Jongen-Lavrencic, Frank Leebeek, Moniek de Maat, Rebekka Schneider-Kraman, Pieter Sonneveld, Peter Valk, Emma de Pater, Bas Wouters, for building up such a good department.

I'm also grateful to Ans Mannens, Leenke de Jong de-Visser, Erik Kreiter, Natasja Vroone-van de Bospoort and Jan van Kapel for their support. Also, thanks to Egied for his help in the design of this thesis layout and the arrangments of the figures.
Thanks to everyone working at the EDC for taking the best care of our precious mice.

Thanks to my friends and colleagues Emmanuele, Cansu, Almira, Tim, Sophie, Adil, Melissa, François, Leonie, Claire, Burak, Andrea, Hèléne, Almira, Inge, Chelsea, Davine, Michiyo, Roger, Joke, Jacqueline… you create a beautiful atmosphere in the department. Do not forget to invite me to your next lab day out, lol! All the best for you!

To Onno, thanks so much for all your help. You taught me key tricks in confocal microscopy but listened to me and tried always to find a solution for me anytime I asked you! Thanks Onnito for all our moments together, I will always keep you as a good friend.

To Kasia, Jana and Roberto, I consider you my aunties and uncle in Rotterdam. Since the beginning you included me as part of your team and I cannot be happier for that. Thanks for opening your arms to me and show how crazy-fun is life. I will always appreciate you all for this!

To Paulete, Julia, Patricia, Joyce, Hans, Eric Bindels, Remco, Mathijs, Claudia, Marije, Michael, Jasper, Mark van Duin, Annelieke and the people of transplantation lab for this memorable years.
I'm grateful to Riccardo Fodde's group for helping me in the optimization of organoid culture and their contribution in the field of stem cell biology.

Thanks to Frederike Schmitz and the other members of Frits Koning's Lab at the LUMC for their training during my internship and their guidance and encouragement to start my

career as a PhD.

I would also like to acknowledge all the people who was part of the ITN STROMA. Thanks for the hard work of the Principal Investigators who unified so much effort to obtain funding and to the organizers and participants to give me exceptional opportunities and trained me as an early stage researcher.

I am also very happy to have met many PhD students in other departments, in particular Shorouk, Lorenzo, Vincenzo and François, Rodrigo and Pablo, and so many more…that thanks to our coffee times and borrels, long days in the lab were much easier and funnier. Looking forward to your PhD parties!

To my friends Josh and Stratos, I would not have been able to make it in Rotterdam without you. Thanks for being always there and teach me so much in life!

To Gizem, Matteo, Geoffrey, Joana and Carlos, my Loveland buddies. Thanks for the incredible time out spent together.

To Cristina, thanks for your energy, you have such an amazing Aurea!

To my dear flat mate Diego, your emotional support has made me a better person. Keep in mind our idea to start up our own foodie's business, it would be a great pleasure! Thanks for everything Dieguito!

To the entire Spanish Ghetto in Leiden, thanks so much for all these special moments we shared since my Erasmus in 2011. Jordi, Elena, Lucia, Guillem, Ander, Xabi, Pietro, Joana, Maria, Victorio, Juan… and everyone else that take good care of me, such as Jean Marc, Joriaan and Nils. You are part of me forever!

To Anna de la Fuente, thanks for your exceptional attitude. I enjoyed and keep on enjoying our special connection with eternal laughs and much more! Merci per tot bonica!

I especially would like to thank my best friend Carla, with who I started this amazing experience in the Netherlands. Thanks for learning English together, practicing oral presentations and showing to me your passion about science and green biology. Thanks also to travel around the world with me and always be there when I was sad. I would need an entire book to thank you for sharing so much with me! And remember that our FaceTime calls to discuss about Wnt signaling have had a special contribution in this thesis. Moltes gràcies Carlins, t'estimo molt!

También quiero agradecer a mi amiga Ane, que des de que nos conocimos en la UAB ha sido un gran apoyo para mí. Eres la chica más inteligente del planeta Ane, gracias por enseñarme tanto!

A toda mi familia también quiero agradecerles todo el apoyo y el cariño que siempre me han dado. Esto lo he conseguido gracias a vosotros, por enseñarme que, en esta vida, con esfuerzo y persistencia, todo es posible! Infinitas gracias por todas las oportunidades que me habéis ofrecido, por toda la paciencia que habéis tenido conmigo y por todas las risas que hemos vivido juntos. No tengo palabras para agradecéroslo. Aunque esté lejos, sé que no hay nadie mejor que vosotros: Papa, Mama, Laura, y Javi, os quiero muchísimo.

A Marco, il mio compagno di vita, voglio ringraziarti per viaggare e scoprire il mondo con me. Sono fiera di te. Grazie per il tuo amore, il tuo sostegno incondizionato. Sei bravissimo, e spero di poter imparare da te tutte le tue abilità. Insieme non ci sarà nessuno che ci fermerà in Canada.

And last but not least, I am really thankful to the Netherlands that has manage to make me feel like home for 6 years. Thanks for your educational programs, your organized system, and specially to your tolerant spirit, which makes possible the coexistence of an amazing multinational community.